GLUTAMATERGIC CALCIUM DYNAMICS

OF

RAT RETINAL GANGLION CELLS

by

Andrew T.E. Hartwick

Submitted in partial fulfillment of the requirements
for the degree of Doctor of Philosophy

at

Dalhousie University
Halifax, Nova Scotia
March 2006

Your file Votre référence
ISBN: 978-0-494-16723-6
Our file Notre référence
ISBN: 978-0-494-16723-6

DALHOUSIE UNIVERSITY

To comply with the Canadian Privacy Act the National Library of Canada has requested that the following pages be removed from this copy of the thesis:

Preliminary Pages
- Examiners Signature Page (pii)
- Dalhousie Library Copyright Agreement (piii)

Appendices
- Copyright Releases (if applicable)

DEDICATION

I would like to dedicate this thesis in memory of my mother,

Elizabeth Hartwick,

for all of her love, support, guidance and encouragement.

TABLE OF CONTENTS

LIST OF TABLES

LIST OF FIGURES

ABSTRACT

Although the release of the neurotransmitter glutamate onto retinal ganglion cell (RGC) dendrites is a normal part of retinal circuitry, prolonged exposure to glutamate is toxic to these retinal output neurons. A rise in intracellular calcium levels has been implicated as the trigger for glutamate excitotoxicity. In this thesis, I characterized the calcium dynamics of RGCs during brief (30 second) and prolonged (1 hour) glutamate exposures, investigated the relationship between calcium and excitotoxic death, examined the effect of adenosine on glutamate-induced calcium influx, and assessed the functional efficiency of retinal glutamate uptake. Using calcium imaging techniques on RGCs in both purified cultures and retinal wholemount preparations, I demonstrated that glutamate-induced calcium influx is mediated primarily by activation of NMDA-type glutamate receptors, but a smaller portion of the signal is mediated by voltage-gated calcium channel and AMPA/kainate-type glutamate receptor activation at saturating glutamate (100 μM) concentrations. One hour exposure to glutamate (10-1000 μM) killed 18-28% of the cultured RGCs, and RGC death was accompanied by delayed calcium deregulation. RGCs that displayed greater glutamate-evoked calcium signals were more likely to undergo calcium deregulation. Inhibition of NMDA receptors reduced calcium influx and significantly protected RGCs from glutamate excitotoxicity. The neuromodulator adenosine was shown to reversibly inhibit glutamate-induced calcium influx through an adenosine A_1 receptor-mediated mechanism, supporting a role for adenosine as a modifier of RGC glutamatergic pathways. In retinal wholemounts, glutamate was much less effective than NMDA in eliciting an RGC calcium response (compared to isolated RGCs) due to the presence of glutamate transporters. Detectable calcium signals with micromolar glutamate concentrations could be obtained if retinal glutamate uptake was pharmacologically inhibited. Imaging RGC calcium dynamics in retinal wholemounts was used to functionally assess glutamate clearance mechanisms in a rat glaucoma model, and no significant defect in glutamate uptake was apparent using this novel methodology. The modulation of RGCs by adenosine and the rapid removal of extracellular glutamate by transporters represent two mechanisms through which glutamatergic signaling is regulated in the retina to counter the excitotoxic actions of this neurotransmitter.

LIST OF ABBREVIATIONS

ADO	adenosine
AGIS	Advanced Glaucoma Intervention Study
AM	acetoxymethyl ester
AMPA	α-amino-3-hydroxy-5-methylisoxazole-4-propionate
ANOVA	analysis of variance
APV	D(-)-2-amino-5-phosphonopentanoic acid
ARVO	Association for Research in Vision and Ophthalmology
ATP	adenosine 5'-triphosphate
BAPTA	1,2-bis(2-aminophenoxy)ethane-N,N,N',N'-tetraacetic acid
BDNF	brain-derived neurotrophic factor
BSA	bovine serum albumin
$[Ca^{2+}]_i$	intracellular calcium concentration
cAMP	cyclic adenosine monophosphate
CCD	charged-coupled device
CHA	N^6-cyclohexyladenosine
CNQX	6-cyano-7-nitroquinoxaline-2,3-dione
CNS	central nervous system
CNTF	ciliary neurotrophic factor
CNTGS	Collaborative Normal-Tension Glaucoma Study
CPCA	5'-(N-cyclopropyl)carboxamidoadenosine
CREB	cAMP response element binding protein
DCD	delayed calcium deregulation
DIC	differential interference contrast
DIV	days in vitro
DMEM	Dulbecco's modified Eagle's medium
DMPX	3,7-dimethyl-1-propargylxanthine
DMSO	dimethyl sulfoxide
DNQX	6,7-dinitroquinoxaline-2,3-dione
DPBS	Dulbecco's phosphate-buffered saline
DPCPX	8-cyclopentyl-1,3-dipropylxanthine
EAAT	excitatory amino acid transporter
EBSS	Earle's balanced salt solution
EGTA	ethylene glycol-bis(2-aminoethylether)-N,N,N',N'-tetraacetic acid
EMGT	Early Manifest Glaucoma Trial
G-protein	guanine nucleotide-binding protein
GCL	ganglion cell layer
GLAST	glutamate aspartate transporter
GLUT	glutamate
GLY	glycine
h	hours
HBSS	Hanks' balanced salt solution
IOP	intraocular pressure
IPL	inner plexiform layer
K_D	dissociation constant
min	minutes

MW	molecular weight
NBQX	2,3-dihydro-6-nitro-7-sulfamoyl-benzo(f)quinoxaline
NMDA	N-methyl-D-aspartate
nNOS	neuronal nitric oxide synthase
OHTS	Ocular Hypertension Treatment Study
PBS	phosphate-buffered saline
PKA	cAMP-dependent protein kinase
-R	receptor
RGC	retinal ganglion cell
s	seconds
SD	standard deviation
SEM	standard error of the mean
SERCA	sarcoplasmic/endoplasmic reticulum calcium ATPase
SNK	Student-Newman-Keuls test
TBOA	DL-threo-β-benzyloxyaspartate
TRP	transient receptor potential channel
VGCC	voltage-gated calcium channel

ACKNOWLEDGEMENTS

There are a number of people I would like to thank for making my experience as a graduate student at Dalhousie University so enjoyable:

- First and foremost, my supervisor **Dr. William Baldridge**. There is not enough space here to express my gratitude to Bill for his guidance, encouragement, and patience. Bill has been a true mentor to me, and his approach to science and life is one I aspire to emulate. A special thanks to the rest of the Baldridge family, **Linda**, **David**, and **Michael** for making my family feel so at home during our stay in Halifax.

- My committee members **Dr. Balwantray Chauhan**, **Dr. David Clarke** and **Dr. Kazue Semba**. I always received useful feedback during my committee meetings that led me to think about my work from a new perspective, and I appreciate their valuable advice. I would also like to thank Dr. Chauhan for his important contributions to the research presented in Chapter 3 of this thesis.

- My external examiner **Dr. Andrew Ishida**. I am thankful to Dr. Ishida for his time commitment in reviewing my thesis and traveling to Halifax for my defence.

- **Dr Steven Barnes**, **Dr. Melanie Kelly** and **Dr. Francois Tremblay**. The Retina and Optic Nerve Research Laboratory was an exciting lab to work in, in large part due to its great team of primary investigators. Through various collaborative projects, I had a chance to learn from each of these scientists, and I thank them for their input.

- My fellow lab-mates: **Michael Davis**, **Anna Stratis**, **Bryan Daniels**, **Jianing Yu**, **Xiaowei Zhang** and **Tim Maillet**. The Baldridge lab has been a great environment to grow intellectually while still being reminded on a daily basis that research is fun.

- **Michele Archibald**, **Christine Jollimore**, **Terry LeVatte**, and **Kelly Stevens**. They always helped me when I needed it and I am grateful for their assistance and advice.

- All other members, past and present, of the Retina Lab. In particular, I would like to thank **Darryl Baptiste**, **Melanie Lalonde** and **John Vessey**, colleagues who were a pleasure to collaborate with, in addition to being good friends.

- Finally, I would like to thank my wife **Tracy**, and my two sons **Samuel** and **Elliott** for everything. I can simply not fully express how much your love and support picked me up and kept me going, particularly in the final writing of this thesis. When I started this graduate work, there were two of us...and now as I finish, we are four. Although I learned a lot about science through the course of my Ph.D. work, it pales in comparison to what I've learned from Sam and Elliott as I've adjusted to fatherhood. I truly am a lucky person and I love you all.

I also gratefully acknowledge my financial support, provided first by an Ezell Fellowship from the **American Optometric Foundation** and then by an E.A. Baker Fellowship from the **Canadian Institute for the Blind** and **Canadian Institutes for Health Research**.

CHAPTER 1: General Introduction

Retinal Ganglion Cells

Vision, the transformation of photons of light into an organism's perception of images, begins in the retina. The vertebrate retina lines the back of the inside of the eye and is anatomically organized into well-defined cellular layers, as illustrated in Figure 1-1. Light passes through the entire retina and is captured by the photoreceptors located in the most posterior retinal layer. The resulting electrochemical signal is then transmitted from photoreceptors to bipolar cells and finally to ganglion cells in a circuit commonly referred to as the 'vertical' visual pathway. The region containing the synaptic connections between photoreceptors (rods and cones) and the second-order retinal neurons, bipolar cells and horizontal cells, is termed the outer plexiform layer. Similarly, the more anterior neuropil, consisting of synapses between bipolar cells and both amacrine and ganglion cells, is denoted as the inner plexiform layer. Input from horizontal and amacrine cells modifies the signal in the vertical visual pathway, and fine-tunes the visual information that is carried from the retina to the brain (for more detailed descriptions of retinal circuits, see Masland 2001a; Kolb 2003; Wassle 2004).

The focus of this thesis will be on retinal ganglion cells (RGCs), the output neurons of the inner retina that project to targets in the brain. Detailed neuroanatomical studies, characterizing soma size, dendritic field width and the dendrite branching level, indicate that there are ten to fifteen morphological types of RGCs in the mammalian retina (Masland 2001b). RGCs can also be classified by their physiological responses to light stimuli, with perhaps the broadest subdivision consisting of two major categories:

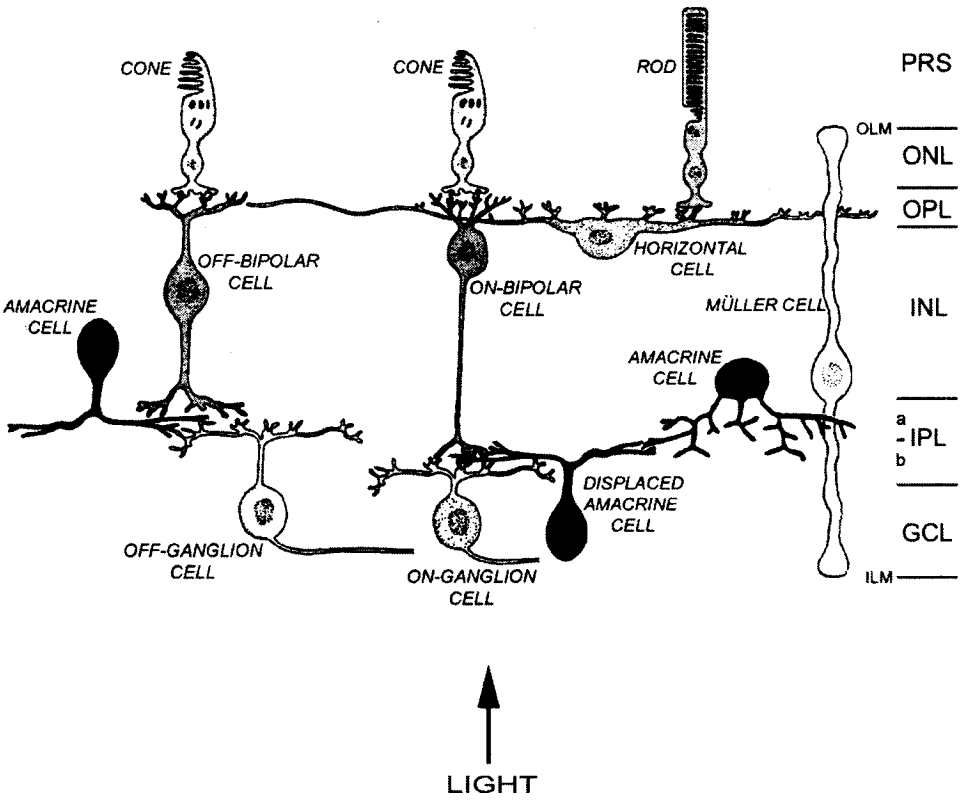

Figure 1- 1 Organization of the retina. Schematic diagram illustrating the cell types present in different layers of the retina. Light passes through the entire retina and is captured by rods and cones. The retinal ganglion cells of the inner retina are the cell type of primary interest for this thesis, and these neurons have axons that exit the eye and project to the brain. The dendrites of OFF-center RGCs receive synaptic contacts in sublamina a of the inner plexiform layer, while the ON-center RGC dendrites arborize in sublamina b. The Müller cells are glial cells and nearly span the width of the retina. PRS, photoreceptor segments; ONL, outer nuclear layer; OPL, outer plexiform layer; INL, inner nuclear layer; IPL, inner plexiform layer; GCL, ganglion cell layer; ILM, inner limiting membrane; OLM, outer limiting membrane. Figure adapted from Tessier-Lavigne (1991).

ON-center RGCs that respond to light areas set against dark backgrounds; and OFF-center RGCs that fire in response to dark areas on light backgrounds (Masland 2001a; Kolb 2003; Wassle 2004). The physiological distinction between these two classes has an anatomical correlate as the dendrites of ON and OFF RGCs branch at specific and segregated levels within the inner plexiform layer. The dendrites of ON RGCs arborize at a more inner level (sublamina b) of the inner plexiform layer relative to those of OFF RGCs (sublamina a). It should be clarified that RGC ON or OFF responses are not due to direct stimulation of these cells by light, as initiation of the visual signal begins with phototransduction by photoreceptors in the outer retina, but these responses are instead determined by the retinal circuitry through which each RGC is synaptically driven.

Additional RGC classifications exist that are based on electrophysiological responses obtained for RGCs exposed to various stimuli (Dowling 1987; Masland 2001b; Dacey *et al.* 2003; Wassle 2004). Example RGC sub-types, using physiological criteria, include: transient (originally named 'Y') RGCs that exhibit brief bursts of activity pulses with either onset (ON-type) or offset (OFF-type) of illumination; sustained (termed 'X') RGCs (again, both ON- and OFF-types) that, as the name implies, fire for the duration of the stimulus; ON-OFF direction-selective RGCs that display transient activity bursts at both the onset and offset of a stationary light spot stimulus, and that respond to light stimuli moving in a certain direction; color-coded RGCs that are excited by blue light and inhibited by yellow light (and vice versa) due to color-opponent synaptic interactions with short-wavelength and long-wavelength cone retinal circuits (a similar red-green system also exists); orientation-selective RGCs that respond preferentially to a given orientation of a bar of light (i.e. horizontal versus vertical); and edge-detector RGCs that fire vigorously in response to a moving target traveling across their receptive field in any direction. Finally, a small group of RGCs (1-2% of the total RGC population) express the

photopigment melanopsin and have recently been shown to be directly light-sensitive. Melanopsin RGCs are thought to provide light/dark input to the brain regions that control circadian rhythms (endogenously controlled daily cycles of physiology and behavior), and their discovery overturned the long-held belief that rods and cones are the sole photoreceptors in the retina (for a review on melanopsin RGCs, see Berson 2003).

The experiments in this thesis will be performed on RGCs from neonatal and adult rats. With the large body of knowledge that exists for the rat nervous system, combined with the relative low cost of animal maintenance, the rat has become an important mammalian model for retinal research. Each rat retina contains roughly 115,000-130,000 RGCs (Potts *et al.* 1982; Perry *et al.* 1983; Dreher *et al.* 1985; Cepurna *et al.* 2005; Chauhan *et al.* 2006), and there appear to be morphologically distinct classes of rat RGCs similar to those characterized in cat, monkey and rabbit retinas (Sun *et al.* 2002a). Rats lose about 35-50% of their RGCs in the first 5 days following birth, but the total number of RGCs at age 7-8 days (the age used in this thesis) is roughly the same as in adult rats (Potts *et al.* 1982). In the rodent retina, RGCs are not the sole neurons in the innermost ganglion cell layer as up to 50% of the cells here are displaced amacrine cells (Perry *et al.* 1983). Unlike amacrine cells, RGCs possess axons, and these axons travel along the inner surface of the retina and exit together from the back of the eye as the optic nerve. As the unmyelinated RGC axons leave the eye, they congregate into bundles and pass through pores in the sheets of connective tissue known as the lamina cribrosa that span the opening of the scleral hole. In this region, there are specialized astrocytes (two types), lamina cribrosa cells and microglia that surround the RGC axons, and these different glial cells can alter the microenvironment and extracellular matrix at the optic nerve head (Hernandez 2000). After passing through the lamina cribrosa, the axons become myelinated and continue

on to their appropriate brain targets. The vast majority of rat RGCs (95-99%) cross at the optic chiasm and project to the contralateral superior colliculus, with some (up to 30%) of these axons splitting into collaterals that synapse in the lateral geniculate nucleus of the thalamus (Dreher *et al.* 1985; Kondo *et al.* 1993). The rodent superior colliculus is connected to the motor centers that control reflex responses, and therefore it is likely that the rat visual system is specialized for the linking of object detection (such as a predator) to the initiation of movement (for example, the escape response). The lateral geniculate nucleus sends projections to the cortical regions that further process the image information into pattern vision.

The retina develops from the neural tube as an outpouching of the diencephalon and is considered part of the central nervous system (Dowling 1987). RGCs share a number of characteristics with neurons in the brain, including: 1) separation from the vascular system by a specialized blood-retinal barrier (analogous to the blood-brain barrier); 2) narrow synaptic clefts that are completely ensheathed by glial cells, resulting in tight regulation of neurotransmitter concentrations; 3) axons that are encased by myelin generated from oligodendrocytes, rather than from Schwann cells; and 4) reduced capacity for axonal regeneration after optic nerve injury. Therefore, in addition to furthering our understanding of retinal function and dysfunction, the study of RGC neurobiology can elucidate fundamental properties of central neurons.

Glutamatergic Neurotransmission

Glutamate is the major excitatory neurotransmitter throughout the central nervous system. Glutamate activates both ionotropic receptors that are ligand-gated cation channels and metabotropic receptors that are seven transmembrane G-protein-

coupled receptors linked to the activation of second messenger pathways (Hollmann and Heinemann 1994). The ionotropic glutamate receptors can be classified into three families with agonist-derived names: N-methyl-D-aspartate (NMDA), α-amino-3-hydroxy-5-methylisoxazole-4-propionate (AMPA), and kainate receptors. The mammalian ionotropic glutamate receptors have been cloned and a total of 18 receptor subunits have been identified (Mayer 2005). There are seven NMDA subunits (NR1, NR2A, NR2B, NR2C, NR2D, NR3A and NR3B), four AMPA subunits (GluR1, GluR2, GluR3 and GluR4), five kainate subunits (GluR5, GluR6, GluR7, KA1 and KA2) and two orphan delta subunits (δ1 and δ2). For metabotropic glutamate receptors, eight genetically distinct receptors have been cloned (mGluR1-8) which are further divided into three groups (Group I, II and III) according to agonist sensitivity, sequence homology and second messenger system coupling (Conn 2003).

The glutamate-induced flow of ions through its ionotropic receptors, a principal topic of this thesis, helps to mediate fast synaptic communication between neurons. There has been significant progress in understanding both the physical and molecular structures of these receptors (for reviews, see Madden 2002; Mayer and Armstrong 2004; Wollmuth and Sobolevsky 2004). Functional ionotropic glutamate receptors consist of four subunits, and there are multiple subunit combinations that have been observed in the CNS. However, there is no evidence for naturally occurring receptors that possess subunits intermingled from different receptor families (i.e. AMPA subunits combining with kainate or NMDA subunits). While homomeric AMPA receptors are possible, AMPA receptors generally consist of GluR2 combined with either GluR1 or GluR3 subunits (Dingledine *et al.* 1999). The kainate subunits GluR 5-7 can form homomeric channels or combine with each other or with KA1-2 subunits to produce heteromeric glutamate receptors (Lerma 2003). Functional NMDA receptors are always

heteromeric and are usually composed of two NR1 subunits and two NR2 subunits, with the glutamate binding site being present on the latter (Dingledine *et al.* 1999; Mayer and Armstrong 2004). The NR1 subunit contains a binding site for glycine, a co-agonist with glutamate for the NMDA receptor (Johnson and Ascher 1987). Although not as common, the NR3 subunit also contains a glycine binding site and can co-assemble with NR1 and NR2 subunits in some neurons (Madden 2002). The physiological properties of the delta subunits (after being cloned, these were referred to as 'orphan' receptors because they do not form functional glutamate-gated ion channels when expressed alone or with other glutamate receptor subunits) are not fully understood, but ion channels containing the δ2 subunit may contribute to cerebellar function (Yuzaki 2003).

The amino acid glutamate is the endogenous ligand for NMDA, AMPA and kainate receptors, although the putative transmitter aspartate can also activate NMDA receptors (Patneau and Mayer 1990). In addition to glycine, there is evidence that D-serine acts as a co-agonist for NMDA receptors in the CNS (Schell *et al.* 1995; Wolosker *et al.* 1999). Immunohistochemical data suggests that D-serine may be the primary ligand for the NR1 subunit in certain regions of the brain while glycine serves this role in others (Schell *et al.* 1997). While NMDA is a selective agonist for its named receptor subtype, it is difficult to specifically target AMPA or kainate receptors pharmacologically. Kainate will activate AMPA receptors and AMPA will activate most kainate receptors, so these receptor classes were initially distinguished by their relative affinities for these two ligands (Huettner 2003). Similarly, antagonists such as the quinoxalines (CNQX, DNQX and NBQX) will block both AMPA and kainate receptors, although it has more recently been discovered that benzodiazepines such as GYKI 53655 will specifically antagonize AMPA but not kainate receptors (Wilding and Huettner 1995). While functional differences between AMPA and kainate receptors are beginning to emerge (Huettner

2003; Lerma 2003), these two classes will often be classified together as AMPA/kainate receptors for the purposes of this thesis.

There are a number of key distinctions between NMDA and AMPA/kainate receptors. Relative to NMDA receptors, AMPA/kainate receptors typically exhibit: 1) a lower affinity for glutamate, requiring higher concentrations of this agonist to be present for activation to occur; 2) faster gating properties (ion channels open quickly upon activation); 3) stronger desensitization (the ion channel closes despite glutamate still being bound to the receptor) that occurs more quickly; and 4) less permeability to calcium ions (Hollmann and Heinemann 1994; Dingledine *et al.* 1999). In addition, the ion channels of NMDA receptors (but not AMPA/kainate receptors) can be blocked by magnesium ions (Mg^{2+}) at concentrations normally present in the extracellular medium. The effect of Mg^{2+} is voltage-dependent; the NMDA receptor channels are blocked while the neuron is sitting at resting membrane potentials, and not affected when the neuron is depolarized (Mayer *et al.* 1984; Nowak *et al.* 1984). The contrasting properties of NMDA and AMPA/kainate receptors likely have functional implications. For example, the rapid activation and brief open time of AMPA/kainate receptors would serve to depolarize the neuron, thus relieving the Mg^{2+}-block of slower-activating NMDA receptors. The intriguing voltage-dependent Mg^{2+}-block of NMDA receptors has led to these receptors being called 'coincidence detectors', as they require both postsynaptic depolarization and presynaptic glutamate release in order to be activated (Stevens and Sullivan 1998). Due to this property, NMDA receptors have garnered significant attention as 'Hebbian' molecules (Hebb 1949) that signal the activity-dependent changes in synaptic strength thought to underlie memory formation and learning (Bliss and Collingridge 1993; Nicoll and Malenka 1995; Lamprecht and LeDoux 2004).

In the retina, glutamate is released by photoreceptors (rods and cones) onto

bipolar and horizontal cell dendrites, and by bipolar cells onto amacrine and RGC dendrites (for review, see Thoreson and Witkovsky 1999). Rods and cones, somewhat counterintuitively, release glutamate constantly in the dark and stop releasing this neurotransmitter in the light. The splitting of the retinal circuitry into parallel ON and OFF visual channels occurs at the photoreceptor/bipolar cell synapse. Whereas OFF bipolar cells possess ionotropic AMPA/kainate receptors (and thus respond to glutamate released from photoreceptors when light is turned off), ON bipolar cell responses are mediated through the metabotropic glutamate receptor mGluR6 (Shiells *et al.* 1981; Slaughter and Miller 1981; Nomura *et al.* 1994). Activation of mGluR6 by glutamate (released in the dark) leads to the closing of G-protein-coupled cation channels on the ON bipolar cells, and conversely these channels open following the uncoupling of the glutamate-mGluR6 interaction with light onset.

With the separation of ON and OFF pathways originating at the dendritic terminals of bipolar cells, transmission of the excitatory signal to either ON or OFF RGCs is mediated through the activation of ionotropic glutamate receptors. Almost every AMPA/kainate (GluR1-7, KA2) and NMDA (NR1, NR2A-C, NR3A) subunit has been identified in the ganglion cell layer of the rat retina in studies using *in situ* hybridization and immunohistochemistry techniques (Hughes *et al.* 1992; Muller *et al.* 1992; Hamassaki-Britto *et al.* 1993; Brandstatter *et al.* 1994; Peng *et al.* 1995; Grunder *et al.* 2000a; Grunder *et al.* 2000b; Sucher *et al.* 2003). The organic cation agmatine can pass through glutamate-gated ion channels, and experiments on the NMDA-driven accumulation of agmatine in the mammalian retina indicates that functional NMDA receptors are present only on RGCs and some amacrine cells (Marc 1999a; Kalloniatis *et al.* 2004). A similar study using kainate instead of NMDA showed that AMPA/kainate receptors are also on RGCs and some amacrine cells, although these receptors can be

identified in OFF bipolar and horizontal cells as well (Marc 1999b). Recordings of the electrical current elicited by NMDA, AMPA, kainate in RGCs from mixed rat retinal cell cultures have confirmed that functional NMDA and AMPA/kainate receptors are present on most, if not all, RGCs (Aizenman *et al.* 1988; Taschenberger *et al.* 1995).

Both ionotropic glutamate receptor subtypes contribute to RGC light responses. In the primate retina, light-evoked neurotransmission from bipolar cells to RGCs occurs predominantly through AMPA/kainate receptor activation (~85% of the light response can be blocked with appropriate antagonists) with NMDA receptors making a smaller (~15%) contribution (Cohen and Miller 1994). Further analysis, using an intact rat retina preparation, suggests the relative contribution of AMPA/kainate versus NMDA receptors to the light response is related to their position along the RGC membrane (Chen and Diamond 2002). This study showed that AMPA/kainate receptors (predominantly AMPA) are located right at the bipolar/RGC synapse, while NMDA receptors are located outside of the synapse (extrasynaptically) and thus encounter less glutamate during an evoked synaptic response. In addition to light responses, NMDA receptors appear to contribute to the background and tonic fluctuations in RGC membrane potential (Gottesman and Miller 1992, 2003). Stimulation of retinal NMDA receptors may be enhanced by either glycine released from glycinergic amacrine cells (Lukasiewicz and Roeder 1995) or by D-serine, which has more recently been shown to be released from glial cells (Müller cells and astrocytes) in the retina (Stevens *et al.* 2003).

Intracellular Calcium Dynamics

Stimulation of ionotropic glutamate receptors results in the flow of positively-charged ions through the channel pore. The influx of calcium into neurons is of

considerable interest to neuroscientists, as it is the changes in intracellular calcium levels ($[Ca^{2+}]_i$) that regulate a wide variety of biochemical cascades involved in diverse neuronal functions. For example, calcium has been implicated as a key intracellular messenger in processes related to cell growth and differentiation, synaptic plasticity, neurotransmitter release, gene transcription, neuronal excitation, neurite outgrowth and cellular death (Deisseroth *et al.* 1995; Berridge 1998; Berridge *et al.* 1998; Sattler and Tymianski 2000; Augustine *et al.* 2003). The resting $[Ca^{2+}]_i$ in most neurons is approximately 50-100 nM, as compared to Ca^{2+} levels of 1-3 mM in the extracellular environment. With a ~10,000-fold concentration gradient across the cell membrane, the opening of calcium channels can result in rapid increases in $[Ca^{2+}]_i$. Relatively small amounts of Ca^{2+} are required to bind to effector molecules that then initiate calcium-dependent pathways such as the opening/closing of ion channels and the activation or inactivation of numerous enzymes (Berridge *et al.* 2003; Orrenius *et al.* 2003).

While all glutamate receptors appear to be permeable to monovalent sodium and potassium ions, specific receptors are also capable of allowing divalent calcium ions to pass through their channel pores. In general, NMDA receptors are more permeable to calcium than kainate or AMPA receptors (Dingledine *et al.* 1999), although AMPA receptors that do not possess a GluR2 subunit are also calcium permeable (Jonas and Burnashev 1995). The calcium influx through NMDA receptors is thought to be an important mediator of both pathological and physiological processes in the CNS. One such process is synaptic plasiticity, as NMDA-receptor mediated Ca^{2+} flow can lead to increases in synaptic strength and connectivity through the activation of a kinase-mediated (most prominently calcium/calmodulin-dependent protein kinase II) pathway that culminates in the insertion of more AMPA receptors into the postsynaptic membrane (Nicoll and Malenka 1995). In RGCs, there is conflicting evidence regarding the relative

contribution of NMDA or AMPA/kainate receptors to glutamatergic alterations of intracellular calcium dynamics, and this issue is addressed in Chapter 4.

Voltage-gated calcium channels (VGCCs) are also present on CNS neurons and these channels are activated by changes in membrane potential. The neuronal depolarization induced by the flow of Ca^{2+} and Na^{+} through glutamate receptors can cause VGCCs to open, thus representing an alternative indirect pathway through which glutamate can alter intracellular calcium dynamics. VGCCs are composed of 5 subunits (often α_1, α_2, δ, β, and γ), with the ion pore and the voltage sensor occurring on the α_1 subunit (Catterall 2000). The family of VGCCs has traditionally been divided into different types based on their physiology and pharmacology (Tsien *et al.* 1995; Ertel *et al.* 2000; Trimmer and Rhodes 2004): L-type channels (the Cav1 group of more recent nomenclature) that are high-voltage-activated, exhibit long-lasting channel opening, and blocked by dihydropyridines (i.e. nifedipine), phenylalkylamines (i.e.verapamil) and benzothiazepines (i.e. diltiazem); N-type, P/Q-type and R-type channels (the Cav2 group) that are high-voltage-activated, found predominantly on neurons, and blocked by the snail and spider venoms ω-conotoxin GVIA, ω-agatoxin IVA, and SNX-482, respectively; and T-type channels (Cav3 group) that are low-voltage-activated and exhibit transient currents. Membrane conductances characteristic of N-type, L-type and T-type VGCCs have been demonstrated in RGCs (Karschin and Lipton 1989; Ishida 1991; Guenther *et al.* 1994; Taschenberger and Grantyn 1995; Bindokas and Ishida 1996; Schmid and Guenther 1999). Calcium influx through VGCCs has long been regarded as the trigger that initiates neurotransmitter release from presynaptic membranes (Katz and Miledi 1967; Llinas 1982). In accord, the synaptic release of glutamate from putative RGCs in mixed cultures has been shown to be VGCC-dependent, as the non-specific VGCC inhibitor cadmium eliminated glutamate release

while the N-type channel antagonist ω-conotoxin GVIA reduced release by about 40% (Taschenberger and Grantyn 1995). Also, calcium influx through VGCCs in fish RGCs (depolarized by elevated extracellular potassium ions) can elicit somatic changes in $[Ca^{2+}]_i$ (Ishida *et al.* 1991), indicating a potential role for these channels in the modulation of RGC activity and the activation of calcium-dependent pathways.

In addition to the flow of Ca^{2+} through membrane-bound channels, a number of intracellular processes contribute to changes in $[Ca^{2+}]_i$ and serve to shape its temporal dynamics. Ca^{2+} can stimulate inositol 1,4,5-trisphosphate and ryanodine receptors on the endoplasmic reticulum, causing the release of more Ca^{2+} into the cytoplasm in a phenomenon known as calcium-induced calcium release (Berridge 1998). In a study of RGCs in mixed retinal cell cultures, it was noted that the release of calcium from intracellular stores contributed up to 50% of the NMDA-induced calcium signal (Lei *et al.* 1992). As a counterbalance to calcium influx and calcium-induced calcium release, various buffers, pumps and exchangers are triggered which act to remove Ca^{2+} and maintain homeostasis (Berridge *et al.* 2003). The calcium buffers include calbindin D-28, calretinin, and parvalbumin and their binding to Ca^{2+} fine-tunes the spatial and temporal properties of the calcium signal (Carafoli *et al.* 2001). To return $[Ca^{2+}]_i$ to resting levels, cytoplasmic Ca^{2+} is extruded from neurons back into the extracellular milieu via Na^+/Ca^{2+} exchangers (Bano *et al.* 2005) and plasma membrane Ca^{2+} pumps (Mata and Sepulveda 2005), or Ca^{2+} can be sequestered internally following its uptake into the endoplasmic reticulum and mitochondria via Ca^{2+}/ATPase (SERCA) pumps (Berridge 1998) and Ca^{2+} uniporters (Kirichok *et al.* 2004), respectively. Finally, the rise in $[Ca^{2+}]_i$ can stimulate Ca^{2+}-dependent enzymes such as calcineurin that inactivate VGCCs, particularly L-, N- and P/Q- types, through the dephosphorylation of these channels (Budde *et al.* 2002). By limiting Ca^{2+} entry through voltage-activated

channels, this negative feedback pathway likely serves to also regulate $[Ca^{2+}]_i$.

To better understand calcium signaling mechanisms, a variety of Ca^{2+} probes and imaging techniques have been developed that enable scientists to monitor real-time fluctuations of $[Ca^{2+}]_i$ in living cells (for review of different methods, see Rudolf *et al.* 2003). Measurements of $[Ca^{2+}]_i$ can also be used as a marker of neuronal activity and to identify potential targets of neurotransmitters and neuromodulators. The fura dyes are the calcium indicator probes used throughout this thesis, and they are part of the family of fluorescent calcium probes developed by Roger Tsien and colleagues in the 1970s and 1980s. These probes, which are structurally similar to the well-known calcium chelator EGTA, undergo a conformational change upon binding to Ca^{2+} that results in altered excitation properties of the attached chromophores (Tsien 1989). The fura dyes are ratiometric, meaning that $[Ca^{2+}]_i$ is measured as the ratio of fluorescence intensities obtained with excitation by two different wavelengths (340 and 380 nm). As illustrated in Figure 1-2, the excitation spectrum of fura changes depending on whether the molecule is bound or unbound to Ca^{2+}. In non-ratiometric dyes, such as the fluo dyes, the resulting fluorescence intensity (one excitation wavelength) simply increases as more of the dye molecules bind to Ca^{2+}. The absolute level of fluorescence, however, is influenced by factors such as dye loading, cell size, dye bleaching, dye leaking, and microscope focus. With a ratiometric dye, dividing the raw fluorescence intensity value at one wavelength by the value obtained with another excitation (or emission) wavelength largely cancels out and corrects for these variables (Grynkiewicz *et al.* 1985). As a result, two cells that have identical $[Ca^{2+}]_i$ but different concentrations of the loaded fura dye (i.e. due to differences in cell volume) would display a similar fura ratio even though the individual fluorescence intensities for the two excitation wavelengths may be vastly different. This property of ratiometric dyes also enables fluorescence

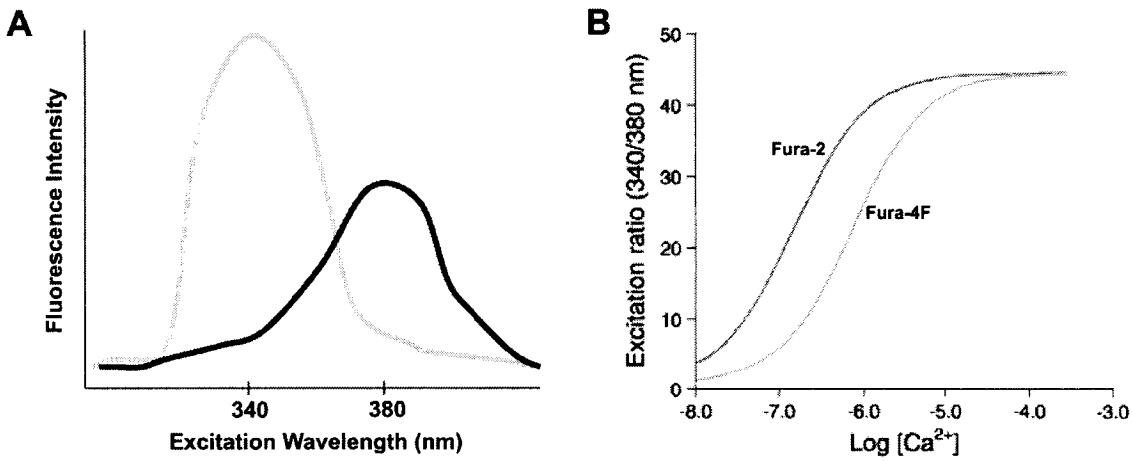

Figure 1- 2. Properties of fura calcium indicator dyes. **(A)** Approximate excitation spectrum (fluorescence measured at 510 nm) for the fura group of dyes in high-calcium (grey line) and calcium-free (black line) conditions. Note that with calcium binding, the excitation curve for fura shifts to the left. As calcium levels rise, the fluorescence measured at 340 nm excitation increases, while the fluorescence measured at 380 nm excitation decreases. Therefore the 340 nm/380 nm fluorescence ratio increases as $[Ca^{2+}]$ increases. **(B)** Typical affinity binding curves (data from Molecular Probes product information) for the high affinity dye fura-2 and the low affinity dye fura-4F. Note that at log $[Ca^{2+}]$ = -6.0 (equal to 1 μM), the fura-2 indicator is approaching saturation. In contrast, this concentration lies well within the dynamic range of fura-4F.

ratios to be converted more easily and accurately to absolute $[Ca^{2+}]_i$ than the fluorescence intensities obtained with non-ratiometric dyes (see Appendix A for more details on the calibration procedure).

Fura-2 AM is the predominant dye used throughout this thesis. As calcium indicator dyes are not membrane permeable, their conjugation to an acetoxymethyl (AM) ester allows them to cross the lipid membrane. With the ester attached, the dye is poorly fluorescent and does not contribute greatly to background fluorescence. Once inside the cell, however, the ester is cleaved from the dye by endogenous esterases and the now-fluorescent dye becomes trapped within the cell. While ester-dyes can be loaded into isolated cells, they are generally ineffective in intact tissue preparations unless they are directly injected into cells using microelectrodes. An alternative method involves the retrograde loading of fura dye that is conjugated to large dextran (inert sugar) molecules (Baldridge 1996), and a modified version of this technique is used for experiments on intact rat retina preparations in this thesis.

The binding affinity for calcium can vary among different calcium indicators and is measured as the dissociation constant K_D, the $[Ca^{2+}]$ at which 50% of the dye is bound to calcium ions. With a K_D of 224 nM, fura-2 is best suited to measure changes in $[Ca^{2+}]_i$ in the nM range (recall that the resting $[Ca^{2+}]_i$ for most neurons is ~50-100 nM), but the dye will become saturated as the $[Ca^{2+}]_i$ rises above roughly 1.5 μM (based on affinity binding curve, see Figure 1-2). The low affinity dye fura-4F is used in Chapter 4, and with a K_D of 770 nM, it is better suited to measure changes in $[Ca^{2+}]_i$ in the low μM range although it has less sensitivity to small variations from resting calcium levels. In addition, the affinity of these dyes for Ca^{2+} varies with pH (Lattanzio and Bartschat 1991), requiring that calcium imaging experiments be performed in strongly buffered physiological solutions to prevent pH perturbations from altering the relationship of the

fura ratio to $[Ca^{2+}]_i$. Thus, all imaging experiments in this thesis are performed on cells or tissue maintained in a balanced salt solution containing HEPES buffer (15 mM).

Glutamate Excitotoxicity

Although glutamate is fundamental to excitatory neurotransmission in the CNS, excessive stimulation of glutamate receptors is associated with neuronal death. The pathological effects of glutamate were first noted in the retina. In the 1950s, two ophthalmologists, Lucas and Newhouse, subcutaneously injected a number of amino acids and neurotransmitters into neonatal mice that displayed eventual deterioration of outer retinal neurons due to a genetic defect. While their results did not yield a new treatment for retinal degeneration, the mice injected with glutamate curiously also exhibited destruction of the inner retina (Lucas and Newhouse 1957). Subsequent work confirmed that glutamate was toxic to inner retinal neurons, and the phenomenon of glutamate-related death was termed excitotoxicity (Olney 1969a, 1969b).

Excitotoxicity is not unique to the retina, and this process has been implicated in a number of pathological conditions of the CNS. For example, there is strong evidence that glutamate contributes to the acute neuronal death that occurs during hypoxia/ischemia (such as stroke or carbon monoxide poisoning) and mechanical trauma (Lipton and Rosenberg 1994). Under normal conditions, extracellular glutamate levels are kept low and prevented from reaching toxic levels through the action of high affinity glutamate transporters (Danbolt 2001). Of the five cloned excitatory amino acid transporters (EAATs), four have been identified in the retina. EAAT2 (also known at GLT-1) has been identified on cone photoreceptors and some bipolar cells; EAAT3 (also termed EAAC1) is associated with certain horizontal, amacrine and ganglion cells;

EAAT5 has been found on some mammalian photoreceptors and bipolar cells; but the majority of retinal glutamate uptake appears to be mediated by EAAT1 (also called GLAST) present on Müller glial cells (for review of glutamate transporters in the retina, see Pow 2001). Throughout the CNS, glial cells play a chief role in clearing extracellular glutamate. This amino acid can then be detoxified within glia by means of its conversion to glutamine and released back to neurons for glutamate recycling (Westergaard *et al.* 1995). With the constant discharge of glutamate that occurs throughout the CNS, the pharmacological inhibition of glutamate transporters leads to an abrupt rise in extracellular glutamate levels within seconds (Jabaudon *et al.* 1999). Excitatory amino acid transporters are energy-dependent and the experimental simulation of hypoxic conditions disrupts glutamate uptake (Jabaudon *et al.* 2000; Rossi *et al.* 2000), thus providing a mechanism for the altered glutamate homeostasis that occurs during acute ischemia. Glutamate-related death has also been associated with more chronic neurodegenerative disorders such as amyotrophic lateral sclerosis, Alzheimer's, Parkinson's and Huntington's diseases, although the exact role of excitotoxicity in these conditions has not been conclusively validated (Lipton and Rosenberg 1994). The means by which extracellular levels of glutamate rise in these chronic diseases is controversial, but altered glutamate clearance has been hypothesized as an underlying cause (Rothstein *et al.* 1994; Danbolt 2001; Rao and Weiss 2004) and there has been interest in searching for therapeutic compounds that stimulate increased glutamate uptake (Fontana *et al.* 2003; Rothstein *et al.* 2005).

The excitotoxic cascade is highly Ca^{2+}-dependent, as *in vitro* studies have shown that it is possible to block glutamate-induced neuronal death by removing Ca^{2+} from the extracellular medium (Choi 1985, 1987). Excessive levels of Ca^{2+} are thought to trigger neuronal death even though this cation is necessary for the regulation of a broad range

of essential cellular processes. To explain how neurotoxic actions of Ca^{2+} are differentiated from physiological Ca^{2+} signaling, two main hypotheses have emerged (Sattler and Tymianski 2000; Hardingham and Bading 2003). In the 'calcium load' hypothesis, cell death is directly related to the magnitude of the rise in $[Ca^{2+}]_i$. Evidence in support of this theory comes from data showing that the occurrence of glutamate-induced death was linearly correlated to the amount of neuronal Ca^{2+} accumulation (Hartley *et al.* 1993; Eimerl and Schramm 1994; Lu *et al.* 1996). The alternative 'source specificity' hypothesis instead proposes that it is not the overall increase in $[Ca^{2+}]_i$, but rather the route of Ca^{2+} entry that is the critical determinant for the initiation of the death pathway. This principle is based on data indicating that Ca^{2+} influx through NMDA receptors is more toxic than similar amounts of Ca^{2+} entering neurons through VGCCs (Tymianski *et al.* 1993; Sattler *et al.* 1998). As a mechanistic explanation for this finding, further research has suggested that NMDA receptors are physically linked to neuronal nitric oxide synthase (nNOS) (Sattler *et al.* 1999; Aarts *et al.* 2002), and therefore Ca^{2+} influx through NMDA receptors may stimulate higher production of the excitotoxic mediator nitric oxide.

Irrespective of whether or not Ca^{2+} toxicity is source specific, a key distinction between physiological and pathological Ca^{2+} signaling is time (Berridge *et al.* 1998). In contrast to the transient changes in $[Ca^{2+}]_i$ that are necessary to activate physiological processes, cell death generally requires extended elevations in $[Ca^{2+}]_i$. In support of this premise, neurons are continuously exposed to brief millisecond pulses of glutamate (Auger and Attwell 2000) during synaptic neurotransmission without deleterious effect. However, it is with prolonged and constant receptor stimulation (that can occur due to dysfunction of glutamate clearance mechanisms, for example) that glutamate switches from neurotransmitter to toxin. The calcium dynamics for various central neurons

subjected to prolonged glutamate exposures has been characterized (Manev *et al.* 1989; DeCoster *et al.* 1992; Randall and Thayer 1992; Tymianski *et al.* 1993; Rajdev and Reynolds 1994). After the initial rise in $[Ca^{2+}]_i$, a stable level of $[Ca^{2+}]_i$ is maintained until there is a secondary irreversible rise in $[Ca^{2+}]_i$ (termed delayed calcium deregulation) in the neurons that undergo excitotoxic death. The relationship of $[Ca^{2+}]_i$ to cell death has not yet been characterized for RGCs and is investigated in Chapter 4.

The protracted rise in $[Ca^{2+}]_i$ is capable of activating enzymes such as nNOS, calpains, protein kinases, calcineurins, and endonucleases that can induce production of toxic free radicals, lethally alter the cytoskeleton, or activate genetically programmed death pathways (Sattler and Tymianski 2000; Orrenius *et al.* 2003). The nitric oxide generated from nNOS is thought to be an important effector of the excitotoxic pathway, as nitric oxide reacts with superoxide to form the noxious free radical peroxynitrate (Dawson *et al.* 1991; Dawson *et al.* 1993; Lipton *et al.* 1993). As previously mentioned, nNOS has been shown to be physically attached (by the scaffolding protein PSD-95) to NMDA receptors in cortical neurons (Sattler *et al.* 1999), and blocking the interaction between these receptors and nNOS protects against both glutamate-induced death to cortical neurons *in vitro* and ischemic damage to the cortex *in vivo* (Aarts *et al.* 2002). There is evidence for the involvement of nitric oxide in glutamate excitotoxic damage to RGCs (for review, see Sucher *et al.* 1997), and mice deficient in nNOS are more resistant to the RGC death caused by intravitreal NMDA injections or retinal arterial occlusion (Vorwerk *et al.* 1997). In addition to cytoplasmic nNOS, mitochondria also appear to be a significant target of pathological glutamatergic signaling. In conditions of elevated $[Ca^{2+}]_i$, the resulting overload of Ca^{2+} into mitochondria can lead to dysfunction of this organelle (Nicholls and Budd 2000). The presence of nitric oxide in the cytoplasm can exacerbate mitochondrial Ca^{2+} uptake (Keelan *et al.* 1999), and the resulting

mitochondria depolarization can induce the generation of more damaging free radicals (Lacza *et al.* 2001; Khodorov 2004).

While the downstream mechanisms of the excitotoxic cascade after the elevation in $[Ca^{2+}]_i$ have not been fully clarified and may involve multiple pathways, the end result is neuronal death. Neurons undergoing glutamate-related death exhibit features consistent with either apoptosis or necrosis (Ankarcrona *et al.* 1995; Bonfoco *et al.* 1995; Leist and Nicotera 1998; Yuan *et al.* 2003). Apoptosis is a form of cell death wherein the cell actively orchestrates its own death through a series of preprogrammed genetic signals and was originally distinguished from necrosis based on morphological criteria. In apoptosis, DNA is disassembled into fragments and the cell nucleus and cytoplasm breaks up into several membrane-wrapped packets, while in necrosis, there is cell swelling and lysis of the plasma membrane (Kerr *et al.* 1972). The resulting spillage of cellular contents into the extracellular milieu that occurs with necrosis can induce an inflammatory response, whereas apoptotic cell bodies are generally quietly cleared away without adverse effect to neighboring cells (Walker *et al.* 1988). Phosphatidylserine is normally present on the inner plasma membrane, and this phospholipid becomes translocated to the outer membrane during apoptosis as a signal to phagocytes that then remove these cell fragments (Orrenius *et al.* 2003). The presence of phosphatidylserine on the cell surface can be detected by staining cells with annexin V, and this technique serves as a marker for the identification of cells in the early stages of apoptosis (Koopman *et al.* 1994). In addition to changes in the plasma membrane, apoptosis involves a complex series of biochemical events that can include activation of the tumor suppressor protein p53, overexpression of Bax protein, release of cytochrome c from the mitochondria, activation of the family of proteases known as caspases, and stimulation of c-Jun N-terminal stress pathways (Adams and Cory 1998; Green and Reed 1998;

Leist and Nicotera 1998; Thornberry and Lazebnik 1998; Linden *et al.* 1999; Spierings *et al.* 2005). There does not appear to be a single universal pathway for apoptosis (see Rubin *et al.* 1994; Yuan *et al.* 2003; Kroemer and Martin 2005), however, and a complete discussion of this complex machinery is beyond the scope of these introductory comments. Although necrosis has generally been considered a more passive and less-ordered mode of death than apoptosis, it is beginning to emerge that there are also evolutionary conserved mechanisms underlying necrosis (Syntichaki and Tavernarakis 2003). Rather than being two completely independent pathways, necrosis and apoptosis likely represent two extremes on the continuum of cell death (Leist and Nicotera 1998; Syntichaki and Tavernarakis 2003). In accord, the type of death (necrosis versus apoptosis) exhibited by neurons challenged with glutamate appears to depend on the intensity of the insult, the resulting functional capacity of mitochondria, and the extent of free radical production (Ankarcrona *et al.* 1995; Bonfoco *et al.* 1995).

Multiple biochemical pathways are also likely to be involved in glutamate-related death of RGCs (Li *et al.* 2002). Therefore, the determination of signals most 'upstream' in the excitotoxic cascade, such as the mechanisms underlying glutamate-induced calcium influx, may present a more attractive target for therapeutic intervention in diseases associated with excitotoxicity. The potential involvement of glutamate excitotoxicity in retinal diseases has generated considerable attention. In animal models of acute ischemia, induced by transient occlusion of the central retinal artery (followed by reperfusion), the resulting damage to RGCs can be attenuated by pre-treating the animals with intravitreal injections of glutamate antagonists and/or NOS inhibitors (Geyer *et al.* 1995; Weber *et al.* 1995; Adachi *et al.* 1998; Kapin *et al.* 1999; Lagreze *et al.* 1999; Osborne 1999; Ju *et al.* 2000; Neufeld *et al.* 2002; Nucci *et al.* 2005). This model of ischemia/reperfusion likely best mimics the type of retinal damage that occurs in humans

with central and branch retinal artery and vein occlusions (Goldblum and Mittag 2002). In addition to acute ischemic conditions, glutamate excitotoxicity has been proposed as a potential contributor to the chronic RGC death that occurs in glaucoma.

Glaucomatous Neurodegeneration of Retinal Ganglion Cells

As RGCs are the final recipients of the visual signal in the retina, damage to these neurons disrupts the transmission of this information from the eye to the brain. Therefore, RGC dysfunction or death leads to significant and irreversible visual disturbances, including blindness. There are a number of retinal diseases and optic neuropathies (disorders affecting the optic nerve) that result in RGC death, with the most prevalent being glaucoma. Glaucoma is ranked as the second leading cause of blindness both in the world (behind cataracts) and in the United States (behind macular degeneration), based on statistics for the year 2002 (Resnikoff *et al.* 2004). In Canada, glaucoma represented the third most common diagnosis for new patients registering for services at the Canadian National Institute for the Blind in 2002 (CNIB 2003).

Glaucoma actually represents a collection of diseases, and in its broadest classification, this disorder can be separated into 'open-angle' and 'closed-angle' sub-types (Foster 2002; Weinreb and Khaw 2004). In closed-angle glaucoma, the iris of the eye blocks the flow of aqueous fluid from draining out through the trabecular meshwork (at the angle formed between the iris and the beginning of the cornea within the eye globe). Aqueous fluid is released from the processes of the ciliary body and circulates around the anterior chamber of the eye before passing through the trabecular meshwork and eventually into the venous system via the episcleral veins. Blockage of aqueous fluid flow causes the pressure inside the eye, termed intraocular pressure (IOP), to rise.

In primary open-angle glaucoma, the flow of fluid to the trabecular meshwork is not blocked by the iris or by another visible obstruction (such as blood vessels or pigment granules) but may be reduced. While elevated IOP is also often associated with primary open-angle glaucoma, the exact relationship of IOP to the progression of this disease has not been without debate (discussed in more detail below).

Regardless of sub-type, all forms of glaucoma culminate in the progressive degeneration of RGCs and their axons in the optic nerve (Quigley 1999), and RGCs appear to be the exclusive neurons affected in this disease. Evidence from cell-counting experiments on human post-mortem tissue and experimental animal models indicate that other retinal neurons (photoreceptors, bipolar cells, horizontal cells, amacrine cells) are not lost during the course of glaucoma (Kendell *et al.* 1995; Vickers *et al.* 1995; Wygnanski *et al.* 1995; Harwerth *et al.* 1999; Jakobs *et al.* 2005; Kielczewski *et al.* 2005). Clinically, both open- and closed-angle glaucoma are characterized by the presence of a distinct optic nerve head appearance and by a reduction in visual function measured as decreased sensitivity at various locations in the field of vision. The glaucomatous optic nerve head appears excavated or "cupped" due to changes in the architectural organization of this structure, and optic nerve head cupping is nearly pathognomonic for glaucoma. As a comparison, ischemic optic neuropathy (essentially a stroke of the optic nerve) also results in the death of RGCs, but this disorder is generally characterized by increased pallor of the optic nerve head without definitive changes in cupping (Burgoyne *et al.* 2005).

An elevation in IOP has long been associated with primary open-angle glaucoma, and all currently approved therapies for this disease involve medical or surgical procedures designed to lower IOP. Data from both prevalence (Sommer *et al.* 1991) and incidence (Armaly *et al.* 1980) studies indicate that patients with higher IOP

are more likely to develop primary open-angle glaucoma, thus supporting IOP as an important risk factor for this disease. However, during the 1980s, the causal relationship of IOP to glaucomatous optic nerve damage, and the value of treating open-angle glaucoma patients with IOP-lowering therapy, was questioned (Bengtsson 1981; Krakau 1981; Eddy *et al.* 1983; Eddy and Billings 1988). Randomized prospective clinical trials have become the gold standard study design in modern health care for scientifically validating the efficacy of a given treatment regime and, at that time, no such trial had been conducted to test the usefulness of lowering IOP in retarding glaucomatous progression. In addressing this issue, a number of large-scale randomized clinical trials were initiated such as the Advanced Glaucoma Intervention Study (AGIS), the Collaborative Normal-Tension Glaucoma Study (CNTGS), the Ocular Hypertension Treatment Study (OHTS), and the Early Manifest Glaucoma Trial (EMGT). Each study was designed to assess different primary questions, but as a whole, these studies demonstrated that lowering IOP can slow or prevent glaucomatous damage. In the AGIS, which evaluated different surgical management strategies for glaucoma after medical therapy had failed, it was noted that patients with IOP < 18 mmHg were least likely to exhibit glaucomatous progression (measured by visual field changes) while those with IOP > 22 mm Hg were most likely to progress (The AGIS Investigators 2000). The CNTGS assessed the role of IOP in patients exhibiting optic nerve damage and/or visual field loss yet having statistically normal IOP (median IOP < 20 mm Hg), and found that IOP-lowering treatment still significantly slowed visual field progression in these 'normal-tension' glaucoma patients (CNTGS Group 1998). The OHTS showed that lowering IOP in patients with ocular hypertension (elevated IOP without definitive evidence for optic nerve damage or visual field loss) delayed the onset of glaucoma as compared to untreated controls (Gordon *et al.* 2002; Kass *et al.* 2002). Finally, the

EMGT examined the effectiveness of lowering IOP in glaucoma patients presenting with an early visual field defect, and found that progression of field loss was significantly less frequent in treated patients versus untreated controls (Heijl *et al.* 2002). In a follow-up study for the EMGT, further data analysis suggested that there was a 10% reduction in the risk of progression for each 1 mm Hg decrease in IOP that was achieved with therapy (Leske *et al.* 2003).

The results of these recent clinical trials have re-affirmed the importance of IOP in primary open-angle glaucoma. However, many of the untreated patients in the CNTGS, OHTS, and EMGT did not exhibit glaucomatous progression (65%, 90.5%, and 38%, respectively, using indicators for progression specific to each study) over the approximate 5-year period that the patients were followed. Furthermore, while the lowering of IOP reduced the risk of glaucoma onset or progression, the treatment paradigms used in these studies did not eliminate disease advancement in every patient (progression was deemed to have occurred in 12%, 4.4%, and 45% of treated patients in the CNGTS, OHTS, and EMGT, respectively). To improve on these statistics through the identification of better detection and novel treatment strategies, experimental laboratory studies have been directed towards understanding how and why RGCs die in glaucoma and the relationship of IOP to optic nerve damage. With a current inability to non-invasively evaluate RGC function and viability in humans, animal models represent a valuable tool for studying the pathogenesis of glaucoma.

If elevated IOP is a potential cause for glaucomatous optic nerve damage (rather than an effect), it follows that the experimental induction of increased IOP in animals should produce a similar pathology. Indeed, as first shown in monkeys, raising IOP through the obstruction of aqueous fluid outflow (by application of argon laser to the trabecular meshwork, or by injection of fixed red blood cells into the anterior chamber)

results in RGC axonal loss and optic nerve head cupping resembling that seen in human glaucoma patients (Gaasterland and Kupfer 1974; Quigley and Addicks 1980). With the considerable expense and animal handling complexities involved in primate research, the rat has emerged as a popular and cost-effective experimental animal for glaucoma models. A variety of techniques have been utilized to reduce aqueous outflow in rats, leading to sustained increases in IOP (Shareef *et al.* 1995; Morrison *et al.* 1997; Ueda *et al.* 1998; WoldeMussie *et al.* 2001; Levkovitch-Verbin *et al.* 2002b). In addition to RGC loss and optic nerve damage, rats with experimentally elevated IOP develop greater optic disk cupping (Sawada and Neufeld 1999; Chauhan *et al.* 2002), a key feature of human glaucoma.

While the information gained from human clinical trials and animal laboratory studies support a link between elevated IOP and optic nerve damage, the exact pathophysiology of primary open-angle glaucoma is not firmly established and has been debated for over one hundred years. Many of the theories regarding the mechanism of damage are traditionally divided into two groups: one mechanical-based and the other centered on vascular factors (Fechtner and Weinreb 1994). There is considerable support from postmortem analyses on tissue obtained from human glaucoma patients, and from animal models of IOP elevation, in favor of the mechanical hypothesis that IOP damages RGC axons by causing structural changes to the optic nerve head. Histological and experimental evidence indicate that glaucomatous optic nerve head cupping involves deformation of the lamina cribrosa, as the sheets of this connective tissue become compressed together and bow outward from the eye globe (Quigley *et al.* 1981; Quigley *et al.* 1983; Bellezza *et al.* 2003; Burgoyne *et al.* 2005; Morrison *et al.* 2005). In human eyes with glaucoma (Quigley *et al.* 1981) and in monkey eyes following high IOP exposure (Anderson and Hendrickson 1974), swelling of RGC axons was

noted in the optic nerve head at the level of the lamina cribrosa, suggesting that the distortion of the lamina may impact RGC axonal transport. Although the rat lamina cribrosa is much more rudimentary than that in primates, the experimental elevation of IOP in rats results in similar RGC axonal changes at their exit site from the eye (Morrison *et al.* 1997). Blockade of axoplasmic flow could interrupt the transport of vital messengers such as neurotrophins, which are released from the brain (or possibly from glia in the optic nerve) and are involved in the development and maintenance of RGCs. If retrogradely transported neurotrophins are prevented from reaching RGC somata (for example, by optic nerve axotomy), the programmed sequence of apoptotic cell death is activated (Berkelaar *et al.* 1994; Garcia-Valenzuela *et al.* 1994). During embryological development, the retrograde transport of molecules such as neurotrophins ensures proper targeting of RGC axons to appropriate brain centers. Roughly 50% of RGCs in the developing retina do not reach their target, and these RGCs are eliminated through apoptosis (Linden *et al.* 1999). The presence of apoptotic RGCs has been detected in human glaucoma (Kerrigan *et al.* 1997) and in monkey (Quigley *et al.* 1995) and rat (Garcia-Valenzuela *et al.* 1995) glaucoma models, indicating that at least some RGCs die by programmed cell death in glaucoma (see Nickells 1996). In support of the neurotrophin deprivation hypothesis, Pease and colleagues (2000) showed that transport of the neurotrophin brain-derived neurotrophic factor (BDNF) to RGC somata was blocked in rats with chronically elevated IOP.

On the other hand, the vascular theory contends that decreased blood perfusion to the anterior optic nerve head is a key cause of glaucomatous optic nerve damage. There is evidence for reduced ocular blood flow in glaucoma patients, and this mechanism has been invoked to explain why some patients develop glaucoma despite having statistically normal IOP (Fechtner and Weinreb 1994; Flammer *et al.* 2002).

However, it has been argued that 'normal-tension' glaucoma should not be treated as a separate disease (Quigley 2005), supported by the finding of the CNTGS that lowering IOP in glaucoma patients with statistically normal IOP is still beneficial (CNTGS Group 1998). In addition, the signature optic disk cupping changes in glaucoma have not been conclusively demonstrated in any pressure-independent optic neuropathy model. For example, the localized application of the vasoconstrictor endothelin-1 to the rat optic nerve head by osmotic pump results in RGC axonal damage and increased pallor of the optic nerve head, but no detectable change in cupping (Chauhan *et al.* 2004). Similar results (optic nerve head pallor without cupping) have been documented for optic nerve axotomy, suggesting that cupping is in fact the result of biomechanical stress at the nerve head rather than an effect simply related to loss of RGC axons (Burgoyne *et al.* 2005). Nevertheless, glaucoma may be a multifactorial disease with both vascular and mechanical components. IOP-induced changes to the lamina cribrosa could collapse the microvasculature at the optic nerve head, resulting in ischemic axonal death or inhibition of energy-dependent axonal transport and subsequent neurotrophin deprivation (Fechtner and Weinreb 1994).

In the search for alternative glaucoma treatments to complement existing IOP-lowering strategies, there is interest in new therapeutic approaches that prevent or slow down RGC degeneration *after* the original insult (i.e. elevated IOP, mechanical stress, ischemia) has occurred. The concept of delayed RGC degeneration, perhaps due to the release of death-inducing cellular factors, meshes well with the commonly held clinical view that some glaucoma patients will continue to progress despite effective IOP-lowering therapy and that this progression is related to the severity of the disease prior to treatment (Grant and Burke 1982; Brubaker 1996). Evidence for delayed, or secondary, degeneration has been observed in a rat model of RGC death involving

partial transection of the optic nerve (Levkovitch-Verbin *et al.* 2003; Blair *et al.* 2005). Lesioning the superior optic nerve resulted in the expected damage, after one week, to RGCs in the superior retina whose axons passed through the lesion site. However, at later timepoints, diffuse damage was also observed in the unlesioned inferior optic nerve (along with RGC loss in the inferior retina) indicating that a more gradual degeneration followed the initial wave of RGC loss (Levkovitch-Verbin *et al.* 2003; Blair *et al.* 2005).

Neuroprotection is a therapeutic paradigm aimed at retarding neuronal death, particularly that mediated by secondary degeneration, in order to keep neurons alive and functional (for reviews of neuroprotection as it applies to glaucoma, see Yoles and Schwartz 1998; Weinreb and Levin 1999; Hartwick 2001; Kuehn *et al.* 2005). Glutamate excitotoxicity has been proposed as a potential contributor to glaucomatous RGC death that could be targeted by neuroprotective agents (for reviews, see Dreyer 1998; Osborne *et al.* 2001; Lipton 2003). Interest in the potential relationship between glutamate and glaucoma increased following the work of Dreyer and colleagues (1996). These researchers examined amino acid concentrations in the vitreous humor collected from patients undergoing cataract surgery and found that glutamate levels in the vitreous of glaucoma patients (~23 μM) was more than double that from a control group (~10 μM) without glaucoma. Furthermore, in monkeys with experimental glaucoma (surgically elevated IOP), the vitreous glutamate concentration was 5 to 6 times higher than that in the fellow control eyes, suggesting that elevated IOP can produce altered extracellular glutamate levels (Dreyer *et al.* 1996). While these findings are controversial (see Chapter 3 for more details), the concept that RGCs are chronically exposed to dangerous concentrations of glutamate implies that the normally proficient glutamate clearance system is dysfunctional (Figure 1-3). In support of this assertion, Martin and colleagues (2002) found reduced glutamate transporter protein levels in rats with

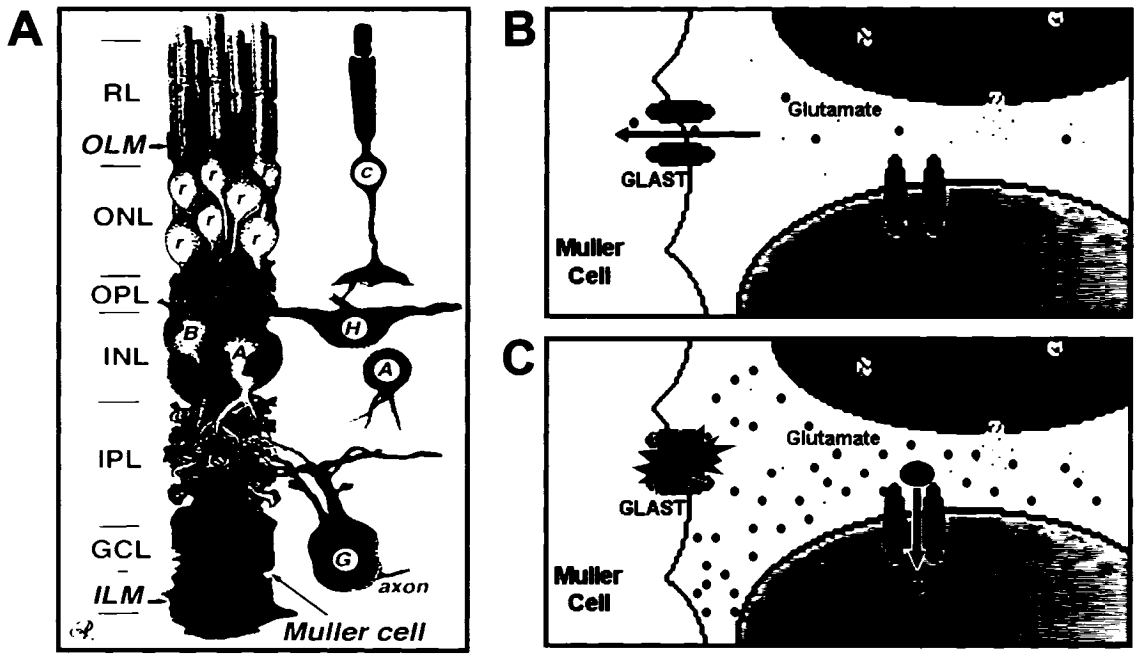

Figure 1- 3. Extracellular glutamate levels in the retina are regulated by excitatory amino acid transporters (EAATs). **(A)** Schematic drawing (figure from Reichenbach *et al.* 1993) illustrating that Müller cells (in pink) completely ensheath RGC (denoted by 'G') somata and their dendrites in the inner plexiform layer. **(B)** Caricature of synapse between a bipolar cell and RGC under normal conditions. Glutamate released from the bipolar cell is rapidly removed from the synaptic cleft by EAATs such as the glutamate aspartate transporter (GLAST) present on adjacent Müller cell processes (Rauen et al. 1998; Pow and Barnett 1999; Rauen 2000). **(C)** For glutamate levels to rise and remain chronically elevated, this highly efficient glutamate clearance mechanism must be compromised. The accumulation of extracellular glutamate could then induce excitotoxic RGC death due to excessive and prolonged glutamate receptor-mediated calcium influx.

experimental glaucoma. However, the reduced protein expression may have been a consequence of RGC loss, rather than a causative factor. To address this issue, I assess the functional capacity of retinal glutamate uptake in a chronic rat glaucoma model in Chapter 3.

Neuromodulatory Actions of the Purine Adenosine

Purine-derived molecules are ubiquitous in living organisms and serve an important role in a diverse array of vital biological processes (Dunwiddie and Masino 2001), such as genetic transmission (the purine base adenine is a component of DNA), cellular metabolism (the nucleotide ATP, comprised of adenine attached to a pentose-triphosphate group, is used as the primary energy source in aerobic cells), and intracellular signaling (cyclic AMP is a key messenger in multiple signal transduction pathways). In addition, the purines adenosine and ATP have emerged as important extracellular signaling compounds in the CNS. While ATP is synaptically released as a neurotransmitter, there is little evidence that adenosine is released from synaptic vesicles in a classical calcium-dependent fashion (Brundege and Dunwiddie 1997). Adenosine is therefore generally considered to be a neuromodulator rather than a true neurotransmitter.

Intracellular concentrations of adenosine are kept low under basal conditions due to its rapid phosphorylation to nucleotides (AMP, ADP, ATP) by adenosine kinase, and its degradation to inosine by adenosine deaminase. Adenosine can be formed intracellularly by the cleavage of S-adenosylhomocysteine (homocysteine is also produced in this reaction), and through degradation of AMP by cytosolic 5'-nucleotidases. During periods of metabolic stress, there is increased catabolism of ATP

and a concurrent elevation in intracellular adenosine levels. Adenosine can then diffuse across the plasma membrane along the concentration gradient through facilitated diffusion nucleoside transporters. The second major source of extracellular adenosine occurs from the degradation of synaptically released ATP by ecto-5'-nucleotidases (these enzymes are present in the extracellular space) and this is likely the primary mechanism under normoxic conditions (for further details on the intracellular and extracellular metabolism of adenosine, see Brundege and Dunwiddie 1997; Dunwiddie and Masino 2001; Latini and Pedata 2001). The breakdown of extracellular ATP to adenosine can occur extremely rapidly, with conversion happening in less than one second (Dunwiddie *et al.* 1997; Cunha *et al.* 1998).

Once present in the extracellular space, adenosine mediates its neuronal effects through membrane-bound receptors. There are four known adenosine receptors, A_1, A_{2A}, A_{2B}, and A_3, all of which are coupled to G-proteins (Fredholm *et al.* 2001). A_1 receptors are coupled to G_i proteins and inhibit adenyl cyclase (causing a decrease in cAMP), while the A_2 receptors are coupled to G_s proteins that stimulate adenyl cyclase (increase in cAMP). The A_3 receptor is more poorly characterized but it appears to be coupled to G_q or G_{i3} proteins and linked to the activation of phospholipase C or the inhibition of adenyl cyclase. The A_1 receptor is the most abundant adenosine receptor type in the CNS and its stimulation is associated with the inhibition of voltage-gated Ca^{2+} channels (Mogul *et al.* 1993; Yawo and Chuhma 1993), leading to reduced synaptic transmission, and activation of potassium channels (Trussell and Jackson 1985; Thompson *et al.* 1992), resulting in neuron hyperpolarization. The A_2 receptors, on the other hand, can stimulate neurotransmitter release (Brown *et al.* 1990) and enhance voltage-gated Ca^{2+} channel currents (Mogul *et al.* 1993; Umemiya and Berger 1994). Inhibitory properties of A_2 receptors have also been observed, and these effects could

be due to A_{2A} receptor-mediated inhibition of Ca^{2+} channels in some cell types (Latini *et al.* 1996; Edwards and Robertson 1999). The role of A_3 receptors is not well understood, but it may serve to modulate other metabotropic receptors (Macek *et al.* 1998).

Adenosine receptors are expressed throughout the brain and adenosine is likely involved in the regulation of sleep and arousal and the autoregulation of blood flow (Dunwiddie and Masino 2001). Caffeine is an adenosine receptor antagonist, and its stimulatory properties are thought to be a consequence of its action in blocking the effects of endogenous adenosine (Fredholm *et al.* 1999). In addition to these physiological roles, there is increasing evidence that adenosine acts as a neuroprotective compound in pathological conditions such as hypoxia/ischemia and epilepsy. As previously mentioned, under conditions of metabolic stress or increased neuronal activity there is a buildup of intracellular adenosine as the energy requirements of the neurons exceeds ATP re-synthesis (Latini and Pedata 2001). With more adenosine diffusing extracellularly under these conditions, the resulting stimulation of neuronal A_1 receptors leads to calcium channel inhibition, reduced neurotransmitter release, and neuron hyperpolarization. These inhibitory effects counter some of the excitatory actions of glutamate (which also increases extracellularly during ischemic conditions), and explains adenosine's demonstrated neuroprotective properties in experimental models of excitotoxicity (de Mendonca *et al.* 2000). Contrary to its effects at A_1 receptors, activation of the A_{2A} receptor by adenosine may have neurodestructive consequences that contribute to ischemic damage (Ongini *et al.* 1997; Chen *et al.* 1999; Popoli *et al.* 2004). However, A_{2A} receptors are also present on arterial walls and platelets and A_{2A} receptor-mediated vasodilation may protect against ischemia, although this remains controversial (Pedata *et al.* 2001; Stone 2002). A potential neuroprotective

role for A_3 receptors has also been suggested, but this is not yet conclusive (von Lubitz 1997; von Lubitz *et al.* 2001).

In the retina, it has been established that 'starburst'-type amacrine cells contain ATP and likely release this neurotransmitter along with acetylcholine (Perez *et al.* 1986; Neal and Cunningham 1994). More recently, it has been demonstrated that ATP can also be released from retinal Müller cells (Newman 2001, 2003, 2004). ATP can directly evoke Ca^{2+} influx in RGCs (Taschenberger *et al.* 1999; Zhang *et al.* 2005), but some of the released ATP likely is rapidly converted into adenosine by extracellular ecto-nucleotidases. Radioactive ligand binding studies suggest that A_1 receptors are present in the inner retina, particularly in the ganglion cell layer and the inner plexiform layer (for review of this data, see Blazynski and Perez 1991; Figure 1-4 is based on the data presented in this review). In agreement with this finding, an *in situ* hybridization study identified A_1 receptor mRNA primarily in the ganglion cell layer, while the A_{2A} receptor mRNA was most prominently found in the inner and outer nuclear layers (Kvanta *et al.* 1997). This same study did not detect message for A_{2B} and A_3 receptors in the retina. Although adenosine receptors appear to be present on RGCs, there is little known about the effect of adenosine on these retinal output neurons. In Chapter 2, I test the effect of adenosine on glutamate-induced calcium influx in RGCs. There is some physiological evidence supporting a role for adenosine signaling in the retina as A_1 receptor activation regulates retinal acetylcholine release in rabbit retinas (Blazynski *et al.* 1992), and inhibits the light-evoked activity recorded from optic nerve fibers in a cat eyecup preparation (Kaelin-Lang *et al.* 1999). Also, adenosine levels have been shown to rise during experimentally-induced retinal ischemia (for reviews, see Ghiardi *et al.* 1999; Roth 2004), and blockade of A_1 adenosine receptors increases ischemic retinal injury

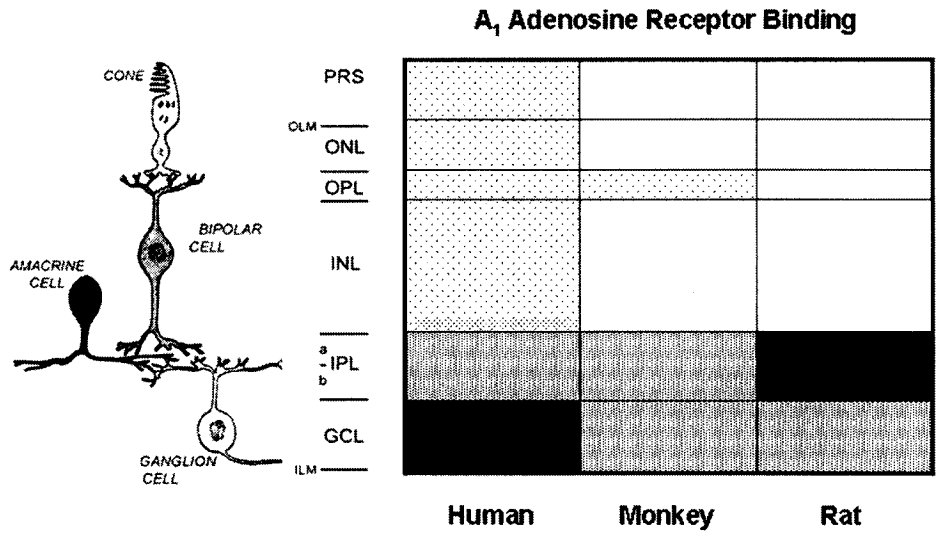

Figure 1- 4. Adenosine A_1 receptor localization in the mammalian retina. Data summary of multiple studies investigating the distribution of binding sites for A_1-selective radioligands in human, monkey, and rat retinas. The darkness of the shading represents the relative density of silver grains (corresponding to uptake of [^{3}H]CHA, a tagged A_1-receptor agonist) in retinas subjected to this autoradiographic localization technique. Note consistent pattern of dense labeling in ganglion cell layer (GC) and inner plexiform layer (IPL), providing anatomical evidence in support of A_1 receptor-mediated adenosine signaling in the inner retina. Based on a similar figure from Blazynski and Perez (1991).

(Li and Roth 1999). Therefore, adenosine may act as an endogenous neuroprotective agent in the retina, serving to limit the excitotoxic actions of glutamate on RGCs.

Goals of Thesis

The work in this thesis is centered on the mechanisms involved in the regulation and control of RGC intracellular calcium dynamics following their stimulation by the excitatory neurotransmitter glutamate. By monitoring the internal calcium concentrations of rat RGCs, using both purified cell cultures and intact retina preparations, I will investigate the underlying pathways involved in glutamate-induced calcium influx, the modification of this calcium signal by an endogenous neuromodulator, the efficiency of retinal glutamate clearance mechanisms that serve to limit glutamate receptor stimulation, and the relationship of glutamate-related fluctuations in RGC calcium levels to excitotoxic death.

In Chapter 2, I assess the effect of adenosine on glutamate-induced calcium influx and identify the adenosine receptor subtype involved. In Chapter 3, I develop a novel method to functionally assess glutamate uptake in the retina, and then I utilize this methodology to probe whether glutamate clearance is compromised in retinas from rat eyes that were chronically exposed *in vivo* to elevated IOP. In Chapter 4, I examine the mechanisms involved in glutamate-induced alterations of RGC calcium levels, and I characterize the calcium dynamics of RGCs undergoing excitotoxic death due to prolonged glutamate exposure. As a whole, it is my hope that these experiments will provide new insights in the distinguishing features that separate physiological and pathophysiological glutamatergic signaling pathways.

CHAPTER 2: Adenosine Modulation of Glutamate-Induced Calcium Influx in Rat Retinal Ganglion Cells

Preface and Significance to Thesis

The retina receives a large range of visual stimuli that are processed into appropriate electrochemical signals for relay to the brain. In order to respond to such a dynamic range of sensory input, neurotransmission within the retinal circuitry (including that mediated by the excitatory neurotransmitter glutamate) must be tightly regulated. The modification of the visual signal through the action of neuromodulators is one such regulatory mechanism. The purine adenosine is a CNS neuromodulator, and although adenosine receptors (both A_1 and A_{2A} types) have been identified in the mammalian retina, the role of adenosine in this tissue is not fully understood. In addition, there is growing evidence that adenosine protects CNS neurons against glutamate excitotoxicity during ischemia by inhibiting excitatory neurotransmission. As adenosine may act as an endogenous neuroprotective agent in the retina, a better understanding of how adenosine exerts its effects could have therapeutic relevance. In this chapter, I investigate the potential neuromodulatory actions of adenosine on glutamate-induced calcium influx in rat RGCs.

To achieve the goals of this thesis, I had to first choose and then optimize experimental protocols that allowed reliable monitoring of RGC calcium dynamics. Initially, I attempted to image retrogradely labeled RGCs in mixed retinal cultures, but I was mostly unsuccessful at eliciting repeatable glutamate responses from positively identified RGCs. In this chapter, I have included results from preliminary experiments

that were performed on unidentified retinal neurons from mixed cultures. I then generated purified RGC cultures using an immunopanning method developed by Dr. Ben Barres and his colleagues at Stanford University. I received a detailed protocol for the immunopanning technique via an email communication with Dr. Barres, and I would like to acknowledge this assistance. As demonstrated in this chapter, I confirmed that the immunopanning method generates nearly pure RGC cultures. These RGCs are capable of responding to consecutive bursts of glutamate exposure in a repeatable fashion, thus enabling the effect of potential neuromodulators, such as adenosine, to be assessed. The calcium imaging of isolated RGCs in purified cultures is a central technique that is utilized throughout this thesis.

Preliminary results of this work were presented at the Association for Research in Vision and Ophthalmology (ARVO) Annual Meeting in 2002 (Hartwick ATE, Baldridge WH. Adenosine modulates glutamate-induced calcium influx in retinal neurons. *Invest. Ophthalmol. & Vis. Sci.* 43: ARVO E-Abstract 4752). Portions of this work were then published in *Investigative Ophthalmology & Vision Science* in 2004 (Hartwick ATE, Lalonde MR, Barnes S, Baldridge WH. Adenosine A_1-receptor modulation of glutamate-induced calcium influx in rat retinal ganglion cells. 45: 3740-3748), and copyright permission for re-printing these results is located in Appendix B. The contribution of Melanie Lalonde (a PhD student at Dalhousie University at that time, supervised by Dr. Steven Barnes) to the published manuscript was to assess the effect of adenosine on voltage-gated calcium currents in rat RGCs that I isolated. I refer to these results in this chapter, but I have not included the data in my thesis. I collected all the data and performed all of the techniques presented in this chapter, with appropriate guidance of my supervisor Dr. William Baldridge.

Introduction

Adenosine is now recognized as an important neuromodulator in the central nervous system (Dunwiddie and Masino 2001). Under normal physiological conditions, the majority of extracellular adenosine is thought to be generated by the conversion of the neurotransmitter adenosine 5'-triphosphate (ATP) by ectonucleotidases (Latini and Pedata 2001). In the retina, the release of ATP from cholinergic amacrine (Neal and Cunningham 1994) and Müller (Newman 2001) cells represent potential sources of adenosine in the inner retina.

Four adenosine receptors have been cloned and characterized, all of which are coupled to G-proteins and are designated as A_1, A_{2A}, A_{2B}, and A_3 (Fredholm *et al.* 2001). Whereas A_3 and A_{2B} adenosine receptors have not yet been identified in the retina, A_1 and A_{2A} receptors (A_1-Rs and A_{2A}-Rs) have been found in the retinas of several vertebrates and appear to have distinct areas of distribution: A_1-Rs predominantly in the inner retina, and A_{2A}-Rs in the outer retina (Blazynski and Perez 1991). In the rat retina, autoradiographic receptor binding (Braas *et al.* 1987) and *in situ* hybridization (Kvanta *et al.* 1997) studies have provided evidence for the presence A_1-Rs in the inner plexiform (IPL) and ganglion cell (GCL) layers.

The presence of A_1-Rs in the IPL and GCL suggests that adenosine may influence retinal ganglion cells (RGCs). Throughout the CNS, A_1-R activation generally results in presynaptic inhibition through modulation of potassium and calcium currents (Dunwiddie and Masino 2001; Fredholm *et al.* 2001). Recently, adenosine has been shown to decrease voltage-gated calcium channel (VGCC) currents in goldfish (Zhang and Schmidt 1998, 1999) and salamander (Sun *et al.* 2002b) RGCs through A_1-R activation, but it is not yet known whether adenosine also modulates calcium currents in mammalian RGCs. The modulation of RGC calcium channels by adenosine may be

relevant to presynaptic inhibition of glutamate release from RGC terminals in the brain, (Zhang and Schmidt 1998, 1999; Hallworth *et al.* 2002). However, RGCs are entirely postsynaptic in the retina, and so the presence of A_1-Rs in the GCL suggests that adenosine may postsynaptically modulate RGC activity. As glutamate is the predominant excitatory neurotransmitter released from bipolar cells onto RGC dendrites (Thoreson and Witkovsky 1999), A_1-R activation could affect the glutamatergic stimulation of RGCs. To evaluate this hypothesis, I assessed the effect of adenosine on glutamate receptor-mediated calcium influx in rat RGCs, using both purified cultures and living retinal wholemount preparations.

Methods

Materials

The Neurobasal-A culture medium, B27 supplements, Dulbecco's phosphate-buffered saline (DPBS), Earle's buffered salt solution (EBSS), Dulbecco's modified Eagle's medium (DMEM), glutamine and trypsin were obtained from Invitrogen-Gibco (Burlington, ON). The papain and DNase were from Worthington Biochemicals (Lakewood, NJ). Rhodamine B dextran, fura dextran, fura-2 acetoxymethyl (AM) ester and pluronic acid F-127 were purchased from Molecular Probes (Eugene, OR). Regeneron (Tarrytown, NY) generously provided the neurotrophic factors brain-derived neurotrophic factor (BDNF) and ciliary neurotrophic factor (CNTF; Axokine protein). The Hibernate-A medium was from BrainBits, (Springfield, IL). Unless noted otherwise, all other chemicals and reagents were obtained from Sigma-Aldrich (Oakville, ON). The suppliers of the above materials were consistent for the entire thesis, and vendor locations for chemicals noted in this chapter are not reiterated in subsequent chapters.

Stock solutions of L-glutamate, glycine, N-methyl-D-aspartate (NMDA), and adenosine were prepared before each experiment and were dissolved in the experimental Hanks' balanced salt solution (HBSS). N^6-cyclohexyladenosine (CHA) and 5'-(N-cyclopropyl)carboxamidoadenosine (CPCA) were first dissolved as a stock solution (10 mM) in 0.1 N HCl. 8-Cyclopentyl-1,3-dipropylxanthine (DPCPX) was first dissolved in dimethyl sulfoxide (DMSO), and 3,7-dimethyl-1-propargylxanthine (DMPX) was first dissolved in purified water (10 mM stock for both). Aliquots of CHA, CPCA, DPCPX and DMPX stock solutions were stored at -30 °C before use.

Retina Dissection and Dissociation

All procedures in this thesis were performed in accordance with the ARVO Statement for the Use of Animals in Ophthalmic and Vision Research and the Dalhousie University Committee for the Use of Laboratory Animals. Natural litters (1-10 pups for each experiment) of Long-Evans rats (Charles River, Montreal, QC) were killed at age 7 to 8 days postnatal by over-exposure to halothane and decapitation. After the eyes were enucleated, the anterior segment and lens were removed, and the posterior eyecups were immersed in dissection medium consisting of Hibernate-A medium (see Brewer 1997) with 2% B27 supplements and 10 μg/ml gentamicin. The retinas were dissected and maintained in the dissection medium until all retinas were isolated.

The retinas were dissociated enzymatically and mechanically to make a single-cell suspension (see Huettner and Baughman 1986). The tissue was first incubated for 30 min at 37°C in a papain solution (165 U in 10 ml) in Ca^{2+}/Mg^{2+}-free DPBS containing 1mM L-cysteine and 0.004% DNase. The papain-treated retinas were then triturated sequentially in DPBS (with Ca^{2+} and Mg^{2+}) containing 1.5 mg/ml ovomucoid (Roche Diagnostics, Laval, QC), 1.5 mg/ml bovine serum albumin (BSA), and 0.004% DNase.

In addition, this solution contained the rabbit anti-rat macrophage antibodies (1:75; Axell brand, Accurate Chemical, Westbury, NY) required for the macrophage panning step (see next section). After 10 min incubation at room temperature to allow antibody binding, the suspension was centrifuged at 200x g for 11 min at 25°C and rewashed in a high concentration ovomucoid/BSA solution (10 mg/ml each in DPBS). Following another centrifugation and removal of the supernatant, the dissociated cells were resuspended in DPBS containing 0.2 mg/ml BSA and 5 μg/ml insulin. To reduce cell clumping, the suspension was filtered through a nylon mesh (20 μm Nitex mesh; Tetko Inc., Elmsford, NY) prior to incubation on the first panning plate.

Immunopanned RGC Cultures

Purified RGC cultures were generated using a two-step immunopanning (antibody-mediated plate adhesion) procedure, essentially as described previously (Barres *et al.* 1988; Meyer-Franke *et al.* 1995). In this technique, a Petri dish coated with anti-Thy1.1 antibodies is used to extract RGCs from a mixed retinal cell suspension. To obtain purified RGC cultures, an initial panning step is necessary to remove macrophages, which also express the Thy1 antigen, from the suspension.

The mixed retinal cell suspension was first incubated for 20 min on a Petri dish that had been pre-coated overnight with affinity-purified goat anti-rabbit IgG (H+L) antibodies (Jackson ImmunoResearch, West Grove, PA), followed by an additional 30 min on a second identical panning plate to remove macrophages (now bound to the rabbit anti-rat macrophage antibodies that were added to the enzyme inhibitor solution) from the suspension. The remaining cells were filtered again through the Nitex mesh and then transferred to a Petri dish that had first been precoated overnight with affinity-purified goat anti-mouse IgM (μ chain) antibodies (Jackson ImmunoResearch) and

second with anti-Thy1.1 monoclonal IgM antibodies (generated in-house; see next section). After 30 min, the dish was repeatedly rinsed (8 to 12 times) with DPBS to remove any non-adherent cells. The remaining adherent cells (RGCs) were incubated in Ca^{2+}/Mg^{2+}-free EBSS containing 0.125% trypsin solution for 8 min at 37°C in a 5% CO_2-air atmosphere. Finally, the cells were released from the plate by gently pipetting an enzyme inhibitor solution (30% fetal bovine serum in Neurobasal-A) along the surface of the dish while observing the progress with an inverted microscope. The resulting cell suspension was removed from the plate, centrifuged at 200x g for 11 min at 25°C, and resuspended in culture medium for plating.

The RGCs were plated onto poly-D-lysine/laminin-coated glass coverslips (12 mm round; Biocoat; BD Biosciences, Bedford, MA) in 4-well Nunclon Delta plastic multidishes (1.9 cm^2/well; Nalge Nunc International, Rochester, NY) at a density of 1.5 x 10^4 cells per well. The cells were cultured in 600 μl of serum-free culture medium consisting of Neurobasal-A with 2% B27 supplements, 1 mM glutamine, 50 ng/ml BDNF, 10 ng/ml CNTF, 5 μM forskolin, and 10 μg/ml gentamicin (Brewer *et al.* 1993; Meyer-Franke *et al.* 1995). Cultures were maintained at 37°C in a humidified 5% CO_2-air atmosphere. All experiments on the isolated RGCs were performed on the two days following the day of cell dissociation and panning.

Thy1.1 Antibody Generation and Panning Plate Preparation

Monoclonal IgM antibodies against mouse Thy1.1 were generated with the mouse hybridoma cell line T11D7e2 (#TIB-103, American Type Culture Collection, Manassas VA). The hybidoma cells were cultured at 37°C in a 5% CO_2-air atmosphere in 75 cm^2 tissue culture flasks in DMEM culture medium with glutamine (4 mM), glucose (4.5 g/l), sodium bicarbonate (1.5 g/l) and fetal bovine serum (10%). The cultures were

maintained at a 10^5 to 10^6 cells/ml concentration, and the supernatant was collected every two days and exchanged with fresh culture medium. This supernatant contained the anti-Thy1.1 antibodies and was kept frozen at -80°C prior to its experimental use.

For the panning plates, one 100 mm and two 150 mm Petri dishes (Fisher Scientific, Nepean, ON) were incubated overnight at 4°C with a Tris buffer solution (50 mM, pH 9.5) containing the secondary antibodies (all from Jackson ImmunoResearch): 120 μg of affinity-purified goat anti-rabbit IgG (H+L-specific) in each 150 mm dish and 100 μg of affinity-purified goat anti-mouse IgM (μ chain specific) in the 100 mm dish.

On the following day, the Tris buffer solution was discarded and the three panning plates were rinsed with DPBS. Approximately 8 ml of thawed supernatant containing the anti-Thy1.1 monoclonal antibodies was added to the 100 mm plate. DPBS with 2 mg/ml BSA was added to the 150 mm plates. All three panning plates were then incubated for 2-4 hours at room temperature prior to use.

Mixed Retinal Cell Cultures

For the mixed retinal cell cultures, retinas were dissected from 7-8 day old Long-Evans rats and enzymatically dissociated into single cell suspensions as described above. The panning steps were omitted and the mixed cell suspension was plated directly onto poly-D-lysine/laminin-coated glass coverslips, in the same serum-free Neruobasal-A/B27 culture medium detailed above for the purified RGC cultures, at a density of approximately of 1 x 10^5 cells per well.

Retrograde Labeling of RGCs

To confirm the purity and yield of RGCs obtained with the panning procedure, experiments were first performed using a retrograde label to identify the RGCs in culture.

RGCs can be distinguished from other retinal cells through the use of a fluorescent retrograde label injected into the superior colliculus, the primary projection site for RGCs in rats. The rats (6 days old) were put under halothane anesthesia, and a longitudinal incision was made along the midline of the scalp to expose the skull. Two injections each of 2 μl rhodamine B dextran (10,000 MW, 10% solution dissolved in water) were made through the skull on each side of the brain using a 10 μl syringe (Hamilton, Reno, NV) fitted with a 26-gauge needle. The injections were performed at a depth of 4 mm and at a position 2 mm lateral to the saggital sinus, just rostral to its intersection with the transverse sinus (Potts *et al.* 1982; Barres *et al.* 1988). To allow for retrograde transport, the RGC cultures were generated from these rats two days after the rhodamine dextran injection. The rhodamine dextran was detected in the cultured RGCs with a rhodamine filter set (XF101-2, excitation 525 nm; emission 565 nm; dichroic 560 nm; Omega Optical, Brattleboro, VT) fitted to the microscope rig described below.

Thy1 Immunostaining

The isolated RGCs were fixed for 10 min in 4% paraformaldehyde in 0.1 mM phosphate-buffered saline (PBS). Following three washes in PBS, the coverslip-plated cells were incubated in a 10% goat serum blocking solution for 30 min. The remainder of the blocking solution was buffer containing 150 mM NaCl, 50 mM Tris buffer, 1% BSA, 100 mM L-lysine and 0.04% sodium azide in distilled water. The cells were then incubated with primary antibodies overnight at 4°C. Primary antibodies were mouse anti-rat Thy1.1 (cat #55895; BD Biosciences PharMingen, San Diego, CA) made up at 1:500 in the buffer solution described above. The cells were rinsed in PBS three times, and then incubated in secondary antibodies (goat anti-mouse IgG, conjugated to Alexa 488 fluorophore; Molecular Probes) at a dilution of 1:300 (in buffer solution) for 1 h at

room temperature. The slips were then rinsed and transferred to the microscope chamber filled with PBS. Fluorescence was captured using the same microscope rig employed for calcium imaging (described below) with the appropriate fluorescein filter set (XF100 set; excitation 475 nm, emission 535 nm; dichroic 505 nm; Omega Optical) and a water-immersion 40x objective.

Calcium Imaging of Isolated Retinal Neurons

The isolated RGCs (and cells from the mixed retinal cultures) were loaded with the ratiometric calcium-indicator dye fura-2. Cells were incubated in 5 μM fura-2 AM dissolved in modified Mg^{2+}-free HBSS (2.6 mM $CaCl_2$, 15 mM HEPES, pH 7.4) for 30 min in the dark at 37 °C. The fura-2 AM was first dissolved in DMSO (0.1% final concentration in HBSS) and then solubilized in HBSS with 0.1% pluronic acid F-127.

Coverslips containing the fura-2 loaded cells were then transferred to a microscope chamber (ΔTC3; Bioptech, Butler, PA) that was constantly superfused with the Mg^{2+}-free HBSS at 34-36 °C (SH-27 Inline heater, TC-324B controller; Warner Instruments, Hamden, CT) and bubbled with 100% oxygen. A 75 W Xenon lamp (LUDL Electronic Products, Hawthorne, NY) and the appropriate filters (XF04 set, excitation 340 or 380 nm; emission 510 nm; dichroic > 430 nm; Omega Optical) were used to generate fura-2 fluorescence. Alternation of the excitation wavelength from 340 to 380 nm was controlled by a Lambda 10-2 optical filter changer (Sutter Instruments, Novato, CA) with an electronic shutter (Uniblitz, Rochester, NY) to limit each period of illumination to 400 ms. To reduce photodamage and photobleaching, excitation illumination was filtered with a -0.5 log neutral density filter and 320 X 256-pixel (4 X 4 binned) images were acquired. Fluorescence images were captured (8-bit) with a cooled charged-coupled device (CCD) camera (Sensicam; PCO Computer Optic, Kelheim, Germany) fitted to a

microscope (Axioskop FS; Carl Zeiss, Oberkochen, Germany) using a water-immersion objective (N.A. 0.80W; Achroplan 40x; Zeiss). The images of cell fluorescence at 340 and 380 nm excitation were converted to ratiometric (340 nm/380 nm) images by an imaging system (Imaging Workbench 2.2; Axon Instruments, Foster City, CA) and saved to the hard disc of a computer. The background fluorescence was measured from a region on the coverslip devoid of cells and subtracted from each image. The mean fura-2 ratio for each neuron was calculated over a large area of the cell soma, well separated from the edge of the cell.

All treatment solutions were dissolved in the Mg^{2+}-free HBSS and delivered to the chamber by a peristaltic pump (Gilson, Middleton, WI) at a rate of approximately 1 ml/min. The intracellular free calcium concentration ($[Ca^{2+}]_i$) was elevated in the isolated RGCs by application of a short pulse (30 s) of 10 μM glutamate plus 10 μM glycine, a co-agonist of glutamate at the NMDA-type glutamate receptor (Johnson and Ascher 1987). During treatments, image pairs were collected as often as every 3 s but to limit photodamage, images were collected less frequently (20 s) during intervening periods. The time between consecutive glutamate exposures was kept at 15 min to allow sufficient time for $[Ca^{2+}]_i$ to return to a baseline level.

For the calcium imaging experiments on the purified RGCs, fura-2 ratios (R) were converted to $[Ca^{2+}]_i$ in separate calibration experiments using the formula:

$$[Ca^{2+}]_i = K_d\ (F_o/F_s)[(R - R_{min})/(R_{max} - R)]$$

with a K_d for fura-2 = 224 nM, and where F_o/F_s is the ratio of fluorescence intensity at 380 nm excitation in calcium-free solution over the intensity in solution with saturated calcium levels (Grynkiewicz *et al.* 1985; Kao 1994). Superfusion of the isolated RGCs with calcium-free HBSS (10 mM Mg^{2+}, 2 mM BAPTA, 10 μM ionomycin) was also used to determine the minimum value for the fura-2 ratio (R_{min}), following which

the cells were superfused with a saturated calcium solution (0.9% saline with 20 mM Ca^{2+}, 10 μM ionomycin) to determine the maximum fura-2 ratio (R_{max}). Mean values for F_o/F_s, R_{min}, and R_{max} were calculated from 5-10 RGCs and the calibration procedure was repeated every three weeks. Conversion of the fura-2 ratios to $[Ca^{2+}]_i$ allowed an approximation of absolute calcium levels, but as all comparisons of the effect of adenosine and related drugs were within-cell comparisons, the conversion to $[Ca^{2+}]_i$ did not alter the presence or absence of a given effect or its statistical significance. Further details on the calibration method are given in Appendix A of this thesis.

Calcium influx was measured as the peak $[Ca^{2+}]_i$ following each glutamate exposure minus the average baseline $[Ca^{2+}]_i$ measured before the first glutamate exposure. RGCs that had a negligible response to glutamate (peak $[Ca^{2+}]_i$ <150 nM) were excluded from analysis (<5% of all RGCs imaged).

Calcium Imaging of RGCs in Retinal Wholemounts

Calcium imaging experiments on RGCs in an intact rat retina preparation were performed using a method that was previously developed for rabbit retinas (Baldridge 1996). Adult Long-Evans rats (>10 weeks old) were killed by pentobarbital overdose and both eyes enucleated. The anterior segment and vitreous were removed and the posterior segment was immersed in the modified Mg^{2+}-free HBSS (2.6 mM $CaCl_2$, 15 mM HEPES, pH 7.4) that was bubbled continuously with 100% oxygen. The underlying sclera was pinned to a silicone-lined (Sylgard; Dow Corning, Midland MI) glass Petri dish, and the vitreous was removed with curved jeweler's forceps. The retina was dissected from the eyecup by slowly peeling the sclera away from the retina with a flat spatula and then cutting its attachment at the optic nerve head with iris scissors. The retina was floated onto a glass microscope slide and the peripheral retinal edges were

trimmed with a scalpel blade. The retina was then mounted on black filters (HABP 045; Millipore, Bedford, MA) with the RGC layer uppermost.

A small amount (~0.5 μl) of 10,000 MW dextran-conjugated fura calcium indicator dye (10% wt/vol; dissolved in purified water) was ejected to the tip of a tapered 26-gauge needle fitted to a 10 μl Hamilton syringe, and the needle tip was then inserted into the flatmounted retina, passing through all the retinal layers. A large portion of the dye stays on the surface of the retina, but as the fura dye is conjugated to large dextran molecules, it remains extracellular and is rinsed off the surface by the superfusing HBSS during calcium imaging. As described previously (Baldridge 1996), some of the dye is taken up by RGC axons that are cut during the injection, and the dextran-conjugated fura is then transported intracellularly along these axons. The retinas were then incubated at room temperature in HBSS bubbled continuously with 100% oxygen for 3 to 5 h before calcium imaging to allow for the retrograde transport of the fura dextran to RGC somata.

The NMDA-induced calcium influx was measured as the peak fura ratio (occurring in response to NMDA treatment) minus the baseline fura ratio (the average ratio measured in the five images prior to each NMDA exposure) in the RGC somata. The time between consecutive NMDA exposures was 20 to 25 min.

Data Analysis

All data are expressed as the means ± standard error of the mean (SEM). For all calcium imaging experiments, the calcium influx was normalized to the initial glutamate (isolated cells) or NMDA (intact retina) treatment. Statistical within-cell comparisons of the effect of adenosine and/or related drugs were made on the normalized data using the nonparametric Freidman repeated measures ANOVA and Student-Newman-Keuls (SNK) multiple-comparison post hoc test using Sigmastat software (SPSS, Chicago, IL).

Results

Effect of Adenosine on Retinal Cells in Mixed Cultures

In initial experiments using mixed retinal cultures, the tested cells exhibited a range of morphological features (Figure 2-1 A, B) that was consistent with the broad range of cell types expected to be present. The effect of adenosine was tested on the calcium response of 36 cells (pooled from 3 separate cultures) during 30 s exposures to 10 μM glutamate. All of these cells exhibited a rise in the fura-2 ratio (indicative of internal calcium levels) of greater than 0.3, ensuring that non-responsive cells such as macrophages were not included in the study. In the vast majority of these cells, adenosine had no effect on glutamate-induced calcium influx. Although adenosine appeared to increase the duration of the glutamate responses in the example trace shown (Figure 2-1 C), this was not a consistent finding. For the 36 neurons, taken as a whole population, there was no significant difference ($P = 0.379$) in the glutamate response whether adenosine was present or absent (Figure 2-1 D). However, there seemed to be small sub-populations of cells in the mixed cultures that were influenced by adenosine. In 3 of the 36 cells there was a repeatable *increase* of the glutamate-induced response amplitude with adenosine present (an example illustrated in Figure 2-1 E), and in 2 other cells adenosine may have caused a small *decrease* in the response (example in Figure 2-1 F). With the use of serum-free culture medium, glial cells nearly completely die off over the first few days in culture (Brewer *et al.* 1993). To ensure it was predominantly retinal neurons that were tested, the mixed cells were cultured for 3 to 5 days (to eliminate glia) prior to imaging and only neurite-bearing cells were imaged. A caveat to these results, therefore, is that the action of adenosine on these isolated cells may have diminished during the culture period.

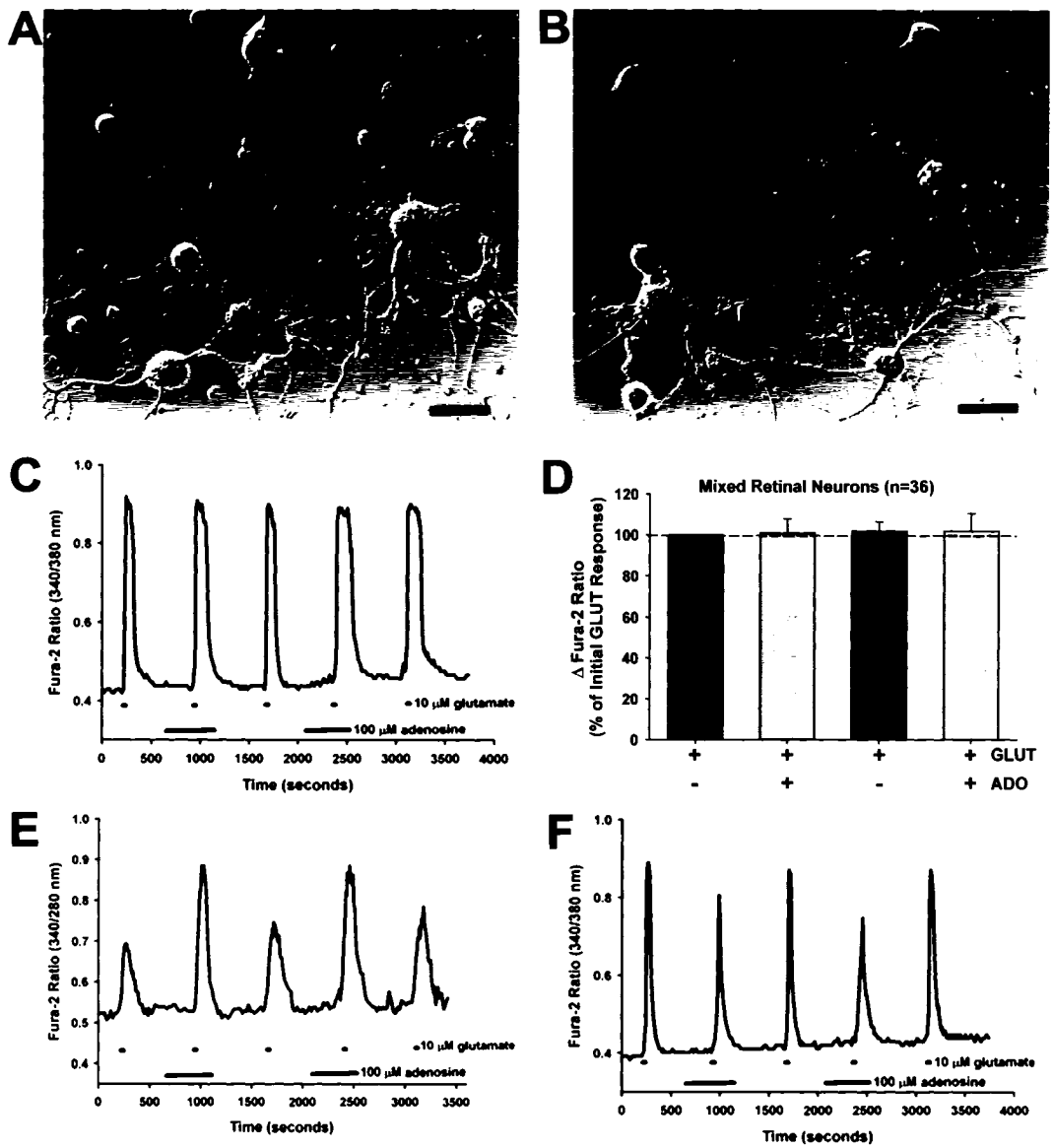

Figure 2- 1. Effect of adenosine on mixed retinal cell cultures. **(A,B)** Differential interference contrast (DIC) images of rat retinal neurons in mixed cultures. **(C)** Example fura-2 ratio trace, indicative of the calcium signal, representative of the majority of neurons tested. **(D)** Summary of data for all tested neurons (n = 36) in the mixed retinal cultures. While adenosine had no effect on the glutamate-induced calcium influx in most of the tested retinal neurons, there was evidence that adenosine could **(E)** enhance (in 3 of the 36 cells) or **(F)** inhibit the glutamate response (in 2 of the 36 cells) in a small subset of the cells present in the mixed cultures.

As adenosine and its A_1 receptor have been identified in the inner layers of the rat retina, I next sought to determine the effect of adenosine specifically on RGCs, the retinal output neurons. RGCs can be retrogradely labeled to enable specific identification in mixed cultures by depositing a neuronal tracer, such as a dextran-conjugated dye, in the brain target sites of RGC axons (i.e. the superior colliculus in rats). However, previous studies have shown that retrogradely labeled RGCs in mixed cultures rapidly die off over the first 2-3 days in culture (Takahashi *et al.* 1991; Taschenberger and Grantyn 1995; Kitano *et al.* 1996). In contrast, it has been reported that RGCs isolated by immunopanning (adhesion to Thy1-coated Petri dishes) and subsequently plated into purified (only RGCs present) cultures exhibit increased viability (Meyer-Franke *et al.* 1995; Otori *et al.* 1998). As there is only one RGC for every 200 cells present in a mixed retinal cell culture immediately after plating (Barres *et al.* 1988; Kitano *et al.* 1996), the immunopanning of RGCs into purified cultures is advantageous for the study of these relatively sparse retinal neurons.

Effect of Adenosine on RGCs in Purified Cultures

In immunopanned cultures generated from rats that had the rhodamine dextran injection in the superior colliculus (n = 3 separate experiments), more than 97% of the plated cells exhibited positive rhodamine fluorescence, thereby confirming their identity as RGCs (Figure 2-2). The few cells not labeled were generally smaller and easy to distinguish morphologically from the identified RGCs and cells of this type were not used in subsequent imaging experiments. The cells extracted through immunopanning using the monoclonal IgM antibody-containing supernatant were verified to be Thy1.1-positive by immunostaining the cultured cells with an IgG antibody directed against Thy1.1, and omitting the primary antibody eliminated the staining in sibling cells (Figure 2-3).

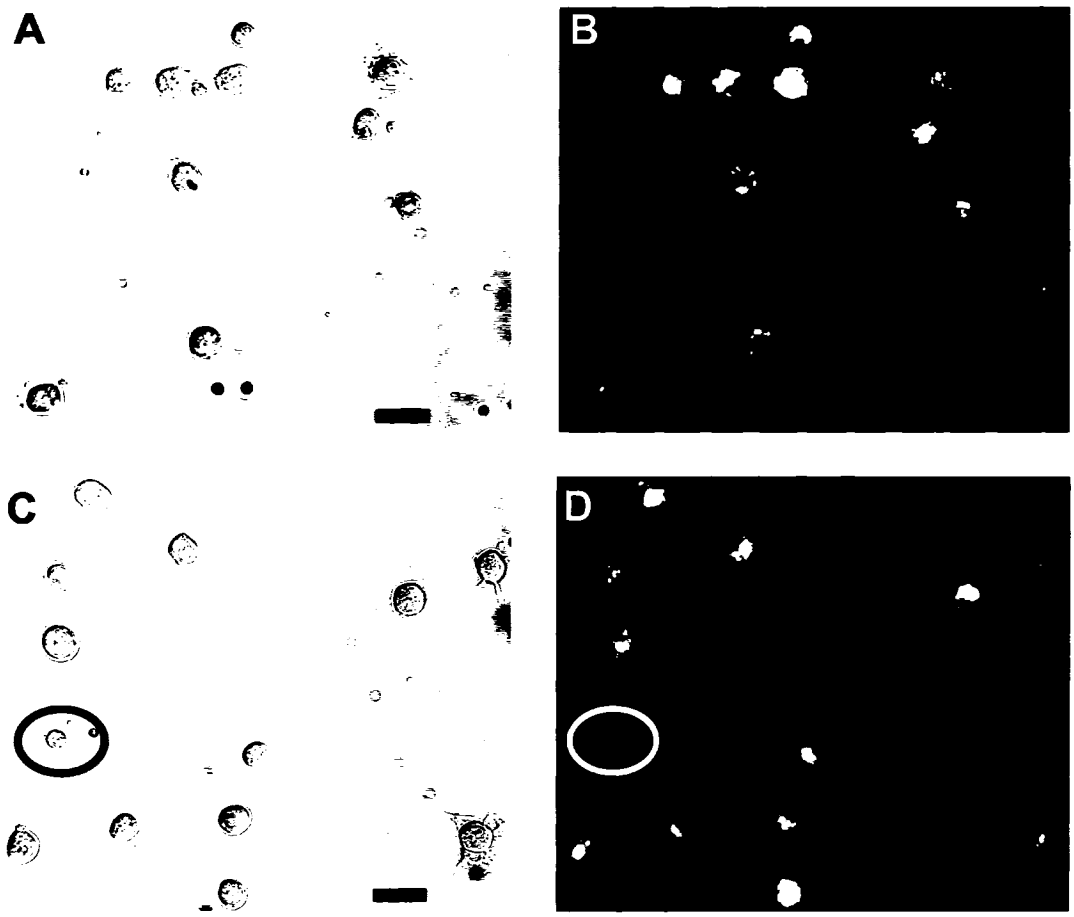

Figure 2- 2. Purified RGC cultures generated using Thy1 immunopanning. **(A, C)** DIC images of cultured cells 6 hours after plating and **(B, D)** fluorescent micrographs of the same cells to identify RGCs retrogradely labeled with rhodamine dextran. The panning method generated RGC cultures >97% pure. The lone cell not exhibiting rhodamine dextran fluorescence is encircled. Scale bar = 25 μm.

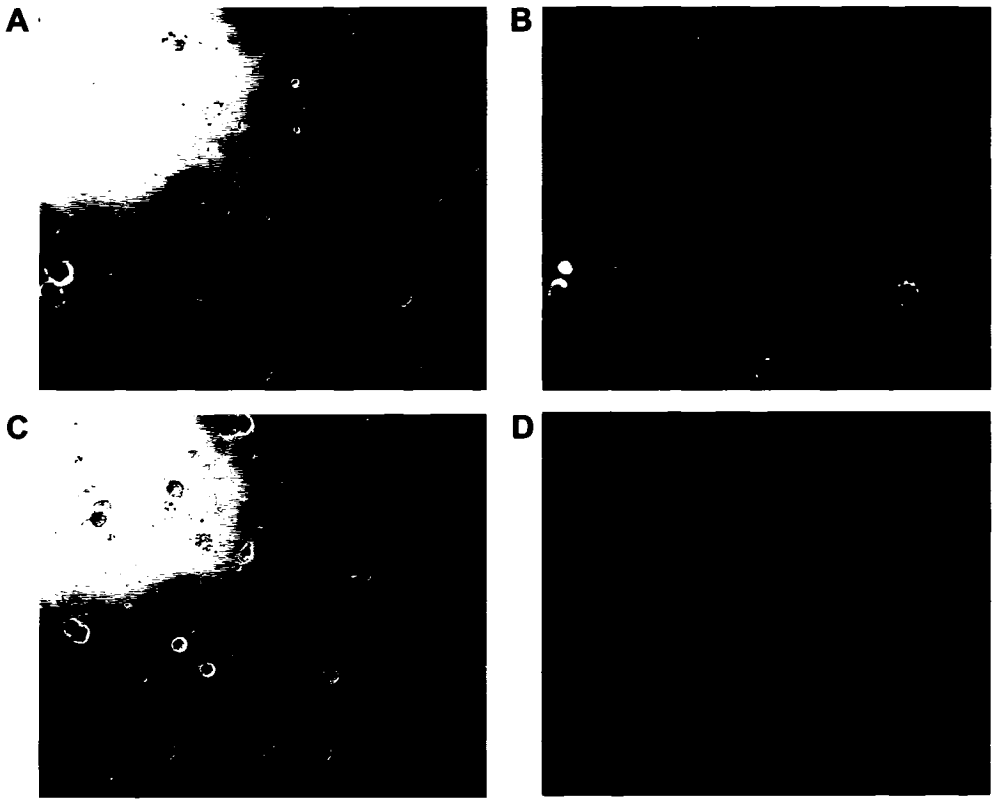

Figure 2- 3. Immunostaining of isolated RGCs by Thy1.1 IgG antibodies. **(A, C)** DIC images of fixed cells (cells were fixed after one day in culture), and **(B, D)** fluorescent micrographs of the same cells after incubation in (B) Thy1.1 primary antibodies and Alexa 488-tagged secondary antibodies or (D) secondary antibodies only (primary omitted). Both fluorescence images (B, D) were captured by a CCD camera (attached to the imaging rig; 40x objective with 0.6x coupling tube) using 400 msec exposure time and 4 X 4 pixel binning. No further processing of the images was performed. The cultured cells were Thy1.1-positive, confirming that the monoclonal supernatant used for immunopanning was selectively isolating cells that express Thy1.1. Scale bar = 25 μm.

In addition, no cells adhered to the final panning plate when Thy1.1 antibodies were omitted and the plate was coated with only secondary antibodies (n = 2 experiments).

The yield of RGCs ranged from 15,000 to 30,000 RGCs per retina. Calcium imaging experiments were performed on the isolated RGCs after 1 to 2 days of culture, and the ratio of fura-2 fluorescence (340 nm/380 nm; converted to $[Ca^{2+}]_i$ after calibration experiments; see Appendix A) was measured in the somata of individual RGCs (Figure 2-4). The protocol of a 30 second exposure to 10 μM glutamate plus 10 μM glycine (hereafter referred to as "glutamate", with the addition of glycine implied) was chosen because it resulted in reproducible increases in $[Ca^{2+}]_i$ within the dynamic range (below saturation) of fura-2 fluorescence in the RGCs.

To test the effect of adenosine, each RGC was exposed to 10 μM glutamate four consecutive times, with the second and fourth treatment occurring with adenosine present (Figure 2-5). HBSS containing either glutamate alone or a mixture of glutamate and adenosine was delivered to the chamber in these studies. In the presence of 10 μM adenosine, calcium influx was significantly reduced (mean influx, 68.7 ± 7.1% and 68.2 ± 6.6% of the initial response; n = 15; $P < 0.01$) compared with the two responses in the absence of adenosine. Increasing the concentration of adenosine from 10 μM to 100 μM resulted in a similar reduction (70.1 ± 3.8% and 62.0 ± 4.5% of initial response; n = 15; $P < 0.01$) of the glutamate-induced calcium influx (Figure 2-5). This suggests that the maximum effect of adenosine is achieved at 10 μM in isolated RGCs.

Pharmacology of Effect of Adenosine on Glutamate-Induced Calcium Influx

To determine whether the inhibitory effect of adenosine on the glutamate-induced calcium response was mediated by either A_1-Rs or A_{2A}-Rs, additional calcium imaging experiments were performed on the cultured RGCs using appropriate adenosine

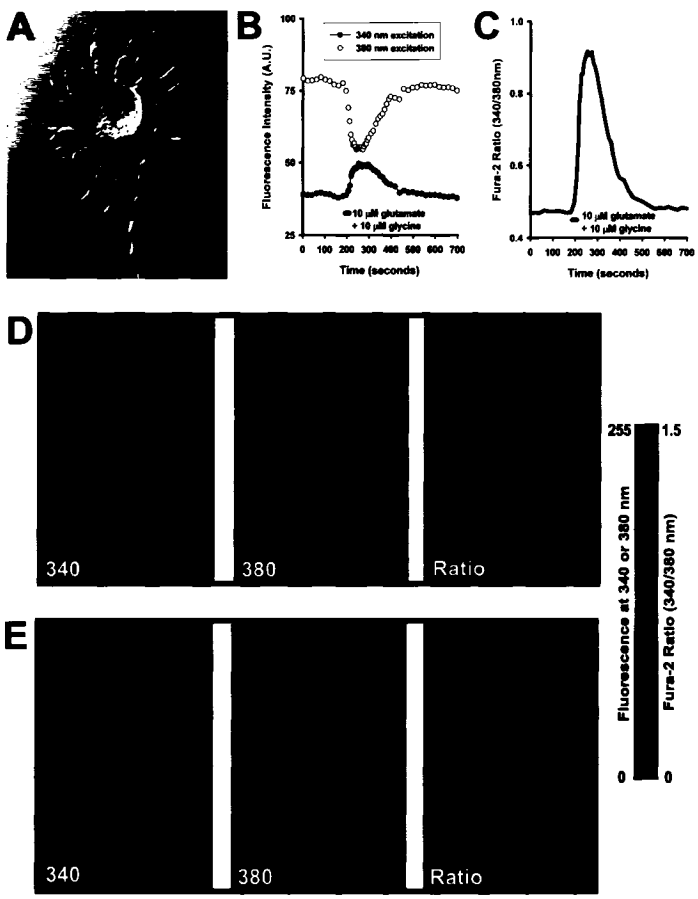

Figure 2- 4. Glutamate increases $[Ca^{2+}]_i$ in rat RGCs in a purified culture. **(A)** DIC image of an RGC one day following dissociation. Scale bar = 25 μm. **(B)** Trace of the fura-2 fluorescence at the excitation wavelengths of 340 and 380 nm (emission 510 nm) and the **(C)** resulting fura-2 ratio (340/380 nm) measured in the soma of this RGC during a 30 s exposure to 10 μm glutamate plus 10 μM glycine. An increase in the fura-2 ratio is indicative of increased internal calcium levels and can be converted to absolute calcium levels through calibration experiments (see Appendix A). **(D)** Pseudocolor representation of the fluorescence at 340 and 380 nm excitation and the resulting fura-2 ratio at baseline and **(E)** during the peak glutamate response for this same RGC.

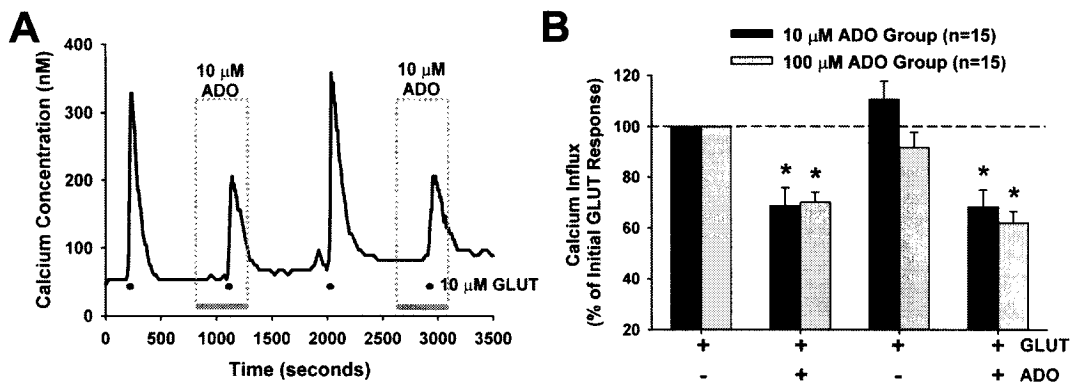

Figure 2- 5. Adenosine (ADO) inhibits glutamate-induced calcium influx in isolated RGCs. **(A)** $[Ca^{2+}]_i$ trace from a cultured RGC illustrating the effect of 10 μM adenosine on the RGC response to 10 μM glutamate (GLUT; with 10 μM glycine). Cells were exposed to glutamate four times with adenosine present during the second and fourth treatment. **(B)** Mean data for all RGCs in studies using 10 μM and 100 μM adenosine, normalized to initial glutamate response (100%, dashed line). * $P < 0.01$ compared with both control glutamate responses (Friedman ANOVA, SNK posthoc).

receptor antagonists and agonists. Individual RGCs were again exposed to four consecutive treatments of 10 μM glutamate. Adenosine was present during the second exposure, and adenosine plus either the A_1-R antagonist DPCPX (Figure 2-6 A) or the A_{2A}-R antagonist DMPX (Figure 2-6 B) were present during the third exposure. Adenosine alone significantly decreased ($P < 0.01$) the glutamate-induced calcium influx in both groups, consistent with the results shown in Figure 2-5, and the effect of adenosine was almost completely blocked by DPCPX but not DMPX. In the presence of both adenosine and DPCPX, the glutamate-induced calcium influx (92.1 ± 8.2% of initial response; n = 14) was not significantly different ($P > 0.05$) from either the initial or the recovery response to glutamate (Figure 2-6 C). In contrast, in the presence of both adenosine and DMPX, the calcium influx (61.2 ± 5.1% of initial response; n = 14) remained significantly reduced ($P < 0.01$) as compared to the responses to glutamate alone (Figure 2-6 C).

In experiments using adenosine agonists, the presence of either 1 or 10 μM of the A_1-R agonist CHA resulted in a significant decrease ($P < 0.01$) in the glutamate-induced calcium influx (to 76.4 ± 7.9% and 64.3 ± 5.9% of the initial response, respectively; n = 15 for both; Figure 2-7). This decrease was similar in magnitude to that observed with adenosine (Figure 2-5). At 1 μM, the A_{2A}-R agonist CPCA did not affect ($P = 0.25$) the glutamate-induced calcium influx (influx 96.0 ± 7.7% of the initial response; n = 15). At 10 μM, CPCA did have a small (influx 85.4 ± 3.6% of the initial response; n = 15) but significant ($P < 0.01$) effect (Figure 2-7). The recovery responses to glutamate in each of the four agonist treatment groups were not significantly different ($P > 0.05$; data not shown) from the initial response, indicating that agonist effects were not due to response 'run-down'. The full recovery of the glutamate response after washing (also see recovery responses in adenosine experiments shown in Figures 2-5

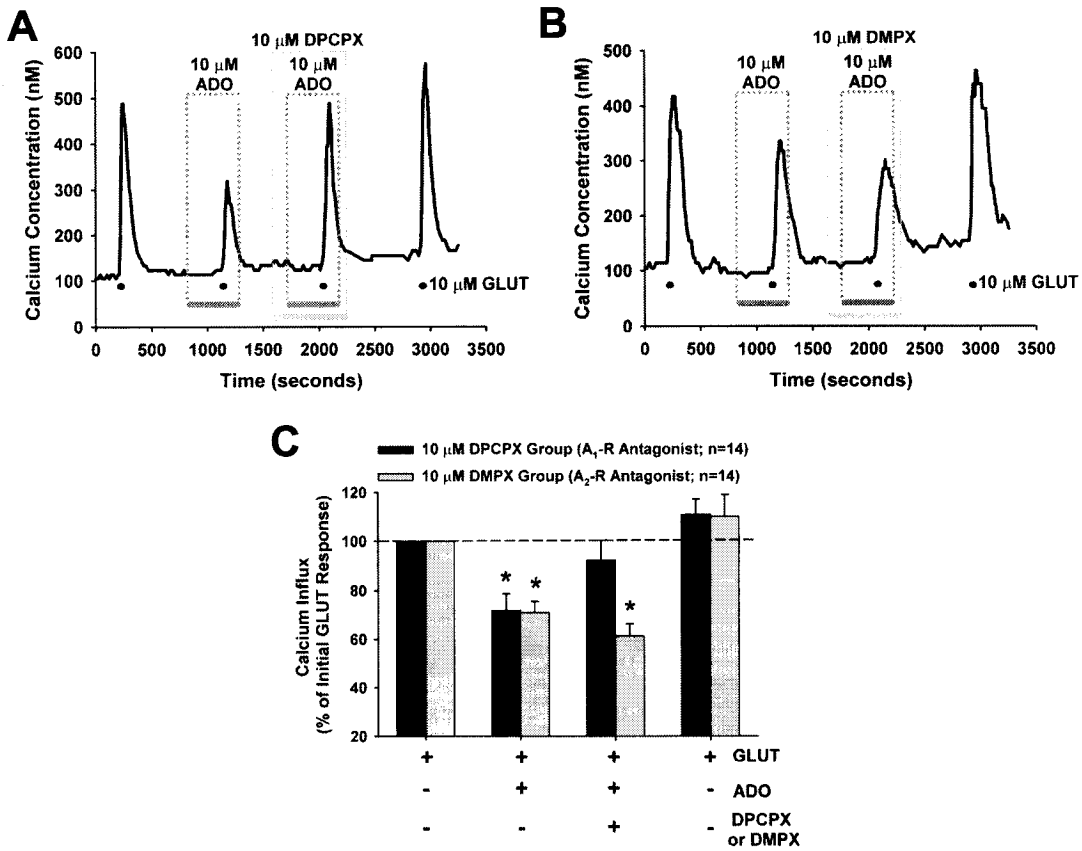

Figure 2- 6. Effects of A_1-R and A_{2A}-R antagonists on glutamate-induced calcium influx in isolated RGCs. $[Ca^{2+}]_i$ traces from individual RGCs showing **(A)** the A_1-R antagonist DPCPX (10 μM) nearly completely blocked the inhibitory effect of 10 μM adenosine (ADO) on increases in $[Ca^{2+}]_i$ induced by 10 μM glutamate (GLUT; with 10 μM glycine), while **(B)** the A_{2A}-R antagonist DMPX (10 μM) had little effect. **(C)** Mean data, normalized to initial response (100%, dashed line). * $P < 0.01$ compared to both the initial and recovery responses to glutamate (Friedman ANOVA, SNK posthoc).

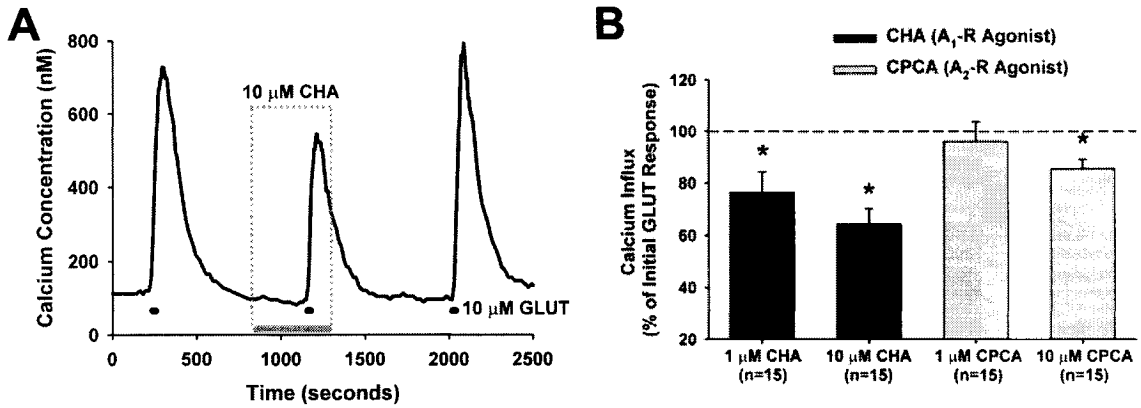

Figure 2- 7. Effects of A_1-R and A_{2A}-R agonists on glutamate-induced calcium influx in isolated RGCs. **(A)** $[Ca^{2+}]_i$ trace illustrating effect of the A_1-R agonist CHA. **(B)** Mean data for studies with the A_1-R agonist CHA (1 or 10 μM) or the A_2-R agonist CPCA (1 or 10 μM), normalized to the initial response (100%, dashed line). * $P < 0.01$ compared to both the initial and recovery responses to glutamate (Friedman ANOVA, SNK posthoc).

and 2-6) indicates that the inhibitory effect of adenosine on glutamate-induced calcium influx in isolated rat RGCs is reversible.

Effect of Adenosine on RGCs in Retinal Wholemounts

Injection of fura dextran into the rat retinal wholemount preparations resulted in the loading of the dye into RGC axons that passed through the injection site. After 3 to 5 h incubation at room temperature, the dye was retrogradely transported to RGC somata. In this study, all experiments were done on retrogradely labeled cells that were at least 200 μM from the injection site, and that were located in the GCL near bundles of labeled axons (Figure 2-8 A). Although there are displaced amacrine cells in the rat GCL, it is rare for these cells to have a dendritic spread larger than 200 μM (Perry 1979). Thus, it is highly likely that the cells used for these experiments were RGCs, and not displaced amacrine cells.

Exogenous application of 200 μM glutamate had no effect on RGC calcium levels in the flatmounted rat retinas (Figure 2-8 B) due to the presence of functional high-affinity glutamate uptake systems, and this is consistent with previous electrophysiological studies using intact retina preparations (Thoreson and Witkovsky 1999). In contrast, the glutamate agonists NMDA and kainate, which are not recognized by the neuronal and glial glutamate transporters, consistently elevated RGC $[Ca^{2+}]_i$ (Figure 2-8 B). Thus, 100 μM NMDA was used to elevate $[Ca^{2+}]_i$ in the experiments to test the effect of adenosine on calcium influx in rat RGCs in the intact retina.

Adenosine (100 μM) significantly decreased ($P < 0.05$) the NMDA-induced calcium influx in the RGCs ($n = 5$; cells from five different retinas from four rats) in the intact rat retina preparation (Figures 2-8 C, D). The mean change in the fura ratio (peak ratio – baseline ratio) in the presence of adenosine was 70.5 ± 9.8% that of the initial

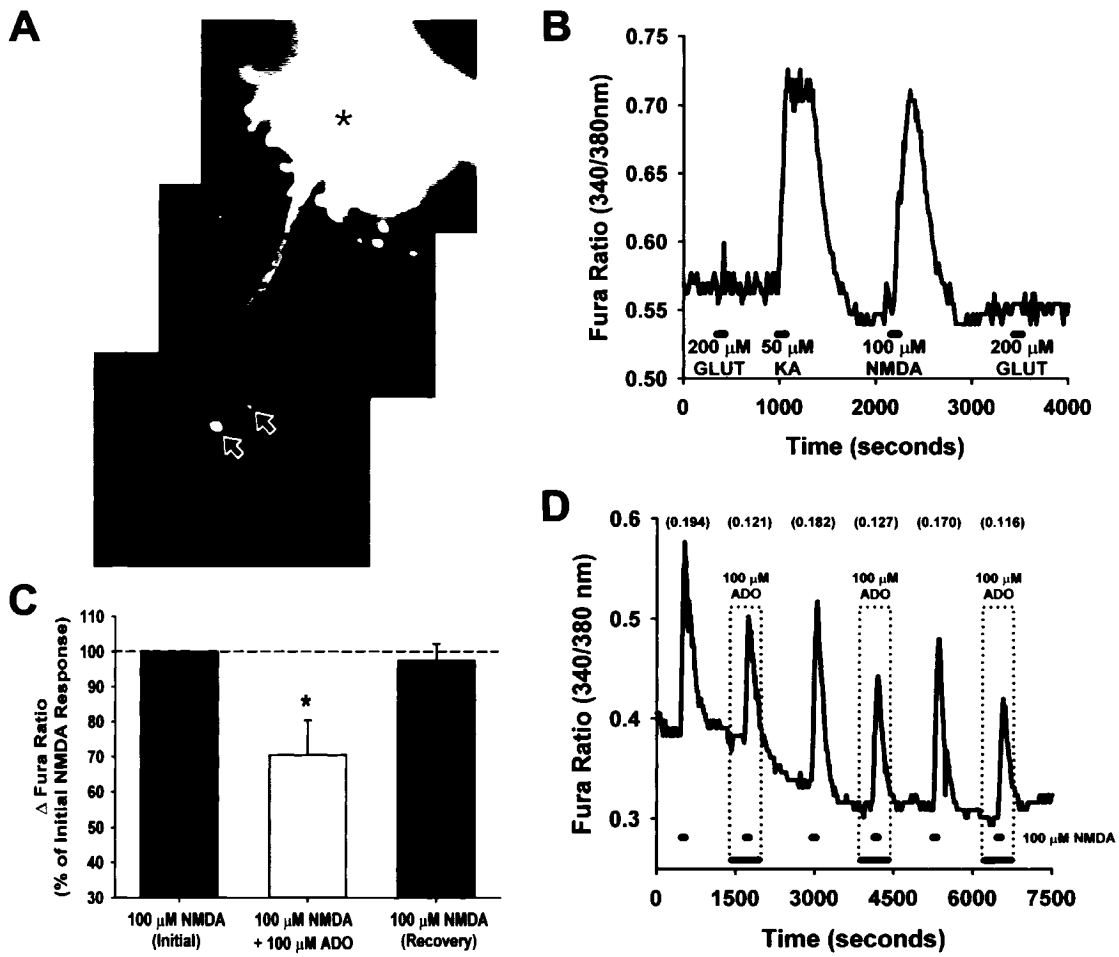

Figure 2- 8. Adenosine (ADO) inhibits NMDA-induced calcium influx in RGCs in rat retinal wholemounts. **(A)** Montage of fluorescence micrographs showing two RGCs (arrows) retrogradely loaded with the fura dextran calcium indicator dye, located in the vicinity of labeled axon bundles. The fura dextran had been injected ~3 hours earlier at the site denoted with an asterisk. Scale bar = 50 µm. **(B)** Representative trace from a RGC illustrating that the glutamate agonists NMDA and kainate (KA) are more effective than glutamate (GLUT) at inducing changes in RGC $[Ca^{2+}]_i$ in this intact retina preparation. **(C)** Summary of data testing the effect of adenosine on RGCs (n = 5) in the retinal wholemounts, normalized to initial NMDA response (dashed line). * $P < 0.05$ compared with both initial and recovery NMDA responses (Friedman ANOVA, SNK posthoc). **(D)** Example trace of RGC exposed to NMDA 6 times with adenosine present during the 2nd, 4th, and 6th treatment. The numbers in parentheses are the Δ fura ratios (peak ratio minus baseline ratio) for each response.

response to NMDA alone. In the third exposure to NMDA following adenosine treatment, the RGCs exhibited recovery as the mean response was 97.6 ± 4.8% that of the initial response. In the optical recording shown in Figure 2-8 D, the tested cell was exposed to NMDA six times, alternating between the presence and absence of adenosine, and illustrates that the effect of adenosine was reversible and repeatable (the first 3 responses in this cell were used for the analysis shown in Figure 2-8 C). The gradual decrease in baseline was sometimes observed in the intact retina experiments and is likely due to the changing background fluorescence as fura dextran on the retinal surface (excess spillage from the injection) is washed away during the experiment. By quantifying calcium influx as the change in fura ratio (calculated as the peak minus baseline ratio) for each response in these experiments on the intact retina, this artifact did not influence the results.

Discussion

In this chapter, I demonstrated that adenosine inhibits glutamate-induced calcium influx in isolated neonatal mammalian (rat) retinal ganglion cells obtained from purified cultures produced by immunopanning. Adenosine also decreased NMDA-induced calcium influx in adult rat RGCs in an intact retina preparation, confirming that the effects of adenosine on RGCs are not unique to neonates or due to an artifact associated with the dissociation of the retina into isolated cells for culture.

Adenosine Modulation of Glutamatergic Calcium Dynamics in RGCs

From the initial experiments on retinal neurons in mixed cultures, it was clear that adenosine does not affect all retinal neurons in the same manner. To specifically assess the effect of adenosine on RGCs, I utilized an immunopanning method that isolates

RGCs using Petri dishes coated with monoclonal Thy1.1 antibodies. In agreement with previous reports (Barres *et al.* 1988; Meyer-Franke *et al.* 1995), I found that the immunopanning technique generated highly purified RGC cultures. Following the retrograde labeling of RGCs by application of rhodamine dextran to the superior colliculus, more than 97% of the panned cells contained the RGC-identifying label. The small percentage (< 3%) of unlabeled cells could be RGCs that were not retrogradely labeled or could represent other retinal neurons that escaped removal during the final rinse of the Thy1.1 panning plate. The latter is most likely given that the unlabelled cells were generally smaller and morphologically distinct from labeled RGCs. Cells of this type were not used for the calcium imaging experiments.

There are a number of advantages to the use of purified RGC cultures as opposed to mixed retinal cell cultures in which RGCs are identified with a retrograde tracing label. First, RGCs comprise only about 0.5% of the cells in a mixed culture (Barres *et al.* 1988; Kitano *et al.* 1996), making the selection of RGCs for study a more tedious task. Second, there is evidence that RGCs undergo rapid cell death in mixed cultures, and are nearly completely eliminated during the first 2-3 days of culture (Takahashi *et al.* 1991; Taschenberger and Grantyn 1995). In contrast, it has been reported that RGCs in purified cultures exhibit a 50-60% survival rate over the first 4 weeks of culture (Meyer-Franke *et al.* 1995). While differences in the dissection and culture methodologies among these research groups may be a contributing factor, the reason for the survival rate discrepancy has not been conclusively demonstrated. Using a consistent dissection protocol for both types of cultures, I also observed more rapid and complete death of RGCs in mixed cultures as compared to purified cultures (data not shown). One possible explanation is that the isolated RGCs, no longer ensheathed by protective glial cells, are vulnerable to potentially neurotoxic agents released from

other cells that are present in the mixed cultures (Otori *et al.* 1998). Finally, a third disadvantage of mixed retinal cell cultures is that it can be difficult to conclusively rule out indirect treatment effects. Exposure of the cultures to a given drug could stimulate adjacent cells to release factors that subsequently act on RGCs. As the immunopanned cultures are comprised almost exclusively of RGCs, an observed treatment effect must be due to the direct action of the tested compound on RGCs.

Glutamate is the principal neurotransmitter of the retina and mediates synaptic communication between bipolar cells and RGCs. Therefore, to assess potential postsynaptic modulation of excitatory input to RGCs, glutamate was used to stimulate calcium influx in the cultured RGCs. Glutamate could increase $[Ca^{2+}]_i$ directly, by activating NMDA-type glutamate receptor (NMDA-R)-gated channels, or indirectly by activation of VGCCs following RGC depolarization due to stimulation of either NMDA- or AMPA/kainate-type glutamate receptors (Berridge 1998). To stimulate both pathways, I used conditions that would promote NMDA-R activation. Specifically, extracellular Mg^{2+} was removed during calcium imaging experiments to eliminate the voltage-dependent block by this cation of NMDA-Rs (Mayer *et al.* 1984; Nowak *et al.* 1984), and glycine, a known co-agonist of glutamate at NMDA-Rs (Johnson and Ascher 1987), was added to the glutamate solution (see Chapter 4).

Despite the benefits associated with the use of the purified RGC cultures, it could be argued that the dissociation and panning procedure, performed on neonatal retinas, generates RGCs with different characteristics than those in the adult retina with retinal synaptic connections intact. My finding that adenosine inhibited NMDA-induced calcium influx in RGCs in retinal wholemount preparations indicates that the neuromodulatory action of adenosine was not unique to isolated RGCs. A possible disadvantage with the intact retina preparation is that there is the potential for adenosine to act 'upstream' from

RGCs in the retinal visual pathway. For example, it has been shown recently in salamanders that adenosine, through A_{2A}-R activation, can inhibit glutamate release from rod photoreceptors (Stella *et al.* 2002; Stella *et al.* 2003). However, NMDA receptors have been localized primarily to RGCs and some amacrine cells in the mammalian retina (Thoreson and Witkovsky 1999), and so it is unlikely that the decrease in NMDA-induced RGC $[Ca^{2+}]_i$ by adenosine observed in the present study was an indirect effect due to an inhibition of glutamate release from photoreceptors or bipolar cells. Taken together with the results from the cultured RGCs, this work provides strong evidence that adenosine modulates the glutamatergic input to mammalian RGCs. The method of retrogradely loading RGC somata with dextran-conjugated calcium indicator dye was originally developed in the rabbit retina (Baldridge 1996), and the present study shows that this technique can be applied to the rat retina as well.

Adenosine Modulates RGCs through A_1-Receptor Activation

Based on receptor binding studies in the rat brain, DPCPX and DMPX have been shown to be selective (relative affinity ratio $[A_{2A}K_i / A_1K_i]$ = 739 for DPCPX and 0.35 for DMPX) adenosine receptor antagonists (Jacobson and Van Rhee 1997). The inhibitory effect of adenosine on glutamate-induced calcium influx was blocked by the A_1-R antagonist DPCPX, while the A_{2A}-R antagonist DMPX had little effect, thus demonstrating an A_1-R-mediated mechanism. In addition, the selective A_1-R agonist CHA (1 and 10 μM) was more effective than the A_{2A}-R agonist CPCA (1 and 10 μM) at reducing glutamate-dependent increases of RGC $[Ca^{2+}]_i$. At 10 μM, CPCA did have a small but significant effect, but this is likely due to an action at A_1-Rs, as CPCA is not completely selective (relative affinity ratio $[A_{2A}K_i / A_1K_i]$ = 392 for CHA and 2.1 for CPCA; from binding studies in rat brain) for the A_{2A}-R (Bruns *et al.* 1986). The pharmacological

characterization in this study of functional A_1-Rs on RGCs is consistent with prior anatomical studies that have identified the presence of these receptors in the GCL (Braas *et al.* 1987; Blazynski and Perez 1991; Kvanta *et al.* 1997).

The inhibitory effect that adenosine exerted on RGCs was rarely observed in the experiments on retinal cells in mixed cultures. This suggests that A_1-R modulation of excitatory input may be a characteristic that is relatively unique to RGCs in comparison to other classes of retinal neurons. As adenosine enhanced the glutamate-induced calcium influx in a small minority of cells in the mixed cultures (this effect was never observed using RGCs from purified cultures), it is possible that adenosine may influence other retinal neurons differently than it does RGCs. As a possible mechanism, the potentiation of the glutamate signal by adenosine may be mediated by A_{2A}-Rs present on these cells, as A_{2A}-R activation elsewhere in the CNS has been associated with increased neuronal activity (Dunwiddie and Masino 2001). However, this hypothesis is only speculative at the present time, as the effect of adenosine on these unidentified cells was not fully characterized.

The best established action of A_1-Rs in the CNS is presynaptic inhibition of neurotransmitter release due to modulation of VGCCs (predominantly N-type) in neuronal terminals (Mogul *et al.* 1993; Yawo and Chuhma 1993; Wu and Saggau 1994; Scammell *et al.* 2003). Indeed, A_1-R-mediated inhibition of presynaptic neurotransmitter release has been demonstrated at RGC axon terminals, which are located in the brain (Zhang and Schmidt 1998, 1999; Hallworth *et al.* 2002). However, the potential colocalization of adenosine and A_1-Rs in the inner retina (Braas *et al.* 1987; Blazynski and Perez 1991; Kvanta *et al.* 1997) implies that adenosine may postsynaptically influence RGCs. By assessing the effect of adenosine on the glutamate-evoked calcium signal, the results of this chapter do support a postsynaptic mechanism for the

neuromodulation of RGCs by adenosine. Similar to my findings in RGCs, the postsynaptic modulation of excitatory input by adenosine has been observed in subpopulations of isolated hippocampal (de Mendonca *et al.* 1995) and hypothalamic (Obrietan *et al.* 1995) neurons.

Concurrent experiments on isolated RGCs in the purified cultures showed that adenosine, acting through A_1-Rs, inhibited RGC calcium currents. The electrophysiology recordings were performed by Melanie Lalonde (a PhD student at that time at Dalhousie University) on RGCs I had isolated into purified cultures, and this data was published in conjunction with the results presented in this chapter (see Figure 4 in Hartwick *et al.* 2004). These data suggest that the observed effect of adenosine on glutamate-induced calcium influx may, at least in part, be attributable to the inhibition of VGCCs. Further evidence for the role of adenosine in the retina was shown in a recent study, in which adenosine was observed to induce an outward potassium (K^+) current in rat RGCs (Newman 2003). The K^+ efflux would serve to hyperpolarize the membrane potential, resulting in reduced RGC excitability. Taking these results together with those presented in this chapter, it is clear that adenosine can act on mammalian RGCs within the retina, influencing RGCs through the modulation of postsynaptic Ca^{2+} and K^+ currents and ligand-gated changes in $[Ca^{2+}]_i$.

Functional Consequences of RGC Neuromodulation by Adenosine

The finding that adenosine can affect glutamate-induced calcium influx in RGCs has potential physiological and pathologic implications. Throughout the CNS, A_1-R activation is associated with a reduction in neuronal activity and energy expenditure and is thought to contribute to tonic depression of synaptic transmission (Wu and Saggau 1994; Dunwiddie and Masino 2001; Johansson *et al.* 2001). There is evidence, from

studies using a perfused feline eye preparation, that there is a tonic level of extracellular adenosine in the retina and that this contributes to an overall inhibition of light-stimulated retinal neuronal activity (Kaelin-Lang *et al.* 1999). The tonic stimulation of RGC A_1-Rs would dampen the excitatory input to these retinal output neurons and could serve as a fine-tuning mechanism controlling the flow of visual information to the brain.

In addition to the role of glutamate in normal synaptic transmission, excessive activation of glutamate receptors can lead to an increase in $[Ca^{2+}]_i$ to toxic levels, resulting in neuronal death (Choi 1988; Leist and Nicotera 1998). Compounds that limit these increases in $[Ca^{2+}]_i$ have been shown to protect retinal neurons against glutamate excitotoxicity (Baptiste *et al.* 2002; Kawasaki *et al.* 2002), and thus our results present a mechanism through which adenosine could mediate neuroprotective effects on RGCs. In fact, it is well-established that extracellular adenosine levels increase following ischemia or excitotoxic insults in the CNS, and A_1-R agonists have exhibited neuroprotective properties in several CNS models of ischemia and excitotoxicity (de Mendonca *et al.* 2000; Dunwiddie and Masino 2001; Latini and Pedata 2001). In support of the role of adenosine as an endogenous neuroprotective agent, mice lacking A_1-Rs show impaired functional recovery following ischemia (Johansson *et al.* 2001). Increased adenosine levels following ischemia have also been reported in the retina, and there is evidence that the subsequent A_1-R activation contributes to an endogenous retinal neuroprotective response to limit damage and increase tolerance to future ischemic episodes (Ghiardi *et al.* 1999; Li and Roth 1999).

Conclusion

In this chapter, I showed that adenosine reduced glutamate-induced calcium influx in rat RGCs through the activation of A_1-Rs. In summary, this work supports the

role of adenosine as a neuromodulator in the mammalian retina, and the postsynaptic effects of adenosine on RGCs could influence both physiological and pathophysiological glutamatergic signaling pathways.

CHAPTER 3: Functional Assessment of Glutamate Clearance Mechanisms in a Chronic Rat Glaucoma Model Using Retinal Ganglion Cell Calcium Imaging

Preface and Significance to Thesis

The retina possesses a powerful glutamate uptake system that keeps extracellular glutamate levels low. In conjunction with the effect of neuromodulatory compounds (investigated in Chapter 2), this glutamate clearance system is an additional mechanism by which neurotransmission can be regulated. The clearing of glutamate from the synaptic cleft by excitatory amino acid transporters helps to shape the visual signal by limiting both temporal (time glutamate remains in the cleft) and spatial (area of spillover of glutamate from the cleft) aspects of neurotransmission. In addition to a physiological role, glutamate transporters protect CNS neurons against the pathological consequences of prolonged or excessive exposure to glutamate (excitotoxicity). In glaucoma, a disease that results in RGC death, it has been proposed that a global and chronic rise in extracellular glutamate levels is a contributing factor. If glutamate levels are chronically elevated, there must be a corresponding deficiency in retinal glutamate clearance mechanisms.

In Chapter 2, I observed that glutamate was less potent than NMDA at inducing RGC calcium influx in the retinal wholemount preparation. This is consistent with many previous electrophysiology studies using intact retina preparations, as glutamate (but not NMDA) is recognized by glutamate transporters in these preparations and rapidly

cleared away. In this chapter, using the retinal wholemount preparation, I better characterize retinal glutamate clearance mechanisms by testing the effects of NMDA versus glutamate in the presence and absence of a glutamate uptake inhibitor, and I compare this to the effects of NMDA versus glutamate in isolated RGC cultures. I found that I could use the imaging of RGC calcium dynamics in retinal wholemounts challenged with exogenous glutamate as a novel methodology to assess glutamate transporter function. In improving on the technique from Chapter 2, I was able to image more RGCs per retina by: 1) dividing each retina into four pieces for separate imaging experiments; 2) incubating for a longer period of time to allow more RGC somata to be retrogradely labeled; 3) switching to an atmospheric culture medium (rather than a salt solution) to enhance tissue viability during the longer incubation; 4) placing a 0.6x tube before the CCD camera to expand the field of view; and 5) increasing excitation exposure time to enhance fluorescence. I then utilized this calcium imaging technique to assess whether the efficiency of glutamate uptake is altered following chronic exposure to elevated intraocular pressure (IOP) in an experimental rat glaucoma model.

Preliminary results of this work were presented at the ARVO Annual Meeting in 2004 (Hartwick ATE, Zhang X, Chauhan BC, Baldridge WH. Evidence for functional glutamate clearance mechanisms in a rat model of chronic pressure-related optic nerve damage. *Invest. Ophthalmol. & Vis. Sci.* 45: ARVO E-Abstract 1116). This work was subsequently published in the *Journal of Neurochemistry* (Hartwick ATE, Zhang X, Chauhan BC, Baldridge WH. 2005. Functional assessment of glutamate clearance mechanisms in a chronic rat glaucoma model using retinal ganglion cell calcium imaging. 94: 794-807), and copyright permission for the use of this paper is located in Appendix B. Dr. Xiaowei Zhang (a postdoctoral fellow at Dalhousie University at that time, co-supervised by Drs. Balwantray Chauhan and William Baldridge) performed the

IOP-elevating surgeries, and made the IOP measurements in these rats with experimental glaucoma. I acknowledge this contribution, and I have included the experimental glaucoma methodology and resulting IOP measurements in this chapter. Although I did not collect this data myself, this information is important to allow comparison of the calcium imaging data to the IOP exposure and optic nerve damage of each rat. I did take all of the pictures of the histological sections myself (taken after the data was tabulated and I was unmasked), and I made the IOP figures from the raw data I obtained from Dr. Zhang. I would also like to acknowledge Michele Archibald and Terry LeVatte, who were the two masked observers that graded axonal damage. Finally, in addition to my supervisor Dr. William Baldridge, I would like to acknowledge the valuable contribution of Dr. Balwantray Chauhan to the initial experimental design and final interpretation of the results presented in this chapter.

Introduction

Excessive or prolonged stimulation of glutamate receptors by the excitatory neurotransmitter glutamate can elevate the intracellular calcium concentration in many CNS neurons to lethal levels (Choi 1988; Sattler and Tymianski 2000). Glutamate excitotoxicity has been implicated in the neuronal death that occurs in acute pathologies such as stroke and trauma, and in several chronic neurodegenerative disorders (Lipton and Rosenberg 1994; Schwartz *et al.* 2003). Glaucoma, for which elevated intraocular pressure (IOP) is the most noxious known risk factor (Armaly *et al.* 1980; Sommer *et al.* 1991), is a chronic disease that culminates in progressive retinal ganglion cell (RGC) death and optic nerve damage (Quigley 1999). While glutamate excitotoxicity has been proposed as a contributing factor in the pathogenesis of glaucoma (Dreyer 1998;

Osborne *et al.* 2001; Lipton 2003), its role in this ocular condition has not been conclusively demonstrated and is controversial (see page 160 for more details).

In contrast to acute ischemia, in which neuronal death occurs on a relatively short timescale, it has been hypothesized that excitotoxic damage in glaucoma occurs following a more long-term exposure of RGCs to moderate extracellular levels of glutamate (Lipton 2003). Initial evidence supporting this hypothesis came from reports of increased vitreous glutamate levels in human patients and monkeys with experimentally elevated IOP (Dreyer *et al.* 1996), and from dogs (Brooks *et al.* 1997) and quails (Dkhissi *et al.* 1999) with spontaneous glaucoma-like conditions. More recent analyses of vitreous from human patients (Honkanen *et al.* 2003), and from monkeys (Carter-Dawson *et al.* 2002; Hare *et al.* 2004a; Wamsley *et al.* 2005) and rats (Levkovitch-Verbin *et al.* 2002a) with experimental glaucoma have refuted these findings. However, vitreous glutamate levels may not be indicative of the levels in the extracellular space surrounding RGC glutamate receptors. Thus, vitreous measurements alone are insufficient to confirm or to exclude that elevated IOP can induce a global rise in retinal glutamate levels sufficient to trigger excitotoxic RGC death.

Excitatory amino acid transporters (EAATs) maintain low extracellular glutamate levels in the CNS (Anderson and Swanson 2000; Danbolt 2001). In the retina, this is accomplished primarily by the action of EAAT1 (also known as the glutamate aspartate transporter, GLAST) on Müller glial cells (Rauen *et al.* 1998; Pow and Barnett 1999; Rauen 2000). Accordingly, a corollary to the hypothesis that a chronic elevation in extracellular glutamate levels contributes to glaucomatous RGC death is that retinal glutamate clearance mechanisms are inadequate. The experimental elevation of IOP in rats (achieved through a variety of techniques) is commonly used to model glaucomatous optic nerve damage (for reviews, see Goldblum and Mittag 2002;

Morrison *et al.* 2005), and a decrease in EAAT protein levels has been demonstrated in a rat glaucoma model (Martin *et al.* 2002). This result provides a potential mechanism underlying a rise in retinal glutamate levels in glaucoma, as it suggests that exposure to elevated IOP may directly affect EAAT expression and disrupt glutamate homeostasis. Nevertheless, the interpretation of this finding is difficult as a decrease in transporter protein levels may not signify a functional deficiency in glutamate uptake. For example, it may instead represent a physiological adaptation to changes in retinal synaptic activity.

If chronic exposure to elevated IOP causes a global reduction in the functional capacity of retinal glutamate clearance mechanisms, exogenously applied glutamate should be able to activate RGC glutamate receptors at lower concentrations. In this work, I tested this hypothesis by assessing the effect of glutamate on RGC calcium dynamics in retinal wholemounts prepared from rats with experimental glaucoma.

Methods

Retinal Wholemount Preparation

RGCs in living retinal wholemount preparations were loaded with calcium indicator dye using a method that was modified from Chapter 2. Immediately following enucleation, the anterior segment of each eye was removed and the eye-cups were immersed in Hibernate-A medium with 2% B27 supplements for the retina dissection. Each retina was carefully dissected and divided into four quadrants by cutting through the optic nerve head with the scalpel blade, and the resulting retinal pieces were then mounted on black filters (HABP 045; Millipore) with the RGC layer uppermost. A small volume (~0.5 μl) of 10% (dissolved in purified water) fura dextran (10,000 MW) was deposited into the approximate center of each retinal piece (passing through all the

retinal layers) using a tapered 26-gauge needle fitted to a 10 μl Hamilton syringe. The retinal dissection and fura injection methods are described in more detail in Chapter 2 on page 49. For the rats with experimental glaucoma, I performed the retinal dissections and calcium imaging experiments while masked both to treatment and to the IOP parameters of the treated and control eye from each rat.

To allow the dextran to be retrogradely transported to RGC somata, the retinal pieces were then incubated in the dark at room temperature in the Hibernate-A/B27 medium. For each rat with experimental glaucoma, there were up to eight retinal pieces consecutively imaged in one session (four retinal quadrants from the treated eye, and four from the control). After 7 h incubation, the first retinal piece (randomly selected) was transferred to the microscope chamber for calcium imaging. The remaining pieces were studied sequentially (alternating between samples from the two eyes), and as the imaging session on each retinal piece took approximately 1 h, all retinal pieces were studied 7-15 h following the fura dextran injection.

Purified RGC Cultures

Natural litters (6-12 pups for each experiment) of Long-Evans rats were killed at age 7 to 8 postnatal days by over-exposure to halothane and decapitation. Retinas were dissected from the eyes and then enzymatically and mechanically dissociated into a single-cell suspension as described on page 42 of this thesis. Purified RGC cultures were produced using a two-step panning procedure described originally by Barres and colleagues (1988), and described in detail earlier in Chapter 2 (beginning on page 43). In brief, the mixed retinal cell suspension was first incubated with rabbit anti-rat macrophage antibodies (1:75; Axell brand, Accurate Chemical) and placed on Petri dishes coated with goat anti-rabbit IgG (H+L) antibodies (Jackson ImmunoResearch) to

remove macrophages. The remaining cells were then transferred to a Petri dish that had first been coated with goat anti-mouse IgM (μ chain) antibodies (Jackson ImmunoResearch) and second with anti-Thy1.1 monoclonal IgM antibodies (cell line T11D7e2; American Type Culture Collection). The adherent RGCs were released by manually pipetting an enzyme inhibitor solution along the surface of the dish after incubation in a 0.125% trypsin solution. This technique yields RGC cultures that are 97-99% pure (Barres *et al.* 1988; and see Chapter 2 of this thesis).

The RGCs were plated onto poly-D-lysine/laminin-coated Biocoat glass coverslips (BD Biosciences) in 4-well tissue culture plates at a density of 3.5×10^4 cells per well. The cells were cultured in 600 μl of serum-free culture medium consisting of Neurobasal-A with 2% B27 supplements, 1 mM glutamine, 50 ng/ml BDNF, 10 ng/ml CNTF, 5 μM forskolin, and 10 μg/ml gentamicin. Cultures were maintained at 37°C in a humidified 5% CO_2-air atmosphere. For calcium imaging, the cells were incubated at 37°C for 30 min in a solution of 5 μM fura-2 AM calcium indicator dye, which was first dissolved in DMSO (0.1% final concentration) and then in modified Mg^{2+}-free Hanks' balanced salt solution (HBSS) containing 0.1% pluronic acid F-127. Calcium imaging on isolated RGCs was performed on the two days following immunopanning.

Rat Glaucoma Model

Adult male Brown Norway rats were housed in a constant low-light (80 lux) environment and given food and water *ad libitum*. The method described by Morrison and colleagues (1997), with modifications (Chauhan *et al.* 2002), was used to elevate IOP in one eye of each animal while the fellow eye served as an untreated control. This procedure was performed by Dr. Xiaowei Zhang, a postdoctoral fellow at Dalhousie University. Briefly, a lateral canthotomy was performed on rats anesthetized with a

ketamine-xylazine cocktail, and a 5.5 mm polypropylene ring with a 1 mm gap was placed around the equator of the eye. The ring was oriented so that blood flow in all vessels was blocked with the exception of one episcleral vein. A micropipette, made using a pipette puller (P-97; Sutter, Novato, CA) and a beveller (1300M; World Precision Instruments, Sarasota, FL), was inserted along the long axis of the unobstructed vein, and 50 μL of a hypertonic saline solution (1.75 M NaCl) was injected into the vein. To standardize the injection force, a syringe pump (sp 200I; World Precision Instruments) was used to set the injection flow rate at 250 μL/min. One week later, the injection procedure was repeated on a second episcleral vein in all treated eyes. The saline injection results in sclerosis of the trabecular meshwork, leading to reduced aqueous outflow and increased IOP.

A handheld tonometer (Tonopen-XL; Innova, North York, ON) was used by Dr. Zhang to measure IOP in conscious animals as described previously (Chauhan *et al.* 2002). Following instillation of a topical anesthetic drop (proparacaine hydrochloride; Alcon, Mississauga, ON), approximately 10 readings were obtained from each eye and the resulting mean was taken as the IOP measurement for the day. The baseline IOP was measured prior to the injection of the episcleral vein, and follow-up measurements were taken at approximately the same time of day. Peak Δ IOP for each rat was recorded as the maximum IOP difference (in mm Hg) between the experimental eye and the untreated eye at any time during follow-up. The duration of IOP elevation was defined as the number of days between the second hypertonic saline injection and the death of the animal. The Δ IOP integral (in mm Hg-days) was calculated as the integral of the IOP difference between the experimental and control eyes over the course of the study, and provided a measure of the cumulative exposure of the treated eye to elevated

IOP. Descriptions of these IOP parameters and their relationship to RGC loss are detailed elsewhere (Chauhan *et al.* 2002).

Optic Nerve Histology

The animals with experimental glaucoma were killed at a variety of times (7-36 weeks) following IOP elevation by overdose of pentobarbital sodium (340 mg/mL) administered intraperitoneally, and the eyes were enucleated. Care was taken to preserve the maximum length of optic nerve, which was then cut approximately 1 mm behind the globe. The nerve stump was fixed immediately in 2.5% glutaraldehyde, embedded in an epoxy mounting medium (Epon Araldite; Mirivac, Halifax, NS) and sectioned. Thick sections (~1 μm) were stained with 1% p-phenylenediamine (Sigma) and axon damage was graded on a scale ranging from 0 (no damage) to 10 (complete damage) under light microscopy using a 40x (NA 0.75) objective. The whole optic nerve section was viewed and the damage grade approximately reflected the estimated percentage of axonal damage in the entire optic nerve section (e.g. grade 7 is equivalent to roughly 70% damage). The final grade was based on agreement between two observers masked to treatment (Michele Archibald and Terry LeVatte, at Dalhousie University). For illustration, I acquired digital images of optic nerve sections using a 100x (NA 1.30) objective (Nikon, Mississauga, ON).

Calcium Imaging

A 75 W Xenon lamp (LUDL Electronic Products) and the appropriate filters (XF04 set, excitation 340 or 380 nm; emission 510 nm; dichroic > 430 nm; Omega Optical) were used to generate fura fluorescence. The details of the imaging rig used in this study are described in Chapter 2 on page 46, with the modification that a 0.6x coupling

tube (HRP060; Diagnostic Instruments, Sterling Heights, MI) was placed between the cooled charged-coupled device (CCD) camera (Sensicam; PCO Computer Optic) and microscope to expand the field of view afforded by the 40x (NA 0.80 W) objective (Carl Zeiss). The period of excitation illumination was set at 1000-1500 ms for the retinal wholemounts and at 400 ms for the isolated cells. The captured fluorescence images (12-bit processing, 4 X 4 binned) were converted to ratiometric (340 nm/380 nm) images by imaging software (Imaging Workbench 2.2; Axon Instruments).

The retinal wholemounts (on filters) and isolated RGCs (on coverslips) were transferred to the microscope chamber that was constantly superfused with Mg^{2+}-free Hanks' balanced salt solution (HBSS; 2.6 mM $CaCl_2$, 15 mM HEPES, pH 7.4). The HBSS was warmed to 34-36°C, bubbled with 100% oxygen, and delivered to the chamber by a peristaltic pump at a rate of approximately 1 ml/min. The treatment solutions of glutamate, NMDA, and DL-threo-β-benzyloxyaspartate (TBOA; Tocris, Ellisville, MO) were dissolved in the Mg^{2+}-free HBSS on the day of each experiment, and delivered to the chamber by the peristaltic pump. Following drug treatment, the retinal pieces were again constantly superfused with the HBSS to allow for drug wash-out. Glycine (10 μM) was included in NMDA and glutamate treatment solutions for the isolated RGCs. During treatments, image pairs were collected as often as every 10 s (5 s for isolated RGCs) but to limit photodamage, images were collected less frequently (40-60 s) during intervening periods.

Data Analysis

Using the imaging software, circular regions of interest were drawn around all visible cell somata that exhibited fluorescence with 380 nm excitation, and the mean fura ratio within each region was monitored throughout the experiments. The response to

each treatment (i.e. NMDA or glutamate) was calculated as the Δ fura ratio, the peak fura ratio minus baseline fura ratio. The baseline fura ratio for every cell was calculated as the average fura ratio measured in the three images prior to each treatment, and the peak ratio was the maximum ratio value obtained in the 400 s following each treatment. For illustration, fura ratio traces of RGCs from retinal wholemounts were corrected for a gradual decrease in baseline ratio due to decreasing background fluorescence, likely attributable to the washing away of fura dextran (excess spillage from the injection) from the retinal surface. All data analysis was performed on the non-baseline-corrected raw data. In experiments on isolated RGCs, background fluorescence remained stable and was measured from a region on the coverslip devoid of RGCs and subtracted from each image. In 28 of the 69 isolated RGCs tested in this work, the minimum (in calcium-free solution) and maximum (in calcium-saturated solution) values of fura-2 fluorescence were determined at the end of the experiment. Using a K_d for fura-2 of 224 nM, the averaged minimum and maximum fluorescence values obtained from these calibrations were used to convert the fura-2 ratios for all of the isolated RGCs to absolute calcium levels (for detailed method, see Kao 1994 and Appendix A of this thesis).

All data in this chapter are expressed as the mean ± 1 SD. In the experiments with TBOA and different NMDA concentrations, statistical within-cell comparisons were made on the normalized data using the nonparametric Friedman repeated-measures ANOVA and the Tukey multiple-comparison post-hoc test. In the experiments on retinas from the rats with unilateral experimental glaucoma, comparisons of the RGC responses from treated versus untreated retinas were made on the normalized data with the Mann-Whitney rank sum test. A value of $P < 0.01$ was used to determine statistical significance.

Results

Optical Imaging of RGC Calcium Dynamics in Living Retinal Wholemounts

Injection of the dextran-conjugated calcium indicator dye into the retinal wholemount preparations resulted in the loading of the dye into RGC axons passing through the injection site (Figure 3-1). Following an incubation period (7-15 h), the fura dextran was transported along the RGC axons in both the anterograde (towards the optic nerve head) and retrograde direction. Retrograde versus anterograde direction was determined by examining the bifurcation pattern of adjacent or overlying retinal blood vessels under white light. In the retrograde direction, many fura-loaded RGC somata, of varying sizes, could be seen in the ganglion cell layer (GCL) in close proximity to the labeled RGC axons. Displaced amacrine cells are also present in the rat GCL, and it is possible that some of the labeled cell somata near (< 100 μm) the injection site were amacrine cells whose neurites had been injected with dextran. Unlike the axonal loading of RGCs, the dendrite or neurite loading of RGCs or displaced amacrine cells, respectively, can occur in any direction from the injection site. Labeled cells more than 100 μm from the injection site were noted in the retrograde direction of RGC axon bundles, but almost never in the anterograde direction (Figure 3-1 A). In this work, all experiments were performed on dextran-loaded cell bodies that were located in the GCL near labeled RGC axon bundles. As the dye injection was made in the approximate center of each retinal piece (each retina had been cut at the optic nerve head into four pieces), the RGCs tested in this study were located in the paracentral to mid-periphery region of the retinas. In selecting the labeled cells for study, the edge of the field of view was set up on the edge of the fura dextran injection site and then moved roughly half a field of view away in the direction of the retrogradely labeled RGC axons.

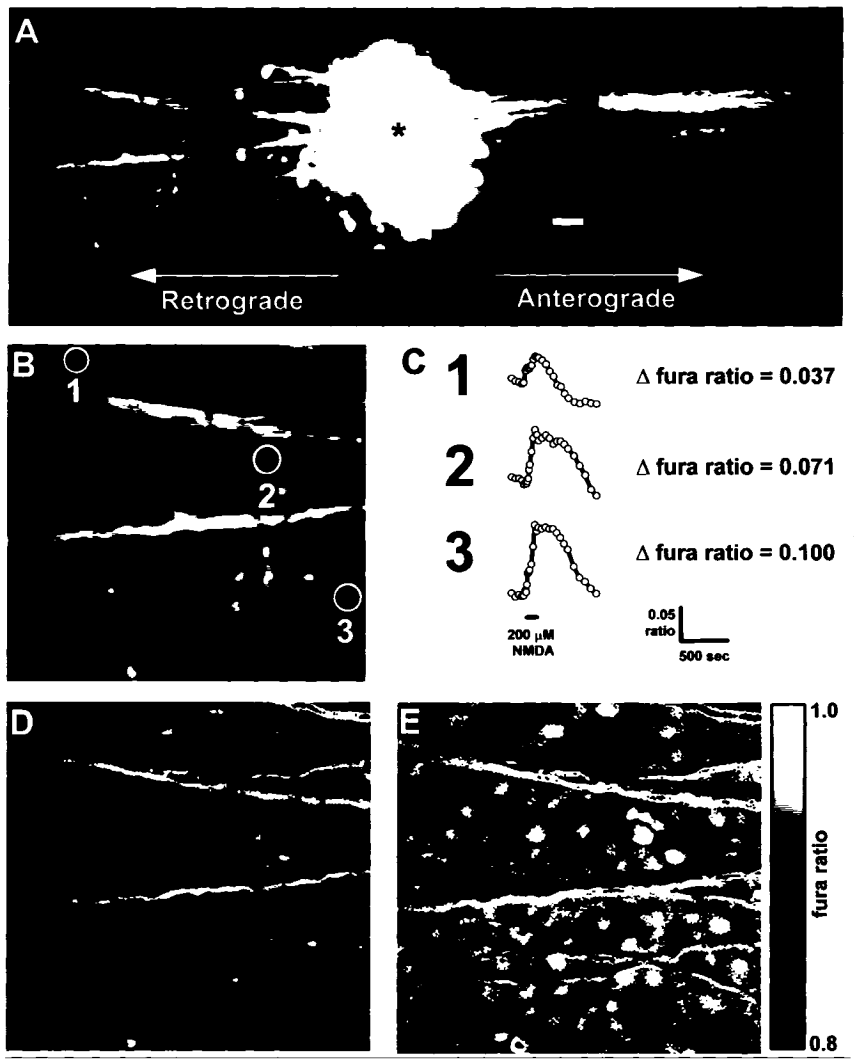

Figure 3-1. Calcium imaging of RGCs in retinal wholemounts. **(A)** Montage of fluorescent micrographs (380 nm excitation, 510 nm emission) showing the retrograde loading of RGC somata following injection of fura dextran calcium indicator dye into the retina (injection site denoted by asterisk). Scale bar, 50 μm. **(B)** Higher magnification view of the cells present at the far left in (A), highlighting three individual RGCs and **(C)** the fura ratio (340/380 nm) traces for these three example cells when the retinal piece was exposed to 200 μM NMDA for 2 minutes (Δ fura ratio = peak minus baseline ratio, and is indicative of the change in RGC internal calcium levels). **(D)** Grayscale fura ratio image, following background subtraction, for the same RGCs at baseline and **(E)** at peak response to 200 μM NMDA.

With a field of view of approximately 400 μm, the imaged cells were therefore located at least 100 μm away from the injection site and generally between 200 and 600 μm away. Thus, it is highly likely that the imaged cells in these studies were exclusively RGCs and not displaced amacrine cells in the RGC layer.

I previously loaded dextran-conjugated fura calcium indicator dye into RGCs in adult rat retinal wholemounts (Chapter 2), and the present work represents an enhancement of this technique. The increased incubation time (7-15 h post-injection), facilitated with the use of Hibernate-A/B27 culture medium, enabled the retrograde loading of fura dye into many more RGC somata (on average, 40-60 RGCs in a given field of view) in the present study. However, the fura injection technique did not appear to load the calcium indicator dye equally into every RGC. In general, the raw fluorescence values (under either 340 or 380 nm excitation) were lower in RGCs furthest from the injection site, suggesting that these cells had lower intracellular fura concentrations relative to cells closer to the injection site (Figure 3-1 A,B). Exposure of the retinal wholemounts to the glutamate agonist NMDA (200 μM) caused an increase in the fura fluorescence ratios (340/380 nm) in RGC somata that is indicative of increased intracellular calcium levels (Figure 3-1 D, E). Although the use of a ratiometric calcium imaging dye such as fura helps to offset differences in dye loading (Kao 1994), the RGCs with lower raw fluorescence tended to display smaller absolute increases in the Δ fura ratio (peak minus baseline fura ratio). To illustrate this point, the NMDA responses of three individual RGCs, located at varying distances from the injection site (Figure 3-1 B), are highlighted in Figure 3-1 C. To compensate for potential inter-cell differences in absolute increases in the fura ratio, which could represent differences in dye loading rather than differences in the calcium signal, all treatment responses in subsequent experiments were normalized to each individual RGC's response to 200 μM NMDA.

Cells that had a Δ fura ratio less than 0.03 in response to the initial NMDA treatment were excluded from analysis, as these responses were deemed too low to distinguish a true calcium signal from background noise. The threshold criteria of 0.03 also ensured that regions not encircling RGC somata were excluded from analysis, as the Δ fura ratio measured in an area of background or in an RGC axon never met this criteria following treatment with NMDA.

Glutamatergic RGC Calcium Dynamics in Retinal Wholemounts and in Purified Cultures

It has been well-established in previous electrophysiological studies that very high (millimolar) concentrations of glutamate must be exogenously applied to increase RGC activity in the intact retina (for review, see Thoreson and Witkovsky 1999). It is presumed that this is because glutamate is cleared by retinal EAATs before it can stimulate RGC glutamate receptors. I demonstrated the presence of functional EAATs in this intact retina preparation by first testing the effect of glutamate on RGCs (n = 215) in retinal wholemounts (N = 4; from 3 eyes) from untreated control rat eyes (Figure 3-2 A, B). Application of 500 μM glutamate had no effect on RGC calcium dynamics, even though these cells responded to 200 μM NMDA. However, in the presence of the EAAT inhibitor TBOA (250 μM; present during the 2-min glutamate treatment and for 1 min both pre- and post-treatment), exposure of these same cells to 500 μM glutamate resulted in significantly increased ($P < 0.01$) fura ratios. Subsequent application of 250 μM TBOA for the same duration (4 min) on its own also induced a detectable calcium signal, but this response was significantly less ($P < 0.01$) than that induced by the glutamate plus TBOA combination. The cells were exposed to NMDA a final time to confirm the stability of NMDA-receptor-mediated RGC responses over time in this

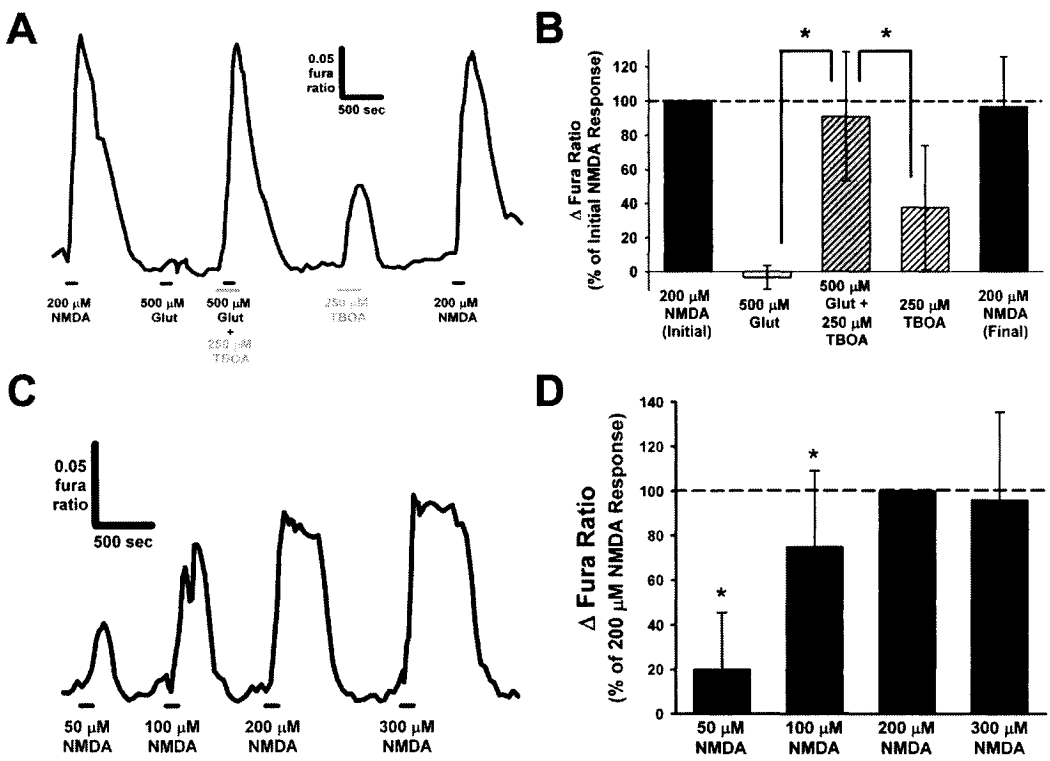

Figure 3-2. Comparative effects of NMDA and glutamate on calcium dynamics of RGCs in retinal wholemounts. **(A)** Example fura ratio trace illustrating the effect of glutamate (500 µM) on RGC calcium dynamics both in the presence and absence of the glutamate transporter inhibitor TBOA (250 µM), and in comparison with the effect of NMDA (200 µM). **(B)** Mean data (± 1 SD) for all RGCs (n = 215) from the retinal wholemounts (N = 4 retinal pieces, from 3 eyes) in which TBOA was tested, normalized to the initial NMDA response (dashed line). * $P < 0.01$, Friedman ANOVA, Tukey post-hoc. **(C)** Example fura trace of an RGC responding to increasing concentrations (50 - 300 µM) of NMDA and **(D)** mean data (± 1 SD) for the NMDA concentrations-response studies (n = 125 RGCs; N = 3 retinal pieces, from 3 eyes), normalized to 200 µM NMDA response (dashed line). * $P < 0.01$, Friedman ANOVA, Tukey post-hoc, compared to 200 µM NMDA response.

wholemount preparation (Figure 3-2 A, B). These experiments serve as a positive control to verify that a decrease in glutamate transporter function, induced pharmacologically, is associated with an increase in the sensitivity of the RGCs in intact retina preparations to exogenously applied glutamate.

To determine the dynamic range and sensitivity limits of this calcium imaging method, I studied the relative effect of different concentrations of NMDA (50-300 μM) on RGC calcium dynamics (Figure 3-2 C, D; n = 125 RGCs; N = 3 retinal pieces from 3 eyes). Application of 50, 100 and 200 μM NMDA elicited detectable calcium responses of increasing magnitude (all responses significantly different from each other; $P < 0.01$), but the response to 300 μM NMDA was, on average, approximately the same as for 200 μM NMDA ($P > 0.05$). This suggests that fura fluorescence may have reached saturation, and that larger treatment responses (roughly equal to or greater than the calcium influx induced by 200 μM NMDA) may be underestimated, such as the response to 500 μM glutamate with 250 μM TBOA present (Figure 3-2 B). However, these results show that the technique was sensitive enough to detect a calcium signal induced by as little as 50 μM NMDA, and that 500 μM glutamate (without TBOA present) was below this detection threshold in retinas from untreated rats (compare Figure 3-2 A, B to C, D).

These results clearly show that NMDA can induce RGC calcium influx at lower concentrations than necessary for glutamate in this intact retina preparation, even though glutamate is a more potent agonist than NMDA at the NMDA-type glutamate receptor (Hollmann and Heinemann 1994). Unlike glutamate, the non-endogenous NMDA is not recognized by EAATs and thus is not influenced by retinal glutamate uptake. To gain an estimate of the efficiency of retinal glutamate clearance mechanisms, I sought to compare the relative calcium signal induced by glutamate and

NMDA in purified rat RGC cultures. In the intact retina, glutamate levels in the extracellular space around RGC glutamate receptors are influenced by the presence of glutamate transporters on other retinal cell types, particularly EAAT1 on Müller cells and EAAT2 on bipolar cells (Rauen 2000). As these retinal cell types are removed in the generation of the purified RGC cultures, the influence of retinal EAATs on exogenously applied glutamate is absent. Thus, the effect of glutamate on individual RGCs in isolation (Figure 3-3 E) can be directly assessed. As in previous work (see Chapter 2), the relatively low concentration of 10 μM glutamate increased the internal calcium levels in the isolated RGCs and each RGC was subsequently exposed to 50, 100 and 200 μM NMDA (as example in Figure 3-3 A; n = 35 RGCs, pooled from 3 separate cultures). The average calcium influx induced by the four treatments, measured as the Δ fura-2 ratio and normalized to the initial 10 μM glutamate response, were significantly different from each other ($P < 0.01$), with the exception of 10 μM glutamate versus 200 μM NMDA ($P > 0.05$) (Figure 3-3 B; dark bars). In these calcium imaging experiments on isolated cells, I also converted the fura-2 ratios to absolute calcium concentrations via a calibration protocol (see Appendix A), but this did not change the findings of statistical significance found using fura-2 ratios (Figure 3-3 B; open bars). To ensure that the similarity of the 10 μM glutamate and 200 μM NMDA responses was not due to saturation of the calcium dye (as appeared to occur at greater treatment concentrations in the retinal wholemount experiments with fura dextran), I tested 200 μM NMDA versus 50 μM glutamate in a separate group of cells (n = 34 RGCs, pooled from 3 separate cultures). The response to 50 μM glutamate was roughly 3 times greater than 200 μM NMDA ($P < 0.01$; Figure 3-3 C, D), indicating that saturation did not occur. Thus, in the absence of EAATs, these results indicate that the calcium influx induced by 200 μM

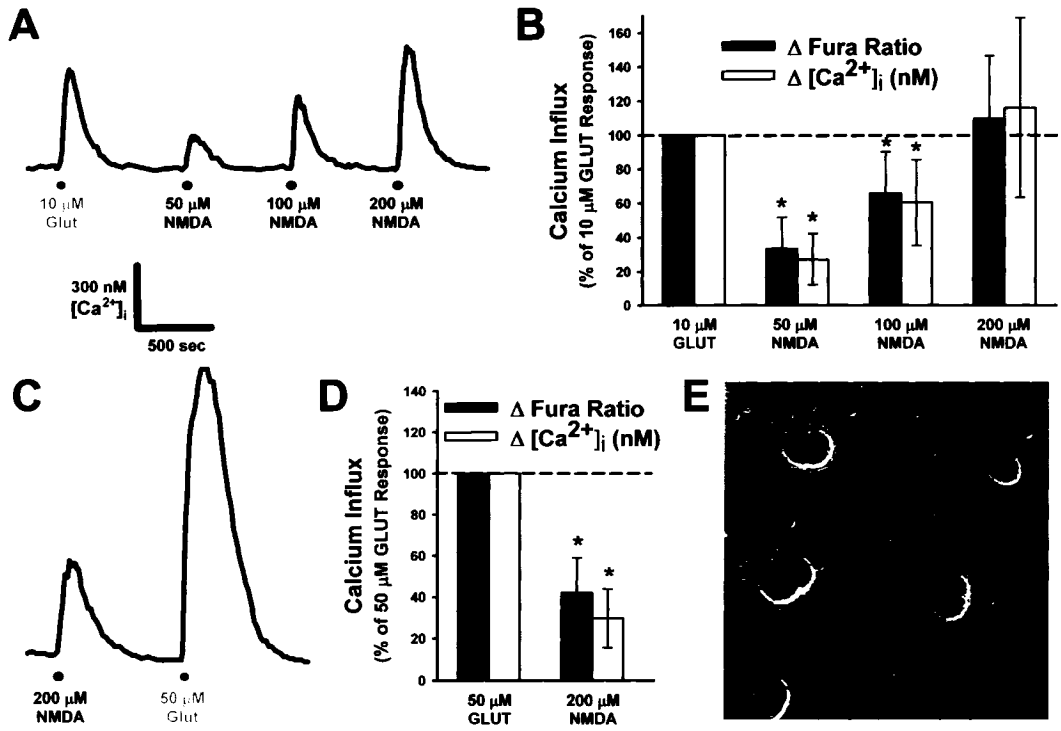

Figure 3-3. Comparative effects of NMDA and glutamate on calcium dynamics of isolated RGCs in purified cultures. **(A)** Trace of the intracellular calcium concentration ($[Ca^{2+}]_i$) in a representative RGC illustrating the effect of glutamate (10 μM) in comparison to the effect of increasing concentrations of NMDA (50 - 200 μM). Scale bar applies to both traces in (A) and (C). **(B)** Mean data (± 1 SD) for all tested RGCs (n = 35, pooled from 3 separate cultures), normalized to the glutamate response (dashed line). Both the Δ fura-2 ratios (dark bars) and Δ $[Ca^{2+}]_i$ (following conversion of the ratios to absolute calcium levels; open bars) are shown. * $P < 0.01$, Friedman ANOVA, Tukey post-hoc, compared to glutamate response. **(C)** Example $[Ca^{2+}]_i$ trace of an RGC responding to 200 μM NMDA and 50 μM glutamate, and **(D)** mean data (± 1 SD) for tested RGCs (n = 34, pooled from 3 separate cultures), normalized to glutamate response (dashed line). The mean baseline $[Ca^{2+}]_i$ for all tested isolated RGCs (n = 69) in these experiments was 75.1 nM ± 40.8 SD. * $P < 0.01$, Friedman ANOVA, Tukey post-hoc, compared to glutamate response. **(E)** Differential interference contrast image of cultured RGCs, one day after plating. Scale bar = 25 μM.

NMDA in rat RGCs is approximately equivalent to 10 μM glutamate, and is much less than that induced by 50 μM glutamate.

Effect of Glutamate on RGCs from Eyes with Experimental Glaucoma

To test the hypothesis that elevated IOP in glaucoma causes a global deficiency in glutamate transporter function, a rat model of chronic IOP elevation was used. This model exhibits RGC death and optic nerve damage resembling the pathology of glaucoma (Morrison et al. 1998; Chauhan et al. 2002). Rats were selected to encompass a range of IOP parameters, and subsequent grading on a scale of 0 to 10 of the optic nerve sections revealed damage that ranged from mild to severe (Table 3-1). The IOP parameters, optic nerve histology, and RGC fura dextran loading for a rat with mild (rat 3; grade 2 damage), moderate (rat 6; grade 7 damage), and severe (rat 5; grade 10 damage) optic nerve damage are shown in Figure 3-4. For rat 3, the IOP started to elevate roughly 2 weeks post-saline injection and remained consistently about 12-13 mm Hg higher than the control eye (Figure 3-4 A) for the duration of follow-up. In comparison to rat 3, rat 6 was maintained for a longer duration of chronic IOP elevation (Δ peak IOP of 13.0 mm Hg; Figure 3-4 B), and rat 5 exhibited a larger IOP rise in its treated eye (Δ peak IOP of 20.9 mm Hg; Figure 3-4 C). Organized bundles of RGC axons were observed in the optic nerve sections from the untreated eyes of these three rats (Figure 3-4 D, H, L). Conversely, in the optic nerve sections from the treated eyes, early signs of axonal degeneration and myelin debris were evident for rat 3 (grade 2 damage; Figure 3-4 E), more extensive axonal degeneration and disorganization of the axon bundles were apparent for rat 6 (grade 7 damage; Figure 3-4 I), and severe damage with near-complete axonal loss and widespread gliosis were noted for rat 5 (grade 10 damage; Figure 3-4 M). The fura dextran injection resulted in similar RGC

Rat ID	Peak Δ IOP (mm Hg)	Δ IOP Integral (mm Hg-days)	Duration of IOP Elevation (days)	Treated Optic Nerve Grading (scale 0-10)
1	21.6	767	84	1
2	21.1	792	51	1
3	13.2	1000	103	2
4	28.6	1728	71	9
5	20.9	1070	70	10
6	13.0	2013	251	7
7	21.8	1291	113	8
8	22.8	2529	145	10

Table 3-1. Summary of intraocular pressure (IOP) parameters and grading of optic nerve damage for eyes treated with saline injection to elevate IOP. Rats 1 to 5 were used to test the effect of 100 and 500 μM glutamate while rats 6 to 8 were used to test the effect of 1000 and 2000 μM glutamate on RGCs in retinal wholemounts. See page 79 for details on the calculation of these parameters.

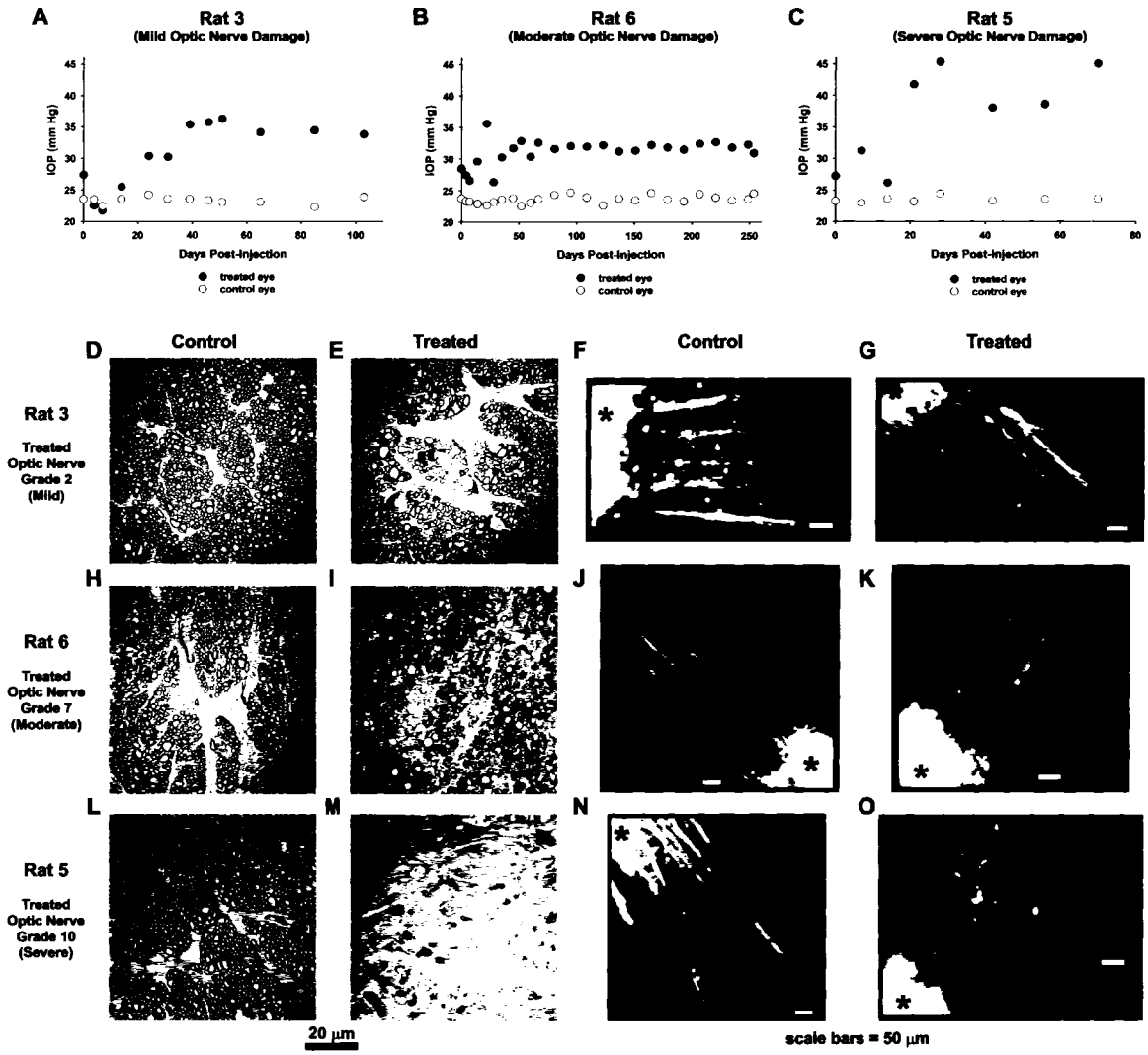

Figure 3-4. Rat glaucoma model of chronic intraocular pressure (IOP) elevation. **(A, B, C)** IOP measurements during course of study for three rats that had histological characteristics of **(D, E)** mild (rat 3), **(H, I)** moderate (rat 6), and **(L, M)** severe (rat 5) optic nerve damage in the treated eyes as compared to the undamaged optic nerve from the fellow untreated eyes. Corresponding fluorescent micrographs (380 nm excitation, 510 nm emission) show the retrograde loading of fura dextran into RGC somata (injection site denoted by asterisk) from representative retinal pieces obtained from these same rats: **(F, G)** rat 3, **(J, K)** rat 6, and **(N, O)** rat 5. Note the reduced number of labeled RGC somata and axons in the retinal piece from rat 5, which exhibited severe optic nerve damage.

loading in retinal pieces from both the treated or untreated eye of rat 3 (Figure 3-4 F,G), but there were only a few faint axons emanating from the injection site and far fewer labeled RGCs in retinal pieces from the treated eye, relative to the untreated eye, of rat 5 (Figure 3-4 N, O). The robustness of the fura-loaded axons and RGCs in rat 6 was more intermediate between that observed for rats 3 and 5 (Figure 3-4 J,K). This was consistent with the expected result that in rats with greater optic nerve damage, there is a greater loss of RGC somata in the retina and thus fewer cells available for loading with calcium indicator dye. Although the number of fura dextran-loaded RGCs present in a microscope view of 3-4 retinal pieces from a given eye likely provides only a crude estimate of relative RGC numbers, there were fewer numbers of RGCs in the retinal pieces from eyes with severe optic nerve damage (see Figures 3-5 and 3-6; n = total RGCs imaged, and N = number of retinal pieces imaged from each eye).

The effects of 100 μM and 500 μM glutamate on RGCs were assessed in retinal wholemounts prepared from five rats (Figure 3-5; Table 3-1). Dividing each retina into four pieces increased the number of RGCs imaged from each eye, although all four pieces per eye were not always successfully imaged. The usual reason for exclusion of a retinal piece is that it did not remain firmly adhered to the filter on which it was mounted, and this occurred most frequently near the end of imaging sessions (~14-15 h). Representative traces from a single RGC and the summary data for all the RGCs from each retina are shown for rat 3 (Figure 3-5 A, B, C) and rat 5 (Figure 3-5 D, E, F), the rats with mild and severe optic nerve damage, respectively, that were profiled in Figure 3-4. Similar results were observed in the retinal preparations from the other three rats (Figure 3-5 G, H, I). Although the RGCs responded to 200 μM NMDA, indicating that functional NMDA receptors were present, the application of 100 or 500 μM glutamate did not affect calcium levels in the RGCs from any of the eyes, regardless of

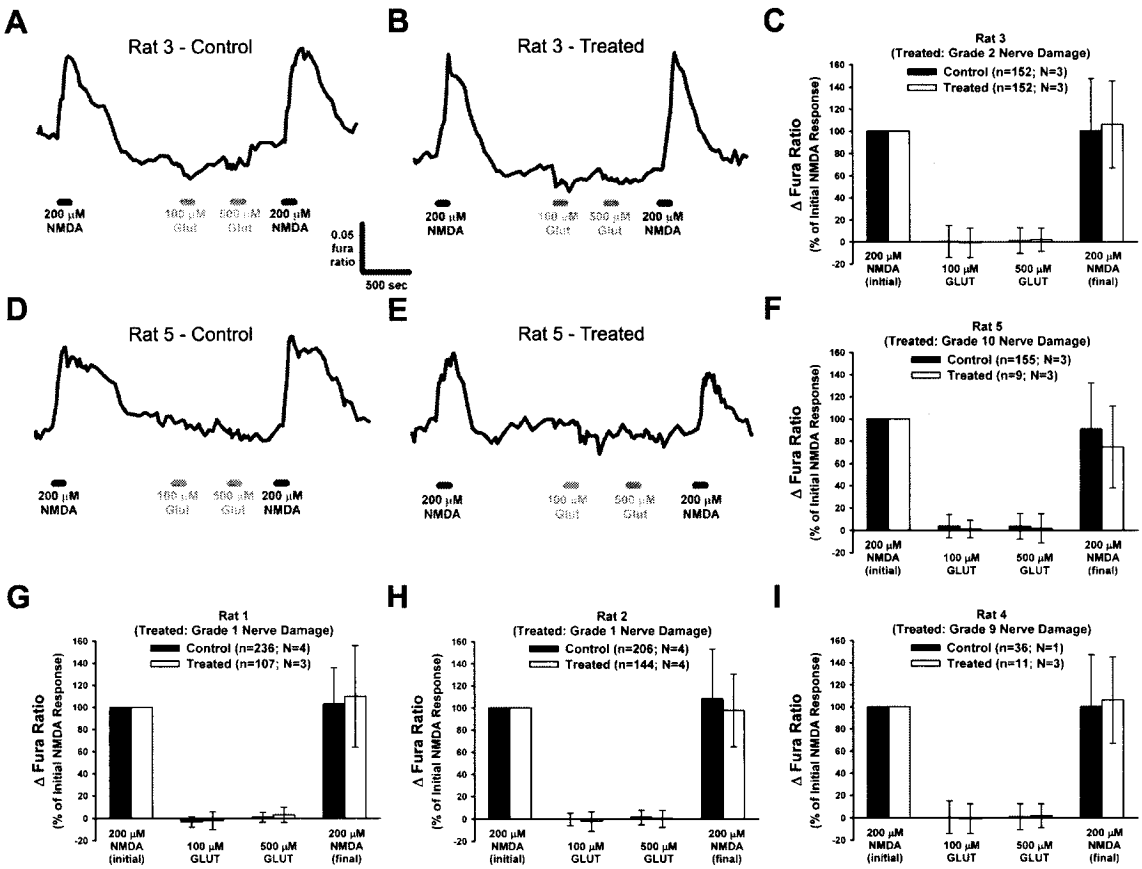

Figure 3-5. Effect of 100 µM and 500 µM glutamate on RGC calcium dynamics in rat glaucoma model. **(A, D)** Example fura ratio traces for RGCs from untreated and **(B, E)** treated (saline-injected to elevate IOP) eyes, and the **(C, F)** mean data (± 1 SD) of RGC responses from two rats (profiled in Figure 3-4) that had (A-C) mild (Grade 2) and (D-F) severe (Grade 10) optic nerve damage. **(G-I)** Data summary for the other three rats tested (n denotes number of RGCs imaged; N denotes number of tested retinal pieces). At these concentrations, glutamate had no detectable effect on RGC calcium dynamics in retinal pieces from either treated or untreated eyes.

the IOP parameters oroptic nerve damage. The Δ fura ratios were essentially zero (the method used to calculate the Δ fura ratio could yield a negative response if the peak ratio following treatment was less than the averaged baseline ratio), and there was no difference ($P > 0.01$) in any of the responses in RGCs from treated versus untreated eyes. The cells responded again to a final exposure to 200 μM NMDA, showing that the lack of an effect by glutamate was not due to response 'run-down' or cell death during the calcium imaging experiments. These results indicate that glutamate clearance mechanisms were functional and able to sufficiently clear glutamate at these concentrations.

Three more rats, all with moderate to severe optic nerve damage in the treated eyes, were chosen to assess the effect of 1000 and 2000 μM glutamate (Figure 3-6; Table 3-1). These concentrations elicited a detectable response, but the average response was less than that induced by 200 μM NMDA. There was no significant difference ($P > 0.01$) in the response to 1000 μM glutamate in RGCs from treated eyes versus untreated eyes in any of the 3 rats. There was a small but statistically significant ($P < 0.01$) increased response to 2000 μM glutamate in RGCs from the treated eye of rat 7, relative to the untreated eye, but the effect of 2000 μM glutamate was not significant in the other two rats (Figure 3-6 A,B,C). Example traces from individual RGCs illustrates the effect of these higher concentrations of glutamate on RGC calcium dynamics, as compared to the effect of 200 μM NMDA (Figure 3-6 D,E). There was a small but significant ($P < 0.01$) decrease in the final NMDA response in the RGCs from the treated eyes of rats 7 and 8, indicating a decrease in the recovery response for these eyes with severe optic nerve damage.

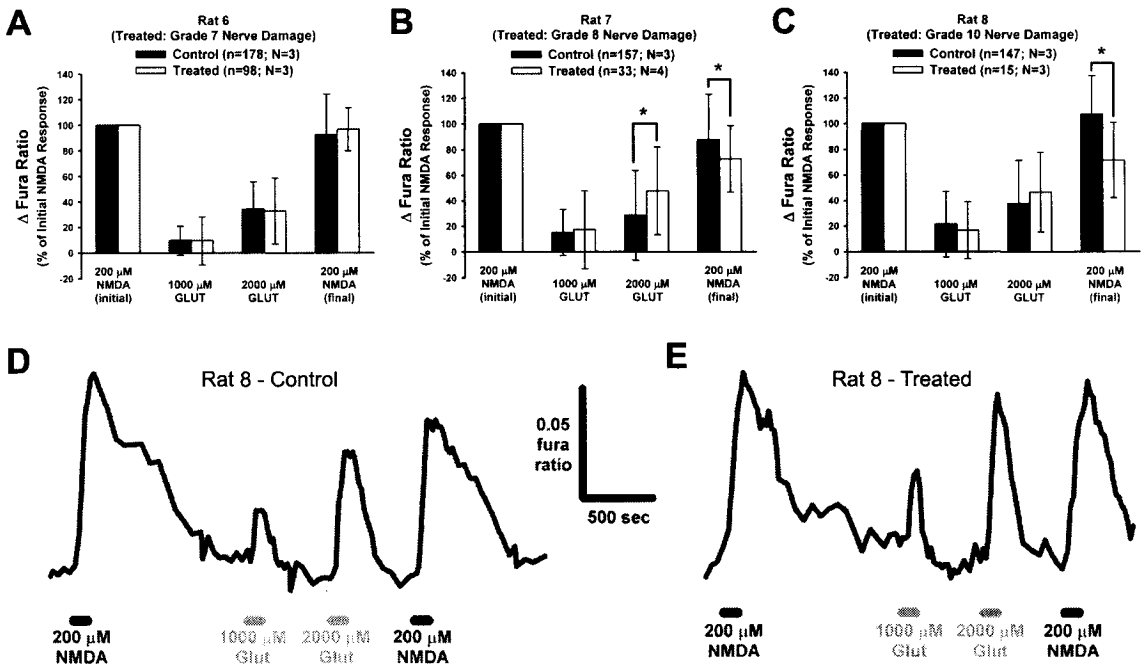

Figure 3-6. Effect of 1000 μM and 2000 μM glutamate on RGC calcium dynamics in rat glaucoma model. **(A-C)** Summary of mean data (± 1 SD) of RGC responses from the three rats tested, showing these glutamate concentrations induced a detectable calcium signal in RGCs from both treated and untreated eyes (n denotes number of RGCs imaged; N denotes number of tested retinal pieces). * $P < 0.01$, Mann-Whitney. **(D, E)** Example fura ratio traces illustrating effect of 1000 and 2000 μM glutamate, relative to 200 μM NMDA, in an RGC from the treated and untreated eye of the same rat.

Discussion

In this work, I functionally assessed glutamate uptake in retinas from rats with experimental glaucoma as compared to untreated control retinas. The optical imaging of RGC calcium dynamics in retinal wholemounts represents a novel methodology to assess the vulnerability of RGCs to excessive glutamate receptor activation. Using this technique, I found that RGCs from eyes with experimental glaucoma were no more sensitive to exogenous glutamate than RGCs from the fellow untreated eyes.

Assessing Retinal Glutamate Clearance through RGC Calcium Imaging

In contrast to isolated RGCs in culture, the loading of membrane-permeable calcium indicator dyes such as fura-2 AM into RGCs in adult mammalian intact retina preparations is generally ineffective, likely because of an inability of the dye to penetrate the neuropil and Müller cell endfeet that envelope RGCs (Baldridge 1996; Kettunen *et al.* 2002). In this work, dextran-conjugated fura dye was retrogradely loaded into RGC somata in wholemount preparations, building on previous studies using rabbit (Baldridge 1996) and rat (Chapter 2 of this thesis) retinas. The RGC intracellular calcium levels were used as a 'sensor' of RGC glutamate receptor stimulation, and therefore as an indicator of the functional capacity of retinal glutamate uptake. Unlike electrophysiological recordings that require one cell to be tested at a time, a strength of this imaging technique is that it allows the simultaneous imaging of a relatively large number of RGCs. I was able to image up to 236 RGCs (and consistently more than 150 RGCs) from a single eye, and thus this technique shows promise for future studies where experimentation on large numbers of RGCs, in an intact retina preparation, is desirable.

While the efficiency of glutamate clearance mechanisms protects neurons from pathological glutamatergic signaling pathways, it is also necessary for the normal control of excitatory synaptic transmission (Higgs and Lukasiewicz 1999; Takayasu *et al.* 2004). By evaluating the relative effect of glutamate on RGC calcium dynamics in retinal wholemounts versus isolated cell cultures, the effectiveness of EAATs in the rat retina was demonstrated. Application of 10 μM glutamate induced a robust calcium signal in RGCs in the purified cultures, while 500 μM glutamate had no detectable effect on RGCs in the retinal wholemounts (compare Figures 3-2 and 3-5 to Figure 3-3). Importantly, I compared glutamate and NMDA responses in each tested RGC, as NMDA is not recognized by EAATs and thus not affected by retinal glutamate uptake. In the cultured RGCs, which are isolated from the influence of EAATs that are present on other retinal cell types in the retinal wholemounts, the calcium signal measured in response to 10 μM glutamate was significantly greater than that caused by 100 μM NMDA and was similar to the response to 200 μM NMDA. This is in agreement with data from ligand binding studies that have shown glutamate, relative to NMDA, to be a more potent agonist (8 - 30 times more potent depending on receptor subtype) for the NMDA-type glutamate receptor (for review, see Hollmann and Heinemann 1994). In contrast, I found that millimolar concentrations of glutamate were necessary to induce a detectable RGC calcium signal in the retinal wholemount preparations, and the response to 1000 and 2000 μM glutamate was still less (~20% and ~40%, respectively) than that caused by 200 μM NMDA (Figure 3-6). The calcium signal induced by 1000 μM glutamate appeared to be at the threshold for detection using the calcium imaging technique, and was similar to the response induced by 50 μM NMDA (Figure 3-2). Comparing these results to the effects of glutamate and NMDA on isolated RGCs (Figure 3-3) suggests

that the effective concentration achieved by exogenous 1000-2000 μM glutamate is < 10 μM. That is, typically < 1% of the exogenous millimolar glutamate applied to the retinal wholemounts escapes uptake.

With a decrease in the functional capacity of retinal glutamate uptake, one would expect that more of the exogenously applied glutamate would evade the glutamate transporter system and activate RGC glutamate receptors. To test this premise, I used TBOA, which has been shown to be a potent pharmacological inhibitor of all known subtypes (EAAT1-5) of glutamate transporters (Shimamoto *et al.* 1998; Shigeri *et al.* 2001). Under these recording conditions, 500 μM glutamate only increased RGC calcium levels when it was applied with TBOA (250 μM) (Figure 3-2). Exposure of the retinal pieces to TBOA alone also increased RGC calcium levels, although this response was significantly less than the response to glutamate plus TBOA. These results are in agreement with that of Izumi *et al.* (2002), who showed that while 100 μM glutamate had no effect on isolated rat retinas, the application of 100 μM glutamate plus TBOA (with riluzole to block endogenous glutamate release) or TBOA alone induced significant excitotoxic neurodegeneration. Unlike other pharmacological inhibitors of glutamate uptake, it has been demonstrated that the non-transportable TBOA does not induce an artificial release of glutamate by heteroexchange, and it does not act as a partial glutamate receptor agonist (Shimamoto *et al.* 1998; Jabaudon *et al.* 1999). Therefore, the effect of TBOA on RGC calcium levels was not due to a direct action of this agent, but rather due to the accumulation of endogenously released glutamate. Prior studies on neonatal rat hippocampal and cortical slices have shown that the activation of NMDA receptors by endogenous glutamate occurs within seconds following TBOA application (Jabaudon *et al.* 1999; Demarque *et al.* 2004). Thus, as in the neonatal brain, these results show that the disruption of glutamate uptake in the adult mammalian retina

results in a rapid elevation of extracellular glutamate levels and this underscores the importance of glutamate transporters for the maintenance of glutamate homeostasis.

Retinal Glutamate Uptake in a Chronic Rat Glaucoma Model

A rise in the extracellular concentration of glutamate has been proposed as a contributing factor in glaucomatous RGC death (Dreyer 1998; Osborne *et al.* 2001; Lipton 2003), and a corollary of this hypothesis is that retinal glutamate uptake is compromised. In support for this theory, Martin *et al.* (2002) found that overall retinal protein levels of EAAT1 and EAAT2 (found mainly on retinal bipolar cells) were decreased in a rat chronic glaucoma model, suggesting that exposure to elevated IOP may directly disrupt retinal glutamate transporter expression. However, a more recent study reported increased retinal protein levels of EAAT1 following IOP elevation in a rat glaucoma model (Woldemussie *et al.* 2004). The difficulty in interpreting these findings is that the relationship between EAAT protein levels and EAAT functional efficiency is not clear. Changes in absolute transporter protein levels may not necessarily be directly related to the integrity of glutamate clearance mechanisms, but may instead occur as a physiological response to changes in synaptic activity during the neurodegenerative cascade. To investigate this unresolved issue, I tested the functional capacity of glutamate uptake in a rat glaucoma model of chronic IOP elevation using RGC calcium imaging. An additional advantage to this approach is that, unlike immunohistochemical or Western blotting techniques, it does not require *a priori* assumptions on the importance of individual EAAT subtypes. For example, although EAAT1 accounts for the majority of glutamate uptake in the mammalian retina, the retinal phenotype of EAAT1-deficient mice appears normal and free from excitotoxic neurodegeneration (Harada *et al.* 1998). Instead, glutamate homeostasis is maintained through alternative

mechanisms, as glutamate uptake in retinas from these mice has been shown to be mediated by other retinal EAATs and by additional unidentified transporters located on Müller cells (Sarthy *et al.* 2005). The imaging methodology in the present work assesses the ability of the overall glutamate transporter system in preventing RGC glutamate receptor activation.

My results showed that the application of 100 and 500 μM glutamate did not induce a detectable calcium signal in RGCs from either treated (elevated IOP) or untreated eyes from rats with experimental glaucoma (Figure 3-5). Therefore, this data indicates that the threshold concentration of exogenous glutamate required to elicit a response was not decreased to ≤ 500 μM in the treated eyes. RGCs did respond to 200 μM NMDA (a glutamate agonist not recognized by transporters) at the beginning and end of every experiment, ruling out the possibility that RGCs were not responding to glutamate because functional NMDA receptors were absent, or because the RGCs became non-responsive during the experiment. The protocol of normalizing all treatment responses to each individual RGC's initial response to 200 μM NMDA ensured that this assay would reflect transporter activity if RGC NMDA receptor expression had changed. For example, if NMDA receptor levels had decreased, the absolute responses to either NMDA or glutamate would also have likely decreased but the ratio of these responses would not have been altered if glutamate clearance were unaffected. Conversely, a defect in glutamate uptake would alter this ratio such that the response to glutamate, relative to NMDA, would increase, as demonstrated in the present study in the experiments using TBOA on retinal wholemounts (inhibition of glutamate uptake) and in the experiments using purified RGC cultures (absence of glutamate uptake). In addition to response amplitudes, no apparent difference (treated versus control) in the time course of the NMDA responses was evident. This suggests that the diffusion of

NMDA through the inner limiting membrane and retinal neuropil was not grossly altered in the treated rats.

Supra-threshold concentrations of glutamate (1000 and 2000 μM) induced similar increases in RGC calcium levels in retinal wholemounts from either treated or untreated eyes (Figure 3-6). If exposure to elevated IOP caused a relatively mild defect in glutamate uptake, it was possible that the functional capacity of the clearance mechanisms in the treated eyes might still have been sufficient to clear 100 and 500 μM glutamate, as observed in Figure 3-5. However, a mild defect should be accompanied by a shift in the threshold sensitivity to exogenous glutamate, and my findings of similar responses to 1000 and 2000 μM glutamate provide evidence that this was not the case. The responses to 1000 μM glutamate were small (on average less than 20% of that induced by 200 μM NMDA) and, as they were not significantly different in treated versus controls, there was no apparent change in the sensitivity to exogenous glutamate in the retinas that had been exposed to chronic IOP elevation. These findings, using a highly selected group of experimental rats, indicate that retinal glutamate clearance mechanisms were not compromised across a broad range of IOP parameters and damage grades (Figure 3-4 and Table 3-1) in this model of glaucomatous RGC death and optic nerve damage.

While my data suggests that a chronic and moderate elevation of IOP does not directly disrupt overall retinal glutamate uptake, it does not completely exclude potential excitotoxic RGC death in this glaucoma model due to transient or localized elevations in glutamate levels. The intracellular glutamate concentration in neurons is likely to be at about 5 to 15 mM (Attwell *et al.* 1993; Anderson and Swanson 2000), and so in a region of RGC death there may be a rapid rise in glutamate levels following the spilling of intracellular contents into the extracellular space. My results do indicate that millimolar

glutamate levels can overcome the transporter system and stimulate RGC glutamate receptors. However, the RGCs from eyes with experimental glaucoma were no more susceptible to this concentration than were the RGCs from control retinas. With glutamate uptake functional, even a significant elevation in extracellular glutamate would only be temporary. This makes it highly unlikely that global glutamate excitotoxicity is a primary cause of RGC death in this model, although I cannot rule out that some RGCs underwent secondary excitotoxic degeneration.

An additional caveat to the results of this study, obtained using a rat glaucoma model based on chronic IOP elevation, is that there may be factors other than IOP that initiate RGC death in human glaucoma. Ischemia has long been debated as a potential etiological factor for glaucoma (Osborne *et al.* 2001; Flammer *et al.* 2002). The simulation of ischemic conditions *in vitro* can result in the inhibition and reversal of glutamate transporters in hippocampal slice cultures (Jabaudon *et al.* 2000; Rossi *et al.* 2000). In the retina, there is immunocytochemical evidence that EAAT activity is disrupted in experimental *in vivo* (Barnett *et al.* 2001) and *in vitro* (Bull and Barnett 2004) models of acute ischemia, and it has been demonstrated that isolated rat retinas become more susceptible to the excitotoxic effects of exogenously applied glutamate under ischemic conditions (Izumi *et al.* 2003). The reduction in retinal glutamate uptake that occurs during acute ischemia may be temporary and not accompanied by a subsequent down-regulation in EAAT expression, as supported by a recent immunocytochemical study (Barnett and Grozdanic 2004). It is likely that the technique used in the present study would not identify a temporary decrease in EAAT activity, as short-term retinal metabolic alterations could normalize during the incubation period required for calcium dye loading. Also, an increase in glutamate release, rather than a decrease in glutamate clearance, would not have been detected using the RGC calcium

imaging methodology. Excessive glutamate release contributes to the spread of neuronal death that follows severe mechanical insult, as in head or spinal cord injury (Lipton 2003). However, in contrast to an acute ischemic insult or mechanical trauma, glaucoma is a chronic and progressive neurodegeneration that culminates in pathological changes that are specific to the optic nerve and the RGC layer (Quigley 1999; Morrison *et al.* 2005). As it has been suggested that a more gradual form of excitotoxicity, as a result of a moderate elevation in retinal glutamate levels, may account for the prolonged time-scale of RGC death that is observed in glaucoma (Dreyer 1998; Lipton 2003), I assessed glutamate uptake in a chronic model of IOP-induced optic nerve damage and RGC death. Further work on glutamate transporter inhibition and recovery in more acute models of RGC death, such as ischemia, is warranted.

Conclusion

In summary, the optical imaging of RGC calcium levels in living retina wholemounts is a novel method to assess the functional capacity of glutamate uptake in the mammalian retina. Using rats with experimental glaucoma, I did not observe any difference in the sensitivity to exogenously applied glutamate in RGCs from either the treated or fellow untreated eyes. Thus, there was no evidence for a global defect in retinal glutamate clearance mechanisms in this rat glaucoma model. Imaging RGC calcium dynamics in retinal wholemounts should serve as a useful technique to probe the relationship between retinal transporters and RGC glutamate receptors and to identify conditions and factors that disrupt glutamate uptake in the CNS.

CHAPTER 4: Glutamatergic Calcium Dynamics and Deregulation in Rat Retinal Ganglion Cells

Preface and Significance to Thesis

The work in this chapter seeks to determine the underlying pathways of calcium entry that contribute to glutamatergic calcium responses in RGCs. A consensus on the mechanisms involved in glutamate-dependent increases in RGC calcium levels has not been reached, and there are discrepancies in the literature concerning the excitotoxic actions of glutamate on RGCs. Understanding the relationship between glutamate and RGC excitotoxicity is essential if potential neuroprotective strategies that target this death pathway are to be properly assessed. In this chapter, I utilize the methodologies that were optimized in previous chapters, namely the calcium imaging of RGCs in purified cultures and in retinal wholemounts, to address these topics and to probe the relationships between glutamate, calcium and RGC death. In addition, I use the relatively novel approach of generating purified RGC cultures from adult rat retinas in order to test for developmental differences in glutamatergic responses.

Preliminary results of this work were presented at the ARVO Annual Meetings in 2003 (Hartwick ATE, Baldridge WH. Glutamate induces calcium influx by NMDA receptor activation in purified retinal ganglion cells cultured from neonatal and adult rats. *Invest. Ophthalmol. & Vis. Sci.* 44: ARVO E-Abstract 5218) and in 2005 (Hartwick ATE, Baldridge WH. Delayed calcium deregulation in rat retinal ganglion cells following prolonged glutamate exposure. *Invest. Ophthalmol. & Vis. Sci.* 46: ARVO E-Abstract

4007). With the important guidance and supervision of Dr. William Baldridge, I performed all of the research and data analysis that is presented in this chapter of work.

Introduction

Glutamate is the predominant excitatory neurotransmitter in the retina (for review, see Thoreson and Witkovsky 1999), as it is elsewhere in the CNS. Retinal ganglion cells (RGCs) are the output neurons of the retina and their axons exit the eye as the optic nerve and project to various brain targets. Although the synaptic release of glutamate onto RGC dendrites is an essential part of the visual pathway, excessive or prolonged exposure to glutamate is thought to be lethal to these retinal neurons. Many CNS neurons are susceptible to glutamate-induced death and this phenomenon, termed excitotoxicity (Olney 1969b), was in fact first documented in the retina (Lucas and Newhouse 1957). The subcutaneous administration of glutamate to neonatal mice (the blood-retina barrier is incomplete at this early age) was shown to produce wide-spread degeneration of the inner retina including the RGC layer (Lucas and Newhouse 1957; Olney 1969a). A similar pattern of damage was later demonstrated in adult rats by circumventing the blood-retina barrier with injections of high glutamate doses into the vitreous body of the eye (Sisk and Kuwabara 1985), thus confirming the susceptibility of the rodent retina to excitotoxic death. Since the initial retinal experiments, glutamate excitotoxicity has been implicated in the pathogenesis of a number of CNS neurodegenerative disorders including ischemic-hypoxic brain injury, epilepsy and mechanical trauma (Choi 1988; Lipton and Rosenberg 1994), and there is evidence that glutamate is involved in the death of RGCs that occurs during retinal ischemia

associated with central and branch retinal artery and vein occlusions (for review, see Osborne *et al.* 2004).

An accumulation of data supports a role for calcium, specifically the rise in the intracellular calcium concentration ($[Ca^{2+}]_i$) that occurs following neuronal stimulation with glutamate, as a key factor in the initiation of the excitotoxic death cascade (reviewed in Sattler and Tymianski 2000; Zipfel *et al.* 2000; Khodorov 2004). N-methyl-D-aspartate-type glutamate receptors (NMDA-Rs) are directly permeable to Ca^{2+} (Mayer and Westbrook 1987; Ascher and Nowak 1988), and excessive stimulation of these receptors has long been linked to CNS excitotoxicity (Choi *et al.* 1988). Consistent with a role for NMDA-Rs in mediating glutamate-related RGC death, the intravitreal injection of the selective agonist NMDA causes destruction of the RGC layer in rodents (Siliprandi *et al.* 1992; Lam *et al.* 1999; Li *et al.* 1999; Schlamp *et al.* 2001; Manabe *et al.* 2005; Nakazawa *et al.* 2005), and treatment of mixed retinal cell cultures with NMDA results in the loss of identified RGCs (Hahn *et al.* 1988; Sucher *et al.* 1991; Kitano *et al.* 1996). However, in addition to NMDA-Rs, electrophysiological recordings of rat RGCs in mixed cultures (Aizenman *et al.* 1988; Taschenberger *et al.* 1995) and in retinal slices (Chen and Diamond 2002) show that these neurons also possess α-amino-3-hydroxy-5-methylisoxazole-4-propionate (AMPA) and kainate-type ionotropic glutamate receptors, which are often grouped together (AMPA/kainate-Rs) due to similar pharmacological profiles. Calcium imaging studies on retinal wholemounts prepared from rabbit (Baldridge 1996) or rat (see Chapter 2 of this thesis) indicate that both NMDA and kainate (an agonist for AMPA/kainate-Rs) are capable of inducing a rise in RGC $[Ca^{2+}]_i$. Although AMPA/kainate-Rs are generally less permeable to Ca^{2+} than NMDA-Rs, AMPA-Rs that lack the GluR2 subunit are Ca^{2+} permeable (Jonas and Burnashev 1995; Dingledine *et al.* 1999). Additionally, the activation of voltage-gated calcium channels

(VGCCs), following membrane depolarization subsequent to NMDA-R and/or AMPA/kainate-R activation, could also contribute to increases in RGC $[Ca^{2+}]_i$ (Ishida *et al.* 1991).

RGCs can be isolated from neonatal rats into purified cultures using Thy-1 immunopanning (Barres *et al.* 1988; Meyer-Franke *et al.* 1995). This system should prove advantageous in assessing the relationships between glutamate, $[Ca^{2+}]_i$, and excitotoxicity in a central neuron as it eliminates the potential for alteration of the glutamatergic response by neuroactive compounds released by other cells present in mixed cultures or intact tissue preparations. For example, treatment of mixed retinal cultures (in which RGCs make up < 1% of the cell population) with kainate causes an endogenous release of glutamate that contributes to the effect of kainate on RGCs (Sucher *et al.* 1991). However, investigations of excitotoxic death in purified RGC cultures have generated conflicting data that contradicts previous *in vitro* and *in vivo* studies (described above) linking NMDA-Rs to RGC death. Otori and colleagues (1998) reported that glutamate-induced calcium influx and excitotoxicity occurs in immunopanned RGCs through activation of AMPA/kainate-Rs rather than NMDA-Rs. In contrast, the findings of Ullian *et al.* (2004) suggest that RGCs in purified cultures, although expressing functional NMDA-Rs, are invulnerable to the excitotoxic actions of glutamate, NMDA or kainate. In light of these discrepancies, the goal of this work was to: 1) characterize the glutamate-evoked calcium dynamics of immunopanned RGCs, and assess the relative contribution of NMDA-Rs, AMPA/kainate-Rs and VGCCs to the glutamate signal; 2) compare the mechanisms of glutamate-induced calcium influx in immunopanned RGCs generated from neonatal versus adult rats, and to determine whether isolated RGCs exhibit differences relative to RGCs in an adult rat retinal wholemount preparation; and 3) characterize the calcium dynamics in RGCs exposed to

glutamate for a prolonged period and investigate the relationship of $[Ca^{2+}]_i$ to excitotoxic RGC death.

Methods

Purified RGC Cultures

Natural litters of Long-Evans rats were killed at age 7 to 8 postnatal days by over-exposure to halothane and decapitation. Following enucleation, the retinas were dissected from the eyes and then placed in 10 ml Ca^{2+}/Mg^{2+}-free Dulbecco's phosphate-buffered saline with 165 units of papain and 0.004% DNase for 30 min at 37°C, followed by mechanical trituration. The dissection and dissociation procedures were the same as described in Chapter 2, and further details can be found on page 42 of this thesis. For some experiments, RGC cultures were instead generated from adult Long-Evans rats that were 6-15 weeks old. Following dissection, the retinas from adult rats were dissociated using the same methodology as for neonatal retinas except that a 60 min incubation period in the papain solution was applied prior to trituration due to the more extensive synaptic connections in these aged retinas. Purified RGC cultures were generated from the single-cell suspensions (produced from either neonatal or adult retinas) using a two-step panning procedure described originally by Barres and colleagues (1988), and described in detail earlier (see page 43). In brief, macrophages were first removed from the mixed retinal cell suspensions through an incubation in anti-rat macrophage antiserum (raised in rabbit; Axell brand, Accurate Chemical) prior to the transfer of the cells to a Petri dish coated with appropriate secondary antibodies (goat anti-rabbit IgG [H+L] antibodies; Jackson ImmunoResearch). The non-adherent cells were then resuspended on a final dish coated with monoclonal supernatant IgM

antibodies against mouse Thy1.1 (cell line T11D7e2; American Type Culture Collection). RGCs adhered to the Thy1.1 plate and were released by manually pipetting an enzyme inhibitor solution along the surface of the dish after incubation in a 0.125% trypsin solution.

The RGCs were plated onto poly-D-lysine/laminin-coated Biocoat glass coverslips (BD Biosciences) in 4-well tissue culture plates at a density of 3.5×10^4 cells per well. The cells were cultured in 600 μl of serum-free culture medium consisting of Neurobasal-A with 2% B27 supplements, 1 mM glutamine, 50 ng/ml BDNF, 10 ng/ml CNTF, 5 μM forskolin, and 10 μg/ml gentamicin. Cultures were maintained at 37°C in a humidified 5% CO_2-air atmosphere. For calcium imaging, coverslips with plated cells were removed from the culture medium and incubated at 37°C for 30 min in a solution containing esterfied calcium indicator dye (5 μM fura-2 AM or 5 μM fura-4F AM, depending on the experiment). The fura dyes were first dissolved in DMSO (0.1% final concentration) and then in the balanced salt solution used for imaging experiments to which 0.1% pluronic acid F-127 had been added.

Retinal Wholemount Preparation

Retinal wholemounts were prepared from adult Long-Evans rats aged 6-10 weeks and RGCs in the wholemounts were loaded with calcium indicator dye using a method essentially as described in Chapter 2 on page 49, with the modifications outlined in Chapter 3 on page 76. The rats were sacrificed by over-exposure to halothane followed by decapitation. The eyes were enucleated, the anterior segment removed, and the posterior eye-cups were immersed in Hibernate-A medium with 2% B27 supplements for the retina dissection. Each retina was carefully dissected and mounted on black filters (HABP 045; Millipore) with the RGC layer uppermost. A small volume

(~0.5 μl) of 10% (dissolved in purified water) fura dextran (10,000 MW) was deposited into each retinal piece (passing through all the retinal layers) using a tapered 26-gauge needle fitted to a 10 μl Hamilton syringe. To allow the dextran to be retrogradely transported to RGC somata, the wholemounts were then incubated in the dark at room temperature in Hibernate-A/B27 medium for 7-12 h prior to calcium imaging.

Calcium Imaging

The retinal wholemounts (on filters) and isolated RGCs (on coverslips) were transferred to a microscope chamber that was constantly superfused with Hanks' balanced salt solution (HBSS) that had been bubbled with 100% oxygen. A peristaltic pump was used to maintain a solution flow rate of approximately 1 ml/min. In most experiments, the HBSS (pH 7.4) was modified to be nominally Mg^{2+}-free and contain 2.6 mM $CaCl_2$ and 15 mM HEPES buffer. For experiments testing the effect of extracellular magnesium, $MgCl_2$ was substituted for some of the $CaCl_2$ so that the final divalent concentrations were 0.8 mM Mg^{2+} and 1.8 mM Ca^{2+}. The HBSS was warmed through an inline heater prior to its delivery to the temperature-regulated chamber, where it was maintained at 34-36°C. The fura-loaded RGCs were alternately stimulated with the excitation wavelengths of 340 and 380 nm using a xenon lamp source and appropriate filters (XF04 set, excitation 340 or 380 nm; emission 510 nm; dichroic > 430 nm) that were housed in a computer-controlled filter wheel. The period of excitation for each wavelength was regulated by an electronic shutter to be 1000-1500 ms for the retinal wholemounts and 400 ms for the isolated cells. During treatments, image pairs were collected as often as every 5 s (10 s for retinal wholemounts) but to limit photodamage, images were collected less frequently (20-40 s) during intervening periods. Fluorescence was captured by a cooled charged-coupled device (CCD) camera using a

40x (NA 0.80 W) water-immersion objective and the resulting images (8-bit processing, 4 X 4 binned) were converted into ratiometric (340 nm/380 nm) data by imaging software (Axon Imaging Workbench 2.2). Manufacturers and additional particulars of the imaging rig and associated equipment are fully described in Chapter 2 beginning on page 46.

Glutamatergic calcium dynamics were assessed in the isolated RGCs using two treatment paradigms. RGCs were either exposed to glutamate receptor agonists (glutamate, glycine, NMDA, kainate; all dissolved directly in HBSS on the day of the experiment) for a relatively brief 30 s pulse, or were constantly superfused with a glutamate/glycine solution for a prolonged 1 h period. RGCs used for the 30 s treatment experiments were loaded with the high affinity dye fura-2 AM (K_D ~ 224 nM), while the 1 h exposures were performed on RGCs loaded with the low affinity fura-4F AM (K_D ~ 770 nM) dye (see Figure 1-2 on page 15). For the fura dextran-loaded RGCs in retinal wholemounts, the treatment period with glutamatergic agonists was 2 min and the glutamate transporter inhibitor DL-threo-β-benzyloxyaspartate (TBOA; Tocris, Ellisville, MO) was added to the glutamate treatment solution. In both the prolonged glutamate exposure experiments on isolated RGCs and the experiments on retinal wholemounts, the imaging rig was modified in that a 0.6x coupling tube (HRP060; Diagnostic Instruments, Sterling Heights, MI) was placed between the CCD camera and microscope, which expanded the field of view afforded by the 40x objective.

Imaging Analysis

For studies on isolated RGCs, circular regions of interest were drawn around individual RGC somata, and the mean fura ratio within each region was monitored throughout the experiments. Background fluorescence was measured from a region on the coverslip devoid of RGCs and subtracted from each image. Using a K_d for fura-2 of

224 nM, the averaged minimum and maximum fluorescence values obtained from separate calibration experiments were used to convert the fura-2 ratios to absolute calcium levels (for detailed method, see Kao 1994 and Appendix A of this thesis) for trials involving 30 s glutamate treatments. Calcium influx was measured as the peak $[Ca^{2+}]_i$ obtained with each glutamate exposure minus the average baseline $[Ca^{2+}]_i$ measured prior to the first glutamate treatment. In the trials assessing the effect of glutamate receptor antagonists and VGCC blockers, RGCs that had a negligible response to glutamate (peak $[Ca^{2+}]_i$ <150 nM) were excluded from analysis (< 5% of RGCs imaged). In the prolonged glutamate exposure (1 h) experiments, initial calcium influx (Δ fura-4F ratio) was measured as the peak fura-4F ratio occurring during the first 400 s of the glutamate treatment minus the average baseline ratio before treatment.

For studies on RGCs in retinal wholemounts, the mean fura ratio was monitored in RGC somata that exhibited fluorescence with 380 nm excitation. As in previous work described in Chapters 2 and 3, all experiments were performed on dextran-loaded cell bodies that were located in the GCL near labeled RGC axon bundles, and that were > 200 μm from the dextran injection site. The response to each treatment was calculated as the Δ fura ratio, the peak fura ratio minus baseline fura ratio. The baseline fura ratio for every cell was calculated as the average fura ratio measured in the three images prior to each treatment, and the peak ratio was the maximum ratio value obtained in the 400 s following each treatment. For illustration, fura ratio traces of RGCs from retinal wholemounts were slope-corrected for a gradual decrease in baseline ratio due to decreasing background fluorescence. However, all data analysis was performed on the non-baseline-corrected raw data.

RGC Death Assay

After the 1 h glutamate exposure, the RGCs were imaged for another 15 min to monitor for recovery. The superfusing HBSS was then stopped and 5 μl of fluorescently-tagged annexin V (Alexa Fluor 488 annexin V; Invitrogen) was added to the microscope chamber (chamber volume ~0.5 ml) to compare the calcium imaging data with a marker of cell death. After 10 min incubation, the flow of HBSS was resumed for 5 min to wash. Images of annexin V fluorescence were captured with the CCD camera using an FITC filter set (XF100 set; excitation 475 nm, emission 535 nm; dichroic 505 nm; Omega Optical) and saved, through the imaging software program, with and without the circular regions of interest that had been drawn for calcium imaging. The images of annexin V fluorescence were assessed independently of the calcium imaging data using Photoshop 5.0 software (Adobe Systems, San Jose CA). Using the histogram function, a cell was deemed annexin V positive if the mean luminance minus 1 SD within its outlined region of interest was greater than background luminance in a section devoid of cells.

Absorbance of Glutamate Receptor Antagonist Solutions

Solutions of 6,7-dinitroquinoxaline-2,3-dione (DNQX; 25 μM), 6-cyano-7-nitroquinoxaline-2,3-dione (CNQX; 25 μM), 2,3-dihydro-6-nitro-7-sulfamoyl-benzo(f)quinoxaline (NBQX; 25 μM) and D(-)-2-amino-5-phosphonopentanoic acid (APV; 100 μM), in HBSS at the concentrations used in the imaging experiments, were put into quartz cuvettes (1 cm width). The cuvettes were placed in the holder of an Ultrospec 2000 single-beam spectrophotometer (Amersham Biosciences, Piscataway NJ) and the absorbance at 340 and 380 nm was determined. The absorbance of HBSS alone (no glutamate receptor antagonists added) was subtracted from each reading.

Results

Glutamatergic Calcium Dynamics of Neonatal Rat Retinal Ganglion Cells

All calcium imaging experiments in this chapter were performed on cultured RGCs 1 to 2 days after their isolation through Thy1.1 immunopanning. Upon loading of the calcium indicator dye fura-2, RGCs typically display a bi-lobed pattern of fluorescence, with either 340 or 380 nm excitation, presumably due to asymmetrical nucleus position (Figure 4-1 A). To investigate the relationship of glutamate concentrations to calcium responses, isolated RGCs (n = 38; pooled from 8 imaging experiments on RGCs from 3 separate cultures) were first challenged with consecutive 30 s treatments of 1, 10, 50 and 100 μM glutamate (Figure 4-1). Glycine (10 μM), a co-agonist with glutamate for NMDA-Rs (Johnson and Ascher 1987), was included in all glutamate treatment solutions, and the superfusing HBSS was nominally Mg^{2+}-free. Under these recording conditions, 1 μM glutamate was below threshold and did not, on average, induce a detectable response. The 30 s exposures to 10, 50 and 100 μM glutamate, however, generally caused an elevation in the fura-2 fluorescence ratio (340/380 nm; measured in RGC somata) that was followed by recovery to baseline levels (Figure 4-1 E). Changes in the ratio of fura-2 fluorescence reflect changes in RGC calcium levels, and these ratios were converted to absolute $[Ca^{2+}]_i$ following calibration experiments (Grynkiewicz *et al.* 1985; Kao 1994; and see Appendix A for further details). This calibration allowed an approximation of the magnitude (in nM) of the $[Ca^{2+}]_i$ change.

As illustrated by the fura-2 ratio images for the four RGCs depicted in Figure 4-1 B-D, the RGC responses to glutamate were highly variable between different cells.

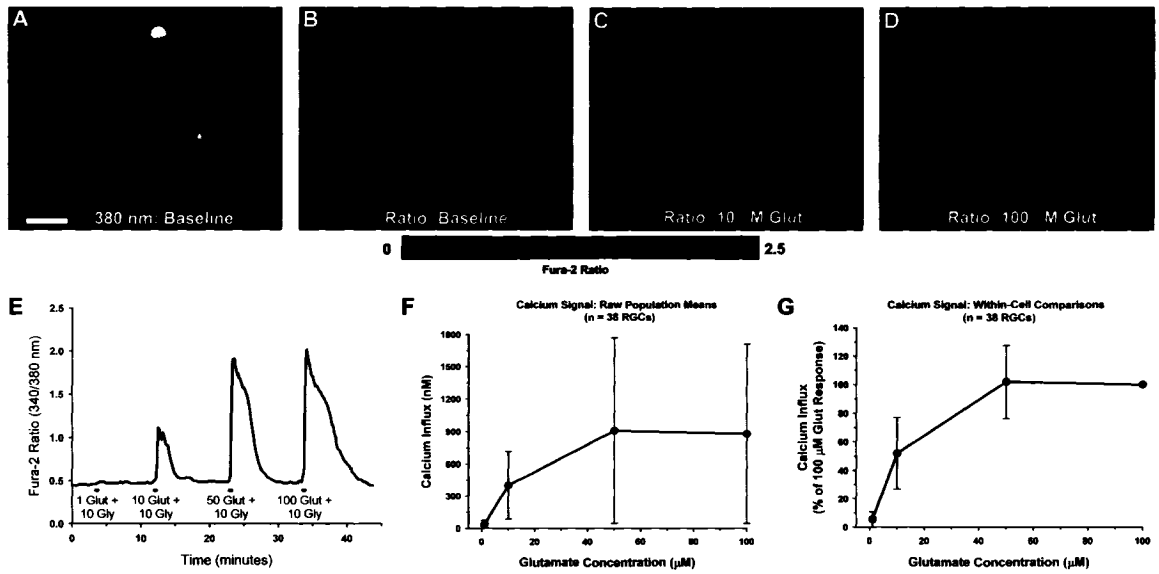

Figure 4-1. Concentration-response relationship for glutamate-induced increases of $[Ca^{2+}]_i$ in cultured RGCs isolated from neonatal rats. **(A)** Fluorescence (380 nm excitation, 510 nm emission) of immunopanned RGCs in culture loaded with the calcium indicator dye fura-2 AM. Scale bar = 25 μm. **(B)** Pseudocolor images of fura-2 fluorescence ratios (340/380 nm) in same RGCs at baseline and at peak response to **(C)** 10 μM and **(D)** 100 μM glutamate, plus 10 μM glycine. **(E)** Fura-2 ratios were monitored in RGC somata during consecutive 30 s exposures to 1, 10, 50 and 100 μM glutamate (with 10 μM glycine; extracellular Mg^{2+} absent). Example trace is full optical recording from uppermost RGC shown in panels A-D. **(F-G)** Summary of mean data (± 1 SD) for calcium influx (peak $[Ca^{2+}]_i$ minus baseline $[Ca^{2+}]_i$; conversion of fura-2 ratios to $[Ca^{2+}]_i$ following calibration experiments) induced by the different glutamate concentrations (n = 38 RGCs). Calcium responses are presented as both (F) raw mean data for all tested RGCs, and as (G) normalized data (responses expressed as a percentage of each RGC's 100 μM glutamate response) for within-cell comparisons.

While there was large variation in the absolute magnitude of the $[Ca^{2+}]_i$ change (data summary for all tested RGCs shown in Figure 4-1 F), within-cell analysis indicated that the response to 10 μM glutamate was roughly one half (51.9 ± 25.2% SD) of that elicited by 100 μM glutamate for a given RGC (Figure 4-1 G). The responses to the different glutamate concentrations were all significantly different from each other ($P < 0.01$, Friedman ANOVA, Tukey; using normalized data) with the exception of 50 versus 100 μM ($P > 0.05$, $q = 0.127$), indicating that 50 μM glutamate was sufficient to evoke the maximum calcium response.

Increases in RGC $[Ca^{2+}]_i$ could also be observed following 30 s treatment with either NMDA or kainate, selective ligands for NMDA-Rs and AMPA/kainate-Rs respectively (Figure 4-2). In a direct comparison of the calcium signal induced by 200 μM NMDA (with 10 μM glycine) to that by increasing concentrations of kainate in isolated RGCs (n = 33), the magnitude of NMDA-induced calcium influx (raw population mean = 363 nM ± 357 SD) was similar ($P > 0.05$, $q = 0.202$, Friedman ANOVA, Tukey) to that due to 200 μM kainate (398 nM ± 499 SD) but was significantly ($P < 0.01$) greater and smaller than the responses elicited by 100 μM (104 nM ± 189 SD) and 300 μM (907 nM ± 786 SD) kainate, respectively (example trace in Figure 4-2 A). RGC responses to NMDA were highly dependent on the presence of the NMDA-R coagonist glycine in the treatment solution (Figure 4-2 B). The RGC calcium signals stimulated by 200 μM NMDA alone were significantly less ($P < 0.001$, Wilcoxon) than the signal produced by 200 μM NMDA plus 10 μM glycine (in n = 34 RGCs tested, the normalized NMDA-induced $\Delta [Ca^{2+}]_i$ was 25.3% ± 11.9 SD, on average, of the same RGC's response to NMDA plus glycine), but glycine did not significantly ($P = 0.134$, Wilcoxon) enhance kainate responses (in n = 19 RGCs treated with 200 μM kainate alone and then 200 μM

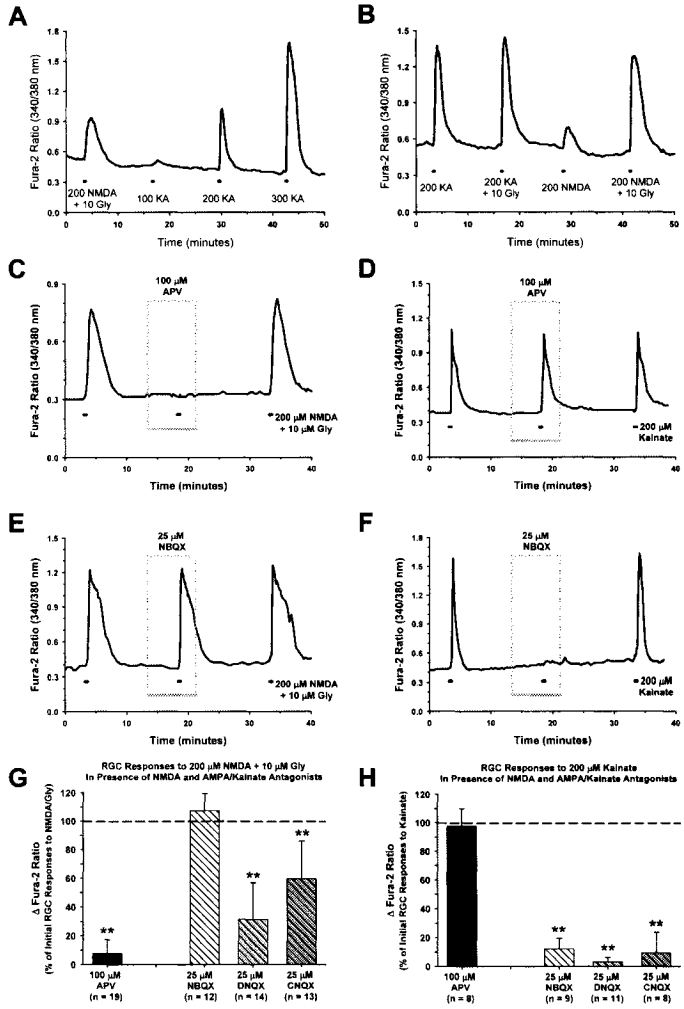

Figure 4- 2. NMDA- and kainate-induced calcium influx in isolated RGCs. **(A)** Example fura-2 ratio trace for an RGC treated with 200 µM NMDA plus 10 µM glycine, and then 100, 200 and 300 µM kainate. **(B)** Glycine (10 µM) significantly enhanced the response evoked by 200 µM NMDA, but not 200 µM kainate, and was included in NMDA treatment solutions. **(C)** The NMDA-R antagonist APV blocked NMDA responses, and **(D)** did not affect kainate responses. **(E)** The AMPA/kainate-R antagonist NBQX did not alter NMDA responses but **(F)** inhibited kainate responses. **(G-H)** Mean data (± 1 SD) showing effect of NMDA-R (dark bar) and AMPA/kainate-R (hatched bars) antagonists on (G) NMDA- and (H) kainate-induced calcium influx (extracellular Mg^{2+} absent), normalized to initial NMDA or kainate responses (dashed line). ** $P < 0.01$, Friedman ANOVA, Tukey, as compared to both initial and recovery responses to NMDA or kainate.

To confirm that changes in RGC calcium dynamics due to NMDA and kainate stimulation were mediated by two independent pathways, I tested the effect of antagonists for the two ionotropic glutamate receptor types on the ligand-gated calcium signals. To generate responses with roughly similar magnitudes, concentrations of 200 μM NMDA (with 10 μM glycine) and 200 μM kainate were employed for these studies. As expected, NMDA responses were blocked by the NMDA-R antagonist APV (Figure 4-2 C), kainate responses were blocked by the AMPA/kainate-R antagonist NBQX (Figure 4-2 F), and these two antagonists did not influence the calcium influx induced by the respective contrary agonists (Figure 4-2 D, E).

An unexpected finding, however, was that the AMPA/kainate-R antagonists DNQX and CNQX appeared to inhibit both kainate and NMDA responses (partially, in the case of NMDA; summary of data in Figure 4-2 G, H). Further analysis showed that the apparent inhibitory effect of DNQX and CNQX on NMDA-evoked signals was an artifact due to the fluorescence quenching properties of these compounds (Figure 4-3). In contrast to the colorless 100 μM APV solution, the DNQX, CNQX, and NBQX solutions, dissolved at 25 μM in HBSS, all were yellow in color. The fura-2 ratio is the quotient obtained after dividing the fluorescence intensity obtained with 340 nm excitation by that obtained with 380 nm excitation (510 nm emission for both excitation wavelengths). With a rise in $[Ca^{2+}]_i$, there is a decrease in 380 nm fluorescence while 340 nm fluorescence increases (see Figure 2-4 on page 57). The addition of the yellow AMPA/kainate-R antagonists to the microscope chamber caused a decrease in fluorescence with either 340 or 380 nm excitation. The quenching effect of DNQX on raw fluorescence intensities is illustrated in Figure 4-3 A, and the resulting fura-2 ratio trace for this same experiment is shown in Figure 4-3 B. For comparison, the fluorescence intensities under 340 and 380 nm excitation for a RGC in which the NMDA-

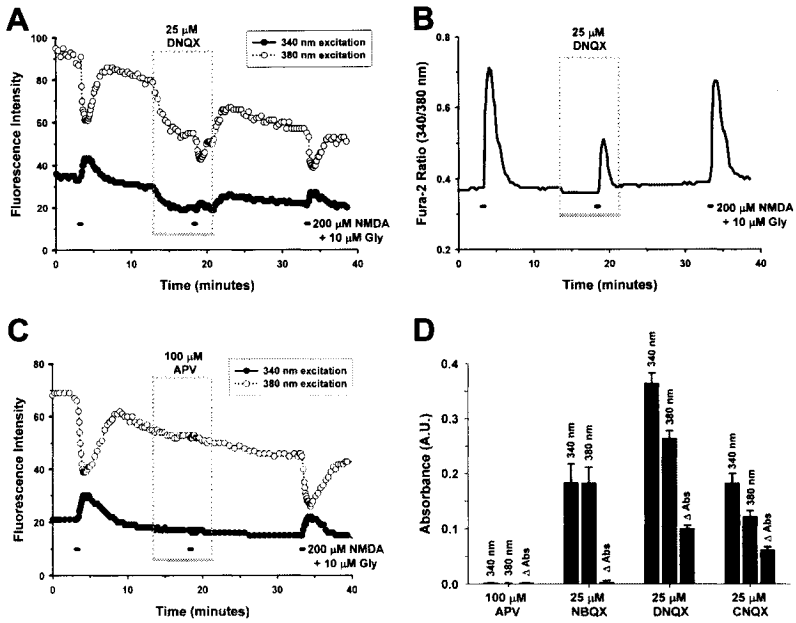

Figure 4- 3. Fluorescence quenching by AMPA/kainate-R antagonists and its effect on ratiometric calcium imaging. **(A)** Fluorescence intensities with 340 and 380 nm excitation (510 emission) for an RGC treated with 200 μM NMDA plus 10 μM glycine in the presence and absence of 25 μM DNQX (AMPA/kainate-R antagonist), and **(B)** the resulting fura-2 ratio trace for same experiment. Note quenching effect of the yellow DNQX solution. **(C)** For comparison, fluorescence intensities are shown for an imaged RGC treated with NMDA in the presence and absence of the colorless NMDA-R antagonist APV (100 μM). The resulting fura-2 trace for this same RGC is depicted in Figure 4-2 C. **(D)** Mean (± 1 SD) absorbance (in arbitrary units) of glutamate antagonist solutions (dissolved in HBSS, from n = 3 separate experiments) at 340 and 380 nm, as measured in a spectrophotometer (path length = 1 cm). The absorbance of HBSS alone was subtracted from each reading. The DNQX and CNQX solutions absorbed more at 340 nm relative to 380 nm (Δ ABS is difference between 340 and 380 nm absorbances), while the NBQX and APV solutions did not exhibit asymmetrical absorbance.

induced calcium signal was blocked by the colorless APV is shown in Figure 4-3 C. The absorbance of the glutamate receptor antagonists, dissolved in HBSS at the same concentrations as for the imaging experiments, was then measured in a spectrophotometer. The absorbance of NBQX (25 μM) at 340 and 380 nm was almost identical, while DNQX (25 μM) and CNQX (25 μM) solutions exhibited greater absorbance at 340 relative to 380 nm (Figure 4-3 D). The differential absorbance at the two excitation wavelengths alters the relationship of the fura-2 ratio to $[Ca^{2+}]_i$ and therefore the apparent decrease in NMDA-evoked signals was artifact due to quenching effects of these compounds on fura-2 fluorescence. As 25 μM NBQX blocked kainate responses and did not affect NMDA responses, this was the AMPA/kainate-R antagonist utilized in subsequent experiments in this chapter.

Mechanisms of Glutamate-Induced Calcium Influx in Isolated RGCs

The experiments with the glutamatergic agonists NMDA and kainate confirmed that there are at least two distinct pathways through which glutamate could potentially influence RGC calcium dynamics. Glutamate is the natural endogenous ligand for these two receptor types, and its action can differ from that of its related agonists. In particular, the activation of AMPA-Rs by glutamate is accompanied by rapid desensitization, but this desensitization is markedly reduced if AMPA-Rs are instead stimulated with kainate (Hollmann and Heinemann 1994; Dingledine *et al.* 1999). Therefore, the magnitude of kainate-induced calcium influx may be exaggerated, as compared to that mediated by glutamate stimulation of AMPA/kainate-Rs.

To test the relative contribution of the NMDA-R and AMPA/kainate-R-mediated pathways, I assessed the effect of APV and NBQX on the calcium signal produced by a 30 s treatment of 10 and 100 μM glutamate (plus 10 μM glycine). Based on the data

shown in Figure 4-1, these concentrations elicited the near-threshold (10 μM) and maximum (100 μM) calcium responses in the isolated RGCs under Mg^{2+}-free conditions. The NMDA-R antagonist APV (100 μM) dramatically ($P < 0.01$, Friedman ANOVA, Tukey; as compared to both initial and recovery responses with APV absent) reduced the elevation in $[Ca^{2+}]_i$ that occurred with either 10 or 100 μM glutamate treatment (Figure 4-4 A, C, D). The AMPA/kainate-R antagonist NBQX (25 μM) did not affect ($P = 0.418$, Friedman ANOVA) 10 μM glutamate responses, but it did have a small yet significant ($P < 0.01$, Friedman ANOVA, Tukey) effect on 100 μM glutamate responses (Figure 4-4 B, C, D). These results indicate that glutamate-induced calcium influx occurs predominantly through NMDA-R activation, although at higher glutamate concentrations there is a small AMPA/kainate-R contribution. 10 μM glycine was included in the glutamate treatment solutions because it significantly ($P < 0.05$, Friedman ANOVA, Tukey) enhanced RGC responses, and increasing the glycine concentration to 50 μM did not further potentiate the calcium signals (Figure 4-4 E, F). As glycine is a co-agonist with glutamate at NMDA-Rs (Johnson and Ascher 1987), the effect of glycine was consistent with NMDA-Rs mediating the glutamate-related rise in RGC $[Ca^{2+}]_i$.

I next sought to assess the contribution of VGCCs to glutamate-evoked changes in $[Ca^{2+}]_i$, as calcium could also pass through VGCCs if RGCs became depolarized during glutamate treatment. I first attempted to inhibit all types of VGCCs with the non-selective blocker cadmium, but this divalent cation interfered with the fura-2 indicator dye (data not shown). Instead, RGCs were stimulated with 10 and 100 μM glutamate, 200 μM NMDA, and 200 μM kainate in the presence of ω-conotoxin GVIA (5 μM) and verapamil (10 μM), selective blockers of N- and L- type VGCCs, respectively. Verapamil was used rather than nifedipine, another commonly used blocker of L-type VGCCs, due

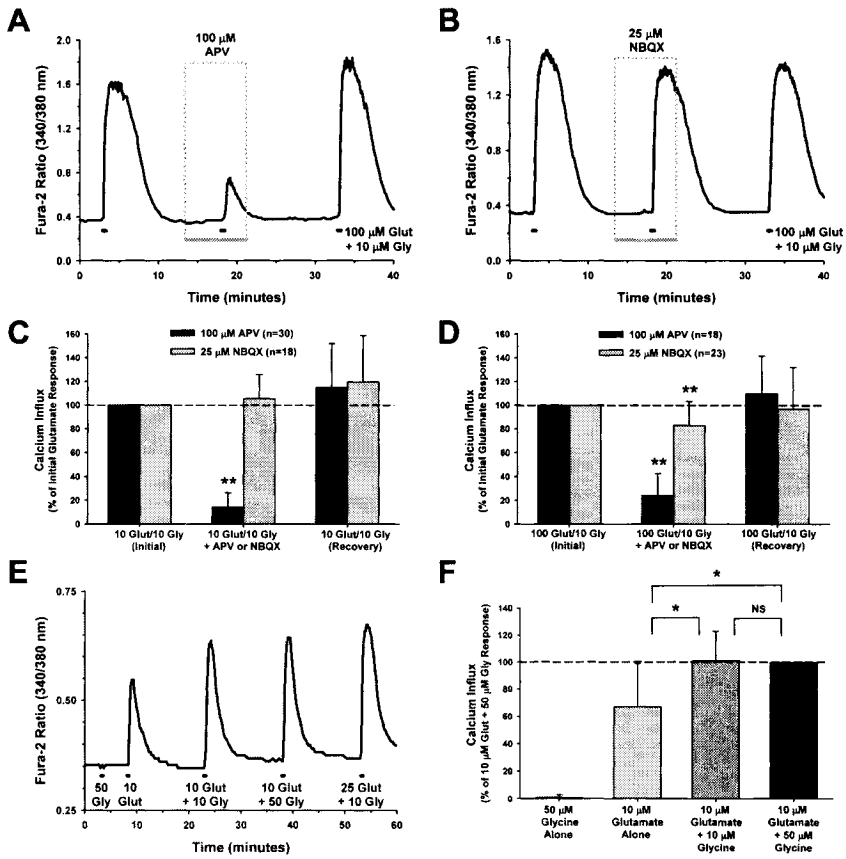

Figure 4-4. Effect of glutamate (Glut) receptor antagonists and glycine (Gly) on glutamate-induced calcium influx in isolated RGCs. **(A-B)** Example fura-2 ratio traces illustrating effects of (A) NMDA-R antagonist APV and (B) AMPA/kainate-R antagonist NBQX on the calcium signal evoked by 100 µM Glut. **(C-D)** Mean data (± 1 SD) showing effect of antagonists on calcium influx due to (C) 10 µM and (D) 100 µM Glut treatments (with 10 µM Gly; extracellular Mg^{2+} absent). Calcium influx in these experiments was calculated as the change in $[Ca^{2+}]_i$, following conversion of the fura-2 ratios through calibration experiments, and data was normalized to initial RGC glutamate responses (dashed line). **(E)** Example fura-2 ratio trace and **(F)** mean normalized data (± 1 SD) summarizing effect of 50 µM Gly alone, 10 µM Glut alone, 10 µM Glut plus 10 µM Gly and 10 µM Glut plus 50 µM Gly on RGCs (n = 14). Gly alone does not affect $[Ca^{2+}]_i$, but potentiates RGC responses to Glut. The RGC in (E) was also exposed to 25 µM Glut plus 10 µM Gly to show that fura-2 dye saturation had not occurred. * $P < 0.05$, ** $P < 0.01$, Friedman ANOVA, Tukey, within-cell comparisons on normalized data.

to the concern that the yellow-colored nifedipine may have had similar fluorescence-quenching effects as the yellow quinoxaline AMPA/kainate-R antagonists (see Figure 4-3). The VGCC blocking cocktail significantly ($P < 0.05$, Friedman ANOVA, Tukey; as compared to both initial and recovery responses with VGCC blockers absent) reduced the calcium influx induced by 100 μM glutamate and 200 μM kainate but did not significantly ($P > 0.05$) alter 10 μM glutamate and 200 μM NMDA responses (Figure 4-5). These results suggest that VGCCs are not involved in calcium signals produced by a near-threshold glutamate dose (10 μM), but these channels do contribute significantly to changes in $[Ca^{2+}]_i$ evoked by saturating glutamate doses (100 μM) in isolated RGCs. A concentration of 200 μM was used for both NMDA and kainate, as these concentrations had previously been shown to elicit roughly equivalent calcium signals (see Figure 4-2 A). In accord, the mean magnitude of calcium responses evoked by 200 μM kainate was not significantly different ($P = 0.91$, t-test) than the magnitude of responses produced by 200 μM NMDA treatment (mean rise in $[Ca^{2+}]_i$ was 412 nM ± 407 SD for kainate-treated RGCs [n = 15] and 425 nM ± 200 SD for NMDA-treated RGCs [n = 18]). These results indicate a greater role for VGCCs in AMPA/kainate-R-mediated calcium signals relative to comparable NMDA-R-driven responses.

The superfusing HBSS used in all calcium imaging experiments presented so far was nominally Mg^{2+}-free. Magnesium is known to exert a voltage-dependent block of the NMDA-R channel pore (Mayer *et al.* 1984; Nowak *et al.* 1984). In the presence of 0.8 mM Mg^{2+}, the magnitude of the calcium signal induced by various glutamate concentrations was blunted as compared to recordings in Mg^{2+}-free HBSS, with 10 and 100 μM glutamate often being below threshold (example trace in Figure 4-6 A). To directly test the effect of extracellular Mg^{2+}, isolated RGCs (n = 12) were exposed to

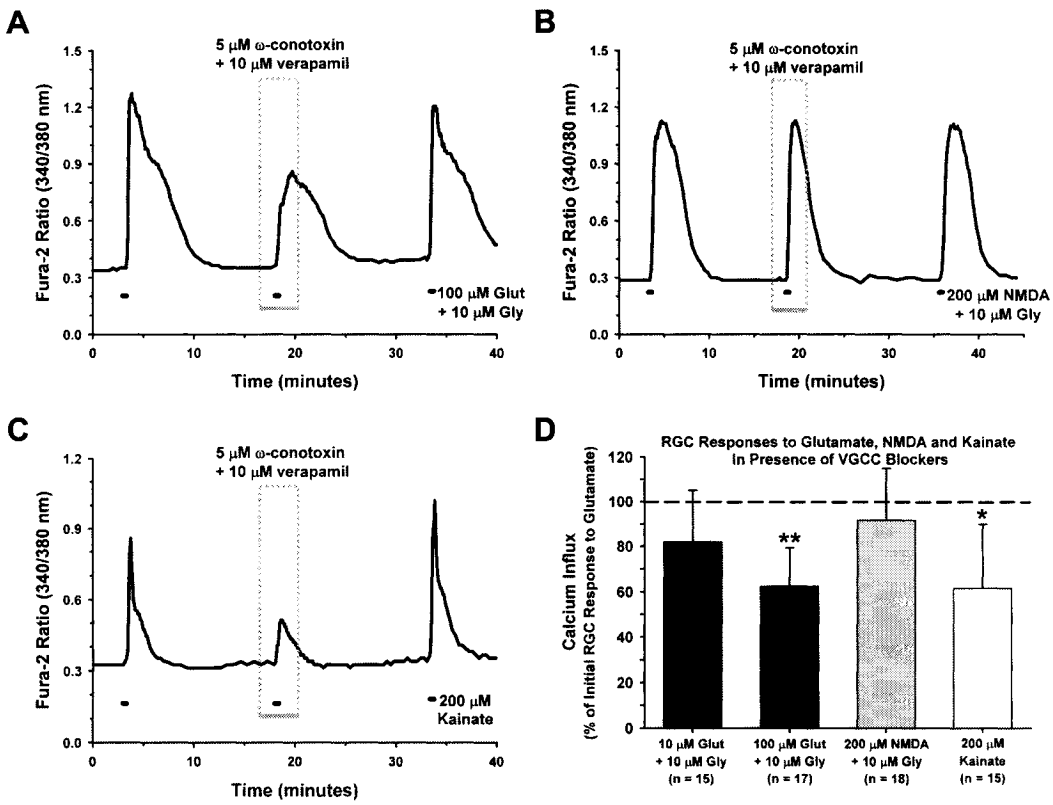

Figure 4-5. Effect of voltage-gated calcium channel (VGCCs) inhibition on glutamatergic calcium influx in isolated RGCs. Representative fura-2 ratio traces of RGCs treated with **(A)** 100 μM glutamate (with 10 μM glycine), **(B)** 200 μM NMDA (with 10 μM glycine), and **(C)** 200 μM kainate in the presence and absence of 5 μM ω-conotoxin GVIA (N-type VGCC blocker) and 10 μM verapamil (L-type VGCC blocker). **(D)** Summary of mean data (± 1 SD) for effect of VGCC blocking cocktail on the calcium influx induced by 10 μM and 100 μM glutamate, 200 μM NMDA, and 200 μM kainate. All recordings were performed under Mg^{2+}-free conditions, and calcium influx was calculated as the peak minus baseline change in $[Ca^{2+}]_i$ following conversion of the fura-2 ratios through calibration experiments. * $P < 0.05$, ** $P < 0.01$, Friedman ANOVA, Tukey, as compared to the initial and recovery responses of each RGC to the glutamatergic agonists with the VGCCs absent.

consecutive glutamate treatments (10 μM; with 10 μM glycine) while the superfusing solution alternated between Mg^{2+}-free HBSS and HBSS containing 0.8 mM Mg^{2+} (Figure 4-6 B). Glutamate-induced calcium influx was greatly diminished ($P < 0.01$, Friedman ANOVA, Tukey) with extracellular Mg^{2+} present as compared to initial and recovery responses in Mg^{2+}-free HBSS; Figure 4-6 C).

The effects of glutamate receptor antagonists were then re-assessed on RGCs challenged with 1000 μM glutamate with 0.8 mM Mg^{2+} present. Only RGCs exhibiting a $\Delta [Ca^{2+}]_i$ of at least 150 nM (roughly equivalent to a Δ fura-2 ratio of 0.2) due to glutamate treatment were included in analysis. Under these conditions, the AMPA-kainate-R antagonist NBQX (25 μM) dramatically ($P < 0.01$, Friedman ANOVA, Tukey, as compared to both initial and recovery responses) reduced glutamate-evoked calcium signals (Figure 4-6 E, F). The NMDA-R antagonist APV, at 100 μM, had a small but significant ($P < 0.05$) effect (Figure 4-6 F). However, the effect of APV was greater at increasing concentrations (data not shown), suggesting that this competitive antagonist was being out-competed by the high (1000 μM) glutamate concentration. To confirm this hypothesis, I tested the non-competitive NMDA-R channel blocker MK-801 (10 μM), and found that this antagonist exhibited a strong inhibitory effect ($P < 0.01$; Figure 4-6 D, F). Therefore, in the presence of external Mg^{2+}, blockade of either NMDA-Rs or AMPA/kainate-Rs will result in near abolishment of glutamate-induced calcium influx.

Glutamate-Induced Calcium Influx in Adult Rat RGCs: Isolated Cells and Retinal Wholemounts

All preceding experiments were performed on purified RGC cultures generated from neonatal rats (age 7-8 postnatal days). At this age, RGC dendrites are just beginning to form functional glutamatergic synapses with bipolar cells in the retina

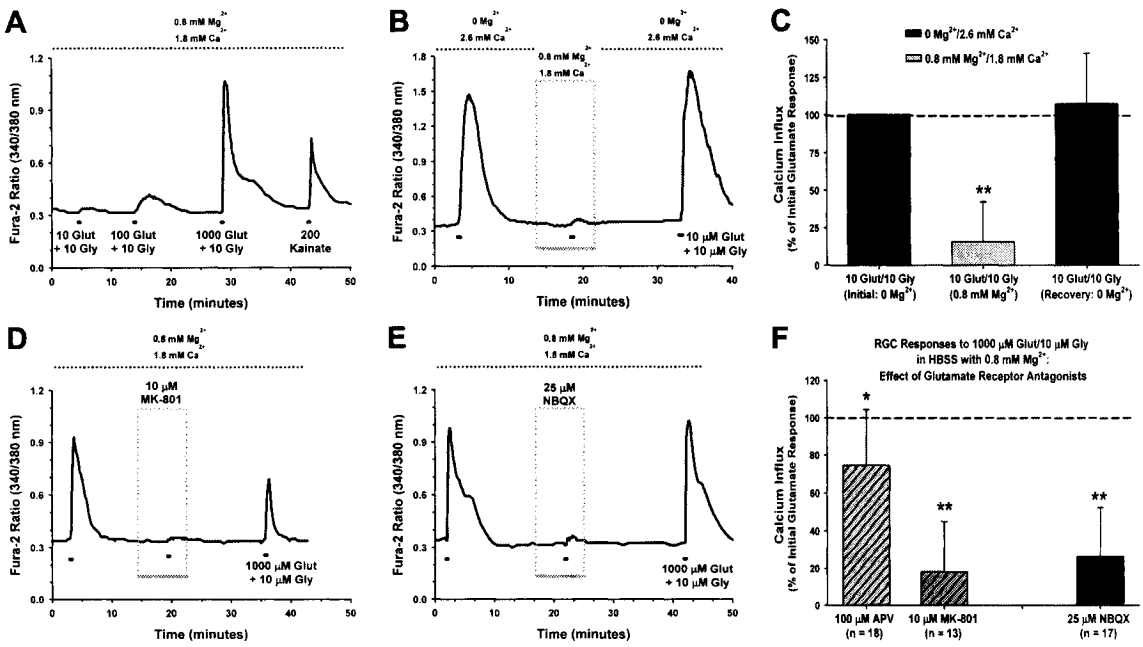

Figure 4-6. Effect of extracellular Mg^{2+} on glutamate-induced calcium influx in isolated RGCs. **(A)** Fura-2 ratio trace for an RGC, in HBSS containing 0.8 mM Mg^{2+}, exposed to 10, 100, and 1000 µM glutamate (plus 10 µM glycine). Responses to lower glutamate concentrations were reduced under these conditions. Note the RGC still responds to 200 µM kainate. **(B)** Representative trace and **(C)** mean normalized calcium influx (change in $[Ca^{2+}]_i$ ± 1 SD) for RGCs (n = 12) treated with 10 µM glutamate in the absence and presence of 0.8 mM Mg^{2+}. **(D-E)** Fura-2 ratio traces illustrating effect of **(D)** NMDA-R antagonist MK-801 (10 µM) and **(E)** AMPA/kainate-R antagonist NBQX (25 µM) on RGC calcium influx evoked by 1000 µM glutamate (plus 10 µM glycine) in HBSS containing 0.8 mM Mg^{2+}. **(F)** Mean data (± 1 SD) for effect of NMDA-R antagonists (hatched bars) and AMPA/kainate-R antagonist (dark bar) on glutamate-induced calcium influx (normalized to initial response; dashed line). * $P < 0.05$, ** $P < 0.01$, Friedman ANOVA, Tukey, as compared to initial and recovery glutamate responses.

(Bansal *et al.* 2000; Wong *et al.* 2000), and so RGC glutamate receptor expression in neonates may differ from adults. Developmental changes in VGCC properties (based on patch-clamp recordings from retinal slices and wholemounts) of rat RGCs have been reported (Schmid and Guenther 1999). In addition, following the opening of rodent eyes around postnatal day 14-15, distinct alterations in AMPA-R to NMDA-R ratios (Chen and Regehr 2000) and NMDA-R subunit compositions (van Zundert *et al.* 2004) have been observed in brain neurons (in the lateral geniculate nucleus and superior colliculus) that receive RGC input. Embryonic or early postnatal animals have traditionally been used for neuronal cultures, as the neurons at younger ages have not yet formed extensive synaptic connections and are generally thought to be less susceptible to damage during dissociation (Banker and Goslin 1991). However, RGCs from adult rats, identified by retrograde labeling, have recently been isolated in mixed retinal cell cultures (Hayashida *et al.* 2004). To test whether the mechanisms underlying glutamate-induced calcium influx change as rats mature, purified RGC cultures were generated from adult rats (age 6-15 weeks) using the Thy1.1 immunopanning technique.

The yield of immunopanned RGCs extracted from adult retinas ranged between 10,000-17,000 RGCs per retina, as compared to 25,000-40,000 RGCs per retina for neonatal rats. This reduction is not due to developmental RGC loss as the total number of RGCs at age 7-8 days is roughly the same as in adult rats (Potts *et al.* 1982), but is likely due to the loss of more cells to damage during dissociation. In contrast to immunopanned RGCs from neonatal rats, RGCs isolated from adult rat retinas displayed little neurite outgrowth in culture (Figure 4-7 A; also see Figure 3-3 E for comparative example of neonatal RGCs 1 day after plating). Despite this morphological difference, glutamate-induced calcium influx (with glycine present and extracellular Mg^{2+} absent) was primarily mediated through NMDA-R activation in cultured adult RGCs as in

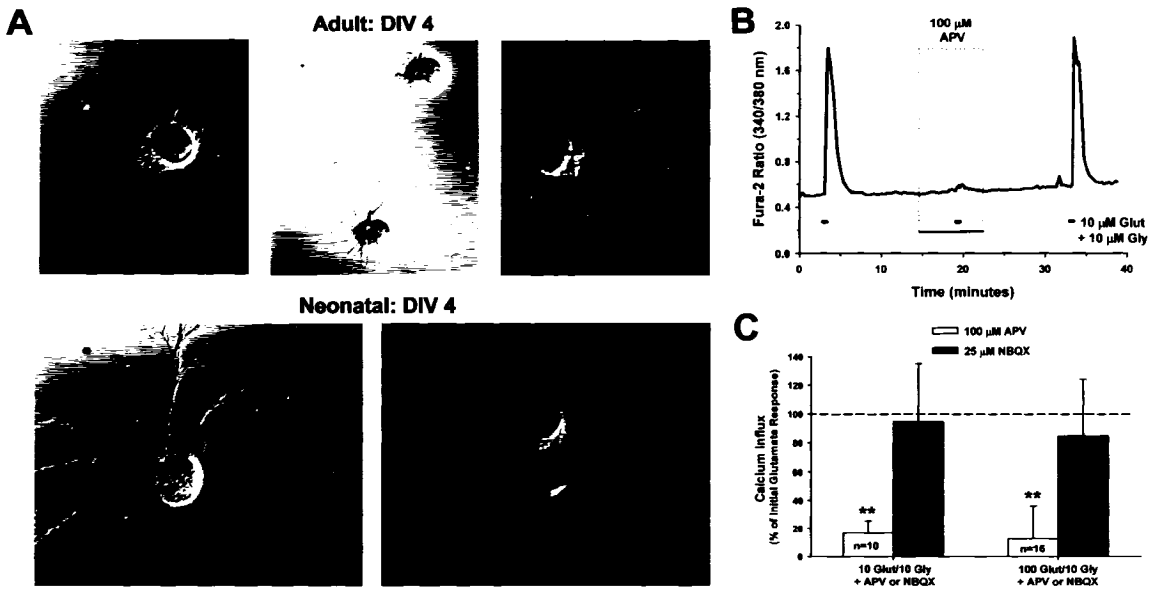

Figure 4- 7. Effect of glutamate receptor antagonists on glutamate-induced calcium influx in immunopanned RGC cultures generated from adult rats. **(A)** DIC images of RGCs isolated from adult (6 weeks old) and neonatal (8 days old) rats after 4 days *in vitro* (DIV). In contrast to neonatal RGCs, adult RGCs exhibited little to no neurite outgrowth. Scale bars = 25 µm. **(B)** Representative trace illustrating effect of NMDA-R antagonist APV on an RGC's response to 10 µM glutamate (with 10 µM glycine; extracellular Mg^{2+} absent). **(C)** Mean data (change in $[Ca^{2+}]_i$ ± 1 SD) showing effect of glutamate receptor antagonists on the calcium responses evoked by 10 and 100 µM glutamate in RGCs isolated from adult rats (normalized to initial response; dashed line). ** $P < 0.01$, Friedman ANOVA, Tukey, compared to initial and recovery glutamate responses with antagonists absent.

neonatal RGCs. The NMDA-R antagonist APV (100 μM) significantly reduced ($P < 0.01$, Friedman ANOVA, Tukey, as compared to both initial and recovery glutamate responses) the calcium influx induced by 10 μM or 100 μM glutamate, while the AMPA/kainate-R antagonist NBQX had negligible ($P > 0.05$) effect (Figure 4-7 B, C).

To determine whether the mechanisms underlying glutamatergic calcium dynamics were altered by the dissociation procedure, I next tested the relative effectiveness of glutamate receptor antagonists on RGCs in retinal wholemounts prepared from adult rats. RGCs were retrogradely loaded with dextran-conjugated fura calcium indicator dye (Figure 4-8 A) following injection of the dye into the filter-mounted retinas (see Baldridge 1996 and Chapter 3 of this thesis for further description of this technique). I first confirmed that both NMDA and kainate produce detectable calcium responses in RGCs in this intact retina preparation, and these responses could be blocked by the appropriate antagonists, 100 μM APV and 25 μM NBQX, respectively (Figure 4-8 B, C). As in previous work (Chapter 3), micromolar concentrations of glutamate were ineffective at stimulating RGC $[Ca^{2+}]_i$ increases. This is due to the efficiency of retinal glutamate uptake that quickly removes glutamate, but not NMDA or kainate, from the extracellular milieu. At 500 μM, glutamate did elicit a detectable calcium signal when co-applied with the glutamate transporter inhibitor TBOA (250 μM). This glutamate-related response was significantly ($P < 0.01$, Friedman ANOVA, Tukey, as compared to initial and recovery glutamate plus TBOA responses) reduced by APV but it was not affected ($P > 0.05$) by NBQX (Figure 4-8 D,E). Therefore, as in isolated RGCs, NMDA-Rs played a predominant role in mediating the rise in RGC calcium levels due to glutamate treatment in this intact retina preparation.

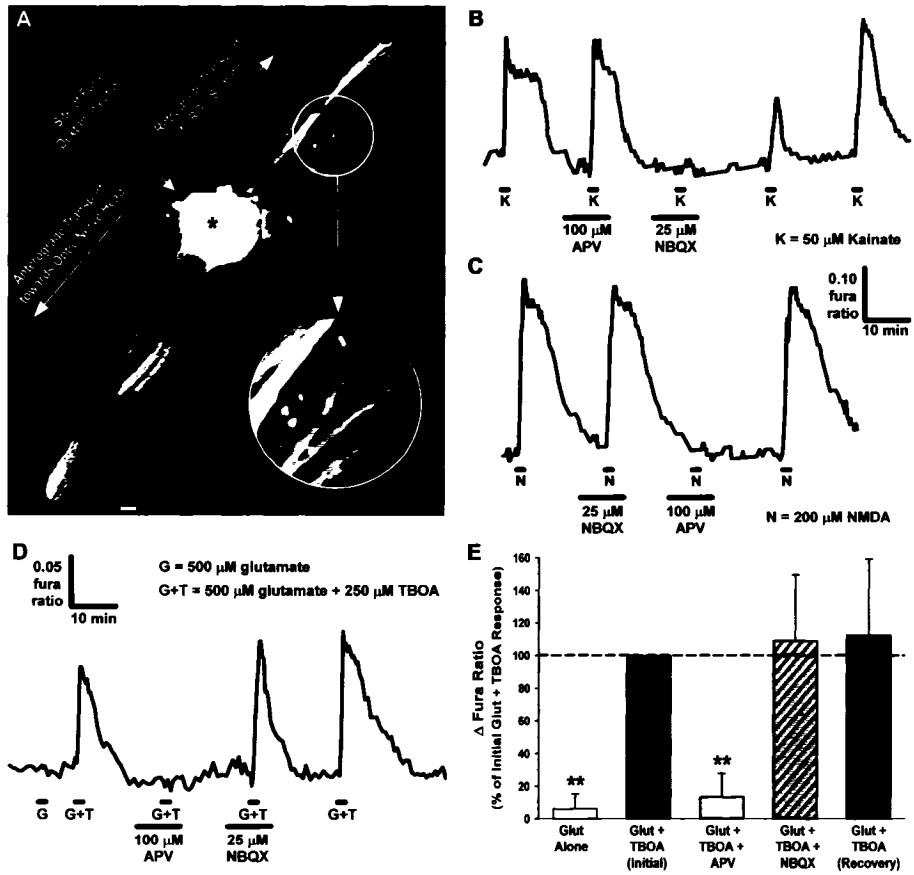

Figure 4- 8. Glutamatergic calcium dynamics in adult rat retinal wholemount preparations. **(A)** Montage of fluorescent micrographs (380 nm excitation, 510 emission) showing retrograde loading of RGC somata following injection of fura dextran calcium indicator dye into the retinal wholemount at the site denoted by an asterisk. Scale bar = 50 µm. The encircled area is shown at higher magnification to highlight individual RGC somata loaded with fura dextran. **(B-C)** Example fura-2 traces showing that (B) kainate-induced calcium influx in RGCs in this intact retina preparation is blocked by the AMPA/kainate-R antagonist NBQX and not affected by the NMDA-R antagonist APV, while (C) the converse is true for NMDA-mediated responses. **(D)** Representative trace illustrating that glutamate is more effective at evoking a detectable calcium signal when co-applied with the glutamate transporter inhibitor TBOA, and the glutamate plus TBOA response is blocked by APV and not affected by NBQX. **(E)** Mean data (Δ fura ratio ± 1 SD) summarizing effect of glutamate receptor antagonists on glutamate responses in RGCs (n = 110) from the retinal wholemount preparations (N = 4 wholemounts; from 4 rats). ** $P < 0.01$, Friedman ANOVA, Tukey, compared to glutamate/TBOA responses.

RGC Calcium Dynamics and Deregulation During Prolonged Glutamate Exposure

RGC calcium dynamics were next monitored during a more prolonged glutamate exposure of 1 h. For these experiments, immunopanned RGCs from neonatal rats were again used, and all experiments were performed in Mg^{2+}-free HBSS unless indicated otherwise. In other central neurons, it has been reported that the high affinity calcium indicator dye fura-2 can underestimate the rise in $[Ca^{2+}]_i$ associated with glutamate excitotoxicity due to saturation (Hyrc *et al.* 1997; Stout and Reynolds 1999). To minimize this possibility, the low-affinity calcium indicator dye fura-4F (K_D ~ 770 nM) was instead employed. The overall design of these experiments is illustrated in Figure 4-9. The fura-4F ratio was continuously monitored in RGCs treated for 1 h with different concentrations of glutamate plus 10 μM glycine. The placement of a 0.6x coupling tube between the microscope and the CCD camera enabled more RGCs to be imaged in each session using the 40x objective. Upon glutamate exposure, RGCs generally exhibited an abrupt rise in the fura-4F ratio that then decreased slightly to a relatively stable level (Figure 4-9 C). Cells that maintained this $[Ca^{2+}]_i$ homeostasis throughout the 1 h exposure showed some recovery to baseline levels during the ensuing 15 min wash-out period. However, certain cells exhibited a latent loss in calcium homeostais that was characterized by a large and irreversible rise in the fura-4F ratio. Cells that underwent this delayed calcium deregulation (DCD), previously described in other central neurons (Manev *et al.* 1989; DeCoster *et al.* 1992; Randall and Thayer 1992; Tymianski *et al.* 1993; Rajdev and Reynolds 1994), showed no recovery during the wash-out period, with the fura-4F ratio remaining elevated. At the end of some of these experiments, fluorescently-tagged annexin V was injected into the microscope chamber. During apoptosis, the lipid phosphatidylserine is translocated from the cytoplasmic side of the

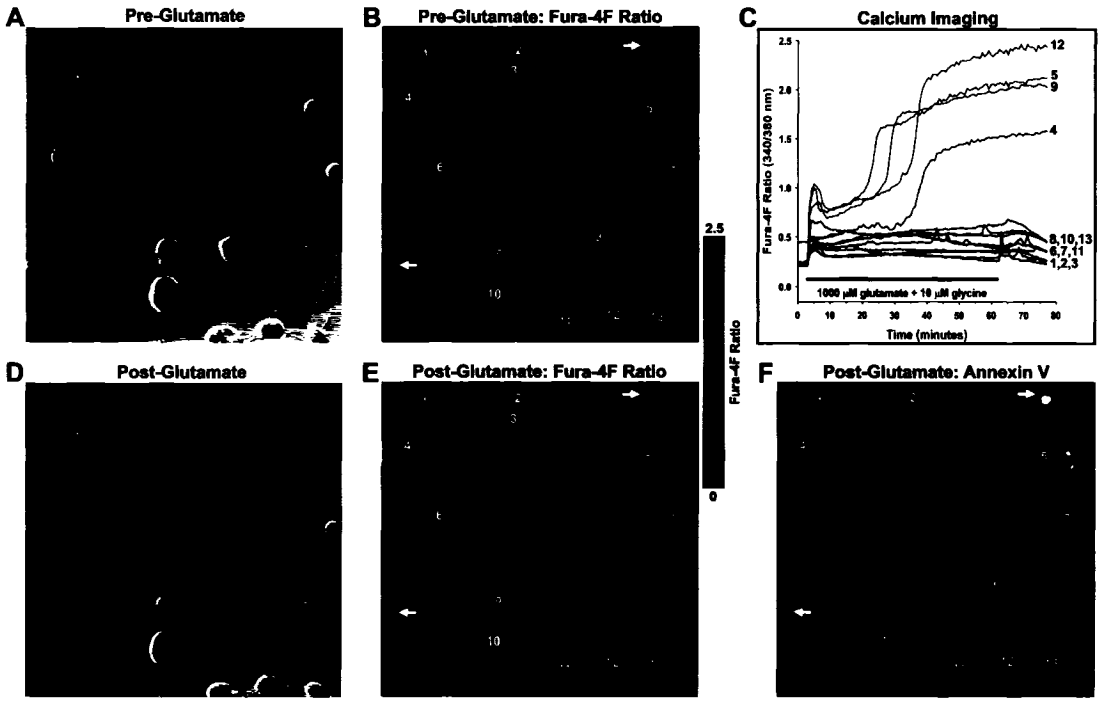

Figure 4- 9. Excitotoxic death of isolated RGCs is associated with delayed calcium deregulation. **(A)** DIC image and **(B)** pseudocolor image of the fura-4F ratio (340/380 nm) of example RGCs, isolated from neonatal rats (1 day in culture), prior to glutamate exposure. **(C)** The fura-4F ratio was monitored in these RGCs while they were continuously superfused with 1000 μM glutamate (plus 10 μM glycine; in Mg^{2+}-free HBSS) for 1 h, followed by a 15 min wash-out period. Of the thirteen RGCs imaged, nine cells maintained homeostatic calcium levels throughout glutamate treatment and recovered towards baseline levels with wash-out (blue traces). In three of the cells (denoted by numbers 5, 9 and 12), there was deregulation of this calcium homeostasis that was characterized by a large increase in the fura ratio with no apparent recovery (red traces). Calcium deregulation was also evident in cell 4 (green trace), but this cell had an elevated fura ratio at the beginning of the experiment and exhibited a negligible initial response to the glutamate treatment. **(D)** DIC image, **(E)** pseudocolor image of the fura-4F ratio and **(F)** annexin V fluorescence in these same cells after glutamate exposure and wash-out. The RGCs numbered 4, 5, 9, and 12 that underwent calcium deregulation stained positive for the death marker annexin V. Note the cells denoted by the arrows also were annexin V-positive, but these cells did not load the calcium indicator dye (absent from fura ratio images) and were therefore not imaged.

plasma membrane to its outer surface (Koopman *et al.* 1994), and therefore annexin V fluorescence can be used to identify apoptotic cells. Necrotic cells can also be stained by annexin V, as this marker can enter lysed cells and stain phosphatidylserine on the inner membrane surface. Annexin V fluorescence was therefore used as a general marker for cell death, rather than to distinguish apoptosis from necrosis. As evident in Figure 4-9 F, the four cells that underwent calcium deregulation (denoted by numbers 4, 5, 9 and 12) were stained by annexin V at the conclusion of the experiment. It is also important to note the two cells denoted by arrows that were also stained by annexin V (Figure 4-9 F). These cells were clearly damaged prior to glutamate exposure (Figure 4-9 A), but were not included in analysis as such unviable cells do not exhibit fura fluorescence (fura-4F AM requires the ester to be cleaved by endogenous esterases) and were therefore not imaged. In addition, cells with elevated fura ratios at baseline (see cell 4, denoted by green trace in Figure 4-9 C) generally were stained by annexin V and these cells, already unhealthy prior to glutamate treatment, were excluded from analysis (a criterion of baseline fura-4F ratio > 0.3 was used to exclude cells; the number of excluded cells was < 5% of total number of cells imaged) to preclude these cells from influencing the results.

Related experiments were routinely performed on RGCs from sibling cultures during the first two days after cell plating, and all results are based on the pooled data from at least three different immunopanned RGC cultures. Calcium influx in these experiments was calculated as the Δ fura-4F ratio, the peak ratio during the first 400 s of glutamate exposure minus the mean baseline ratio before glutamate treatment. The timeframe of 400 s was utilized in order to compare the calcium levels, prior to the onset of DCD, of those cells that deregulated versus those that did not (no cells underwent deregulation during the first 400 s). Also, the peak fura ratio (not including the increase

associated with DCD) generally occurred during this initial response before decaying to a stable level. There was no significant difference in the mean initial calcium influx between cells treated with either 100 μM or 1000 μM glutamate, while the influx induced by 10 μM glutamate was slightly less ($P < 0.05$, $Q = 3.001$, Kruskal-Wallis ANOVA, Dunn's) than that for 100 μM (Figure 4-10 A). These results are consistent with the findings in Figure 4-1 that showed that 100 μM glutamate was sufficient to evoke maximum calcium responses in isolated RGCs, and verifies that the earlier findings were not due to saturation of the high-affinity fura-2 dye. DCD occurred in 18-28% of the RGCs exposed to 10, 100, and 1000 μM glutamate for 1 h (Figure 4-10 B), and there was no significant difference ($P = 0.351$, Chi-square) in the proportion of cells undergoing DCD during treatment with the different glutamate concentrations. As a control, DCD was not observed in any RGCs ($n = 41$) that were maintained in HBSS (no glutamate) for 1 h. Pooling the data together for the three glutamate concentrations, the incidence of DCD was related to the magnitude of the glutamate-induced calcium responses, as RGCs with larger calcium responses were most likely to deregulate (Figure 4-10 C). This susceptibility was not linked to baseline calcium levels (Figure 4-10 D), indicating that the DCD-exhibiting cells were not already injured prior to glutamate exposure. The presence of annexin V fluorescence was determined at the conclusion of the experiment for 186 of the RGCs treated with glutamate (Figure 4-10 E). The vast majority of deregulating RGCs in this group were stained by annexin V (42 of 44 cells), while RGCs that recovered from glutamate treatment usually exhibited negligible annexin V fluorescence (139 of 142 cells). Therefore, these results indicate that the RGCs that underwent DCD were indeed dead or dying, and would not have recovered had a longer wash-out period been employed.

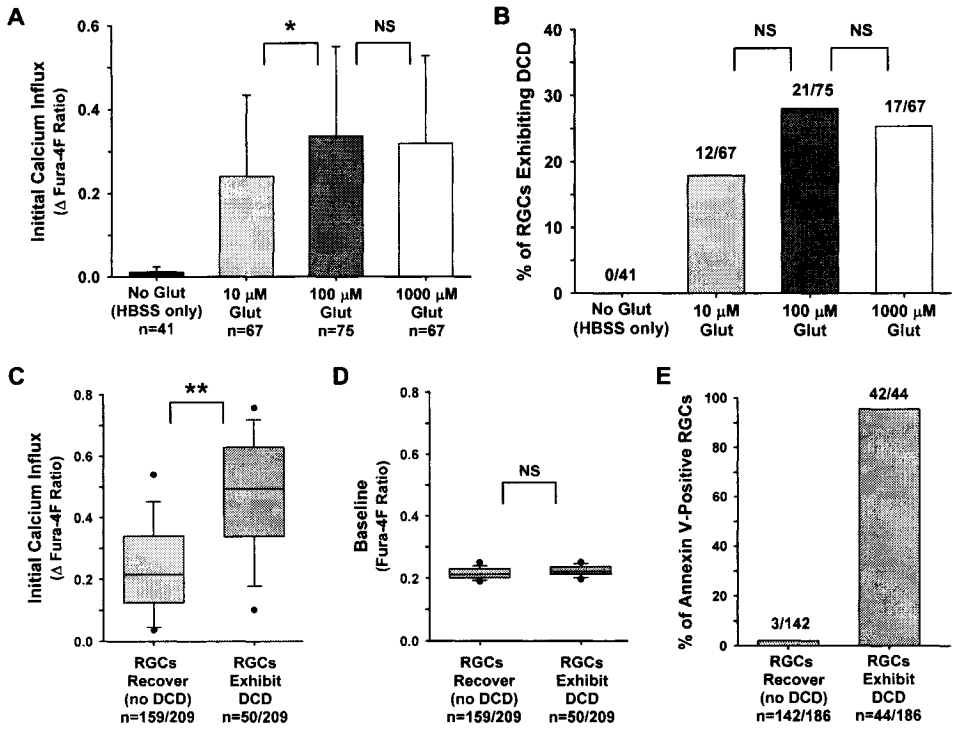

Figure 4- 10. Relationship of glutamate concentration and calcium influx to the incidence of delayed calcium deregulation in isolated RGCs. **(A)** Mean calcium influx (peak fura-4F ratio over first 400 s of glutamate exposure minus baseline ratio; ± 1 SD) induced by 10, 100, and 1000 μM glutamate (plus 10 μM glycine; in Mg^{2+}-free HBSS) during the 1 h glutamate exposure. **(B)** The proportion of cells exhibiting DCD in each treatment group. A group of RGCs were maintained in HBSS for 1 h (glutamate absent) and this control group is included for reference in (A) and (B). **(C)** Box-plots of pooled data for all RGCs treated with glutamate (10-1000 μM; n = 209) illustrating that calcium responses were significantly related to initial calcium influx, but not to **(D)** baseline calcium levels. The upper and lower boundaries of the box indicate the 75th and 25th percentiles, the line within the box marks the median, the whiskers above and below the box indicate the 90th and 10th percentiles, while the points represent outlying data. **(E)** Of the 209 RGCs treated with glutamate, 186 of these RGCs were examined for annexin V fluorescence at the conclusion of the experiment. Annexin V staining paralleled the imaging data, confirming that DCD was associated with cellular death. * $P < 0.05$, ** $P < 0.01$, Kruskal Wallis ANOVA, Dunn's posthoc for calcium influx data (comparing the three glutamate-treated groups); Chi-square for DCD incidence data (comparing the three glutamate-treated groups); Mann-Whitney for comparison of box-plot data.

To assess the effect of glutamate receptor inhibition on DCD occurrence, RGCs were exposed for 1 h to 100 μM glutamate (plus 10 μM glycine; in Mg^{2+}-free HBSS) with AMPA/kainate-R and NMDA-R antagonists present. Each of the tested agents of NBQX (25 μM; AMPA/kainate-R antagonist), APV (100 μM; NMDA-R antagonist) and MK-801 (10 μM; NMDA-R antagonist) significantly ($P < 0.05$, Kruskal-Wallis ANOVA, as compared to group treated only with 100 μM glutamate) reduced the initial calcium influx (Figure 4-11 A). RGCs treated with compounds targeting NMDA-Rs exhibited a significant reduction ($P < 0.01$, Chi square, as compared to 100 μM glutamate-treated group) in DCD occurrence (Figure 4-11 B). Consistent with the observed relationship of calcium influx to DCD incidence (Figure 4-10 C), there was a trend suggesting that greater reductions in glutamate-induced calcium influx were associated with fewer cell numbers exhibiting DCD. APV (100 μM) was not as effective at blocking glutamate-induced calcium signals as in the brief (30 s) glutamate pulse experiments (see Figure 4-4), but this is likely because APV is a competitive antagonist and competes with glutamate throughout the 1 h exposure period. The non-competitive antagonist MK-801 provided near-complete protection, and its effect on glutamate-induced calcium influx and DCD incidence is perhaps best illustrated by examining the optical recordings for all RGCs (n = 40) treated with 100 μM glutamate in the presence of MK-801 (Figure 4-11 D) as compared to traces for RGCs (n = 75) treated with 100 μM glutamate alone (Figure 4-11 C). Calibration of fura-4F ratios to $[Ca^{2+}]_i$ was not performed because the irreversible rise in $[Ca^{2+}]_i$ exceeded the dynamic range of the fura-4F indicator dye. In agreement with the previous experiments employing 30 s glutamate treatments (Figure 4-4), blockade of NMDA-Rs nearly abolished calcium influx, and significantly prevented the incidence of calcium deregulation and ensuing cell death.

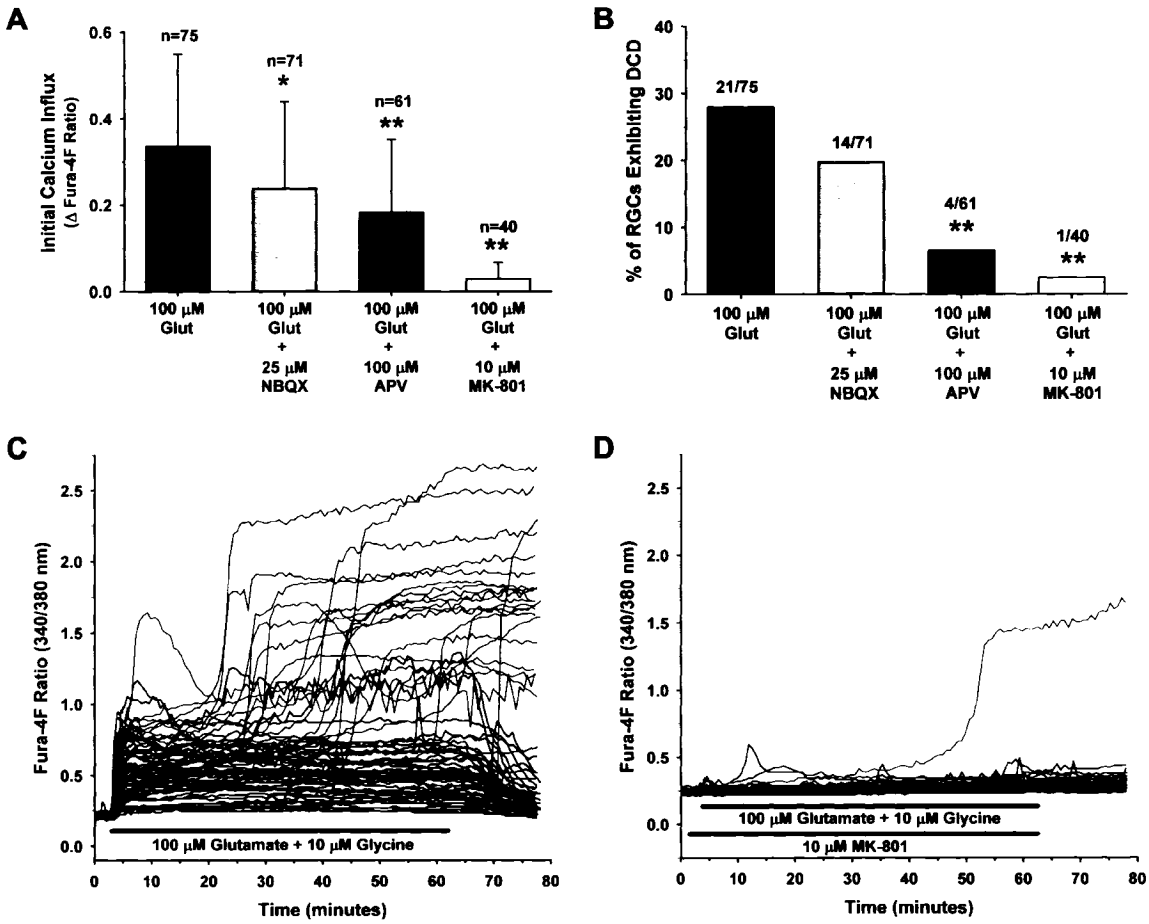

Figure 4- 11. Effect of glutamate receptor inhibition on calcium influx and incidence of delayed calcium deregulation (DCD) in isolated RGCs. **(A)** Mean calcium influx (peak fura-4F ratio over first 400 s of glutamate exposure minus baseline ratio; ± 1 SD) induced by 100 μM glutamate (plus 10 μM glycine; in Mg^{2+}-free HBSS) in the presence and absence of AMPA/kainate-R (NBQX) and NMDA-R (APV and MK-801) antagonists. The data for 100 μM glutamate (blockers absent) is re-plotted from data shown in Figure 4-10. **(B)** The proportion of cells exhibiting DCD in each treatment group. **(C)** Fura-4F ratio traces of all RGCs (n = 75) treated with 100 μM glutamate plus 10 μM glycine for 1 h (with 15 min wash-out) alone, and **(D)** in the presence of the non-competitive NMDA-R antagonist MK-801. RGCs exhibiting DCD are denoted by red traces while RGCs surviving the glutamate insult are denoted by blue traces. * $P < 0.05$, ** $P < 0.01$, as compared to 100 μM glutamate-treated group; Kruskal Wallis ANOVA, Dunn's posthoc for calcium influx data; Chi-square for DCD incidence data.

Discussion

The identification of the mechanisms underlying the excitotoxic pathway, particularly those that distinguish it from physiological glutamatergic signaling, could aid in the development of therapeutic strategies to minimize neuronal loss in pathologies involving glutamate-related death such as ischemic insult. Using calcium imaging techniques, I characterized the mechanisms of glutamate-induced increases in $[Ca^{2+}]_i$, and monitored $[Ca^{2+}]_i$ changes in RGCs undergoing death due to prolonged glutamate exposure.

Glutamate-Induced RGC Calcium Influx is Primarily Mediated by NMDA-Rs

An increase in RGC $[Ca^{2+}]_i$ occurred following stimulation of either NMDA-Rs or AMPA/kainate-Rs with their respective selective agonists, NMDA and kainate, and confirmed that there are multiple pathways through which glutamate can alter RGC calcium dynamics. Under Mg^{2+}-free conditions, the NMDA-R antagonist APV essentially abolished the calcium response induced by a low glutamate concentration (10 μM), and blocked a large part of the response caused by a higher saturating glutamate concentration (100 μM) in neonatal RGCs. The AMPA/kainate-R antagonist NBQX had a small but significant effect on only the RGC responses to the larger glutamate concentration (100 μM). As compared to NMDA-Rs, AMPA/kainate-Rs have a lower affinity for glutamate and desensitize quickly with prolonged stimulation by glutamate (Hollmann and Heinemann 1994; Dingledine *et al.* 1999). These characteristics offer a mechanistic explanation for the findings of the present study: at concentrations of glutamate near the threshold for NMDA-R activation, AMPA/kainate-Rs are not stimulated and so the calcium response is entirely NMDA-R-mediated; and, at high

glutamate concentrations, AMPA/kainate-Rs are activated but desensitize quickly and therefore contribute only a minor portion (relative to NMDA-Rs) of the overall calcium signal.

NBQX was used as the AMPA/kainate-R antagonist in these experiments because of the observation that the AMPA/kainate antagonists DNQX and CNQX quenched fura-2 fluorescence and absorbed light preferentially at 340 nm relative to 380 nm. The differential absorbance of these compounds at the two excitation wavelengths made any true effect of these compounds on the calcium signal difficult to interpret. A compound that quenches both excitation wavelengths equally, as occurred with 25 μM NBQX, has an effect equivalent to a perfect neutral density filter and does not alter the relationship of the fura-2 ratio to $[Ca^{2+}]_i$. It is not my intent to assert that DNQX or CNQX not be used in any studies employing fura-2 imaging. The potential artifact induced by these compounds is dependent on their working concentration and the type of microscope used. The artifact is more pronounced with the use of an upright imaging rig, as used in this study (necessary for the experiments on retinal wholemounts), as the excitation light travels a longer path through the absorbing solution than with an inverted microscope. The results of this study indicate, however, that caution must be exercised in the interpretation of ratiometric data from optical imaging experiments involving fluorescence-quenching solutions such as quinoxaline AMPA/kainate-R antagonists.

Calcium can flow directly through glutamate receptor channels or through the opening of VGCCs subsequent to glutamate receptor-mediated depolarization. Using a cocktail of L- and N-type VGCC blockers, it was determined that the calcium influx through VGCCs contributes at least one-third, on average, of the overall calcium response in isolated RGCs exposed to a saturating concentration of 100 μM glutamate. It is possible that the contribution of VGCCs was underestimated, as only L- and N-type

VGCCs were targeted in these experiments, but these channels have been shown to carry 60-85% of the calcium current in rat RGCs (Karschin and Lipton 1989; Guenther *et al.* 1994; Taschenberger and Grantyn 1995; Schmid and Guenther 1999). AMPA/ kainate-Rs are generally less permeable to Ca^{2+} than NMDA-Rs, and so the contribution of AMPA/kainate-Rs to 100 μM glutamate responses may have occurred through VGCCs rather than direct flow through the receptor-associated channel. The presence of the GluR2 subunit in AMPA-Rs confers their relative impermeability to Ca^{2+}, and *in situ* hybridization (Hamassaki-Britto *et al.* 1993) and immunohistochemical (Hof *et al.* 1998) studies did not find evidence for rat RGCs lacking GluR2. This does not exclude the possibility that RGCs possess both Ca^{2+}-permeable and impermeable AMPA/kainate-Rs, and there is physiological data from rat RGCs *in vitro* that supports this premise (Rorig and Grantyn 1993; Leinders-Zufall *et al.* 1994; Zhang *et al.* 1995). In this study, the calcium influx induced by the non-desensitizing agonist kainate was reduced by roughly 40% in the presence of L- and N-type VGCC blockers, indicating that VGCCs likely contribute to AMPA/kainate-R-mediated calcium signals. Nevertheless, the blockade of VGCCs did not eliminate the kainate responses, thereby supporting a role for Ca^{2+}-permeable AMPA/kainate-Rs. The calcium responses induced by 10 μM glutamate and 200 μM NMDA (these concentrations elicited roughly equivalent calcium signals in the immunopanned RGCs; also, see Chapter 3 of this thesis) were not significantly affected by the VGCC blocking cocktail. This suggests that the calcium signal was mediated by direct flow through NMDA-R-associated channels, although there may have been an additional contribution from calcium-induced calcium release from intracellular stores (Lei *et al.* 1992).

Extracellular Mg^{2+} is known to block NMDA-Rs, but not AMPA/kainate-Rs, in a voltage-dependent manner (Mayer *et al.* 1984; Nowak *et al.* 1984; Patneau and Mayer

1990). By changing the superfusing HBSS from Mg^{2+}-free to that containing 0.8 mM Mg^{2+}, RGC responses to 10 μM glutamate were dramatically reduced. With extracellular Mg^{2+} present, RGC responses to 1000 μM glutamate (higher glutamate concentrations of glutamate were necessary to elicit repeatable robust responses, as compared to experiments in Mg^{2+}-free HBSS) were nearly eliminated by treating the cells with either NMDA-R or AMPA/kainate-R antagonists. The most parsimonious explanation for the difference in the results obtained under Mg^{2+}-free versus Mg^{2+}-containing conditions is that the activation of AMPA/kainate-Rs serves to depolarize the cell and relieve the Mg^{2+}-block of NMDA-Rs. Therefore, activation of both NMDA-Rs and AMPA/kainate-Rs by glutamate is necessary for robust RGC calcium responses with external Mg^{2+} present, but the calcium signal itself is primarily mediated by NMDA-Rs.

Experiments on immunopanned RGCs from adult rats yielded similar results as those on RGCs from neonatal rats in that glutamate-induced calcium influx was significantly reduced by treating the RGCs with the NMDA-R antagonist APV. These results argue against a developmental difference in mechanisms underlying glutamatergic calcium dynamics between 8 day old and adult (> 6 week old) rats. A potential concern with the use of either neonatal or adult RGC cultures is that the dissociation and immunopanning procedure alters the relative expression of NMDA-Rs or AMPA/kainate-Rs as compared to RGCs *in vivo*. Recordings of rat RGCs *in situ* indicate that AMPA/kainate-Rs are present within RGC synaptic clefts, while NMDA-Rs are located extrasynaptically (Chen and Diamond 2002). As RGCs in purified cultures develop few synapses (Ullian *et al.* 2001), AMPA/kainate-Rs may be underrepresented in immunopanned RGCs. The calcium imaging of RGCs in retinal wholemounts prepared from adult rats served to address this issue. In contrast to purified RGC cultures, RGCs and their dendrites in this intact retina preparation are encased by Müller

glial cells possessing high affinity excitatory amino acid transporters that rapidly clear away exogenously applied glutamate (Rauen 2000). Consistent with previous work demonstrating the efficiency of retinal glutamate clearance mechanisms (see Chapter 3 of this thesis), 500 μM glutamate had no effect on RGCs when it was applied by itself to the retinal wholemounts but it induced a detectable calcium signal with the co-application of the glutamate transporter inhibitor TBOA. The bath application of glutamate plus TBOA is meant to mimic the rise in extracellular glutamate levels that occurs when glutamate transporter function is disrupted in conditions such as ischemia/hypoxia (Camacho and Massieu 2006). RGC responses to glutamate with TBOA present were blocked by the NMDA-R antagonist APV but not by the AMPA/kainate-R antagonist NBQX. These antagonists blocked the calcium influx due to their respective receptor agonists (NMDA and kainate), so there was not an issue of poor retinal penetration for these drugs. Thus, as in immunopanned RGCs from neonatal or adult rats, glutamate-induced calcium influx in RGCs in a retinal wholemount preparation was mediated primarily through NMDA-Rs.

Excitotoxic RGC Death is Accompanied by Delayed Calcium Deregulation

During prolonged exposure (1 h) to glutamate (10 - 1000 μM), approximately one-quarter (18 - 28%) of the immunopanned RGCs exhibited a latent loss of calcium homeostasis. This phenomenon has been termed delayed calcium deregulation (DCD) and has been described in other CNS neurons, including cerebellar granule (Manev *et al.* 1989), hippocampal (Randall and Thayer 1992), spinal (Tymianski *et al.* 1993) and cortical neurons (Rajdev and Reynolds 1994). RGCs undergoing DCD did not show recovery in $[Ca^{2+}]_i$ during the 15 min wash-out period following glutamate exposure, while RGCs that maintained a plateau $[Ca^{2+}]_i$ throughout the glutamate treatment

recovered towards baseline levels. The injection of the death marker annexin V into the microscope chamber at the culmination of the imaging experiments resulted in essentially exclusive labeling of RGCs that had underwent DCD, consistent with previous work showing that DCD precedes, or at least coincides with, excitotoxic neuronal death (Tymianski *et al.* 1993). A recent study has demonstrated, using cerebellar granule neurons, that the secondary irreversible rise in $[Ca^{2+}]_i$ is due to calpain-mediated proteolysis of plasma membrane Na^+/Ca^{2+} exchangers, which renders the neurons incapable of extruding Ca^{2+} in sufficient amounts to maintain homeostasis (Bano *et al.* 2005). There is evidence from calcium imaging experiments on isolated goldfish RGCs that these neurons can regulate intracellular $[Ca^{2+}]_i$ through Na^+/Ca^{2+} exchangers (Bindokas *et al.* 1994), and immunohistochemical studies have found Na^+/Ca^{2+} exchangers to be present in the inner retina of salamander, likely on sub-populations of RGCs and amacrine cells (Krizaj *et al.* 2004). It has also been suggested that, rather than a defect in calcium efflux, the large rise in $[Ca^{2+}]_i$ associated with DCD may instead be due to increased activation of certain transient receptor potential (TRP) channels which leads to excessive calcium influx (Chinopoulos *et al.* 2004; Chinopoulos and Adam-Vizi 2006). Activation of TRP channels appears to be modulated by extracellular divalent cations (MacDonald *et al.* 2006), such as Mg^{2+} and Ca^{2+}, and calcium influx through TRP channels may contribute to excitotoxic death during prolonged ischemic insult (Aarts *et al.* 2003). The nature of the secondary $[Ca^{2+}]_i$ increase during DCD remains unknown in RGCs and should be a topic of future study.

In the prolonged glutamate exposure experiments, blockade of NMDA-R activation with the competitive antagonist APV or the non-competitive antagonist MK-801 reduced RGC calcium responses and significantly lowered the percentage of cells showing DCD. The AMPA/kainate-R antagonist NBQX had a small effect on the peak

calcium responses, but its effect in preventing DCD was not statistically significant. Therefore, activation of NMDA-Rs was a major contributor in the initiation of DCD and the occurrence of glutamate-induced cell death. These results differ from those of a recent study that reported RGCs to be completely invulnerable to NMDA and glutamate excitotoxicity (Ullian *et al.* 2004). However, although NMDA-driven currents were identified on the isolated RGCs in this study using a Mg^{2+}-free solution, the excitotoxicity experiments were performed in Mg^{2+}-containing culture medium (Ullian *et al.* 2004). NMDA-Rs would remain blocked by Mg^{2+} with application of NMDA alone, and NMDA-R-driven responses to glutamate would be blunted, as illustrated in the present study. Unlike isolated RGCs in culture, RGCs *in vivo* retain their synaptic input which would serve to depolarize the cell and relieve the NMDA-R Mg^{2+}-block. This offers a potential reason for why a number of *in vivo* studies have reported NMDA excitotoxicity of RGCs (Siliprandi *et al.* 1992; Lam *et al.* 1999; Li *et al.* 1999; Schlamp *et al.* 2001; Manabe *et al.* 2005; Nakazawa *et al.* 2005), yet previous experiments on immunopanned RGCs cultured in Mg^{2+}-containing medium have demonstrated negligible NMDA neurotoxicity (Otori *et al.* 1998; Ullian *et al.* 2004).

The AM ester must be enzymatically cleaved from the fura dye in order for the RGCs to exhibit fura fluorescence, and so unviable cells (i.e. those injured during the dissociation procedure) were not imaged and therefore precluded from influencing the results regarding the neurotoxicity of glutamate. RGCs with elevated baseline fura-4F ratios generally did not respond to glutamate and did not demonstrate any recovery upon wash-out, and these unhealthy cells were also excluded from analysis. As there was no significant difference in the baseline fura-4F ratios between the cells that developed DCD and those that did not, and RGCs maintained in only HBSS (no glutamate added) did not exhibit DCD, it is unlikely that the occurrence of DCD and

subsequent cell death was not related to glutamate treatment. To make certain that the isolated RGCs were exposed to a stable glutamate concentration, the glutamate-containing HBSS was constantly superfused over the cells in the microscope chamber. With continuous superfusion, it is improbable that any endogenous release of glutamate (or other neuroactive compounds) altered individual RGC responses. Also, as the glutamate transporter EAAC1 has been identified on rat RGCs (Rauen *et al.* 1996; Schultz and Stell 1996), the constant flow of glutamate into the chamber ensured that the cells were exposed to extracellular glutamate for the full 1 h period. An additional difference between this study and previous excitotoxicity studies on immunopanned RGCs (Otori *et al.* 1998; Ullian *et al.* 2004) is that the RGCs were transferred to HBSS for glutamate treatments (and calcium imaging), rather than adding glutamate to the Neurobasal/B27 culture medium. Besides Mg^{2+}, this culture medium contains vitamins, minerals, and antioxidants that are designed to enhance neuronal survival (Brewer *et al.* 1993). In particular, oxidative stress caused by the formation of free radicals (such as peroxynitrate generated from nitric oxide) has been implicated as a downstream effector of NMDA-R-mediated excitotoxicity (Dawson *et al.* 1991; Dawson *et al.* 1993; Dugan *et al.* 1995; Reynolds and Hastings 1995; Sattler *et al.* 1999). The antioxidants present in Neurobasal/B27 have been shown to be neuroprotective in models of glutamate-induced neuronal death (Perry *et al.* 2004), indicating that this culture medium may confound studies directed at elucidating the excitotoxic death pathway.

In either the experiments using the high affinity dye fura-2 (RGCs exposed to glutamate for 30 s) or those with the low affinity dye fura-4F (RGCs exposed to glutamate for 1 h), it was apparent that there was considerable inter-neuronal variability in the size of the calcium signal induced by glutamate in immunopanned RGCs. While the dissociation procedure may have contributed to this variability, studies that have

assessed the accumulation of cation channel permeant agmatine in mammalian retinas exposed to glutamatergic agonists indicate that RGCs are indeed a heterogeneous group of neurons with a broad spectrum of responses to excitatory input (Marc 1999a, 1999b; Marc and Jones 2002; Sun *et al.* 2003; Sun and Kalloniatis 2006). The magnitude of an individual RGC's glutamate-induced calcium signal was linked to its susceptibility to excitotoxic death, as RGCs that displayed larger calcium responses were more likely to undergo DCD and die during the 1 hour treatment period. This finding is in general agreement with the "Ca^{2+} load" hypothesis, which suggests that excitotoxic neuronal death is correlated to the rise in $[Ca^{2+}]_i$ (Hartley *et al.* 1993; Eimerl and Schramm 1994; Lu *et al.* 1996). A competing, yet not mutually exclusive, proposal is that the route by which calcium enters the cell is a greater determinant of cell death than the overall change in $[Ca^{2+}]_i$ (the "source specificity" hypothesis), with calcium influx through NMDA-Rs being more likely to initiate the death pathway than influx through VGCCs or AMPA/kainate-Rs (Tymianski *et al.* 1993; Sattler *et al.* 1998). As NMDA-R activation was the major contributor to the RGC calcium signal, the blockade of NMDA-Rs dramatically reduced calcium influx and essentially eliminated the occurrence of DCD. Therefore, the results of these experiments are potentially compatible with either the "Ca^{2+} load" or the "source specificity" hypothesis. However, as the focus of this work was to characterize the mechanisms underlying glutamate-induced calcium influx and excitotoxicity in RGCs, further research is necessary to determine if the influx of Ca^{2+} through NMDA-Rs is more lethal to RGCs than equivalent Ca^{2+} influx through either VGCCs or AMPA/kainate-Rs.

All Ca^{2+} probes, including the fura dyes, bind to calcium and so act as calcium buffers (Rudolf *et al.* 2003). Thus, the monitoring of calcium levels during the prolonged glutamate exposure experiments may have buffered $[Ca^{2+}]_i$ from reaching neurotoxic

levels, reducing the vulnerability of RGCs to glutamate-induced DCD during the 1 h treatment. It is also likely that longer glutamate exposures (1 h was chosen as it was deemed long enough to induce RGC death, yet short enough to allow accurate imaging of RGC $[Ca^{2+}]_i$ over the entire time period) would result in a higher percentage of cells undergoing DCD. Nevertheless, the percentage of RGCs exhibiting DCD (roughly one-quarter of RGCs exposed for 1 h to 100 or 1000 μM glutamate; slightly less for 10 μM glutamate) was much less than the approximate 80% rate of DCD occurrence that has been observed in mixed cultures of cortical (Chinopoulos *et al.* 2004) or spinal (Tymianski *et al.* 1993) neurons using similar glutamate exposures and calcium imaging protocols. There is also good evidence that RGCs are much less vulnerable to excitotoxic insult than retinal amacrine cells (Ullian *et al.* 2004). The results presented in this work indicate that the magnitude of the NMDA-R calcium response is a key determinant of RGC vulnerability to excitotoxicity, raising the possibility that there may be subgroups of RGCs that are more susceptible to glutamate-related death in pathological conditions such as ischemia. It remains to be determined whether the observed variation in NMDA-R-driven RGC calcium signals, or the relative resistance of some RGCs to excitotoxic death (as compared to other CNS neurons), is due to differences in the total number of NMDA-Rs expressed, the NMDA-R subunit composition, the regulation of NMDA-R function (such as through phosphorylation), or the intracellular calcium buffering properties.

Conclusion

It has been nearly 50 years since Lucas and Newhouse (1957) first documented the lethal effects of glutamate with the observation that excessive levels of this excitatory amino acid destroyed inner retinal neurons, including retinal ganglion cells. In this work,

I showed that excitotoxic RGC death was characterized by delayed calcium deregulation, a phenomenon that has been observed in other CNS neurons. RGCs that displayed larger glutamate-evoked calcium responses were more likely to undergo DCD and subsequent cell death. Glutamate-induced calcium influx was shown to occur predominantly through NMDA receptor activation in isolated RGCs generated from either neonatal or adult rats, and in RGCs from retinal wholemounts prepared from adult rats. Glutamatergic calcium responses were attenuated with extracellular Mg^{2+} present, and the blockade of NMDA receptors with selective antagonists or by Mg^{2+} significantly reduced the occurrence of DCD and subsequent excitotoxic RGC death.

CHAPTER 5: Global Discussion

Overall Thesis Summary

Using calcium imaging techniques I demonstrated that the calcium influx induced by the endogenous agonist glutamate is mediated primarily by NMDA-Rs in isolated RGCs purified from neonatal or adult rats. Voltage-gated calcium channels (VGCCs) and AMPA/kainate-Rs contributed to the calcium signal at saturating glutamate levels, but at near-threshold glutamate concentrations, the response was essentially entirely mediated by NMDA-Rs. Consistent with NMDA-R involvement, the presence of extracellular magnesium inhibited RGC responses to glutamate, while glycine had an enhancing effect. Although glutamate is an essential excitatory neurotransmitter, prolonged (1 hour) glutamate exposure was shown to induce RGC death. Glutamate-related death was accompanied by delayed calcium deregulation (DCD), and RGCs that displayed greater glutamate-evoked calcium signals were more likely to undergo DCD and excitotoxic death. Inhibition of NMDA-Rs reduced calcium influx and significantly protected RGCs from the excitotoxic effects of prolonged glutamate exposure.

It is clear from these findings that glutamatergic input to RGCs must be tightly controlled to prevent excessive glutamate receptor stimulation, and this is accomplished through the modulation of glutamate receptors by neuromodulators and through the removal of glutamate from the synaptic cleft by glutamate transporters. Both of these regulatory mechanisms were examined in this thesis. The neuromodulator adenosine was shown to reversibly inhibit glutamate-induced calcium influx through an adenosine A_1 receptor-mediated mechanism. These results support a role for adenosine in retinal

circuitry as a modifier of RGC glutamatergic pathways. The efficiency of retinal glutamate clearance mechanisms was also demonstrated, evident by the finding that glutamate was much less effective than the related agonist NMDA in eliciting a calcium response in RGCs maintained in retinal wholemounts, as compared to isolated RGCs. Pharmacological inhibition of glutamate transporters enabled lower concentrations of glutamate to provoke detectable RGC calcium signals in this intact retina preparation and these responses could be blocked by antagonizing NMDA-Rs but not AMPA/kainate-Rs, consistent with the findings for isolated immunopanned RGCs. Imaging RGC calcium dynamics in retinal wholemounts was used as a novel method to functionally assess glutamate clearance mechanisms, and no significant defect in glutamate uptake was apparent in a rat model of glaucoma as determined with this methodology. These results suggest that while chronic IOP elevation can induce RGC death, it is not sufficient to cause chronic and global alterations in glutamate transport function.

The remainder of this general discussion will focus on topics not fully addressed in the individual chapters. Particular emphasis is given to the implications of the results from Chapter 4 for the earlier findings that were reported in Chapters 2 and 3. Also, I hope to raise unresolved issues that warrant further investigation and to highlight potential future directions and ideas that would extend and advance the body of research presented in this thesis.

Mechanism of Adenosine's Action on Retinal Ganglion Cells

Revealing the actions of modulators such as adenosine on RGCs not only aids in a better understanding of the visual pathway, but also of how neuromodulation may

shape synaptic circuits elsewhere in the CNS. Although the work in Chapter 2 demonstrated that activation of RGC adenosine A_1-receptors reduces glutamate-induced calcium influx, the mechanism through which these receptors regulate the calcium signal was not directly assessed. The modulation of VGCCs (particularly N-type VGCCs) in the CNS by adenosine's activation of A_1-receptors has long been recognized (Mogul *et al.* 1993; Yawo and Chuhma 1993; Wu and Saggau 1994). G-protein-coupled receptor-mediated inhibition of VGCCs is now a well-established phenomenon that has been associated with muscarinic acetylcholine, GABA, opioid, prostaglandin, adrenergic and adenosine receptors (Hille 1994; Zamponi and Snutch 1998). Upon stimulation of these receptors by their respective ligands, the $G_{\beta\gamma}$ subunit separates from the G_{α} subunit of the G-protein and can directly bind to the α1 subunit of N- and P/Q-type VGCCs to cause a reduction in the flow of calcium current (Dolphin 2003). This type of VGCC modulation likely serves a negative feedback function for the control of synaptic neurotransmitter release from dendrites (Chernevskaya *et al.* 1991; Brambilla *et al.* 2005), but it has also been observed for VGCCs located on cell bodies (Holz *et al.* 1986; Ikeda 1991). The inhibition can be reversed ($G_{\beta\gamma}$ subunit uncouples from the VGCC) with strong depolarization of the neuron (Bean 1989), and the membrane potential-associated relief of tonic VGCC inhibition by adenosine has been proposed as a mechanism for the facilitation of short-term synaptic plasticity in central neurons (Brody and Yue 2000).

In accord with the well-known action of adenosine on VGCCs, adenosine inhibited VGCC-mediated calcium currents (through activation of A_1-receptors) in the immunopanned RGCs isolated from neonatal rats (recordings performed by Melanie Lalonde, Dalhousie University; see Hartwick *et al.* 2004). However, as the contribution of VGCCs to RGC glutamate responses was unknown through the course of

experiments performed in Chapter 2, the mechanism of adenosine's action remained speculative. With the characterization of the pathways underlying glutamate-induced calcium influx in Chapter 4, VGCCs were shown to contribute up to a third of the glutamate-induced calcium signal. This indicates that it is possible that A_1-receptor activation inhibited the flow of Ca^{2+} through this pathway. To confirm this hypothesis, future experiments could test the effect of adenosine on RGC glutamate responses in the presence of VGCC inhibitors, particularly the N-type VGCC blocker ω-conotoxin GVIA. If adenosine acts through VGCC inhibition, the effect of adenosine on the resulting glutamate responses should be abolished or highly diminished. In addition, greater adenosine-mediated inhibition would be observed on RGC responses with larger VGCC components, such as RGC responses elicited by treatment with kainate (see Figure 4-5 in Chapter 4) or with elevated extracellular potassium (Ishida *et al.* 1991).

Besides a potential physical interaction between A_1-receptors and VGCCs, adenosine may affect glutamatergic RGC calcium dynamics through secondary messenger pathways. A_1-receptors are coupled to G_i proteins that inhibit adenyl cyclase, thereby leading to a decrease in intracellular cAMP levels (Fredholm *et al.* 2001). The secondary messenger cAMP is essential for the activation of cAMP-dependent protein kinase (PKA), and PKA-mediated phosphorylation of glutamate receptors is a key step in maintaining the functional capacity of these ionotropic receptors (for review, see Gray *et al.* 1998). Inhibition of PKA in hippocampal neurons reduces glutamate-related currents, while treatment with the adenyl cyclase-activating compound forskolin causes an enhancement of glutamate-induced currents through a PKA-mediated mechanism (Greengard *et al.* 1991; Wang *et al.* 1991). Similarly, phosphorylation of NMDA-R NR2 subunits by the tyrosine kinase Src (and related kinases) can enhance NMDA-R currents, and these kinases have also been linked to

upstream signaling cascades involving PKA and G-protein-coupled receptor pathways (for review, see Salter and Kalia 2004). Therefore, an alteration in glutamate receptor phosphorylation, mediated by the actions of a secondary messenger like cAMP, is another potential pathway through which adenosine may modify glutamatergic calcium dynamics. To assess this hypothesis, the effect of adenosine could be tested on RGCs exposed to glutamate with the PKA inhibitor H-89 (Han and Slaughter 1998; Li *et al.* 2004) present, and then assessed on a comparison group of glutamate-stimulated RGCs concurrently treated with forskolin to ensure cAMP levels are elevated for PKA activation. If a cAMP/PKA pathway is involved, adenosine would not affect glutamate responses in the RGCs treated with H-89 but would inhibit the responses elicited in the forskolin-treated RGCs (in addition, larger glutamate responses, with adenosine absent, would be expected for the forskolin-treated RGCs as compared to the H-89-treated RGCs). In determining a role for Src kinases, a more complex, yet theoretically possible, set of experiments could investigate the effect of adenosine on RGCs treated with an inhibitory peptide that disrupts Src kinase (Yu *et al.* 1997). To make the peptide membrane-permeant for cell loading (and negate the need for direct injection into individual RGCs), it could be fused to the human immunodeficiency virus-type 1 Tat protein as has been done for other NMDA-R-interacting peptides (Aarts *et al.* 2002).

Adenosine levels rise during retinal ischemic insult, and the resulting activation of A_1-receptors has been proposed to function as part of the retina's counter-response to limit the extent of neuronal damage (Ghiardi *et al.* 1999; Roth 2004). As shown in Chapter 4, the magnitude of the glutamate-related rise in RGC $[Ca^{2+}]_i$ was associated with the ensuing occurrence of delayed calcium deregulation and cell death. These results suggest that the inhibitory effect of adenosine on glutamate-induced influx (~30% reduction in RGC $[Ca^{2+}]_i$) would confer some degree of neuroprotection against

excitotoxicity. A logical future line of research would be to assess the occurrence of calcium deregulation in RGCs exposed to glutamate for one hour in the presence of adenosine. A reduction in the incidence of calcium deregulation would definitively demonstrate a postsynaptic protective mechanism for adenosine in a central neuron, adding to its more established role of presynaptically inhibiting glutamate release via N-type VGCC modulation (de Mendonca *et al.* 2000). With the determination of adenosine's mechanism of action (described in the experiments at the start of this section), the extent of adenosine's neuroprotection could also be used to confirm or refute the 'calcium load' versus 'source specificity' hypotheses of glutamate excitotoxicity (for review of these theories, see Chapter 1 on page 19). In agreement with the calcium load hypothesis, one would expect that adenosine would have a protective effect roughly proportional to its inhibitory action on calcium influx. In accord with the latter proposal, adenosine would be a relatively less neuroprotective, as compared to an NMDA-R antagonist used at a concentration to achieve similar $[Ca^{2+}]_i$ reduction, if this neuromodulator acts solely through VGCC inhibition. Also in favor of the source specificity theory, adenosine may confer greater neuroprotection than comparable VGCC blockers if its primary action is to regulate NMDA-R phosphorylation.

The results in Chapter 4 showed that the non-competitive NMDA-R antagonist MK-801 essentially abolished glutamate-related calcium influx and prevented RGCs from dying during the one hour glutamate exposure. While this work established the importance of NMDA-Rs in mediating the excitotoxic effects of glutamate on RGCs, it is not my suggestion that the application of MK-801 be considered as a potential neuroprotective retinal therapy. MK-801 has been shown to impair normal neuronal functions (Olney *et al.* 1989) and its NMDA-R blocking action is difficult to reverse (Dingledine *et al.* 1999). As NMDA-Rs have a fundamental role in learning and memory

formation in the brain (Bliss and Collingridge 1993; Nicoll and Malenka 1995; Lamprecht and LeDoux 2004) and in the generation of light-evoked RGC responses in the retina (Cohen and Miller 1994; Chen and Diamond 2002), a compound that completely blocks these receptors is unlikely to be acceptable for clinical use. Indeed, too little Ca^{2+} flowing through NMDA-Rs over time can be as lethal to neurons as excessive Ca^{2+} influx (Hardingham and Bading 2003; Biegon *et al.* 2004), and many of the NMDA-R antagonists assessed in clinical trials have been associated with a high incidence of adverse side effects (Ikonomidou and Turski 2002). The clinical application of NMDA-R antagonists can produce symptoms resembling those observed in schizophrenia patients (in contrast to excitotoxicity, *reduced* NMDA-R stimulation has been proposed as a potential etiology for schizophrenia), including hallucinations, transient psychosis and cognitive defects (Moghaddam 2003). Due to this precarious balance between efficacy and clinical tolerance, there has been more optimism for drugs that act at NMDA-Rs as partial antagonists or as low-affinity channel blockers (Kemp and McKernan 2002). An example of the latter is memantine, an open-channel blocker of NMDA-Rs with rapid kinetics (Chen *et al.* 1992) that is more reversible (it does not get trapped within the channel during closed states) than MK-801 (Blanpied *et al.* 1997). It has been suggested that the properties of memantine make it more effective during sustained NMDA-R activation, and therefore it hinders pathological stimulation more than it does normal synaptic transmission (Lipton 2003).

Due to its low-affinity characteristics, memantine has had some success in clinical neuroprotection trials (Parsons *et al.* 1999) and is currently approved for treatment of Alzheimer's disease in North America (Kemp and McKernan 2002). However, a different therapeutic approach is to reduce, rather than block, glutamate-induced increases in $[Ca^{2+}]_i$. Increasing the concentration of adenosine from 10 to 100

μM did not lead to greater inhibition of RGC glutamate responses (see Chapter 2), suggesting that adenosine only affects a portion of the calcium signal at its maximum effect. Perhaps there is an ideal range of $[Ca^{2+}]_i$ necessary for normal neuronal function (Hardingham and Bading 2003), and adenosine acts to maintain $[Ca^{2+}]_i$ within this spectrum. As an apparent endogenous neuroprotective agent, the elucidation of the mechanisms underlying adenosine's actions could therefore have important therapeutic implications. It is not difficult to envision that such a neuromodulator, refined and optimized through centuries of evolution, may act to specifically prevent key steps in the excitotoxic cascade without negatively influencing physiological glutamatergic signaling pathways.

Neuroprotective Therapy for Glaucoma

Of the vast number of prospective neuroprotective agents that have been studied in various animal models of neurodegeneration, there are few (memantine, as discussed above, for Alzheimer's disease is one exception) that have proven beneficial in human clinical trials (DeGraba and Pettigrew 2000). The poor translation of therapeutics from the lab to the clinic is a problem that has plagued research on neuroprotection. As an example of interest to the work in this thesis, glutamate receptor antagonists have yet to be successfully utilized in the treatment of stroke patients despite the overwhelming evidence that glutamate contributes to neuronal death in acute ischemic conditions. There are several likely reasons for this, including the aforementioned side effects of NMDA-R antagonists, but a basic problem is related to the therapeutic time window (De Keyser *et al.* 1999). In laboratory models, glutamate-related drugs are generally most effective when given before or shortly (minutes rather than hours) after the insult, and

this speed of treatment is rarely attained in human patients. As shown in Chapter 4, applying MK-801 just before and during the 1 hour glutamate treatment largely prevented excitotoxic RGC death. In RGCs treated with glutamate alone, the number of cells exhibiting irreversible calcium deregulation (shown to be associated with cell death) increased steadily over the 1 hour exposure. Therefore, although this was not directly evaluated, it is likely reasonable to extrapolate the following dictum: with longer exposure periods to glutamate prior to treatment, more RGCs will undergo irreversible calcium deregulation, and therefore the effectiveness of treatment will be inversely related to the delay in its application.

The finding by Dreyer and colleagues (1996) of elevated glutamate levels in the vitreous of human glaucoma patients and monkeys with experimentally raised IOP generated considerable optimism that glutamate-related therapies might be well-suited for glaucoma. In addition to the eye being potentially more accessible for drug delivery than the brain (although the blood-retina barrier and the retinal bioavailability of topically applied drugs present significant hurdles), the chronic nature of this disease suggested that the therapeutic time window may be longer than in acute ischemic conditions such as stroke. It was proposed that, in contrast to the abrupt and sharp rise in glutamate levels during ischemic insult, RGCs in glaucomatous retinas are gradually being lost due to constant exposure to low-level elevations (~25 μM or less) of extracellular glutamate (Dreyer *et al.* 1996; Vorwerk *et al.* 1996; Lipton 2003). In accord, I observed that relatively low glutamate concentrations can be lethal to RGCs as a 1 hour exposure to 10 μM glutamate (with glycine present and magnesium absent) was sufficient to kill ~20% of cultured RGCs over this time period. Based largely on the finding of elevated vitreous glutamate levels in glaucoma patients (Dreyer *et al.* 1996), the established history of RGC susceptibility to excitotoxicity (beginning with Lucas and Newhouse

1957), and the relative success of memantine in clinical trials of other CNS neurodegenerative disorders such as Alzheimer's disease (Parsons *et al.* 1999), the NMDA-R antagonist memantine became the first (and so far only) non-IOP-lowering drug to be assessed as a neuroprotective treatment for glaucoma (Weinreb 2005). Currently, there is a large-scale phase 3 randomized clinical trial in North America testing the effectiveness of memantine in human glaucoma patients (who are also being treated with IOP-lowering therapy) and the results from this study are still pending.

However, in the five years that has now passed since subject recruitment ended for the memantine clinical trial, the association between excitotoxicity and glaucoma remains controversial (for editorials on the debate, see Dalton 2001; Kwon *et al.* 2005; Lotery 2005; Salt and Cordeiro 2005; Osborne *et al.* 2006). The IOP-related rise in vitreous glutamate levels has been disputed (see Introduction of Chapter 3), leaving the fundamental question of whether glutamate levels do indeed rise in the retinal space surrounding RGCs during glaucoma. As demonstrated in Chapter 3, the retina under normal conditions possesses a highly efficient glutamate transporter system that can rapidly clear away exogenously applied glutamate. For RGCs *in vivo* to be constantly exposed to extracellular glutamate for 1 hour (as the isolated RGCs were in Chapter 4) or longer (as suggested to occur in glaucoma), there must be a coexisting defect in retinal glutamate clearance mechanisms. One proposal put forth is that elevated IOP impacts Müller cell physiology and consequently hinders glutamate uptake (Dreyer 1998), and support for this hypothesis came with the finding of reduced glutamate transporter protein levels in retinas from rats with experimentally elevated IOP (Martin *et al.* 2002). Using calcium imaging of RGCs in retinal wholemounts (Chapter 3), I could not find evidence for a functional deficit in retinal glutamate uptake for rats with experimental glaucoma. These results indicate that chronic exposure to elevated IOP

(at levels that cause RGC loss) is not sufficient to induce a long-term reduction in overall retinal glutamate transporter function, and suggests that RGCs in this glaucoma model were not being continuously exposed to a global rise in extracellular glutamate levels. It is also interesting to use the delayed calcium deregulation experiments in Chapter 4 to consider the effect of transient RGC stimulation by high concentrations of glutamate, presumably which could occur with the spillage of intracellular glutamate from dying adjacent cells. Even at 1000 μM glutamate, only about one-quarter of the RGCs deregulated after 1 hour, showing a similar steady loss of cells as the 1 hour treatment with 10 or 100 μM glutamate. This finding insinuates that it is extended exposure periods, and not brief contact with high concentrations, that triggers glutamate's toxic effects on RGCs.

The experiments in Chapter 3 were designed to assess glutamate transporter function in a rat glaucoma model and, on their own, do not rule out a role for excitotoxicity in glaucoma (certain caveats are described in the Discussion of Chapter 3). Nevertheless, recent work by other researchers using various animal glaucoma models support the argument that, at the very least, chronic IOP elevation (distinguished from short-term increases in IOP to levels greater than systolic blood pressure, which occludes the central retinal artery and induces acute retinal ischemia) can cause RGC death through mechanisms that are largely independent of excitotoxicity. Using a rat model of elevated IOP, achieved through hypertonic saline injections into episcleral veins similar to the method used in Chapter 3, Pang *et al.* (2005) could find no evidence for increased nitric oxide synthase (NOS) activation and NOS inhibitors were shown to be ineffective in protecting against RGC loss. NOS activation has been shown to be an important downstream effector of NMDA-R-mediated excitotoxicity in other central neurons (Dawson *et al.* 1991; Dawson *et al.* 1993; Vorwerk *et al.* 1997; Sattler *et al.*

1999). Libby and colleagues (2005) showed that RGC death in a genetic mouse model of spontaneous IOP elevation occurs through a pathway distinctly different from NMDA-R-induced excitotoxic RGC death, with the former (but not the latter) requiring the proapoptotic BAX protein. Also, in a monkey glaucoma model, in which argon laser burns were applied to the anterior chamber angle to disrupt aqueous outflow, there was no significant difference in the total RGC counts in glaucomatous eyes of monkeys treated with the NMDA-R antagonist memantine versus glaucomatous eyes from untreated monkeys after approximately 16 months of IOP elevation (Hare *et al.* 2004b). Furthermore, it is difficult to reconcile the exclusive nature of IOP-related RGC death with an increase in retinal glutamate levels; amacrine cells are clearly susceptible to excitotoxicity (Sabel *et al.* 1995; Ullian *et al.* 2004) but there is no evidence that these other inner retinal neurons are lost in animal models of chronic IOP elevation (Vickers *et al.* 1995; Harwerth *et al.* 1999; Jakobs *et al.* 2005; Kielczewski *et al.* 2005).

All of the studies referenced in the preceding paragraph employed animal glaucoma models (monkey, rat, or mouse) wherein the IOP increases are likely due to reduced aqueous outflow through the trabecular meshwork. An alternative methodology for IOP elevation in rats involves the ablation of episcleral veins through either cautery (Shareef *et al.* 1995) or laser photocoagulation (WoldeMussie *et al.* 2001). Using these models, two research papers have reported that glutamate antagonists exert a neuroprotective effect against pressure-related RGC loss. Chaudhary *et al.* (1998) found a protective effect for MK-801 (~14% loss of RGCs in untreated rats versus ~3% loss in MK-801-treated rats 4 weeks after episcleral vein cautery), while WoldeMussie *et al.* (2002) observed a similar statistically significant effect with memantine (~12% RGC loss in untreated rats versus ~37% in memantine-treated group after 3 weeks after episcleral vein photocoagulation). One possible reason for the discrepancy of these two

reports with the previously described studies is related to the variability of most animal glaucoma models of IOP elevation. As evident by examining the parameters for the rats studied in Chapter 3 (see Table 3-1), individual rats showed different IOP elevation patterns and an assortment of optic nerve injury grades even though they all received the same saline injection surgical procedure. This variability has also been demonstrated in the episcleral vein cautery model, with a recent study noting that "a number of eyes subjected to experimental glaucoma can resist a significant loss of RGCs" (Danias *et al.* 2006). The sample size of 3 rats (Chaudhary *et al.* 1998) and 8 rats (WoldeMussie *et al.* 2002) per treatment group used in these two studies may not have been sufficient to determine the efficacy of the glutamate antagonists against the background variability inherent in the RGC counts. Alternatively, there may be differences between the various models in that glutamate-related RGC death occurs to a greater extent following episcleral vein occlusion. In agreement, nitric oxide synthase activation, a downstream effector of excitotoxicity, has been implicated in the vein cautery model (Neufeld *et al.* 1999; Shareef *et al.* 1999) but not in the hypertonic saline injection model (Pang *et al.* 2005). It has been suggested that the vortex veins may be affected by the cauterization, and the resulting reduction in blood outflow from the choroid may trigger non-IOP-related damage to RGCs that is vascular in origin (Goldblum and Mittag 2002; Morrison *et al.* 2005).

Although neuroprotection may serve as a useful adjunct therapy for glaucoma in the future, this therapeutic strategy has not yet been clinically validated. Regardless of the cellular pathway targeted, a crucial issue for the successful development of novel glaucoma treatments is the concurrent development of better techniques to assess neuroprotection both in animal models and in human patients. The monitoring of visual function in the clinic is primarily achieved through automated static perimetry, in which

the threshold level of brightness required for detection of a white target light on a white background is measured at different locations across the visual field (Johnson 1996; Harwerth *et al.* 2002). Unfortunately, this type of conventional perimetry appears to be relatively insensitive to early RGC loss in glaucoma. Research on human cadaver eyes from glaucoma patients suggests that definitive visual field defects are not evident until about half of the overall RGC population in the eye has been lost (Quigley *et al.* 1982). This was confirmed more recently in monkeys with experimental glaucoma that were trained to perform clinical perimetry, as roughly a 50-60% loss in RGCs was necessary before initial visual field defects became distinguishable (Harwerth *et al.* 1999). With the goal of achieving better sensitivity than conventional perimetry, a number of diagnostic instruments have been developed that detect changes in either visual function (more selective perimetric tests) or retinal anatomy (devices that monitor optic disc structure or nerve fiber layer integrity) due to glaucomatous progression (reviewed in Girkin 2004). However, the relationship between structure and function, as determined by these newer methods, is relatively poor and the correlation of measured defects to actual RGC death is still not clear (Artes and Chauhan 2005). Animal glaucoma models permit direct evaluation of the loss of RGCs through post-sacrifice histological analyses of the retina and optic nerve (as done for the rat glaucoma model used in Chapter 3), and consequently the assessment of potentially neuroprotective agents is usually based on counts of surviving RGC somata or axons. A key question that remains unanswered for either human or experimental glaucoma is whether individual RGCs undergo a period of dysfunction prior to death or whether functional RGC life and RGC death form an essentially binary system. The former situation would be particularly more amenable to neuroprotective strategies, as these therapies could then target 'sick' RGCs for their rescue and functional restoration. In addition, a better understanding of RGC

dysfunction could aid in the development of more sensitive clinical tests to detect early glaucomatous changes before RGCs are irreversibly lost.

I believe that a focus of future glaucoma research therefore should include studies that probe for RGC dysfunction at a cellular level. The calcium imaging of RGCs in retinal wholemounts represents a valuable technique to address this issue. To my knowledge, the study described in Chapter 3 represents one of only two studies in which physiological recordings have been obtained for individual RGCs that were exposed *in vivo* to chronic IOP elevation. In the other recently published study, Weber and Harman (2005) measured the biophysical properties of RGCs from a monkey glaucoma model using intracellular microelectrode recordings. An advantage of the calcium imaging methodology is that it allows multiple RGCs to be monitored simultaneously, in contrast to the recording of RGCs one at a time using conventional electrophysiological techniques. Although the experiments on the rat glaucoma model in Chapter 3 were designed to assess retinal glutamate uptake rather than properties of the RGCs themselves, the NMDA-R-mediated responses of the surviving RGCs from the glaucomatous retinas did not appear that different from untreated RGCs. A direct comparison in the absolute magnitude of the responses was not possible due to technical considerations (the absolute responses were dependent on the degree of dye loading; see Figure 3-1), but RGCs from eyes with raised IOP exhibited repeatable and robust responses with little evidence for increased fragility. For instance, the incidence of RGC calcium deregulation or death during the 2-minute NMDA and glutamate exposures was not observed, although two of the rats with severe damage exhibited slightly reduced responses to NMDA following recovery from the millimolar glutamate treatments (Figure 3-6). Weber and Harmon (2005) noted that RGCs from glaucomatous eyes were essentially normal in their intrinsic membrane properties, as

they did not display significantly different resting membrane potentials, activation thresholds, whole cell input resistances, or mean amplitudes of the activity spikes generated by electrical stimulation, as compared to RGCs from control eyes. However, these researchers did find that RGCs from eyes with experimental glaucoma responded less to visual stimulation (the retinal pigment epithelium was present in these retinal preparations, and rod/cone phototransduction was maintained), particularly to patterned stimuli consisting of square-wave gratings. What type of characteristics might distinguish a 'dysfunctional RGC' as determined through the calcium imaging technique described in this thesis? RGCs from monkey and mouse glaucoma models appear to have a reduced dendritic density (Weber *et al.* 1998; Jakobs *et al.* 2005; Weber and Harman 2005), and this anatomical change may signify altered synaptic organization. As AMPA/kainate-Rs are the predominant glutamate receptor located at RGC synapses, with NMDA-Rs mostly present extrasynaptically (Chen and Diamond 2002), one might expect that the ratio of kainate-driven response amplitudes to NMDA-driven response amplitudes would decrease if RGCs from glaucomatous eyes do possess fewer synapses. To test this hypothesis, the relative concentration of kainate required to elicit an equivalent calcium signal as that evoked by 200 μM NMDA could be determined for RGCs in retinal wholemounts prepared from both glaucomatous and control rat eyes.

In conjunction with studies investigating RGC dysfunction, it would be extremely beneficial to determine whether early RGC degeneration is due to axonal or somatic injury. In other words, is glaucomatous progression associated with a sick retina or a sick optic nerve (or both)? As an example for future inquiry, it would be interesting to determine if the altered RGC dendritic architecture that has been linked to experimental glaucoma (Weber *et al.* 1998; Jakobs *et al.* 2005; Weber and Harman 2005) is due to the direct retinal effects of elevated IOP or whether it is a downstream result of axonal

injury. In favor of an axonal mechanism, it has been shown in developing frog RGCs that the transport of neurotrophins (specifically, brain-derived neurotrophic factor [BDNF]) from RGC brain targets is necessary for dendritic arborization, recruitment of AMPA/kainate-Rs to dendrites, and subsequent synapse development (Du and Poo 2004). Therefore, the obstruction of BDNF at the optic nerve head, shown to occur in rat glaucoma models (Pease *et al.* 2000), could stimulate the consequent dendritic disorganization and reduction in synaptic integrity prior to the death of RGCs. This has important implications for neuroprotection, as saving RGC somata and dendrites may be of small benefit if the RGC axon has already been lost. As a crude analogy, it makes little sense to fix a broken telephone if the phone line has been damaged beyond repair. There is increasing evidence that axonal degeneration pathways can be quite different from the mechanisms involved in somal death (Coleman and Perry 2002; Raff *et al.* 2002). The possible importance of axon-specific degeneration in glaucoma has recently been supported by the findings of Libby and colleagues (2005). Using a genetic mouse model of spontaneous IOP elevation (which occurs following pigment dispersion due to iris atrophy), these researchers showed that knocking out the proapoptotic protein BAX resulted in near-complete protection of RGC somata but did not affect the degeneration of RGC axons in the optic nerve. There is considerable evidence supporting the optic nerve head as a primary site of injury in glaucoma (see summary and related references in Chapter 1 on page 27), and the progression of typical glaucomatous visual field defects often corresponds better with the topography of the optic nerve head rather than the retina (Quigley 1999). The principal theory that has been put forward in support of RGC damage (primary or secondary degeneration) originating within the retina is the excitotoxic hypothesis that elevated IOP induces increased glutamate levels around RGC dendrites (Dreyer 1998; Lipton 2003). As already discussed, my findings in

Chapter 3 do not support this hypothesis. Nonetheless, instead of retinal actions, could glutamate excitotoxicity contribute to axonal degeneration? This premise has generally not been considered as glutamate receptors are thought to be present on RGC somata and dendrites rather than RGC axons. However, the previously unrecognized existence of NMDA-Rs on myelin and oligodendrocytes in the rodent optic nerve has only just come to light (Micu *et al.* 2005; Salter and Fern 2005). These studies showed that the induction of ischemia to the optic nerve, through oxygen and glucose deprivation or chemical ischemia, resulted in NMDA-R-mediated damage to oligodendrocyte processes (Salter and Fern 2005) and myelin (Micu *et al.* 2005). Also of importance, the NMDA-Rs on these non-neuronal cells may be less susceptible to blockade by extracellular magnesium ions (Karadottir *et al.* 2005). My findings in Chapter 3 with the rat glaucoma model do not rule out the possibility for glutamate-related damage to oligodendrocytes and myelin within the optic nerve, which could result if the cupping changes to the optic nerve head (known to occur in this model; see Morrison *et al.* 1998; Chauhan *et al.* 2002) were associated with collapse of capillaries and localized ischemia within the optic nerve. As the myelination by oligodendrocytes is essential for maintaining functional RGC axons, this raises the novel idea that secondary RGC degeneration in glaucoma may occur following excitotoxic damage to these optic nerve glial cells.

Probing Neuronal Function in Individual Cells and Intact Tissue

To study the glutamatergic calcium dynamics of rat RGCs, a variety of preparations were utilized in this thesis that broadly span the *in vitro* to *in vivo* spectrum of methodologies. At one extreme, the generation of purified cultures of RGCs eliminated all other cell types and therefore enabled these retinal output neurons to be

directly studied in isolation. In mixed retinal cell cultures (a few initial experiments in Chapter 2 were performed using these cultures), RGCs represent only a small minority (< 1%) of the dissociated cells and it can be difficult to positively identify neuronal types. Regardless of the type of cell culture, a potential drawback is that neuronal dendrites and axons are destroyed during dissociation. Preparing the retina as a living wholemount allows the fundamental architecture of the retina to remain intact. Retinal wholemounts were extensively employed in RGC calcium imaging experiments, permitting *in vitro* studies on RGCs possessing similar dendritic structures and cell contacts as in the living animal. Finally, at the *in vivo* end of the spectrum, an animal glaucoma model was used to induce RGC death and optic nerve damage and to study the effects of elevated IOP on glutamate uptake.

Purified RGC cultures, obtained using Thy1 immunopanning, represent a reductionist approach to the study of retinal neurobiology, and some advantages of this technique have been reiterated in previous chapters. Nevertheless, it is important to consider whether RGCs extracted by immunopanning are indeed 'normal', and whether all morphological and physiological classes of RGCs are appropriately represented in these cultures. Thy1 is a cell-surface glycoprotein that has been identified on many CNS neurons (MacLeish *et al.* 1983), but in the retina it was originally described as an exclusive marker for RGCs (Barnstable and Drager 1984). The functional role of Thy1 is not fully established, but it has been hypothesized to play a role in RGC development and synaptogenesis (Schmid *et al.* 1995; Liu *et al.* 1996). Although retrograde labeling experiments suggest that essentially all superior colliculus-projecting RGCs express Thy1, there is also evidence that a small group of inner retinal neurons besides RGCs, likely a subpopulation of amacrine cells, also express this glycoprotein (Hinds and Hinds 1983; Perry *et al.* 1984; Takahashi *et al.* 1991). In the original description of the

immunopanning technique, these non-RGC Thy1-positive rat neurons could be immunohistochemically labeled by anti-rat Thy1 IgG antibodies but not by monoclonal anti-mouse Thy1 IgM antibodies (Barres *et al.* 1988). In this same study, up to 75% of retrogradely labeled RGCs were stained by the IgM antibody (in contrast to the 100% labeling by IgG antibodies), and immunopanning using the IgM antibody resulted in nearly pure (~99%) RGC cultures (Barres *et al.* 1988). In this thesis, I similarly used monoclonal anti-Thy1 IgM antibodies for immunopanning (see page 44 in Chapter 2), thus sacrificing yield for specificity. It appears that the difference between the anti-Thy1 IgM and IgG antibodies is related to their relative affinity for Thy1, and smaller cells (like the putative Thy1-positive amacrine cells) presumably do not express enough of the protein to be labeled by the IgM antibody (Barres *et al.* 1988). As a caveat to immunopanning, this size bias indicates that RGC classes consisting of predominantly smaller RGCs may be underrepresented in the cultures generated using this technique.

The existence of inter-RGC variability became most apparent during the prolonged glutamate exposure experiments in Chapter 4. Although the relative effect of adenosine and the various glutamate receptor antagonists on glutamate-induced calcium influx was generally consistent for the overall population of isolated RGCs, the absolute magnitude of the glutamatergic responses was highly variable. This variability in the calcium signal was linked to RGC vulnerability, as RGCs that displayed greater responses were more likely to undergo calcium deregulation and subsequent excitotoxic death. The underlying mechanism that distinguished larger responses from smaller ones was not determined, and there are a number of possibilities. Perhaps the simplest explanation is that more glutamate receptors, particularly the NMDA-type, were expressed on the RGCs that displayed bigger responses. An alternative theory is that the calcium signal is related to specific NMDA-R subunits present on individual RGCs.

Certain properties of NMDA-Rs, including the size of glutamate-induced currents, can vary depending on the NR2 (NR2A, B, C or D) subunit expressed. NMDA-Rs comprised of NR2A or NR2B subunits generally are associated with large currents and a high sensitivity to Mg^{2+} block, whereas those with NR2C or NR2D subunits usually have smaller currents and a lower sensitivity to extracellular Mg^{2+} (Cull-Candy *et al.* 2001). There is also evidence NMDA-R subunit composition is related to receptor location, as extrasynaptic NMDA-Rs have been reported to consist mostly of NR1 and NR2B subunits while synaptic NMDA-Rs incorporate NR2A subunits (Vanhoutte and Bading 2003). Most of the known subunits for glutamate receptors (both NMDA-Rs and AMPA/kainate-Rs) have been identified on RGCs (for references, see page 9 in Chapter 1), but it is not clear if different RGCs possess different combinations. Using immunohistochemistry, Ullian *et al.* (2004) noted that all immunopanned RGCs exhibit heavy somatic and dendritic labeling for NR1, NR2A, and NR2B subunits, but the presence of NR2C and NR2D was not assessed. Furthermore, NMDA-Rs that contain the NR3A subunit (often in a tetramer with one NR2A and two NR1 subunits) are associated with reduced whole-cell currents and calcium permeability (Dingledine *et al.* 1999), and the NR3A has been identified in RGCs (Sucher *et al.* 2003). As NMDA-Rs are located on the plasma membrane, NMDA-R subunits can be immunostained without necessitating neuron permeabilization (see Ullian *et al.* 2004). Therefore, comparable to the procedure for annexin V staining that was utilized in Chapter 4, antibodies for NR3A could be injected into the microscope chamber (along with appropriate fluorescent-tagged secondary antibodies) following prolonged glutamate exposure to determine if the RGCs with smaller responses (and reduced incidence of delayed calcium deregulation) express higher levels of NR3A. Similarly, the relative staining for other NR2 subunits in the isolated RGCs could be compared to the calcium imaging data to

assess a possible correlation between their expression and excitotoxic death. If these studies find no apparent dissimilarities, the variability in RGC glutamatergic calcium responses may instead be related to intracellular mechanisms. Examples include disparities in the intracellular buffering capacity of different RGCs (Mann *et al.* 2005), or differential regulation of NMDA-Rs through phosphorylation (Chen and Huang 1992) or tyrosine kinase-mediated pathways (Zheng *et al.* 1998).

Physiological characterizations of mammalian RGCs, in which glutamatergic accumulations of the cation channel-permeable compound agmatine are assessed, indicate that RGCs are a heterogeneous population of neurons that can be classified into different groups with distinct ionotropic receptor-mediated responses (Marc and Jones 2002; Sun and Kalloniatis 2006). That inter-RGC variability exists for the relative distributions and proportions of NMDA, AMPA, and kainate receptors would not be that surprising given the assortment of responses (brisk, sluggish, transient, sustained) that are evident for different physiological classes of RGCs (for review of these classes ,see page 3 in Chapter 1). It should be noted that the presence of glutamate receptors in the plasma membrane is not a static process, with receptors constantly being inserted and removed through receptor trafficking (Borgdorff and Choquet 2002; Tovar and Westbrook 2002; Collingridge *et al.* 2004). In cultured cortical (Gascon *et al.* 2005) and pyramidal (Wu *et al.* 2005) neurons treated with glutamate, an autoregulatory protective response against excitotoxicity has been reported in which there is an active downregulation of glutamate receptor function. However, I observed that the overall change in RGC calcium levels (measured in the soma) due to glutamate receptor stimulation was relatively stable over the 30-90 minutes that most imaging sessions lasted. Evidence for this stability is noted throughout the thesis, as the recovery responses obtained at the end of a given experiment were rarely significantly different

from the initial responses to similar glutamatergic treatments. Could the relative magnitude of the glutamate-induced calcium signals (and therefore the relative vulnerability to delayed calcium deregulation) in immunopanned RGCs be used to consistently identify specific morphological and physiological classes of RGCs? If so, it might enable the determination of which RGC types are most susceptible to excitotoxic damage *in vivo* during retinal ischemia. As an initial step, future experiments could compare the magnitude of NMDA- and kainate-driven responses (and the ratio of these responses to each other) to precise measurements of somal size to determine if differential glutamatergic responses have morphological correlates. Also, it would be important to know if the amplitude of the calcium response induced by brief pulses of glutamate agonists can be used to reliably predict whether that cell will undergo excitotoxic death in ensuing experiments involving prolonged glutamate exposure.

In addition to differences in cell morphology (i.e. soma size) and glutamate-driven responses, Marc and Jones (2002) found that groups of RGCs could be distinguished from each other on the basis of chemically discriminated molecular phenotypes (intracellular glutamate, aspartate, glutamine, GABA, glycine and taurine metabolic signatures). If specific membrane-bound markers for various RGC types are also uncovered, it may be possible to identify different RGC groups following calcium imaging using fixative-free immunohistochemistry (similar to the method of annexin V staining used in Chapter 4), or even to use these markers to isolate specific classes of RGCs through immunopanning. One group of RGCs that would be particularly interesting to study *in vitro* would be the recently-discovered melanopsin-expressing RGCs. In contrast to other rat RGCs that predominantly project to the superior colliculus, these neurons are directly photosensitive (Berson *et al.* 2002; Hattar *et al.* 2002) and project to the hypothalamus via the retinohypothalamic tract (Moore and Lenn 1972; Pickard

1980). Melanopsin RGCs are thought to provide input to non-visual light-regulated systems such as circadian rhythm photoentrainment and pupillary constriction (Berson 2003). The rarity of these neurons ensures that their identification in cell cultures would be a daunting challenge. As melanopsin RGCs constitute approximately 1-2% of the total RGC population (Hattar *et al.* 2002), one would expect that they would represent only 1 of every 10,000-20,000 cells in a mixed retinal cell culture and 1 of every 100 cells in a purified RGC culture. That melanopsin RGCs would even be extracted by Thy1 immunopanning assumes that these RGCs express this glycoprotein, but this has not yet been demonstrated. However, the melanopsin protein is embedded in the plasma membrane throughout these neurons, including the soma (Belenky *et al.* 2003). This raises the possibility that these photosensitive neurons could be isolated into purified cultures by modifying the immunopanning technique. As it has been demonstrated that melanopsin RGC somata respond to light even when physically dissociated from their dendrites by microdissection (Berson *et al.* 2002), this novel culture method could serve as an ideal system for characterizing these rare neurons.

During the course of this thesis work, I had the opportunity to test this hypothesis while on a summer Grass Fellowship at the Marine Biological Laboratory in Woods Hole, Massachussetts. I used an immunopanning procedure based on the same method outlined in Chapter 2 on page 43, but an anti-rat melanopsin N-terminus antibody (#JHU-71, American Type Cell Collection, Manassas VA) was employed rather than Thy1 antibodies. The N-terminus of this opsin is located on the extracellular side of the plasma membrane in these cells (Provencio *et al.* 1998). Using pooled retinas from 6-day old rats, approximately 4,000 cells per dissociated retina were extracted following their adherence to melanopsin antibody-coated panning plates (images of these cells, taken shortly after dissociation and after two days in culture, are shown in Figure 5-1 A).

Fura-2 calcium imaging was then used to determine if these neurons exhibited intrinsic light sensitivity as it had previously been shown, using retinal flatmounts prepared from genetically altered mice that lack rods and cones, that light-evoked responses in photosensitive RGCs are associated with increases in intracellular calcium levels (Sekaran *et al.* 2003). While not every melanopsin-panned RGC exhibited detectable responses to light, light-sensitive cells could be reliably identified by scanning the coverslip under white light and looking for cells (roughly 20-40% of the plated cells on the day following dissociation) with elevated fura-2 ratios (elevated calcium levels) that then recovered to baseline following return to dark conditions. In the initial recordings of light-evoked responses from melanopsin-panned cells, it became apparent that the cells had reduced responses if a stimulus occurred too soon (< 10 min) after the stimulus preceding it. The 'adaptation' to the light stimulus was reversible if these cells were left in the dark for a longer period (> 20 min) before the next stimulation (Figure 5-1 B). This type of 'photoreceptor adaptation' is in agreement with a recent report showing that the responses of light-sensitive RGCs (identified in retinal wholemounts through retrograde labeling from the hypothalamic suprachiasmatic nucleus) are influenced by prior light exposure (Wong *et al.* 2005). As a control, I tested for similar light responses in many (> 200) Thy1-immunopanned RGCs. I did not observe any detectable responses (Figure 5-1 D), although these cells did respond to glutamate and were therefore viable. As melanopsin RGCs are directly photosensitive, it is not inherently necessary that they receive synaptic input, and the presence of functional glutamate receptors on melanopsin RGCs had not been previously demonstrated. However, it has been shown that synaptic connections do exist between these photoreceptors and both bipolar and amacrine cells (Belenky *et al.* 2003). In preliminary work, an increase in calcium levels was elicited in every light-sensitive melanopsin-panned RGC challenged with glutamate

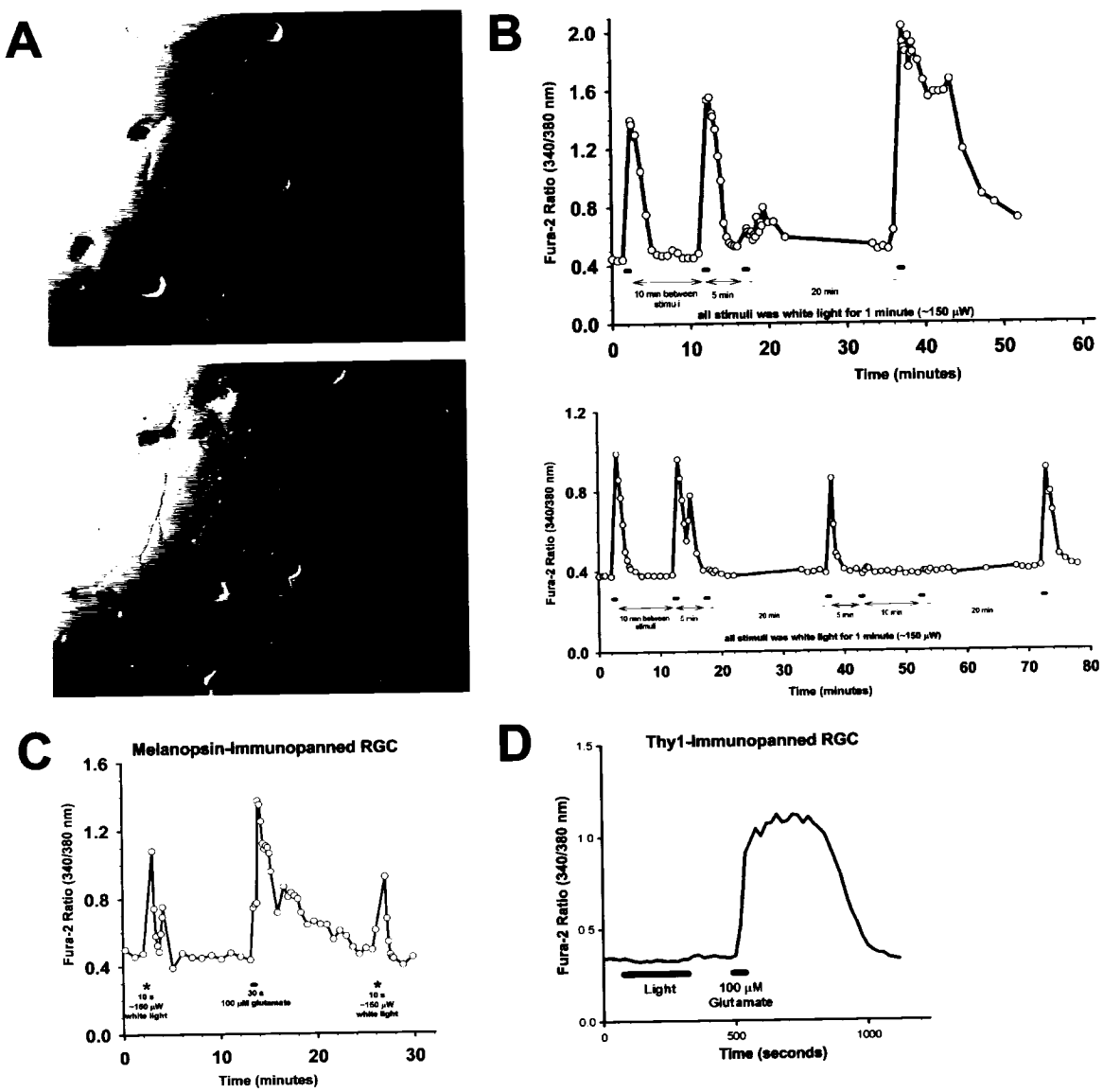

Figure 5- 1. Immunopanned melanopsin RGC cultures. **(A)** DIC image of cells, 6 hours (top) and 2 days (bottom) after plating, that were isolated through immunopanning technique using melanopsin N-terminus antibodies. Scale bar = 25 µM. **(B)** Two example fura-2 imaging traces illustrating calcium responses of melanopsin-panned RGCs exposed to white light. Note that when a subsequent stimulus was presented 5 minutes following its preceding stimulus, there was no response. A response was again observed after the cell was left to recover for 20 minutes. **(C)** Fura-2 imaging data for a melanopsin-panned RGC that responded both to light stimulation and to 30 second treatment with glutamate. **(D)** In contrast, Thy-1-panned RGCs respond to glutamate but not light, as a detectable response to light stimuli was never observed in these cells.

(n = 4; see Figure 5-1 C), indicating that melanopsin RGCs do indeed possess functional glutamate receptors and thus may receive excitatory input within the retina. In the future, I plan to expand these studies to identify the cation channel mediating the light-evoked calcium influx and to determine whether glutamatergic input (in addition to the potential inhibitory effects of GABA, glycine and adenosine) modifies the light responses. Related to the work in this thesis, it would be interesting to determine whether melanopsin RGCs are more, less, or equally vulnerable to excitotoxicity or to death caused by chronic IOP elevation. There is currently nothing known about whether these neurons, and consequently the systems they provide input to, are affected in glaucoma or retinal ischemia.

While the further refinement of the immunopanning approach could make specific RGC types more accessible for study, enhancement of the calcium imaging technique on retinal wholemounts could provide additional important insights on how pathological glutamatergic signaling pathways are activated. In comparison to isolated cell cultures, the effectiveness of exogenous glutamate in eliciting an RGC calcium signal was greatly reduced in the retinal wholemounts (Chapter 3), providing an example of how cell cultures can be limited in their modeling of certain whole-retina interactions. The use of the purified cultures represents a useful system for understanding the direct effects of prolonged glutamate exposure on RGCs, but the retinal wholemount preparation provides a better system for determining the circumstances under which RGCs would be exposed to glutamate for prolonged periods *in vivo*. The possible perturbation of glutamate uptake by conditions such as anoxia, ischemia, and hypoglycemia represent future topics of interest that could be studied using this calcium imaging methodology.

The prolonged glutamate exposure experiments on the isolated RGCs warrants future corroborative studies using the retinal wholemount preparation. As the calcium

signal in fura dextran-loaded RGCs may saturate relatively early (see Figure 3-2), a low affinity dextran-conjugated calcium dye (such as the non-ratiometric fluo-4 dextran dye; see Nikolaeva *et al.* 2005) may may be better at distinguishing the large secondary rise in Ca^{2+} associated with delayed calcium deregulation. Annexin V could be used again to mark dead RGCs following glutamate exposure, with TBOA present to block glutamate uptake and allow glutamate receptor activation. It would be valuable to determine if the proportion of dying RGCs in retinal wholemounts is comparable to that for the isolated RGCs as it is possible that the dissociation and culture procedures altered the susceptibility of immunopanned RGCs to excitotoxicity. For instance, it has been suggested that alternative splicing may occur in RGCs in the days (prior to cell death) following optic nerve axotomy (Kreutz *et al.* 1998), and splice variation can lead to altered glutamate receptor function (Madden 2002). The dissociation process also destroys synapses, which then are reformed to a lesser extent in culture. Differences in the role of extrasynaptic and synaptic NMDA-type glutamate receptors have been reported, as Hardingham and colleagues (2002) showed that stimulation of extrasynaptic NMDA-Rs can induce apoptosis, while the stimulation of synaptic NMDA-Rs is neuroprotective (acting through a cAMP response element binding protein [CREB] pathway) in hippocampal neurons. In RGCs, only extrasynaptic NMDA-Rs have been identified (Chen and Diamond 2002), and it is interesting to speculate whether this is an important factor in the separation of physiological and pathological glutamatergic signaling for these retinal output neurons. In the dark, OFF RGCs would receive relatively constant glutamatergic synaptic input (likely bursts of glutamate in millimolar levels), while the same would be true for ON RGCs under light conditions. The efficiency of retinal glutamate transporters could aid in preventing excess spill-over during normal synaptic transmission and serve to protect RGCs from prolonged

stimulation of extrasynaptic NMDA-Rs and subsequent excitotoxicity. In the retinal wholemount experiments (see Chapter 3 and 4), the bath application of glutamate plus the glutamate transporter TBOA was designed to mimic the rise in extracellular glutamate levels that occurs when glutamate uptake is disrupted in conditions such as ischemia/hypoxia (Camacho and Massieu 2006). The resulting RGC calcium signal was abolished by NMDA-R antagonism, suggesting that, under such conditions, glutamate alters RGC calcium dynamics primarily through extrasynaptic NMDA-Rs. Unfortunately, due to technical considerations, it may be difficult to validate the correlation between the magnitude of the glutamate-induced calcium signal and subsequent RGC excitotoxic death in this intact retina preparation. The size of the signal is related to the extent of dye loading, which is influenced by the distance of the RGC from the fura dextran injection site and by the incubation time following the injection (see Figure 3-1). Nevertheless, this technique could provide a useful complementary approach to the findings of Chapter 4 in elucidating the relationship betwen calcium influx and excitotoxic RGC death.

Finally, in the field of neuroscience as a whole, there is an overall aspiration to continue to push imaging techniques towards *in vivo* applications in order to observe functioning neurons in their normal environment (Lichtman and Fraser 2001). This has been accomplished in the brain to some extent by replacing a section of the skull with a glass coverslip in order to create a window to the underlying cortex (Svoboda *et al.* 1997; Helmchen *et al.* 1999; Sullivan *et al.* 2005). The eye represents the chance to observe neuronal activity through a natural window – the optically transparent cornea and the lens. RGCs have been previously visualized *in vivo* following the retrograde loading of fluorescent dyes injected into the superior colliculus using confocal laser microscopy (Sabel *et al.* 1997) and conventional epifluorescence microscopy (Thanos *et*

al. 2002). In addition, annexin V fluorescence has been followed *in vivo,* using confocal laser scanning ophthalmoscopy, to allow observation of retinal cell apoptosis due to various insults (Cordeiro *et al.* 2004). While these indicators can be used to monitor the presence of RGCs and their death, I believe that with enhanced adaptive optics (Doble 2005) it may be possible to perform calcium imaging experiments *in vivo* using dextran-conjugated calcium indicator dyes by adjusting the technique used in this thesis for retinal wholemounts. One could load dextran-conjugated dyes into RGC axons via puncture through the sclera or by injecting the dye into the optic nerve at its exit site behind the globe. The link between $[Ca^{2+}]_i$ and cell death is not exclusive to excitotoxicity, as non-glutamate-related apoptotic signaling pathways are also thought to be regulated by calcium (Berridge *et al.* 1998; Orrenius *et al.* 2003). It has even been hypothesized that perturbations in Ca^{2+} homeostasis is a major cause in the loss of neurons associated with ageing (Verkhratsky and Toescu 1998; Toescu *et al.* 2004). Clearly, the ability to study RGC function and dysfunction in living animals could provide enormous insights into the calcium dynamics that occur during RGC neurodegeneration and allow the 'calcium hypothesis' of neuronal ageing to be better assessed.

In closing, I feel that the major strength of this thesis is that RGCs were studied both in purified cultures and in retinal wholemount preparations. This two-pronged approach enabled these retinal neurons to be directly probed without interference from other cell types, yet allowed an appreciation of the cellular interactions that influence RGC responses in the intact retina. In addition to the specific findings regarding glutamatergic calcium dynamics in RGCs that were presented in the individual chapters, I hope this work encourages future studies to utilize multiple methodologies in advancing our understanding of RGCs at both cellular and whole-animal levels.

Appendix A: Calibration of Fura-2 Ratios

For the calcium imaging experiments on the purified RGCs, fura-2 ratios (R) were converted to $[Ca^{2+}]_i$ in calibration experiments using the formula:

$$[Ca^{2+}]_i = K_d (F_o/F_s)[(R - R_{min})/(R_{max} - R)]$$

with a K_d for fura-2 = 224 nM, and where F_o/F_s is the ratio of fluorescence intensity at 380 nm excitation in calcium-free solution over the intensity in solution with saturated calcium levels (for derivation of formula and K_d value, see Grynkiewicz *et al* 1985). The calibration protocol was based on the method described by Kao (1994), and is illustrated in Figure 6-1 A. At the conclusion of a representative experiment in which the effect of 100 μM APV on the calcium influx induced by 100 μM glutamate was assessed, the RGC was superfused with calcium-free HBSS (10 mM Mg^{2+}, 2 mM BAPTA, 10 μM ionomycin) to determine the minimum value for the fura-2 ratio (R_{min}). The added magnesium helps to keep the RGCs viable, as cells can become leaky and detach from the coverslip with severe calcium deprivation. Ionomycin is a calcium ionophore that makes the plasma and endoplasmic reticulum membranes more permeable to Ca^{2+}. The spike in the fura-2 ratios that occurs shortly after superfusion of this cocktail is due to the dumping of Ca^{2+} from intracellular stores. BAPTA is a calcium chelator which is used to bind to Ca^{2+} and prevent the ion from being again sequestered internally. The R_{min} under the Ca^{2+}-free conditions was determined to be 0.3267 for the cell displayed in Figure 6-1. After a 2 minute wash in 0.9% saline (buffered with 15 mM HEPES and pH 7.4, the same as the HBSS), the cells were superfused with a saturating calcium solution

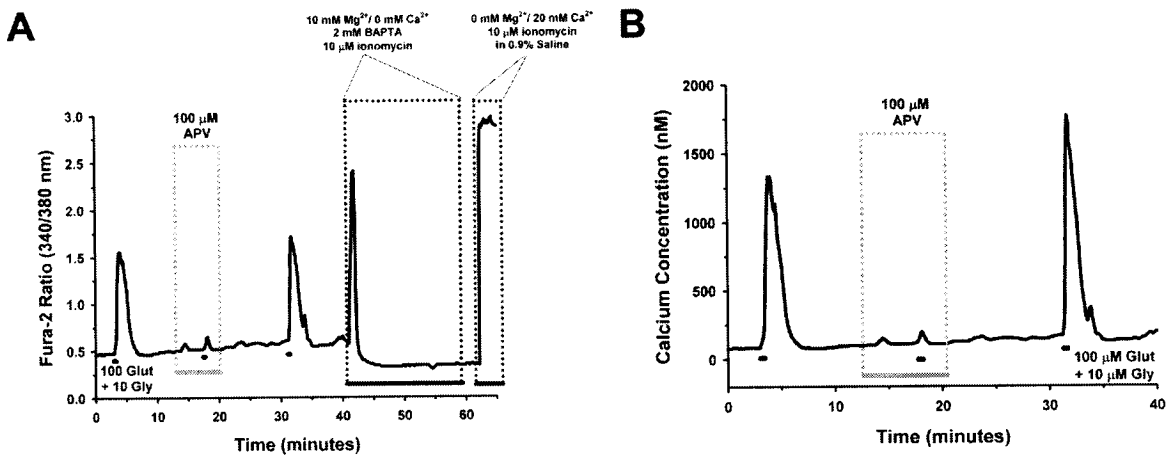

Figure 6- 1. Conversion of fura-2 ratios to $[Ca^{2+}]_i$ through calibration experiments. **(A)** Fura-2 ratio trace of an isolated RGC treated with glutamate in the presence and absence of the NMDA-R antagonist APV. At the end of the experiment, the cell was exposed to Ca^{2+}-free and Ca^{2+}-saturating solutions to determine the minimum and maximum fura-2 ratios (see text for further details). **(B)** The $[Ca^{2+}]_i$ trace for the same RGC shown in (A) after calibration.

(20 mM Ca^{2+}, 10 μM ionomycin in the 0.9% saline solution) to determine the maximum fura-2 ratio (R_{max}). Saline was employed rather than HBSS, as the phosphate salts in HBSS can form precipitates with Ca^{2+} when it is present in high levels. With the entry of the saturating calcium solution into the microscope chamber, there is an abrupt rise in the ratio as Ca^{2+} rushes back inside the cell (which remains permeable due to the continued presence of ionomycin). The R_{max} was 2.9267 for this particular RGC. The F_o/F_s ratio (fluorescence intensity at 380 nm excitation in Ca^{2+}-free solution over the intensity at 380 nm excitation in Ca^{2+}-saturating solution) for this cell was 5.647.

If we substitute these values (F_o/F_s=5.647; R_{min}=0.3267 ;R_{max}=2.9267; using a K_D=224 nM) into the equation at the start of this appendix, we find that a fura-2 ratio of 0.5 corresponds to 90 nM, a ratio of 1.0 is 442 nM, while a ratio of 1.5 converts to 1040 nM. In addition to the cell shown in Figure 6-1, the calibration procedure was applied to four other RGCs in the same imaging session. The F_o/F_s, R_{min} and R_{max} for each of the 5 cells is shown in Table 6-1 (the RGC shown in Figure 6-1 is Cell 1), along with the subsequent $[Ca^{2+}]_i$ conversion for fura-2 ratios of 0.5, 1.0, and 1.5. The mean values for F_o/F_s, R_{min} and R_{max}, averaging the data from the 5 cells, are also shown along with the accompanying conversions. These average values were then used to convert all of the ratiometric data in the imaging session to $[Ca^{2+}]_i$. The $[Ca^{2+}]_i$ trace in Figure 6-1 B was calculated from the ratio trace in Figure 6-1 A using the average values.

There are a number of assumptions with the use of the calibration equation (Moore *et al.* 1990; Roe *et al.* 1990). It requires that: 1) only de-esterfied fura dye is present inside the cell; 2) only the fura dye contributes to the measured fluorescence in cells; 3) the K_d of fura dye used for the equation matches that for the type of cell studied *in situ* and has not been altered by fluctuations in viscosity, temperature, and ionic strength; and 4) that photobleaching has not altered the properties of the dye during the

Cell #	R_{min}	R_{max}	F_o/F_s	Ratio 0.5 Conversion $[Ca^{2+}]_i$	Ratio 1.0 Conversion $[Ca^{2+}]_i$	Ratio 1.5 Conversion $[Ca^{2+}]_i$
1	0.3267	2.9267	5.647	90 nM	442 nM	1040 nM
2	0.3000	2.2867	4.281	107 nM	521 nM	1462 nM
3	0.3000	2.5000	4.520	101 nM	472 nM	1215 nM
4	0.3267	2.6467	5.541	100 nM	507 nM	1270 nM
5	0.3133	2.7933	5.821	106 nM	499 nM	1196 nM
AVG	**0.3133**	**2.6307**	**5.162**	101 nM	487 nM	1213 nM

Table 6-1. Summary of data for a representative calibration experiment. The mininimum and maximum fura-2 ratios (R_{min} and R_{max}) were determined by superfusing the cells with Ca^{2+}-free and Ca^{2+}-saturating solutions. F_o/F_s is the ratio of fluorescence intensity at 380 nm excitation in calcium-free solution over the intensity in solution with saturated calcium levels. The conversion of fura-2 ratios of 0.5, 1.0, and 1.5 to $[Ca^{2+}]_i$ (in nM) is shown using the data for each individual cell (see text for equation). The average R_{min}, R_{max}, and F_o/F_s was calculated for the 5 cells, and the calibrated $[Ca^{2+}]_i$ for the fura-2 ratios of 0.5, 1.0 and 1.5 are shown using these average values. The raw and calibrated (using the average R_{min}, R_{max}, and F_o/F_s) traces for Cell 1 are displayed in Figure 6-1.

recordings and calibrations. Unfortunately, these conditions are likely rarely met. Nevertheless, the calibration of the fura ratio into $[Ca^{2+}]_i$ allows a useful approximation of the relative magnitude of changes in the calcium signal induced and modulated by various compounds. As the assessment of various drug treatments throughout this thesis were generally based on within-cell comparisons, the conversion to $[Ca^{2+}]_i$ did not alter the presence or absence of a given effect or its statistical significance. This is evident in Figure 3-3, in which both the Δ fura-2 ratio and the Δ $[Ca^{2+}]_i$ data are shown graphically. As glutamate-related responses (due to 30 second treatments) normally did not reach levels past 1.5 μM (see Figure 4-1), the increases $[Ca^{2+}]_i$ would have occurred primarily within the linear portion of the fura-2 binding curve (see Figure 1-2).

Appendix B: Copyright Permissions

November 3, 2005

Investigative Ophthalmology and Vision Science

I am preparing my Ph.D. thesis for submission to the Faculty of Graduate Studies at Dalhousie University, Halifax, Nova Scotia, Canada. I am seeking your permission to include a manuscript version of the following paper as a chapter in the thesis:

Hartwick ATE, Lalonde MR, Barnes S, Baldridge WH. 2004. Adenosine A_1-receptor modulation of glutamate-induced calcium influx in rat retinal ganglion cells. *Investigative Ophthalmology & Vision Science* 45: 3740-3748.

Canadian graduate theses are reproduced by the Library and Archives of Canada (formerly National Library of Canada) through a non-exclusive, world-wide license to reproduce, loan, distribute, or sell theses. I am also seeking your permission for the material described above to be reproduced and distributed by the LAC(NLC). Further details about the LAC(NLC) thesis program are available on the LAC(NLC) website (www.nlc.bnc.ca).

Full publication details and a copy of this permission letter will be included in the thesis.

Yours sincerely,

Andrew Hartwick

Permission is granted for:

a) the inclusion of the material described above in your thesis.
b) For the material described above to be included in the copy of your thesis that is sent to the Library and Archives of Canada (formerly National Library of Canada) for reproduction and distribution.

Name: KAREN Schools Colson Title: Director, Publishing & Communications

Signature: x Date: 12/6/05

November 3, 2005

Journal of Neurochemistry

I am preparing my Ph.D. thesis for submission to the Faculty of Graduate Studies at Dalhousie University, Halifax, Nova Scotia, Canada. I am seeking your permission to include a manuscript version of the following paper as a chapter in the thesis:

Hartwick ATE, Zhang X, Chauhan BC, Baldridge WH. 2005. Functional assessment of glutamate clearance mechanisms in a chronic rat glaucoma model using retinal ganglion cell calcium imaging. *Journal of Neurochemistry* 94: 794-807.

Canadian graduate theses are reproduced by the Library and Archives of Canada (formerly National Library of Canada) through a non-exclusive, world-wide license to reproduce, loan, distribute, or sell theses. I am also seeking your permission for the material described above to be reproduced and distributed by the LAC(NLC). Further details about the LAC(NLC) thesis program are available on the LAC(NLC) website (www.nlc.bnc.ca).

Full publication details and a copy of this permission letter will be included in the thesis.

Yours sincerely,

Andrew Hartwick

(email reply on next page)

Thu, 17 Nov 2005

From: Journals Rights <JournalsRights@oxon.blackwellpublishing.com>

To: Andrew.Hartwick@dal.ca

Subject: Re: Permissions Request

Part(s): Download All Attachments (in .zip file)

Headers: Show All Headers

Dear Andrew

Thank you for your email request. Permission is granted for you to use the material below for your thesis subject to the usual acknowledgements and on the understanding that you will reapply for permission if you wish to distribute or publish your thesis commercially.

Re: Functional assessment of glutamate clearance mechanisms in a chronic rat glaucoma model using retinal ganglion cell calcium imaging. Journal of Neurochemistry 94: 794-807

Regards

Gemma Lynch
Permissions Assistant
Rights Department
Blackwell Publishing Ltd
PO Box 805
9600 Garsington Road
Oxford
OX4 2ZG
United Kingdom

Fax: 0044 1865 471158

Permissions Requests can now be sent to journalsrights@oxon.blackwellpublishing.com

REFERENCES

Aarts M., Iihara K., Wei W. L., Xiong Z. G., Arundine M., Cerwinski W., MacDonald J. F. and Tymianski M. (2003) A key role for TRPM7 channels in anoxic neuronal death. *Cell* **115,** 863-877.

Aarts M., Liu Y., Liu L., Besshoh S., Arundine M., Gurd J. W., Wang Y. T., Salter M. W. and Tymianski M. (2002) Treatment of ischemic brain damage by perturbing NMDA receptor- PSD-95 protein interactions. *Science* **298,** 846-850.

Adachi K., Kashii S., Masai H., Ueda M., Morizane C., Kaneda K., Kume T., Akaike A. and Honda Y. (1998) Mechanism of the pathogenesis of glutamate neurotoxicity in retinal ischemia. *Graefes Arch Clin Exp Ophthalmol* **236,** 766-774.

Adams J. M. and Cory S. (1998) The Bcl-2 protein family: arbiters of cell survival. *Science* **281,** 1322-1326.

Aizenman E., Frosch M. P. and Lipton S. A. (1988) Responses mediated by excitatory amino acid receptors in solitary retinal ganglion cells from rat. *J Physiol* **396,** 75-91.

Anderson C. M. and Swanson R. A. (2000) Astrocyte glutamate transport: review of properties, regulation, and physiological functions. *Glia* **32,** 1-14.

Anderson D. R. and Hendrickson A. (1974) Effect of intraocular pressure on rapid axoplasmic transport in monkey optic nerve. *Invest Ophthalmol* **13,** 771-783.

Ankarcrona M., Dypbukt J. M., Bonfoco E., Zhivotovsky B., Orrenius S., Lipton S. A. and Nicotera P. (1995) Glutamate-induced neuronal death: a succession of necrosis or apoptosis depending on mitochondrial function. *Neuron* **15,** 961-973.

Armaly M. F., Krueger D. E., Maunder L., Becker B., Hetherington J., Jr., Kolker A. E., Levene R. Z., Maumenee A. E., Pollack I. P. and Shaffer R. N. (1980) Biostatistical analysis of the collaborative glaucoma study. I. Summary report of the risk factors for glaucomatous visual-field defects. *Arch Ophthalmol* **98,** 2163-2171.

Artes P. H. and Chauhan B. C. (2005) Longitudinal changes in the visual field and optic disc in glaucoma. *Prog Retin Eye Res* **24,** 333-354.

Ascher P. and Nowak L. (1988) The role of divalent cations in the N-methyl-D-aspartate responses of mouse central neurones in culture. *J Physiol* **399,** 247-266.

Attwell D., Barbour B. and Szatkowski M. (1993) Nonvesicular release of neurotransmitter. *Neuron* **11,** 401-407.

Auger C. and Attwell D. (2000) Fast removal of synaptic glutamate by postsynaptic transporters. *Neuron* **28,** 547-558.

Augustine G. J., Santamaria F. and Tanaka K. (2003) Local calcium signaling in neurons. *Neuron* **40,** 331-346.

Baldridge W. H. (1996) Optical recordings of the effects of cholinergic ligands on neurons in the ganglion cell layer of mammalian retina. *J Neurosci* **16,** 5060-5072.

Banker G. and Goslin K. (1991) *Culturing nerve cells.* MIT Press, Cambridge, MA.

Bano D., Young K. W., Guerin C. J., Lefeuvre R., Rothwell N. J., Naldini L., Rizzuto R., Carafoli E. and Nicotera P. (2005) Cleavage of the plasma membrane Na+/Ca2+ exchanger in excitotoxicity. *Cell* **120,** 275-285.

Bansal A., Singer J. H., Hwang B. J., Xu W., Beaudet A. and Feller M. B. (2000) Mice lacking specific nicotinic acetylcholine receptor subunits exhibit dramatically altered spontaneous activity patterns and reveal a limited role for retinal waves in forming ON and OFF circuits in the inner retina. *J Neurosci* **20,** 7672-7681.

Baptiste D. C., Hartwick A. T., Jollimore C. A., Baldridge W. H., Chauhan B. C., Tremblay F. and Kelly M. E. (2002) Comparison of the neuroprotective effects of adrenoceptor drugs in retinal cell culture and intact retina. *Invest Ophthalmol Vis Sci* **43,** 2666-2676.

Barnett N. L. and Grozdanic S. D. (2004) Glutamate transporter localization does not correspond to the temporary functional recovery and late degeneration after acute ocular ischemia in rats. *Exp Eye Res* **79,** 513-524.

Barnett N. L., Pow D. V. and Bull N. D. (2001) Differential perturbation of neuronal and glial glutamate transport systems in retinal ischaemia. *Neurochem Int* **39,** 291-299.

Barnstable C. J. and Drager U. C. (1984) Thy-1 antigen: a ganglion cell specific marker in rodent retina. *Neuroscience* **11,** 847-855.

Barres B. A., Silverstein B. E., Corey D. P. and Chun L. L. (1988) Immunological, morphological, and electrophysiological variation among retinal ganglion cells purified by panning. *Neuron* **1,** 791-803.

Bean B. P. (1989) Neurotransmitter inhibition of neuronal calcium currents by changes in channel voltage dependence. *Nature* **340,** 153-156.

Belenky M. A., Smeraski C. A., Provencio I., Sollars P. J. and Pickard G. E. (2003) Melanopsin retinal ganglion cells receive bipolar and amacrine cell synapses. *J Comp Neurol* **460,** 380-393.

Bellezza A. J., Rintalan C. J., Thompson H. W., Downs J. C., Hart R. T. and Burgoyne C. F. (2003) Deformation of the lamina cribrosa and anterior scleral canal wall in early experimental glaucoma. *Invest Ophthalmol Vis Sci* **44,** 623-637.

Bengtsson B. (1981) Aspects of the epidemiology of chronic glaucoma. *Acta Ophthalmol Suppl,* 1-48.

Berkelaar M., Clarke D. B., Wang Y. C., Bray G. M. and Aguayo A. J. (1994) Axotomy results in delayed death and apoptosis of retinal ganglion cells in adult rats. *J Neurosci* **14,** 4368-4374.

Berridge M. J. (1998) Neuronal calcium signaling. *Neuron* **21,** 13-26.

Berridge M. J., Bootman M. D. and Lipp P. (1998) Calcium--a life and death signal. *Nature* **395,** 645-648.

Berridge M. J., Bootman M. D. and Roderick H. L. (2003) Calcium signalling: dynamics, homeostasis and remodelling. *Nat Rev Mol Cell Biol* **4,** 517-529.

Berson D. M. (2003) Strange vision: ganglion cells as circadian photoreceptors. *Trends Neurosci* **26,** 314-320.

Berson D. M., Dunn F. A. and Takao M. (2002) Phototransduction by retinal ganglion cells that set the circadian clock. *Science* **295,** 1070-1073.

Biegon A., Fry P. A., Paden C. M., Alexandrovich A., Tsenter J. and Shohami E. (2004) Dynamic changes in N-methyl-D-aspartate receptors after closed head injury in mice: Implications for treatment of neurological and cognitive deficits. *Proc Natl Acad Sci U S A* **101,** 5117-5122.

Bindokas V. P. and Ishida A. T. (1996) Conotoxin-sensitive and conotoxin-resistant Ca2+ currents in fish retinal ganglion cells. *J Neurobiol* **29,** 429-444.

Bindokas V. P., Yoshikawa M. and Ishida A. T. (1994) Na(+)-Ca2+ exchanger-like immunoreactivity and regulation of intracellular Ca2+ levels in fish retinal ganglion cells. *J Neurophysiol* **72,** 47-55.

Blair M., Pease M. E., Hammond J., Valenta D., Kielczewski J., Levkovitch-Verbin H. and Quigley H. (2005) Effect of glatiramer acetate on primary and secondary degeneration of retinal ganglion cells in the rat. *Invest Ophthalmol Vis Sci* **46,** 884-890.

Blanpied T. A., Boeckman F. A., Aizenman E. and Johnson J. W. (1997) Trapping channel block of NMDA-activated responses by amantadine and memantine. *J Neurophysiol* **77,** 309-323.

Blazynski C. and Perez M. T. (1991) Adenosine in vertebrate retina: localization, receptor characterization, and function. *Cell Mol Neurobiol* **11,** 463-484.

Blazynski C., Woods C. and Mathews G. C. (1992) Evidence for the action of endogenous adenosine in the rabbit retina: modulation of the light-evoked release of acetylcholine. *J Neurochem* **58,** 761-767.

Bliss T. V. and Collingridge G. L. (1993) A synaptic model of memory: long-term potentiation in the hippocampus. *Nature* **361,** 31-39.

Bonfoco E., Krainc D., Ankarcrona M., Nicotera P. and Lipton S. A. (1995) Apoptosis and necrosis: two distinct events induced, respectively, by mild and intense insults with

N-methyl-D-aspartate or nitric oxide/superoxide in cortical cell cultures. *Proc Natl Acad Sci U S A* **92,** 7162-7166.

Borgdorff A. J. and Choquet D. (2002) Regulation of AMPA receptor lateral movements. *Nature* **417,** 649-653.

Braas K. M., Zarbin M. A. and Snyder S. H. (1987) Endogenous adenosine and adenosine receptors localized to ganglion cells of the retina. *Proc Natl Acad Sci U S A* **84,** 3906-3910.

Brambilla D., Chapman D. and Greene R. (2005) Adenosine mediation of presynaptic feedback inhibition of glutamate release. *Neuron* **46,** 275-283.

Brandstatter J. H., Hartveit E., Sassoe-Pognetto M. and Wassle H. (1994) Expression of NMDA and high-affinity kainate receptor subunit mRNAs in the adult rat retina. *Eur J Neurosci* **6,** 1100-1112.

Brewer G. J. (1997) Isolation and culture of adult rat hippocampal neurons. *J Neurosci Methods* **71,** 143-155.

Brewer G. J., Torricelli J. R., Evege E. K. and Price P. J. (1993) Optimized survival of hippocampal neurons in B27-supplemented Neurobasal, a new serum-free medium combination. *J Neurosci Res* **35,** 567-576.

Brody D. L. and Yue D. T. (2000) Relief of G-protein inhibition of calcium channels and short-term synaptic facilitation in cultured hippocampal neurons. *J Neurosci* **20,** 889-898.

Brooks D. E., Garcia G. A., Dreyer E. B., Zurakowski D. and Franco-Bourland R. E. (1997) Vitreous body glutamate concentration in dogs with glaucoma. *Am J Vet Res* **58,** 864-867.

Brown S. J., James S., Reddington M. and Richardson P. J. (1990) Both A1 and A2a purine receptors regulate striatal acetylcholine release. *J Neurochem* **55,** 31-38.

Brubaker R. F. (1996) Delayed functional loss in glaucoma. LII Edward Jackson Memorial Lecture. *Am J Ophthalmol* **121,** 473-483.

Brundege J. M. and Dunwiddie T. V. (1997) Role of adenosine as a modulator of synaptic activity in the central nervous system. *Adv Pharmacol* **39,** 353-391.

Bruns R. F., Lu G. H. and Pugsley T. A. (1986) Characterization of the A2 adenosine receptor labeled by [3H]NECA in rat striatal membranes. *Mol Pharmacol* **29,** 331-346.

Budde T., Meuth S. and Pape H. C. (2002) Calcium-dependent inactivation of neuronal calcium channels. *Nat Rev Neurosci* **3,** 873-883.

Bull N. D. and Barnett N. L. (2004) Retinal glutamate transporter activity persists under simulated ischemic conditions. *J Neurosci Res* **78,** 590-599.

Burgoyne C. F., Downs J. C., Bellezza A. J., Suh J. K. and Hart R. T. (2005) The optic nerve head as a biomechanical structure: a new paradigm for understanding the role of IOP-related stress and strain in the pathophysiology of glaucomatous optic nerve head damage. *Prog Retin Eye Res* **24,** 39-73.

Camacho A. and Massieu L. (2006) Role of glutamate transporters in the clearance and release of glutamate during ischemia and its relation to neuronal death. *Arch Med Res* **37,** 11-18.

Carafoli E., Santella L., Branca D. and Brini M. (2001) Generation, control, and processing of cellular calcium signals. *Crit Rev Biochem Mol Biol* **36,** 107-260.

Carter-Dawson L., Crawford M. L., Harwerth R. S., Smith E. L., 3rd, Feldman R., Shen F. F., Mitchell C. K. and Whitetree A. (2002) Vitreal glutamate concentration in monkeys with experimental glaucoma. *Invest Ophthalmol Vis Sci* **43,** 2633-2637.

Catterall W. A. (2000) Structure and regulation of voltage-gated Ca2+ channels. *Annu Rev Cell Dev Biol* **16,** 521-555.

Cepurna W. O., Kayton R. J., Johnson E. C. and Morrison J. C. (2005) Age related optic nerve axonal loss in adult Brown Norway rats. *Exp Eye Res* **80,** 877-884.

Chaudhary P., Ahmed F. and Sharma S. C. (1998) MK801-a neuroprotectant in rat hypertensive eyes. *Brain Res* **792,** 154-158.

Chauhan B. C., Pan J., Archibald M. L., LeVatte T. L., Kelly M. E. and Tremblay F. (2002) Effect of intraocular pressure on optic disc topography, electroretinography, and axonal loss in a chronic pressure-induced rat model of optic nerve damage. *Invest Ophthalmol Vis Sci* **43,** 2969-2976.

Chauhan B. C., Levatte T. L., Garnier K. L., Tremblay F., Pang I. H., Clark A. F. and Archibald M. L. (2006) Semiquantitative optic nerve grading scheme for determining axonal loss in experimental optic neuropathy. *Invest Ophthalmol Vis Sci* **47,** 634-640.

Chauhan B. C., LeVatte T. L., Jollimore C. A., Yu P. K., Reitsamer H. A., Kelly M. E., Yu D. Y., Tremblay F. and Archibald M. L. (2004) Model of endothelin-1-induced chronic optic neuropathy in rat. *Invest Ophthalmol Vis Sci* **45,** 144-152.

Chen C. and Regehr W. G. (2000) Developmental remodeling of the retinogeniculate synapse. *Neuron* **28,** 955-966.

Chen H. S., Pellegrini J. W., Aggarwal S. K., Lei S. Z., Warach S., Jensen F. E. and Lipton S. A. (1992) Open-channel block of N-methyl-D-aspartate (NMDA) responses by memantine: therapeutic advantage against NMDA receptor-mediated neurotoxicity. *J Neurosci* **12,** 4427-4436.

Chen J. F., Huang Z., Ma J., Zhu J., Moratalla R., Standaert D., Moskowitz M. A., Fink J. S. and Schwarzschild M. A. (1999) A(2A) adenosine receptor deficiency attenuates brain injury induced by transient focal ischemia in mice. *J Neurosci* **19,** 9192-9200.

Chen L. and Huang L. Y. (1992) Protein kinase C reduces Mg2+ block of NMDA-receptor channels as a mechanism of modulation. *Nature* **356,** 521-523.

Chen S. and Diamond J. S. (2002) Synaptically released glutamate activates extrasynaptic NMDA receptors on cells in the ganglion cell layer of rat retina. *J Neurosci* **22,** 2165-2173.

Chernevskaya N. I., Obukhov A. G. and Krishtal O. A. (1991) NMDA receptor agonists selectively block N-type calcium channels in hippocampal neurons. *Nature* **349,** 418-420.

Chinopoulos C. and Adam-Vizi V. (2006) Calcium, mitochondria and oxidative stress in neuronal pathology. *Febs J* **273,** 433-450.

Chinopoulos C., Gerencser A. A., Doczi J., Fiskum G. and Adam-Vizi V. (2004) Inhibition of glutamate-induced delayed calcium deregulation by 2-APB and La3+ in cultured cortical neurones. *J Neurochem* **91,** 471-483.

Choi D. W. (1985) Glutamate neurotoxicity in cortical cell culture is calcium dependent. *Neurosci Lett* **58,** 293-297.

Choi D. W. (1987) Ionic dependence of glutamate neurotoxicity. *J Neurosci* **7,** 369-379.

Choi D. W. (1988) Glutamate neurotoxicity and diseases of the nervous system. *Neuron* **1,** 623-634.

Choi D. W., Koh J. Y. and Peters S. (1988) Pharmacology of glutamate neurotoxicity in cortical cell culture: attenuation by NMDA antagonists. *J Neurosci* **8,** 185-196.

CNIB (2003) CNIB client statistics 2002. From www.cnib.ca. Accessed March 29, 2006.

Cohen E. D. and Miller R. F. (1994) The role of NMDA and non-NMDA excitatory amino acid receptors in the functional organization of primate retinal ganglion cells. *Vis Neurosci* **11,** 317-332.

Coleman M. P. and Perry V. H. (2002) Axon pathology in neurological disease: a neglected therapeutic target. *Trends Neurosci* **25,** 532-537.

Collaborative Normal-tension Glaucoma Study Group (1998) Comparison of glaucomatous progression between untreated patients with normal-tension glaucoma and patients with therapeutically reduced intraocular pressures. *Am J Ophthalmol* **126,** 487-497.

Collingridge G. L., Isaac J. T. and Wang Y. T. (2004) Receptor trafficking and synaptic plasticity. *Nat Rev Neurosci* **5,** 952-962.

Conn P. J. (2003) Physiological roles and therapeutic potential of metabotropic glutamate receptors. *Ann N Y Acad Sci* **1003,** 12-21.

Cordeiro M. F., Guo L., Luong V., Harding G., Wang W., Jones H. E., Moss S. E., Sillito A. M. and Fitzke F. W. (2004) Real-time imaging of single nerve cell apoptosis in retinal neurodegeneration. *Proc Natl Acad Sci U S A* **101,** 13352-13356.

Cull-Candy S., Brickley S. and Farrant M. (2001) NMDA receptor subunits: diversity, development and disease. *Curr Opin Neurobiol* **11,** 327-335.

Cunha R. A., Sebastiao A. M. and Ribeiro J. A. (1998) Inhibition by ATP of hippocampal synaptic transmission requires localized extracellular catabolism by ecto-nucleotidases into adenosine and channeling to adenosine A1 receptors. *J Neurosci* **18,** 1987-1995.

Dacey D. M., Peterson B. B., Robinson F. R. and Gamlin P. D. (2003) Fireworks in the primate retina: in vitro photodynamics reveals diverse LGN-projecting ganglion cell types. *Neuron* **37,** 15-27.

Dalton R. (2001) Private investigations. *Nature* **411,** 129-130.

Danbolt N. C. (2001) Glutamate uptake. *Prog Neurobiol* **65,** 1-105.

Danias J., Shen F., Kavalarakis M., Chen B., Goldblum D., Lee K., Zamora M. F., Su Y., Podos S. M. and Mittag T. (2006) Characterization of retinal damage in the episcleral vein cauterization rat glaucoma model. *Exp Eye Res* **82,** 219-228.

Dawson V. L., Dawson T. M., London E. D., Bredt D. S. and Snyder S. H. (1991) Nitric oxide mediates glutamate neurotoxicity in primary cortical cultures. *Proc Natl Acad Sci U S A* **88,** 6368-6371.

Dawson V. L., Dawson T. M., Bartley D. A., Uhl G. R. and Snyder S. H. (1993) Mechanisms of nitric oxide-mediated neurotoxicity in primary brain cultures. *J Neurosci* **13,** 2651-2661.

De Keyser J., Sulter G. and Luiten P. G. (1999) Clinical trials with neuroprotective drugs in acute ischaemic stroke: are we doing the right thing? *Trends Neurosci* **22,** 535-540.

de Mendonca A., Sebastiao A. M. and Ribeiro J. A. (1995) Inhibition of NMDA receptor-mediated currents in isolated rat hippocampal neurones by adenosine A1 receptor activation. *Neuroreport* **6,** 1097-1100.

de Mendonca A., Sebastiao A. M. and Ribeiro J. A. (2000) Adenosine: does it have a neuroprotective role after all? *Brain Res Brain Res Rev* **33,** 258-274.

DeCoster M. A., Koenig M. L., Hunter J. C. and Tortella F. C. (1992) Calcium dynamics in neurons treated with toxic and non-toxic concentrations of glutamate. *Neuroreport* **3,** 773-776.

DeGraba T. J. and Pettigrew L. C. (2000) Why do neuroprotective drugs work in animals but not humans? *Neurol Clin* **18,** 475-493.

Deisseroth K., Bito H., Schulman H. and Tsien R. W. (1995) Synaptic plasticity: A molecular mechanism for metaplasticity. *Curr Biol* **5,** 1334-1338.

Demarque M., Villeneuve N., Manent J. B., Becq H., Represa A., Ben-Ari Y. and Aniksztejn L. (2004) Glutamate transporters prevent the generation of seizures in the developing rat neocortex. *J Neurosci* **24,** 3289-3294.

Dingledine R., Borges K., Bowie D. and Traynelis S. F. (1999) The glutamate receptor ion channels. *Pharmacol Rev* **51,** 7-61.

Dkhissi O., Chanut E., Wasowicz M., Savoldelli M., Nguyen-Legros J., Minvielle F. and Versaux-Botteri C. (1999) Retinal TUNEL-positive cells and high glutamate levels in vitreous humor of mutant quail with a glaucoma-like disorder. *Invest Ophthalmol Vis Sci* **40,** 990-995.

Doble N. (2005) High-resolution, in vivo retinal imaging using adaptive optics and its future role in ophthalmology. *Expert Rev Med Devices* **2,** 205-216.

Dolphin A. C. (2003) G protein modulation of voltage-gated calcium channels. *Pharmacol Rev* **55,** 607-627.

Dowling J. E. (1987) *The retina: An approachable part of the brain.* Belknap Press, Cambridge, MA.

Dreher B., Sefton A. J., Ni S. Y. and Nisbett G. (1985) The morphology, number, distribution and central projections of Class I retinal ganglion cells in albino and hooded rats. *Brain Behav Evol* **26,** 10-48.

Dreyer E. B. (1998) A proposed role for excitotoxicity in glaucoma. *J Glaucoma* **7,** 62-67.

Dreyer E. B., Zurakowski D., Schumer R. A., Podos S. M. and Lipton S. A. (1996) Elevated glutamate levels in the vitreous body of humans and monkeys with glaucoma. *Arch Ophthalmol* **114,** 299-305.

Du J. L. and Poo M. M. (2004) Rapid BDNF-induced retrograde synaptic modification in a developing retinotectal system. *Nature* **429,** 878-883.

Dugan L. L., Sensi S. L., Canzoniero L. M., Handran S. D., Rothman S. M., Lin T. S., Goldberg M. P. and Choi D. W. (1995) Mitochondrial production of reactive oxygen species in cortical neurons following exposure to N-methyl-D-aspartate. *J Neurosci* **15,** 6377-6388.

Dunwiddie T. V. and Masino S. A. (2001) The role and regulation of adenosine in the central nervous system. *Annu Rev Neurosci* **24,** 31-55.

Dunwiddie T. V., Diao L. and Proctor W. R. (1997) Adenine nucleotides undergo rapid, quantitative conversion to adenosine in the extracellular space in rat hippocampus. *J Neurosci* **17,** 7673-7682.

Eddy D. M. and Billings J. (1988) The quality of medical evidence: implications for quality of care. *Health Aff (Millwood)* **7,** 19-32.

Eddy D. M., Sanders L. E. and Eddy J. F. (1983) The value of screening for glaucoma with tonometry. *Surv Ophthalmol* **28,** 194-205.

Edwards F. A. and Robertson S. J. (1999) The function of A2 adenosine receptors in the mammalian brain: evidence for inhibition vs. enhancement of voltage gated calcium channels and neurotransmitter release. *Prog Brain Res* **120,** 265-273.

Eimerl S. and Schramm M. (1994) The quantity of calcium that appears to induce neuronal death. *J Neurochem* **62,** 1223-1226.

Ertel E. A., Campbell K. P., Harpold M. M., Hofmann F., Mori Y., Perez-Reyes E., Schwartz A., Snutch T. P., Tanabe T., Birnbaumer L., Tsien R. W. and Catterall W. A. (2000) Nomenclature of voltage-gated calcium channels. *Neuron* **25,** 533-535.

Fechtner R. D. and Weinreb R. N. (1994) Mechanisms of optic nerve damage in primary open angle glaucoma. *Surv Ophthalmol* **39,** 23-42.

Flammer J., Orgul S., Costa V. P., Orzalesi N., Krieglstein G. K., Serra L. M., Renard J. P. and Stefansson E. (2002) The impact of ocular blood flow in glaucoma. *Prog Retin Eye Res* **21,** 359-393.

Fontana A. C., Guizzo R., de Oliveira Beleboni R., Meirelles E. S. A. R., Coimbra N. C., Amara S. G., dos Santos W. F. and Coutinho-Netto J. (2003) Purification of a neuroprotective component of Parawixia bistriata spider venom that enhances glutamate uptake. *Br J Pharmacol* **139,** 1297-1309.

Foster P. J. (2002) The epidemiology of primary angle closure and associated glaucomatous optic neuropathy. *Semin Ophthalmol* **17,** 50-58.

Fredholm B. B., Battig K., Holmen J., Nehlig A. and Zvartau E. E. (1999) Actions of caffeine in the brain with special reference to factors that contribute to its widespread use. *Pharmacol Rev* **51,** 83-133.

Fredholm B. B., AP I. J., Jacobson K. A., Klotz K. N. and Linden J. (2001) International Union of Pharmacology. XXV. Nomenclature and classification of adenosine receptors. *Pharmacol Rev* **53,** 527-552.

Gaasterland D. and Kupfer C. (1974) Experimental glaucoma in the rhesus monkey. *Invest Ophthalmol* **13,** 455-457.

Garcia-Valenzuela E., Gorczyca W., Darzynkiewicz Z. and Sharma S. C. (1994) Apoptosis in adult retinal ganglion cells after axotomy. *J Neurobiol* **25,** 431-438.

Garcia-Valenzuela E., Shareef S., Walsh J. and Sharma S. C. (1995) Programmed cell death of retinal ganglion cells during experimental glaucoma. *Exp Eye Res* **61,** 33-44.

Gascon S., Deogracias R., Sobrado M., Roda J. M., Renart J., Rodriguez-Pena A. and Diaz-Guerra M. (2005) Transcription of the NR1 subunit of the N-methyl-D-aspartate receptor is down-regulated by excitotoxic stimulation and cerebral ischemia. *J Biol Chem* **280,** 35018-35027.

Geyer O., Almog J., Lupu-Meiri M., Lazar M. and Oron Y. (1995) Nitric oxide synthase inhibitors protect rat retina against ischemic injury. *FEBS Lett* **374,** 399-402.

Ghiardi G. J., Gidday J. M. and Roth S. (1999) The purine nucleoside adenosine in retinal ischemia-reperfusion injury. *Vision Res* **39,** 2519-2535.

Girkin C. A. (2004) Relationship between structure of optic nerve/nerve fiber layer and functional measurements in glaucoma. *Curr Opin Ophthalmol* **15,** 96-101.

Goldblum D. and Mittag T. (2002) Prospects for relevant glaucoma models with retinal ganglion cell damage in the rodent eye. *Vision Res* **42,** 471-478.

Gordon M. O., Beiser J. A., Brandt J. D., Heuer D. K., Higginbotham E. J., Johnson C. A., Keltner J. L., Miller J. P., Parrish R. K., 2nd, Wilson M. R. and Kass M. A. (2002) The Ocular Hypertension Treatment Study: baseline factors that predict the onset of primary open-angle glaucoma. *Arch Ophthalmol* **120,** 714-720.

Gottesman J. and Miller R. F. (1992) Pharmacological properties of N-methyl-D-aspartate receptors on ganglion cells of an amphibian retina. *J Neurophysiol* **68,** 596-604.

Gottesman J. and Miller R. F. (2003) N-methyl-D-aspartate receptors contribute to the baseline noise of retinal ganglion cells. *Vis Neurosci* **20,** 329-333.

Grant W. M. and Burke J. F., Jr. (1982) Why do some people go blind from glaucoma? *Ophthalmology* **89,** 991-998.

Gray P. C., Johnson B. D., Westenbroek R. E., Hays L. G., Yates J. R., 3rd, Scheuer T., Catterall W. A. and Murphy B. J. (1998) Primary structure and function of an A kinase anchoring protein associated with calcium channels. *Neuron* **20,** 1017-1026.

Green D. R. and Reed J. C. (1998) Mitochondria and apoptosis. *Science* **281,** 1309-1312.

Greengard P., Jen J., Nairn A. C. and Stevens C. F. (1991) Enhancement of the glutamate response by cAMP-dependent protein kinase in hippocampal neurons. *Science* **253,** 1135-1138.

Grunder T., Kohler K. and Guenther E. (2000a) Distribution and developmental regulation of AMPA receptor subunit proteins in rat retina. *Invest Ophthalmol Vis Sci* **41,** 3600-3606.

Grunder T., Kohler K., Kaletta A. and Guenther E. (2000b) The distribution and developmental regulation of NMDA receptor subunit proteins in the outer and inner retina of the rat. *J Neurobiol* **44,** 333-342.

Grynkiewicz G., Poenie M. and Tsien R. Y. (1985) A new generation of Ca2+ indicators with greatly improved fluorescence properties. *J Biol Chem* **260,** 3440-3450.

Guenther E., Rothe T., Taschenberger H. and Grantyn R. (1994) Separation of calcium currents in retinal ganglion cells from postnatal rat. *Brain Res* **633,** 223-235.

Hahn J. S., Aizenman E. and Lipton S. A. (1988) Central mammalian neurons normally resistant to glutamate toxicity are made sensitive by elevated extracellular Ca2+: toxicity is blocked by the N-methyl-D-aspartate antagonist MK-801. *Proc Natl Acad Sci U S A* **85,** 6556-6560.

Hallworth R., Cato M., Colbert C. and Rea M. A. (2002) Presynaptic adenosine A1 receptors regulate retinohypothalamic neurotransmission in the hamster suprachiasmatic nucleus. *J Neurobiol* **52,** 230-240.

Hamassaki-Britto D. E., Hermans-Borgmeyer I., Heinemann S. and Hughes T. E. (1993) Expression of glutamate receptor genes in the mammalian retina: the localization of GluR1 through GluR7 mRNAs. *J Neurosci* **13,** 1888-1898.

Han Y. and Slaughter M. M. (1998) Protein kinases modulate two glycine currents in salamander retinal ganglion cells. *J Physiol* **508,** 681-690.

Harada T., Harada C., Watanabe M., Inoue Y., Sakagawa T., Nakayama N., Sasaki S., Okuyama S., Watase K., Wada K. and Tanaka K. (1998) Functions of the two glutamate transporters GLAST and GLT-1 in the retina. *Proc Natl Acad Sci U S A* **95,** 4663-4666.

Hardingham G. E. and Bading H. (2003) The Yin and Yang of NMDA receptor signalling. *Trends Neurosci* **26,** 81-89.

Hardingham G. E., Fukunaga Y. and Bading H. (2002) Extrasynaptic NMDARs oppose synaptic NMDARs by triggering CREB shut-off and cell death pathways. *Nat Neurosci* **5,** 405-414.

Hare W. A., WoldeMussie E., Lai R. K., Ton H., Ruiz G., Chun T. and Wheeler L. (2004a) Efficacy and safety of memantine treatment for reduction of changes associated with experimental glaucoma in monkey, I: functional measures. *Invest Ophthalmol Vis Sci* **45,** 2625-2639.

Hare W. A., WoldeMussie E., Weinreb R. N., Ton H., Ruiz G., Wijono M., Feldmann B., Zangwill L. and Wheeler L. (2004b) Efficacy and Safety of Memantine Treatment for Reduction of Changes Associated with Experimental Glaucoma in Monkey, II: Structural Measures. *Invest Ophthalmol Vis Sci* **45,** 2640-2651.

Hartley D. M., Kurth M. C., Bjerkness L., Weiss J. H. and Choi D. W. (1993) Glutamate receptor-induced 45Ca2+ accumulation in cortical cell culture correlates with subsequent neuronal degeneration. *J Neurosci* **13,** 1993-2000.

Hartwick A. T. (2001) Beyond intraocular pressure: neuroprotective strategies for future glaucoma therapy. *Optom Vis Sci* **78,** 85-94.

Hartwick A. T., Lalonde M. R., Barnes S. and Baldridge W. H. (2004) Adenosine A1-receptor modulation of glutamate-induced calcium influx in rat retinal ganglion cells. *Invest Ophthalmol Vis Sci* **45,** 3740-3748.

Hartwick A. T., Zhang X., Chauhan B. C. and Baldridge W. H. (2005) Functional assessment of glutamate clearance mechanisms in a chronic rat glaucoma model using retinal ganglion cell calcium imaging. *J Neurochem* **94,** 794-807.

Harwerth R. S., Carter-Dawson L., Shen F., Smith E. L., 3rd and Crawford M. L. (1999) Ganglion cell losses underlying visual field defects from experimental glaucoma. *Invest Ophthalmol Vis Sci* **40,** 2242-2250.

Harwerth R. S., Crawford M. L., Frishman L. J., Viswanathan S., Smith E. L., 3rd and Carter-Dawson L. (2002) Visual field defects and neural losses from experimental glaucoma. *Prog Retin Eye Res* **21,** 91-125.

Hattar S., Liao H. W., Takao M., Berson D. M. and Yau K. W. (2002) Melanopsin-containing retinal ganglion cells: architecture, projections, and intrinsic photosensitivity. *Science* **295,** 1065-1070.

Hayashida Y., Partida G. J. and Ishida A. T. (2004) Dissociation of retinal ganglion cells without enzymes. *J Neurosci Methods* **137,** 25-35.

Hebb D. O. (1949) *The organization of behavior: A neuropsychological theory*. Wiley, New York, NY.

Heijl A., Leske M. C., Bengtsson B., Hyman L. and Hussein M. (2002) Reduction of intraocular pressure and glaucoma progression: results from the Early Manifest Glaucoma Trial. *Arch Ophthalmol* **120,** 1268-1279.

Helmchen F., Svoboda K., Denk W. and Tank D. W. (1999) In vivo dendritic calcium dynamics in deep-layer cortical pyramidal neurons. *Nat Neurosci* **2,** 989-996.

Hernandez M. R. (2000) The optic nerve head in glaucoma: role of astrocytes in tissue remodeling. *Prog Retin Eye Res* **19,** 297-321.

Higgs M. H. and Lukasiewicz P. D. (1999) Glutamate uptake limits synaptic excitation of retinal ganglion cells. *J Neurosci* **19,** 3691-3700.

Hille B. (1994) Modulation of ion-channel function by G-protein-coupled receptors. *Trends Neurosci* **17,** 531-536.

Hinds J. W. and Hinds P. L. (1983) Development of retinal amacrine cells in the mouse embryo: evidence for two modes of formation. *J Comp Neurol* **213,** 1-23.

Hof P. R., Lee P. Y., Yeung G., Wang R. F., Podos S. M. and Morrison J. H. (1998) Glutamate receptor subunit GluR2 and NMDAR1 immunoreactivity in the retina of macaque monkeys with experimental glaucoma does not identify vulnerable neurons. *Exp Neurol* **153,** 234-241.

Hollmann M. and Heinemann S. (1994) Cloned glutamate receptors. *Annu Rev Neurosci* **17,** 31-108.

Holz G. G. t., Rane S. G. and Dunlap K. (1986) GTP-binding proteins mediate transmitter inhibition of voltage-dependent calcium channels. *Nature* **319,** 670-672.

Honkanen R. A., Baruah S., Zimmerman M. B., Khanna C. L., Weaver Y. K., Narkiewicz J., Waziri R., Gehrs K. M., Weingeist T. A., Boldt H. C., Folk J. C., Russell S. R. and Kwon Y. H. (2003) Vitreous amino acid concentrations in patients with glaucoma undergoing vitrectomy. *Arch Ophthalmol* **121,** 183-188.

Huettner J. E. (2003) Kainate receptors and synaptic transmission. *Prog Neurobiol* **70,** 387-407.

Huettner J. E. and Baughman R. W. (1986) Primary culture of identified neurons from the visual cortex of postnatal rats. *J Neurosci* **6,** 3044-3060.

Hughes T. E., Hermans-Borgmeyer I. and Heinemann S. (1992) Differential expression of glutamate receptor genes (GluR1-5) in the rat retina. *Vis Neurosci* **8,** 49-55.

Hyrc K., Handran S. D., Rothman S. M. and Goldberg M. P. (1997) Ionized intracellular calcium concentration predicts excitotoxic neuronal death: observations with low-affinity fluorescent calcium indicators. *J Neurosci* **17,** 6669-6677.

Ikeda S. R. (1991) Double-pulse calcium channel current facilitation in adult rat sympathetic neurones. *J Physiol* **439,** 181-214.

Ikonomidou C. and Turski L. (2002) Why did NMDA receptor antagonists fail clinical trials for stroke and traumatic brain injury? *Lancet Neurol* **1,** 383-386.

Ishida A. T. (1991) Regenerative sodium and calcium currents in goldfish retinal ganglion cell somata. *Vision Res* **31,** 477-485.

Ishida A. T., Bindokas V. P. and Nuccitelli R. (1991) Calcium ion levels in resting and depolarized goldfish retinal ganglion cell somata and growth cones. *J Neurophysiol* **65,** 968-979.

Izumi Y., Shimamoto K., Benz A. M., Hammerman S. B., Olney J. W. and Zorumski C. F. (2002) Glutamate transporters and retinal excitotoxicity. *Glia* **39,** 58-68.

Izumi Y., Hammerman S. B., Kirby C. O., Benz A. M., Olney J. W. and Zorumski C. F. (2003) Involvement of glutamate in ischemic neurodegeneration in isolated retina. *Vis Neurosci* **20,** 97-107.

Jabaudon D., Scanziani M., Gahwiler B. H. and Gerber U. (2000) Acute decrease in net glutamate uptake during energy deprivation. *Proc Natl Acad Sci U S A* **97,** 5610-5615.

Jabaudon D., Shimamoto K., Yasuda-Kamatani Y., Scanziani M., Gahwiler B. H. and Gerber U. (1999) Inhibition of uptake unmasks rapid extracellular turnover of glutamate of nonvesicular origin. *Proc Natl Acad Sci U S A* **96,** 8733-8738.

Jacobson K. A. and Van Rhee A. M. (1997) Development of selective purinoceptor agonists and antagonists, in *Purinergic Approaches in Experimental Therapeutics* (Jacobson K. A. and Jarvis M. F., eds), pp 101-128. Wiley-Liss, New York.

Jakobs T. C., Libby R. T., Ben Y., John S. W. and Masland R. H. (2005) Retinal ganglion cell degeneration is topological but not cell type specific in DBA/2J mice. *J Cell Biol* **171,** 313-325.

Johansson B., Halldner L., Dunwiddie T. V., Masino S. A., Poelchen W., Gimenez-Llort L., Escorihuela R. M., Fernandez-Teruel A., Wiesenfeld-Hallin Z., Xu X. J., Hardemark A., Betsholtz C., Herlenius E. and Fredholm B. B. (2001) Hyperalgesia, anxiety, and decreased hypoxic neuroprotection in mice lacking the adenosine A1 receptor. *Proc Natl Acad Sci U S A* **98,** 9407-9412.

Johnson C. A. (1996) Standardizing the measurement of visual fields for clinical research: Guidelines from the Eye Care Technology Forum. *Ophthalmology* **103,** 186-189.

Johnson J. W. and Ascher P. (1987) Glycine potentiates the NMDA response in cultured mouse brain neurons. *Nature* **325,** 529-531.

Jonas P. and Burnashev N. (1995) Molecular mechanisms controlling calcium entry through AMPA-type glutamate receptor channels. *Neuron* **15,** 987-990.

Ju W. K., Kim K. Y., Park S. J., Park D. K., Park C. B., Oh S. J., Chung J. W. and Chun M. H. (2000) Nitric oxide is involved in sustained and delayed cell death of rat retina following transient ischemia. *Brain Res* **881,** 231-236.

Kaelin-Lang A., Jurklies B. and Niemeyer G. (1999) Effects of adenosinergic agents on the vascular resistance and on the optic nerve response in the perfused cat eye. *Vision Res* **39,** 1059-1068.

Kalloniatis M., Sun D., Foster L., Haverkamp S. and Wassle H. (2004) Localization of NMDA receptor subunits and mapping NMDA drive within the mammalian retina. *Vis Neurosci* **21,** 587-597.

Kao J. P. (1994) Practical aspects of measuring [Ca2+] with fluorescent indicators. *Methods Cell Biol* **40,** 155-181.

Kapin M. A., Doshi R., Scatton B., DeSantis L. M. and Chandler M. L. (1999) Neuroprotective effects of eliprodil in retinal excitotoxicity and ischemia. *Invest Ophthalmol Vis Sci* **40,** 1177-1182.

Karadottir R., Cavelier P., Bergersen L. H. and Attwell D. (2005) NMDA receptors are expressed in oligodendrocytes and activated in ischaemia. *Nature* **438,** 1162-1166.

Karschin A. and Lipton S. A. (1989) Calcium channels in solitary retinal ganglion cells from post-natal rat. *J Physiol* **418,** 379-396.

Kass M. A., Heuer D. K., Higginbotham E. J., Johnson C. A., Keltner J. L., Miller J. P., Parrish R. K., 2nd, Wilson M. R. and Gordon M. O. (2002) The Ocular Hypertension Treatment Study: a randomized trial determines that topical ocular hypotensive medication delays or prevents the onset of primary open-angle glaucoma. *Arch Ophthalmol* **120,** 701-713.

Katz B. and Miledi R. (1967) Ionic requirements of synaptic transmitter release. *Nature* **215,** 651.

Kawasaki A., Han M. H., Wei J. Y., Hirata K., Otori Y. and Barnstable C. J. (2002) Protective effect of arachidonic acid on glutamate neurotoxicity in rat retinal ganglion cells. *Invest Ophthalmol Vis Sci* **43,** 1835-1842.

Keelan J., Vergun O. and Duchen M. R. (1999) Excitotoxic mitochondrial depolarisation requires both calcium and nitric oxide in rat hippocampal neurons. *J Physiol* **520,** 797-813.

Kemp J. A. and McKernan R. M. (2002) NMDA receptor pathways as drug targets. *Nat Neurosci* **5 Suppl,** 1039-1042.

Kendell K. R., Quigley H. A., Kerrigan L. A., Pease M. E. and Quigley E. N. (1995) Primary open-angle glaucoma is not associated with photoreceptor loss. *Invest Ophthalmol Vis Sci* **36,** 200-205.

Kerr J. F., Wyllie A. H. and Currie A. R. (1972) Apoptosis: a basic biological phenomenon with wide-ranging implications in tissue kinetics. *Br J Cancer* **26,** 239-257.

Kerrigan L. A., Zack D. J., Quigley H. A., Smith S. D. and Pease M. E. (1997) TUNEL-positive ganglion cells in human primary open-angle glaucoma. *Arch Ophthalmol* **115,** 1031-1035.

Kettunen P., Demas J., Lohmann C., Kasthuri N., Gong Y., Wong R. O. and Gan W. B. (2002) Imaging calcium dynamics in the nervous system by means of ballistic delivery of indicators. *J Neurosci Methods* **119,** 37-43.

Khodorov B. (2004) Glutamate-induced deregulation of calcium homeostasis and mitochondrial dysfunction in mammalian central neurones. *Prog Biophys Mol Biol* **86,** 279-351.

Kielczewski J. L., Pease M. E. and Quigley H. A. (2005) The effect of experimental glaucoma and optic nerve transection on amacrine cells in the rat retina. *Invest Ophthalmol Vis Sci* **46,** 3188-3196.

Kirichok Y., Krapivinsky G. and Clapham D. E. (2004) The mitochondrial calcium uniporter is a highly selective ion channel. *Nature* **427,** 360-364.

Kitano S., Morgan J. and Caprioli J. (1996) Hypoxic and excitotoxic damage to cultured rat retinal ganglion cells. *Exp Eye Res* **63,** 105-112.

Kolb H. (2003) How the retina works. *American Scientist* **91,** 28-35.

Kondo Y., Takada M., Honda Y. and Mizuno N. (1993) Bilateral projections of single retinal ganglion cells to the lateral geniculate nuclei and superior colliculi in the albino rat. *Brain Res* **608,** 204-215.

Koopman G., Reutelingsperger C. P., Kuijten G. A., Keehnen R. M., Pals S. T. and van Oers M. H. (1994) Annexin V for flow cytometric detection of phosphatidylserine expression on B cells undergoing apoptosis. *Blood* **84,** 1415-1420.

Krakau C. E. (1981) Intraocular pressure elevation-cause or effect in chronic glaucoma? *Ophthalmologica* **182,** 141-147.

Kreutz M. R., Bockers T. M., Bockmann J., Seidenbecher C. I., Kracht B., Vorwerk C. K., Weise J. and Sabel B. A. (1998) Axonal injury alters alternative splicing of the retinal NR1 receptor: the preferential expression of the NR1b isoforms is crucial for retinal ganglion cell survival. *J Neurosci* **18,** 8278-8291.

Krizaj D., Liu X. and Copenhagen D. R. (2004) Expression of calcium transporters in the retina of the tiger salamander (Ambystoma tigrinum). *J Comp Neurol* **475,** 463-480.

Kroemer G. and Martin S. J. (2005) Caspase-independent cell death. *Nat Med* **11,** 725-730.

Kuehn M. H., Fingert J. H. and Kwon Y. H. (2005) Retinal ganglion cell death in glaucoma: mechanisms and neuroprotective strategies. *Ophthalmol Clin North Am* **18,** 383-395.

Kvanta A., Seregard S., Sejersen S., Kull B. and Fredholm B. B. (1997) Localization of adenosine receptor messenger RNAs in the rat eye. *Exp Eye Res* **65,** 595-602.

Kwon Y. H., Rickman D. W., Baruah S., Zimmerman M. B., Kim C. S., Boldt H. C., Russell S. R. and Hayreh S. S. (2005) Reply to: Glutamate excitotoxicity in glaucoma: throwing the baby out with the bathwater? *Eye* (Epub ahead of print; June 10 2005).

Lacza Z., Puskar M., Figueroa J. P., Zhang J., Rajapakse N. and Busija D. W. (2001) Mitochondrial nitric oxide synthase is constitutively active and is functionally upregulated in hypoxia. *Free Radic Biol Med* **31,** 1609-1615.

Lagreze W. A., Otto T. and Feuerstein T. J. (1999) [Neuroprotection in ischemia of the retina in an animal model]. *Ophthalmologe* **96,** 370-374.

Lam T. T., Abler A. S., Kwong J. M. and Tso M. O. (1999) N-methyl-D-aspartate (NMDA)--induced apoptosis in rat retina. *Invest Ophthalmol Vis Sci* **40,** 2391-2397.

Lamprecht R. and LeDoux J. (2004) Structural plasticity and memory. *Nat Rev Neurosci* **5,** 45-54.

Latini S. and Pedata F. (2001) Adenosine in the central nervous system: release mechanisms and extracellular concentrations. *J Neurochem* **79,** 463-484.

Latini S., Pazzagli M., Pepeu G. and Pedata F. (1996) A2 adenosine receptors: their presence and neuromodulatory role in the central nervous system. *Gen Pharmacol* **27,** 925-933.

Lattanzio F. A., Jr. and Bartschat D. K. (1991) The effect of pH on rate constants, ion selectivity and thermodynamic properties of fluorescent calcium and magnesium indicators. *Biochem Biophys Res Commun* **177,** 184-191.

Lei S. Z., Zhang D., Abele A. E. and Lipton S. A. (1992) Blockade of NMDA receptor-mediated mobilization of intracellular Ca2+ prevents neurotoxicity. *Brain Res* **598,** 196-202.

Leinders-Zufall T., Rand M. N., Waxman S. G. and Kocsis J. D. (1994) Differential role of two Ca(2+)-permeable non-NMDA glutamate channels in rat retinal ganglion cells: kainate-induced cytoplasmic and nuclear Ca2+ signals. *J Neurophysiol* **72,** 2503-2516.

Leist M. and Nicotera P. (1998) Apoptosis, excitotoxicity, and neuropathology. *Exp Cell Res* **239,** 183-201.

Lerma J. (2003) Roles and rules of kainate receptors in synaptic transmission. *Nat Rev Neurosci* **4,** 481-495.

Leske M. C., Heijl A., Hussein M., Bengtsson B., Hyman L. and Komaroff E. (2003) Factors for glaucoma progression and the effect of treatment: the early manifest glaucoma trial. *Arch Ophthalmol* **121,** 48-56.

Levkovitch-Verbin H., Martin K. R., Quigley H. A., Baumrind L. A., Pease M. E. and Valenta D. (2002a) Measurement of amino acid levels in the vitreous humor of rats after chronic intraocular pressure elevation or optic nerve transection. *J Glaucoma* **11,** 396-405.

Levkovitch-Verbin H., Quigley H. A., Martin K. R., Valenta D., Baumrind L. A. and Pease M. E. (2002b) Translimbal laser photocoagulation to the trabecular meshwork as a model of glaucoma in rats. *Invest Ophthalmol Vis Sci* **43,** 402-410.

Levkovitch-Verbin H., Quigley H. A., Martin K. R., Zack D. J., Pease M. E. and Valenta D. F. (2003) A model to study differences between primary and secondary degeneration of retinal ganglion cells in rats by partial optic nerve transection. *Invest Ophthalmol Vis Sci* **44,** 3388-3393.

Li B. and Roth S. (1999) Retinal ischemic preconditioning in the rat: requirement for adenosine and repetitive induction. *Invest Ophthalmol Vis Sci* **40,** 1200-1216.

Li J., Guo Y., Schroeder F. A., Youngs R. M., Schmidt T. W., Ferris C., Konradi C. and Akbarian S. (2004) Dopamine D2-like antagonists induce chromatin remodeling in striatal neurons through cyclic AMP-protein kinase A and NMDA receptor signaling. *J Neurochem* **90,** 1117-1131.

Li Y., Schlamp C. L. and Nickells R. W. (1999) Experimental induction of retinal ganglion cell death in adult mice. *Invest Ophthalmol Vis Sci* **40,** 1004-1008.

Li Y., Schlamp C. L., Poulsen G. L., Jackson M. W., Griep A. E. and Nickells R. W. (2002) p53 regulates apoptotic retinal ganglion cell death induced by N-methyl-D-aspartate. *Mol Vis* **8,** 341-350.

Libby R. T., Li Y., Savinova O. V., Barter J., Smith R. S., Nickells R. W. and John S. W. (2005) Susceptibility to neurodegeneration in a glaucoma is modified by Bax gene dosage. *PLoS Genet* **1,** 17-26.

Lichtman J. W. and Fraser S. E. (2001) The neuronal naturalist: watching neurons in their native habitat. *Nat Neurosci* **4 Suppl,** 1215-1220.

Linden R., Rehen S. K. and Chiarini L. B. (1999) Apoptosis in developing retinal tissue. *Prog Retin Eye Res* **18,** 133-165.

Lipton S. A. (2003) Possible role for memantine in protecting retinal ganglion cells from glaucomatous damage. *Surv Ophthalmol* **48 Suppl 1,** S38-46.

Lipton S. A. and Rosenberg P. A. (1994) Excitatory amino acids as a final common pathway for neurologic disorders. *N Engl J Med* **330,** 613-622.

Lipton S. A., Choi Y. B., Pan Z. H., Lei S. Z., Chen H. S., Sucher N. J., Loscalzo J., Singel D. J. and Stamler J. S. (1993) A redox-based mechanism for the neuroprotective and neurodestructive effects of nitric oxide and related nitroso-compounds. *Nature* **364,** 626-632.

Liu C. J., Chaturvedi N., Barnstable C. J. and Dreyer E. B. (1996) Retinal Thy-1 expression during development. *Invest Ophthalmol Vis Sci* **37,** 1469-1473.

Llinas R. R. (1982) Calcium in synaptic transmission. *Sci Am* **247,** 56-65.

Lotery A. J. (2005) Glutamate excitotoxicity in glaucoma: truth or fiction? *Eye* **19,** 369-370.

Lu Y. M., Yin H. Z., Chiang J. and Weiss J. H. (1996) Ca(2+)-permeable AMPA/kainate and NMDA channels: high rate of Ca2+ influx underlies potent induction of injury. *J Neurosci* **16,** 5457-5465.

Lucas D. R. and Newhouse J. P. (1957) The toxic effect of sodium L-glutamate on the inner layers of the retina. *Arch Opthalmol* **58,** 193-201.

Lukasiewicz P. D. and Roeder R. C. (1995) Evidence for glycine modulation of excitatory synaptic inputs to retinal ganglion cells. *J Neurosci* **15,** 4592-4601.

MacDonald J. F., Xiong Z. G. and Jackson M. F. (2006) Paradox of Ca2+ signaling, cell death and stroke. *Trends Neurosci* **29,** 75-81.

Macek T. A., Schaffhauser H. and Conn P. J. (1998) Protein kinase C and A3 adenosine receptor activation inhibit presynaptic metabotropic glutamate receptor (mGluR) function and uncouple mGluRs from GTP-binding proteins. *J Neurosci* **18,** 6138-6146.

MacLeish P. R., Barnstable C. J. and Townes-Anderson E. (1983) Use of a monoclonal antibody as a substrate for mature neurons in vitro. *Proc Natl Acad Sci U S A* **80,** 7014-7018.

Madden D. R. (2002) The structure and function of glutamate receptor ion channels. *Nat Rev Neurosci* **3,** 91-101.

Manabe S., Gu Z. and Lipton S. A. (2005) Activation of matrix metalloproteinase-9 via neuronal nitric oxide synthase contributes to NMDA-induced retinal ganglion cell death. *Invest Ophthalmol Vis Sci* **46,** 4747-4753.

Manev H., Favaron M., Guidotti A. and Costa E. (1989) Delayed increase of Ca2+ influx elicited by glutamate: role in neuronal death. *Mol Pharmacol* **36,** 106-112.

Mann M., Haq W., Zabel T., Guenther E., Zrenner E. and Ladewig T. (2005) Age-dependent changes in the regulation mechanisms for intracellular calcium ions in ganglion cells of the mouse retina. *Eur J Neurosci* **22,** 2735-2743.

Marc R. E. (1999a) Mapping glutamatergic drive in the vertebrate retina with a channel-permeant organic cation. *J Comp Neurol* **407,** 47-64.

Marc R. E. (1999b) Kainate activation of horizontal, bipolar, amacrine, and ganglion cells in the rabbit retina. *J Comp Neurol* **407,** 65-76.

Marc R. E. and Jones B. W. (2002) Molecular phenotyping of retinal ganglion cells. *J Neurosci* **22,** 413-427.

Martin K. R., Levkovitch-Verbin H., Valenta D., Baumrind L., Pease M. E. and Quigley H. A. (2002) Retinal glutamate transporter changes in experimental glaucoma and after optic nerve transection in the rat. *Invest Ophthalmol Vis Sci* **43,** 2236-2243.

Masland R. H. (2001a) The fundamental plan of the retina. *Nat Neurosci* **4,** 877-886.

Masland R. H. (2001b) Neuronal diversity in the retina. *Curr Opin Neurobiol* **11,** 431-436.

Mata A. M. and Sepulveda M. R. (2005) Calcium pumps in the central nervous system. *Brain Res Brain Res Rev* **49,** 398-405.

Mayer M. L. (2005) Glutamate receptor ion channels. *Curr Opin Neurobiol* **15,** 282-288.

Mayer M. L. and Westbrook G. L. (1987) Permeation and block of N-methyl-D-aspartic acid receptor channels by divalent cations in mouse cultured central neurones. *J Physiol* **394,** 501-527.

Mayer M. L. and Armstrong N. (2004) Structure and function of glutamate receptor ion channels. *Annu Rev Physiol* **66,** 161-181.

Mayer M. L., Westbrook G. L. and Guthrie P. B. (1984) Voltage-dependent block by Mg2+ of NMDA responses in spinal cord neurones. *Nature* **309,** 261-263.

Meyer-Franke A., Kaplan M. R., Pfrieger F. W. and Barres B. A. (1995) Characterization of the signaling interactions that promote the survival and growth of developing retinal ganglion cells in culture. *Neuron* **15,** 805-819.

Micu I., Jiang Q., Coderre E., Ridsdale A., Zhang L., Woulfe J., Yin X., Trapp B. D., McRory J. E., Rehak R., Zamponi G. W., Wang W. and Stys P. K. (2006) NMDA receptors mediate calcium accumulation in myelin during chemical ischaemia. *Nature* **439**, 988-92.

Moghaddam B. (2003) Bringing order to the glutamate chaos in schizophrenia. *Neuron* **40,** 881-884.

Mogul D. J., Adams M. E. and Fox A. P. (1993) Differential activation of adenosine receptors decreases N-type but potentiates P-type Ca2+ current in hippocampal CA3 neurons. *Neuron* **10,** 327-334.

Moore E. D., Becker P. L., Fogarty K. E., Williams D. A. and Fay F. S. (1990) Ca2+ imaging in single living cells: theoretical and practical issues. *Cell Calcium* **11,** 157-179.

Moore R. Y. and Lenn N. J. (1972) A retinohypothalamic projection in the rat. *J Comp Neurol* **146,** 1-14.

Morrison J. C., Johnson E. C., Cepurna W. and Jia L. (2005) Understanding mechanisms of pressure-induced optic nerve damage. *Prog Retin Eye Res* **24,** 217-240.

Morrison J. C., Nylander K. B., Lauer A. K., Cepurna W. O. and Johnson E. (1998) Glaucoma drops control intraocular pressure and protect optic nerves in a rat model of glaucoma. *Invest Ophthalmol Vis Sci* **39,** 526-531.

Morrison J. C., Moore C. G., Deppmeier L. M., Gold B. G., Meshul C. K. and Johnson E. C. (1997) A rat model of chronic pressure-induced optic nerve damage. *Exp Eye Res* **64,** 85-96.

Muller F., Greferath U., Wassle H., Wisden W. and Seeburg P. (1992) Glutamate receptor expression in the rat retina. *Neurosci Lett* **138,** 179-182.

Nakazawa T., Shimura M., Endo S., Takahashi H., Mori N. and Tamai M. (2005) N-Methyl-D-Aspartic acid suppresses Akt activity through protein phosphatase in retinal ganglion cells. *Mol Vis* **11,** 1173-1182.

Neal M. and Cunningham J. (1994) Modulation by endogenous ATP of the light-evoked release of ACh from retinal cholinergic neurones. *Br J Pharmacol* **113,** 1085-1087.

Neufeld A. H., Sawada A. and Becker B. (1999) Inhibition of nitric-oxide synthase 2 by aminoguanidine provides neuroprotection of retinal ganglion cells in a rat model of chronic glaucoma. *Proc Natl Acad Sci U S A* **96,** 9944-9948.

Neufeld A. H., Kawai S., Das S., Vora S., Gachie E., Connor J. R. and Manning P. T. (2002) Loss of retinal ganglion cells following retinal ischemia: the role of inducible nitric oxide synthase. *Exp Eye Res* **75,** 521-528.

Newman E. A. (2001) Propagation of intercellular calcium waves in retinal astrocytes and Muller cells. *J Neurosci* **21,** 2215-2223.

Newman E. A. (2003) Glial cell inhibition of neurons by release of ATP. *J Neurosci* **23,** 1659-1666.

Newman E. A. (2004) Glial modulation of synaptic transmission in the retina. *Glia* **47,** 268-274.

Nicholls D. G. and Budd S. L. (2000) Mitochondria and neuronal survival. *Physiol Rev* **80,** 315-360.

Nickells R. W. (1996) Retinal ganglion cell death in glaucoma: the how, the why, and the maybe. *J Glaucoma* **5,** 345-356.

Nicoll R. A. and Malenka R. C. (1995) Contrasting properties of two forms of long-term potentiation in the hippocampus. *Nature* **377,** 115-118.

Nikolaeva M. A., Mukherjee B. and Stys P. K. (2005) Na+-dependent sources of intra-axonal Ca2+ release in rat optic nerve during in vitro chemical ischemia. *J Neurosci* **25,** 9960-9967.

Nomura A., Shigemoto R., Nakamura Y., Okamoto N., Mizuno N. and Nakanishi S. (1994) Developmentally regulated postsynaptic localization of a metabotropic glutamate receptor in rat rod bipolar cells. *Cell* **77,** 361-369.

Nowak L., Bregestovski P., Ascher P., Herbet A. and Prochiantz A. (1984) Magnesium gates glutamate-activated channels in mouse central neurones. *Nature* **307,** 462-465.

Nucci C., Tartaglione R., Rombola L., Morrone L. A., Fazzi E. and Bagetta G. (2005) Neurochemical evidence to implicate elevated glutamate in the mechanisms of high intraocular pressure (IOP)-induced retinal ganglion cell death in rat. *Neurotoxicology* **26,** 935-941.

Obrietan K., Belousov A. B., Heller H. C. and van den Pol A. N. (1995) Adenosine pre- and postsynaptic modulation of glutamate-dependent calcium activity in hypothalamic neurons. *J Neurophysiol* **74,** 2150-2162.

Olney J. W. (1969a) Glutamate-induced retinal degeneration in neonatal mice. Electron microscopy of the acutely evolving lesion. *J Neuropathol Exp Neurol* **28,** 455-474.

Olney J. W. (1969b) Brain lesions, obesity, and other disturbances in mice treated with monosodium glutamate. *Science* **164,** 719-721.

Olney J. W., Labruyere J. and Price M. T. (1989) Pathological changes induced in cerebrocortical neurons by phencyclidine and related drugs. *Science* **244,** 1360-1362.

Ongini E., Adami M., Ferri C. and Bertorelli R. (1997) Adenosine A2A receptors and neuroprotection. *Ann N Y Acad Sci* **825,** 30-48.

Orrenius S., Zhivotovsky B. and Nicotera P. (2003) Regulation of cell death: the calcium-apoptosis link. *Nat Rev Mol Cell Biol* **4,** 552-565.

Osborne N. N. (1999) Memantine reduces alterations to the mammalian retina, in situ, induced by ischemia. *Vis Neurosci* **16,** 45-52.

Osborne N. N., Chidlow G. and Wood J. P. (2006) Glutamate excitotoxicity in glaucoma: truth or fiction? By AJ Lotery. *Eye* (Epub ahead of print; Jan 27 2006).

Osborne N. N., Melena J., Chidlow G. and Wood J. P. (2001) A hypothesis to explain ganglion cell death caused by vascular insults at the optic nerve head: possible implication for the treatment of glaucoma. *Br J Ophthalmol* **85,** 1252-1259.

Osborne N. N., Casson R. J., Wood J. P., Chidlow G., Graham M. and Melena J. (2004) Retinal ischemia: mechanisms of damage and potential therapeutic strategies. *Prog Retin Eye Res* **23,** 91-147.

Otori Y., Wei J. Y. and Barnstable C. J. (1998) Neurotoxic effects of low doses of glutamate on purified rat retinal ganglion cells. *Invest Ophthalmol Vis Sci* **39,** 972-981.

Pang I. H., Johnson E. C., Jia L., Cepurna W. O., Shepard A. R., Hellberg M. R., Clark A. F. and Morrison J. C. (2005) Evaluation of inducible nitric oxide synthase in glaucomatous optic neuropathy and pressure-induced optic nerve damage. *Invest Ophthalmol Vis Sci* **46,** 1313-1321.

Parsons C. G., Danysz W. and Quack G. (1999) Memantine is a clinically well tolerated N-methyl-D-aspartate (NMDA) receptor antagonist--a review of preclinical data. *Neuropharmacology* **38,** 735-767.

Patneau D. K. and Mayer M. L. (1990) Structure-activity relationships for amino acid transmitter candidates acting at N-methyl-D-aspartate and quisqualate receptors. *J Neurosci* **10,** 2385-2399.

Pease M. E., McKinnon S. J., Quigley H. A., Kerrigan-Baumrind L. A. and Zack D. J. (2000) Obstructed axonal transport of BDNF and its receptor TrkB in experimental glaucoma. *Invest Ophthalmol Vis Sci* **41,** 764-774.

Pedata F., Corsi C., Melani A., Bordoni F. and Latini S. (2001) Adenosine extracellular brain concentrations and role of A2A receptors in ischemia. *Ann N Y Acad Sci* **939,** 74-84.

Peng Y. W., Blackstone C. D., Huganir R. L. and Yau K. W. (1995) Distribution of glutamate receptor subtypes in the vertebrate retina. *Neuroscience* **66,** 483-497.

Perez M. T., Ehinger B. E., Lindstrom K. and Fredholm B. B. (1986) Release of endogenous and radioactive purines from the rabbit retina. *Brain Res* **398,** 106-112.

Perry S. W., Norman J. P., Litzburg A. and Gelbard H. A. (2004) Antioxidants are required during the early critical period, but not later, for neuronal survival. *J Neurosci Res* **78,** 485-492.

Perry V. H. (1979) The ganglion cell layer of the retina of the rat: a Golgi study. *Proc R Soc Lond B Biol Sci* **204,** 363-375.

Perry V. H., Henderson Z. and Linden R. (1983) Postnatal changes in retinal ganglion cell and optic axon populations in the pigmented rat. *J Comp Neurol* **219,** 356-368.

Perry V. H., Morris R. J. and Raisman G. (1984) Is Thy-1 expressed only by ganglion cells and their axons in the retina and optic nerve? *J Neurocytol* **13,** 809-824.

Pickard G. E. (1980) Morphological characteristics of retinal ganglion cells projecting to the suprachiasmatic nucleus: a horseradish peroxidase study. *Brain Res* **183,** 458-465.

Popoli P., Minghetti L., Tebano M. T., Pintor A., Domenici M. R. and Massotti M. (2004) Adenosine A2A receptor antagonism and neuroprotection: mechanisms, lights, and shadows. *Crit Rev Neurobiol* **16,** 99-106.

Potts R. A., Dreher B. and Bennett M. R. (1982) The loss of ganglion cells in the developing retina of the rat. *Brain Res* **255,** 481-486.

Pow D. V. (2001) Amino acids and their transporters in the retina. *Neurochem Int* **38,** 463-484.

Pow D. V. and Barnett N. L. (1999) Changing patterns of spatial buffering of glutamate in developing rat retinae are mediated by the Muller cell glutamate transporter GLAST. *Cell Tissue Res* **297,** 57-66.

Provencio I., Jiang G., De Grip W. J., Hayes W. P. and Rollag M. D. (1998) Melanopsin: An opsin in melanophores, brain, and eye. *Proc Natl Acad Sci U S A* **95,** 340-345.

Quigley H. A. (1999) Neuronal death in glaucoma. *Prog Retin Eye Res* **18,** 39-57.

Quigley H. A. (2005) New paradigms in the mechanisms and management of glaucoma. *Eye* **19,** 1241-1248.

Quigley H. A. and Addicks E. M. (1980) Chronic experimental glaucoma in primates. II. Effect of extended intraocular pressure elevation on optic nerve head and axonal transport. *Invest Ophthalmol Vis Sci* **19,** 137-152.

Quigley H. A., Addicks E. M. and Green W. R. (1982) Optic nerve damage in human glaucoma. III. Quantitative correlation of nerve fiber loss and visual field defect in glaucoma, ischemic neuropathy, papilledema, and toxic neuropathy. *Arch Ophthalmol* **100,** 135-146.

Quigley H. A., Addicks E. M., Green W. R. and Maumenee A. E. (1981) Optic nerve damage in human glaucoma. II. The site of injury and susceptibility to damage. *Arch Ophthalmol* **99,** 635-649.

Quigley H. A., Hohman R. M., Addicks E. M., Massof R. W. and Green W. R. (1983) Morphologic changes in the lamina cribrosa correlated with neural loss in open-angle glaucoma. *Am J Ophthalmol* **95,** 673-691.

Quigley H. A., Nickells R. W., Kerrigan L. A., Pease M. E., Thibault D. J. and Zack D. J. (1995) Retinal ganglion cell death in experimental glaucoma and after axotomy occurs by apoptosis. *Invest Ophthalmol Vis Sci* **36,** 774-786.

Raff M. C., Whitmore A. V. and Finn J. T. (2002) Axonal self-destruction and neurodegeneration. *Science* **296,** 868-871.

Rajdev S. and Reynolds I. J. (1994) Glutamate-induced intracellular calcium changes and neurotoxicity in cortical neurons in vitro: effect of chemical ischemia. *Neuroscience* **62,** 667-679.

Randall R. D. and Thayer S. A. (1992) Glutamate-induced calcium transient triggers delayed calcium overload and neurotoxicity in rat hippocampal neurons. *J Neurosci* **12,** 1882-1895.

Rao S. D. and Weiss J. H. (2004) Excitotoxic and oxidative cross-talk between motor neurons and glia in ALS pathogenesis. *Trends Neurosci* **27,** 17-23.

Rauen T. (2000) Diversity of glutamate transporter expression and function in the mammalian retina. *Amino Acids* **19,** 53-62.

Rauen T., Rothstein J. D. and Wassle H. (1996) Differential expression of three glutamate transporter subtypes in the rat retina. *Cell Tissue Res* **286,** 325-336.

Rauen T., Taylor W. R., Kuhlbrodt K. and Wiessner M. (1998) High-affinity glutamate transporters in the rat retina: a major role of the glial glutamate transporter GLAST-1 in transmitter clearance. *Cell Tissue Res* **291,** 19-31.

Reichenbach A., Stolzenburg J. U., Eberhardt W., Chao T. I., Dettmer D. and Hertz L. (1993) What do retinal muller (glial) cells do for their neuronal 'small siblings'? *J Chem Neuroanat* **6,** 201-213.

Resnikoff S., Pascolini D., Etya'ale D., Kocur I., Pararajasegaram R., Pokharel G. P. and Mariotti S. P. (2004) Global data on visual impairment in the year 2002. *Bull World Health Organ* **82,** 844-851.

Reynolds I. J. and Hastings T. G. (1995) Glutamate induces the production of reactive oxygen species in cultured forebrain neurons following NMDA receptor activation. *J Neurosci* **15,** 3318-3327.

Roe M. W., Lemasters J. J. and Herman B. (1990) Assessment of Fura-2 for measurements of cytosolic free calcium. *Cell Calcium* **11,** 63-73.

Rorig B. and Grantyn R. (1993) Rat retinal ganglion cells express Ca(2+)-permeable non-NMDA glutamate receptors during the period of histogenetic cell death. *Neurosci Lett* **153,** 32-36.

Rossi D. J., Oshima T. and Attwell D. (2000) Glutamate release in severe brain ischaemia is mainly by reversed uptake. *Nature* **403,** 316-321.

Roth S. (2004) Endogenous neuroprotection in the retina. *Brain Res Bull* **62,** 461-466.

Rothstein J. D., Martin L., Levey A. I., Dykes-Hoberg M., Jin L., Wu D., Nash N. and Kuncl R. W. (1994) Localization of neuronal and glial glutamate transporters. *Neuron* **13,** 713-725.

Rothstein J. D., Patel S., Regan M. R., Haenggeli C., Huang Y. H., Bergles D. E., Jin L., Dykes Hoberg M., Vidensky S., Chung D. S., Toan S. V., Bruijn L. I., Su Z. Z., Gupta P. and Fisher P. B. (2005) Beta-lactam antibiotics offer neuroprotection by increasing glutamate transporter expression. *Nature* **433,** 73-77.

Rubin L. L., Gatchalian C. L., Rimon G. and Brooks S. F. (1994) The molecular mechanisms of neuronal apoptosis. *Curr Opin Neurobiol* **4,** 696-702.

Rudolf R., Mongillo M., Rizzuto R. and Pozzan T. (2003) Looking forward to seeing calcium. *Nat Rev Mol Cell Biol* **4,** 579-586.

Sabel B. A., Engelmann R. and Humphrey M. F. (1997) In vivo confocal neuroimaging (ICON) of CNS neurons. *Nat Med* **3,** 244-247.

Sabel B. A., Sautter J., Stoehr T. and Siliprandi R. (1995) A behavioral model of excitotoxicity: retinal degeneration, loss of vision, and subsequent recovery after intraocular NMDA administration in adult rats. *Exp Brain Res* **106,** 93-105.

Salt T. E. and Cordeiro M. F. (2005) Glutamate excitotoxicity in glaucoma: throwing the baby out with the bathwater? *Eye* (Epub ahead of print; June 10 2005).

Salter M. G. and Fern R. (2005) NMDA receptors are expressed in developing oligodendrocyte processes and mediate injury. *Nature* **438,** 1167-1171.

Salter M. W. and Kalia L. V. (2004) Src kinases: a hub for NMDA receptor regulation. *Nat Rev Neurosci* **5,** 317-328.

Sarthy V. P., Pignataro L., Pannicke T., Weick M., Reichenbach A., Harada T., Tanaka K. and Marc R. (2005) Glutamate transport by retinal Muller cells in glutamate/aspartate transporter-knockout mice. *Glia* **49,** 184-196.

Sattler R. and Tymianski M. (2000) Molecular mechanisms of calcium-dependent excitotoxicity. *J Mol Med* **78,** 3-13.

Sattler R., Charlton M. P., Hafner M. and Tymianski M. (1998) Distinct influx pathways, not calcium load, determine neuronal vulnerability to calcium neurotoxicity. *J Neurochem* **71,** 2349-2364.

Sattler R., Xiong Z., Lu W. Y., Hafner M., MacDonald J. F. and Tymianski M. (1999) Specific coupling of NMDA receptor activation to nitric oxide neurotoxicity by PSD-95 protein. *Science* **284,** 1845-1848.

Sawada A. and Neufeld A. H. (1999) Confirmation of the rat model of chronic, moderately elevated intraocular pressure. *Exp Eye Res* **69,** 525-531.

Scammell T. E., Arrigoni E., Thompson M. A., Ronan P. J., Saper C. B. and Greene R. W. (2003) Focal deletion of the adenosine A1 receptor in adult mice using an adeno-associated viral vector. *J Neurosci* **23,** 5762-5770.

Schell M. J., Molliver M. E. and Snyder S. H. (1995) D-serine, an endogenous synaptic modulator: localization to astrocytes and glutamate-stimulated release. *Proc Natl Acad Sci U S A* **92,** 3948-3952.

Schell M. J., Brady R. O., Jr., Molliver M. E. and Snyder S. H. (1997) D-serine as a neuromodulator: regional and developmental localizations in rat brain glia resemble NMDA receptors. *J Neurosci* **17,** 1604-1615.

Schlamp C. L., Johnson E. C., Li Y., Morrison J. C. and Nickells R. W. (2001) Changes in Thy1 gene expression associated with damaged retinal ganglion cells. *Mol Vis* **7,** 192-201.

Schmid S. and Guenther E. (1999) Voltage-activated calcium currents in rat retinal ganglion cells in situ: changes during prenatal and postnatal development. *J Neurosci* **19,** 3486-3494.

Schmid S., Guenther E. and Kohler K. (1995) Changes in Thy-1 antigen immunoreactivity in the rat retina during pre- and postnatal development. *Neurosci Lett* **199,** 91-94.

Schultz K. and Stell W. K. (1996) Immunocytochemical localization of the high-affinity glutamate transporter, EAAC1, in the retina of representative vertebrate species. *Neurosci Lett* **211,** 191-194.

Schwartz M., Shaked I., Fisher J., Mizrahi T. and Schori H. (2003) Protective autoimmunity against the enemy within: fighting glutamate toxicity. *Trends Neurosci* **26,** 297-302.

Sekaran S., Foster R. G., Lucas R. J. and Hankins M. W. (2003) Calcium imaging reveals a network of intrinsically light-sensitive inner-retinal neurons. *Curr Biol* **13,** 1290-1298.

Shareef S., Sawada A. and Neufeld A. H. (1999) Isoforms of nitric oxide synthase in the optic nerves of rat eyes with chronic moderately elevated intraocular pressure. *Invest Ophthalmol Vis Sci* **40,** 2884-2891.

Shareef S. R., Garcia-Valenzuela E., Salierno A., Walsh J. and Sharma S. C. (1995) Chronic ocular hypertension following episcleral venous occlusion in rats. *Exp Eye Res* **61,** 379-382.

Shiells R. A., Falk G. and Naghshineh S. (1981) Action of glutamate and aspartate analogues on rod horizontal and bipolar cells. *Nature* **294,** 592-594.

Shigeri Y., Shimamoto K., Yasuda-Kamatani Y., Seal R. P., Yumoto N., Nakajima T. and Amara S. G. (2001) Effects of threo-beta-hydroxyaspartate derivatives on excitatory amino acid transporters (EAAT4 and EAAT5). *J Neurochem* **79,** 297-302.

Shimamoto K., Lebrun B., Yasuda-Kamatani Y., Sakaitani M., Shigeri Y., Yumoto N. and Nakajima T. (1998) DL-threo-beta-benzyloxyaspartate, a potent blocker of excitatory amino acid transporters. *Mol Pharmacol* **53,** 195-201.

Siliprandi R., Canella R., Carmignoto G., Schiavo N., Zanellato A., Zanoni R. and Vantini G. (1992) N-methyl-D-aspartate-induced neurotoxicity in the adult rat retina. *Vis Neurosci* **8,** 567-573.

Sisk D. R. and Kuwabara T. (1985) Histologic changes in the inner retina of albino rats following intravitreal injection of monosodium L-glutamate. *Graefes Arch Clin Exp Ophthalmol* **223,** 250-258.

Slaughter M. M. and Miller R. F. (1981) 2-amino-4-phosphonobutyric acid: a new pharmacological tool for retina research. *Science* **211,** 182-185.

Sommer A., Tielsch J. M., Katz J., Quigley H. A., Gottsch J. D., Javitt J. and Singh K. (1991) Relationship between intraocular pressure and primary open angle glaucoma among white and black Americans. The Baltimore Eye Survey. *Arch Ophthalmol* **109,** 1090-1095.

Spierings D., McStay G., Saleh M., Bender C., Chipuk J., Maurer U. and Green D. R. (2005) Connected to death: the (unexpurgated) mitochondrial pathway of apoptosis. *Science* **310,** 66-67.

Stella S. L., Jr., Bryson E. J. and Thoreson W. B. (2002) A2 adenosine receptors inhibit calcium influx through L-type calcium channels in rod photoreceptors of the salamander retina. *J Neurophysiol* **87,** 351-360.

Stella S. L., Jr., Bryson E. J., Cadetti L. and Thoreson W. B. (2003) Endogenous adenosine reduces glutamatergic output from rods through activation of A2-like adenosine receptors. *J Neurophysiol* **90,** 165-174.

Stevens C. F. and Sullivan J. (1998) Synaptic plasticity. *Curr Biol* **8,** R151-153.

Stevens E. R., Esguerra M., Kim P. M., Newman E. A., Snyder S. H., Zahs K. R. and Miller R. F. (2003) D-serine and serine racemase are present in the vertebrate retina and contribute to the physiological activation of NMDA receptors. *Proc Natl Acad Sci U S A* **100,** 6789-6794.

Stone T. W. (2002) Purines and neuroprotection. *Adv Exp Med Biol* **513,** 249-280.

Stout A. K. and Reynolds I. J. (1999) High-affinity calcium indicators underestimate increases in intracellular calcium concentrations associated with excitotoxic glutamate stimulations. *Neuroscience* **89,** 91-100.

Sucher N. J., Aizenman E. and Lipton S. A. (1991) N-methyl-D-aspartate antagonists prevent kainate neurotoxicity in rat retinal ganglion cells in vitro. *J Neurosci* **11,** 966-971.

Sucher N. J., Lipton S. A. and Dreyer E. B. (1997) Molecular basis of glutamate toxicity in retinal ganglion cells. *Vision Res* **37,** 3483-3493.

Sucher N. J., Kohler K., Tenneti L., Wong H. K., Grunder T., Fauser S., Wheeler-Schilling T., Nakanishi N., Lipton S. A. and Guenther E. (2003) N-methyl-D-aspartate receptor subunit NR3A in the retina: developmental expression, cellular localization, and functional aspects. *Invest Ophthalmol Vis Sci* **44,** 4451-4456.

Sullivan M. R., Nimmerjahn A., Sarkisov D. V., Helmchen F. and Wang S. S. (2005) In vivo calcium imaging of circuit activity in cerebellar cortex. *J Neurophysiol* **94,** 1636-1644.

Sun D. and Kalloniatis M. (2006) Mapping glutamate responses in immunocytochemically identified neurons of the mouse retina. *J Comp Neurol* **494,** 686-703.

Sun D., Rait J. L. and Kalloniatis M. (2003) Inner retinal neurons display differential responses to N-methyl-D-aspartate receptor activation. *J Comp Neurol* **465,** 38-56.

Sun W., Li N. and He S. (2002a) Large-scale morphological survey of mouse retinal ganglion cells. *J Comp Neurol* **451,** 115-126.

Sun X., Barnes S. and Baldridge W. H. (2002b) Adenosine inhibits calcium channel currents via A1 receptors on salamander retinal ganglion cells in a mini-slice preparation. *J Neurochem* **81,** 550-556.

Svoboda K., Denk W., Kleinfeld D. and Tank D. W. (1997) In vivo dendritic calcium dynamics in neocortical pyramidal neurons. *Nature* **385,** 161-165.

Syntichaki P. and Tavernarakis N. (2003) The biochemistry of neuronal necrosis: rogue biology? *Nat Rev Neurosci* **4,** 672-684.

Takahashi N., Cummins D. and Caprioli J. (1991) Rat retinal ganglion cells in culture. *Exp Eye Res* **53,** 565-572.

Takayasu Y., Iino M. and Ozawa S. (2004) Roles of glutamate transporters in shaping excitatory synaptic currents in cerebellar Purkinje cells. *Eur J Neurosci* **19,** 1285-1295.

Taschenberger H. and Grantyn R. (1995) Several types of Ca2+ channels mediate glutamatergic synaptic responses to activation of single Thy-1-immunolabeled rat retinal ganglion neurons. *J Neurosci* **15,** 2240-2254.

Taschenberger H., Engert F. and Grantyn R. (1995) Synaptic current kinetics in a solely AMPA-receptor-operated glutamatergic synapse formed by rat retinal ganglion neurons. *J Neurophysiol* **74,** 1123-1136.

Taschenberger H., Juttner R. and Grantyn R. (1999) Ca2+-permeable P2X receptor channels in cultured rat retinal ganglion cells. *J Neurosci* **19,** 3353-3366.

Tessier-Lavigne M. (1991) Phototransduction and information processing in the retina, in *Principles of Neural Science* (Kandel E. R., Schwartz J. H. and Jessell T. M., eds), pp 400-418. Appleton & Lange, East Norwalk, CT.

Thanos S., Indorf L. and Naskar R. (2002) In vivo FM: using conventional fluorescence microscopy to monitor retinal neuronal death in vivo. *Trends Neurosci* **25,** 441-444.

The AGIS Investigators (2000) The Advanced Glaucoma Intervention Study (AGIS): 7. The relationship between control of intraocular pressure and visual field deterioration. *Am J Ophthalmol* **130,** 429-440.

Thompson S. M., Haas H. L. and Gahwiler B. H. (1992) Comparison of the actions of adenosine at pre- and postsynaptic receptors in the rat hippocampus in vitro. *J Physiol* **451,** 347-363.

Thoreson W. B. and Witkovsky P. (1999) Glutamate receptors and circuits in the vertebrate retina. *Prog Retin Eye Res* **18,** 765-810.

Thornberry N. A. and Lazebnik Y. (1998) Caspases: enemies within. *Science* **281,** 1312-1316.

Toescu E. C., Verkhratsky A. and Landfield P. W. (2004) Ca2+ regulation and gene expression in normal brain aging. *Trends Neurosci* **27,** 614-620.

Tovar K. R. and Westbrook G. L. (2002) Mobile NMDA receptors at hippocampal synapses. *Neuron* **34,** 255-264.

Trimmer J. S. and Rhodes K. J. (2004) Localization of voltage-gated ion channels in mammalian brain. *Annu Rev Physiol* **66,** 477-519.

Trussell L. O. and Jackson M. B. (1985) Adenosine-activated potassium conductance in cultured striatal neurons. *Proc Natl Acad Sci U S A* **82,** 4857-4861.

Tsien R. W., Lipscombe D., Madison D., Bley K. and Fox A. (1995) Reflections on Ca(2+)-channel diversity, 1988-1994. *Trends Neurosci* **18,** 52-54.

Tsien R. Y. (1989) Fluorescent probes of cell signaling. *Annu Rev Neurosci* **12,** 227-253.

Tymianski M., Charlton M. P., Carlen P. L. and Tator C. H. (1993) Source specificity of early calcium neurotoxicity in cultured embryonic spinal neurons. *J Neurosci* **13,** 2085-2104.

Ueda J., Sawaguchi S., Hanyu T., Yaoeda K., Fukuchi T., Abe H. and Ozawa H. (1998) Experimental glaucoma model in the rat induced by laser trabecular photocoagulation after an intracameral injection of India ink. *Jpn J Ophthalmol* **42,** 337-344.

Ullian E. M., Sapperstein S. K., Christopherson K. S. and Barres B. A. (2001) Control of synapse number by glia. *Science* **291,** 657-661.

Ullian E. M., Barkis W. B., Chen S., Diamond J. S. and Barres B. A. (2004) Invulnerability of retinal ganglion cells to NMDA excitotoxicity. *Mol Cell Neurosci* **26,** 544-557.

Umemiya M. and Berger A. J. (1994) Activation of adenosine A1 and A2 receptors differentially modulates calcium channels and glycinergic synaptic transmission in rat brainstem. *Neuron* **13,** 1439-1446.

van Zundert B., Yoshii A. and Constantine-Paton M. (2004) Receptor compartmentalization and trafficking at glutamate synapses: a developmental proposal. *Trends Neurosci* **27,** 428-437.

Vanhoutte P. and Bading H. (2003) Opposing roles of synaptic and extrasynaptic NMDA receptors in neuronal calcium signalling and BDNF gene regulation. *Curr Opin Neurobiol* **13,** 366-371.

Verkhratsky A. and Toescu E. C. (1998) Calcium and neuronal ageing. *Trends Neurosci* **21,** 2-7.

Vickers J. C., Schumer R. A., Podos S. M., Wang R. F., Riederer B. M. and Morrison J. H. (1995) Differential vulnerability of neurochemically identified subpopulations of retinal neurons in a monkey model of glaucoma. *Brain Res* **680,** 23-35.

von Lubitz D. K. (1997) Adenosine A3 receptor and brain. A culprit, a hero, or merely yet another receptor? *Ann N Y Acad Sci* **825,** 49-67.

von Lubitz D. K., Simpson K. L. and Lin R. C. (2001) Right thing at a wrong time? Adenosine A3 receptors and cerebroprotection in stroke. *Ann N Y Acad Sci* **939,** 85-96.

Vorwerk C. K., Lipton S. A., Zurakowski D., Hyman B. T., Sabel B. A. and Dreyer E. B. (1996) Chronic low-dose glutamate is toxic to retinal ganglion cells. Toxicity blocked by memantine. *Invest Ophthalmol Vis Sci* **37,** 1618-1624.

Vorwerk C. K., Hyman B. T., Miller J. W., Husain D., Zurakowski D., Huang P. L., Fishman M. C. and Dreyer E. B. (1997) The role of neuronal and endothelial nitric oxide synthase in retinal excitotoxicity. *Invest Ophthalmol Vis Sci* **38,** 2038-2044.

Walker N. I., Harmon B. V., Gobe G. C. and Kerr J. F. (1988) Patterns of cell death. *Methods Achiev Exp Pathol* **13,** 18-54.

Wamsley S., Gabelt B. T., Dahl D. B., Case G. L., Sherwood R. W., May C. A., Hernandez M. R. and Kaufman P. L. (2005) Vitreous glutamate concentration and axon loss in monkeys with experimental glaucoma. *Arch Ophthalmol* **123,** 64-70.

Wang L. Y., Salter M. W. and MacDonald J. F. (1991) Regulation of kainate receptors by cAMP-dependent protein kinase and phosphatases. *Science* **253,** 1132-1135.

Wassle H. (2004) Parallel processing in the mammalian retina. *Nat Rev Neurosci* **5,** 747-757.

Weber A. J. and Harman C. D. (2005) Structure-function relations of parasol cells in the normal and glaucomatous primate retina. *Invest Ophthalmol Vis Sci* **46,** 3197-3207.

Weber A. J., Kaufman P. L. and Hubbard W. C. (1998) Morphology of single ganglion cells in the glaucomatous primate retina. *Invest Ophthalmol Vis Sci* **39,** 2304-2320.

Weber M., Bonaventure N. and Sahel J. A. (1995) Protective role of excitatory amino acid antagonists in experimental retinal ischemia. *Graefes Arch Clin Exp Ophthalmol* **233,** 360-365.

Weinreb R. N. (2005) Clinical trials of neuroprotective agents in glaucoma. *Retina* **25,** S78-S79.

Weinreb R. N. and Levin L. A. (1999) Is neuroprotection a viable therapy for glaucoma? *Arch Ophthalmol* **117,** 1540-1544.

Weinreb R. N. and Khaw P. T. (2004) Primary open-angle glaucoma. *Lancet* **363,** 1711-1720.

Westergaard N., Sonnewald U. and Schousboe A. (1995) Metabolic trafficking between neurons and astrocytes: the glutamate/glutamine cycle revisited. *Dev Neurosci* **17,** 203-211.

Wilding T. J. and Huettner J. E. (1995) Differential antagonism of alpha-amino-3-hydroxy-5-methyl-4- isoxazolepropionic acid-preferring and kainate-preferring receptors by 2,3-benzodiazepines. *Mol Pharmacol* **47,** 582-587.

Woldemussie E., Wijono M. and Ruiz G. (2004) Muller cell response to laser-induced increase in intraocular pressure in rats. *Glia* **47,** 109-119.

WoldeMussie E., Ruiz G., Wijono M. and Wheeler L. A. (2001) Neuroprotection of retinal ganglion cells by brimonidine in rats with laser-induced chronic ocular hypertension. *Invest Ophthalmol Vis Sci* **42,** 2849-2855.

WoldeMussie E., Yoles E., Schwartz M., Ruiz G. and Wheeler L. A. (2002) Neuroprotective effect of memantine in different retinal injury models in rats. *J Glaucoma* **11,** 474-480.

Wollmuth L. P. and Sobolevsky A. I. (2004) Structure and gating of the glutamate receptor ion channel. *Trends Neurosci* **27,** 321-328.

Wolosker H., Blackshaw S. and Snyder S. H. (1999) Serine racemase: a glial enzyme synthesizing D-serine to regulate glutamate-N-methyl-D-aspartate neurotransmission. *Proc Natl Acad Sci U S A* **96,** 13409-13414.

Wong K. Y., Dunn F. A. and Berson D. M. (2005) Photoreceptor adaptation in intrinsically photosensitive retinal ganglion cells. *Neuron* **48,** 1001-1010.

Wong W. T., Myhr K. L., Miller E. D. and Wong R. O. (2000) Developmental changes in the neurotransmitter regulation of correlated spontaneous retinal activity. *J Neurosci* **20,** 351-360.

Wu H. Y., Yuen E. Y., Lu Y. F., Matsushita M., Matsui H., Yan Z. and Tomizawa K. (2005) Regulation of N-methyl-D-aspartate receptors by calpain in cortical neurons. *J Biol Chem* **280,** 21588-21593.

Wu L. G. and Saggau P. (1994) Adenosine inhibits evoked synaptic transmission primarily by reducing presynaptic calcium influx in area CA1 of hippocampus. *Neuron* **12,** 1139-1148.

Wygnanski T., Desatnik H., Quigley H. A. and Glovinsky Y. (1995) Comparison of ganglion cell loss and cone loss in experimental glaucoma. *Am J Ophthalmol* **120,** 184-189.

Yawo H. and Chuhma N. (1993) Preferential inhibition of omega-conotoxin-sensitive presynaptic Ca2+ channels by adenosine autoreceptors. *Nature* **365,** 256-258.

Yoles E. and Schwartz M. (1998) Potential neuroprotective therapy for glaucomatous optic neuropathy. *Surv Ophthalmol* **42,** 367-372.

Yu X. M., Askalan R., Keil G. J., 2nd and Salter M. W. (1997) NMDA channel regulation by channel-associated protein tyrosine kinase Src. *Science* **275,** 674-678.

Yuan J., Lipinski M. and Degterev A. (2003) Diversity in the mechanisms of neuronal cell death. *Neuron* **40,** 401-413.

Yuzaki M. (2003) The delta2 glutamate receptor: 10 years later. *Neurosci Res* **46,** 11-22.

Zamponi G. W. and Snutch T. P. (1998) Modulation of voltage-dependent calcium channels by G proteins. *Curr Opin Neurobiol* **8,** 351-356.

Zhang C. and Schmidt J. T. (1998) Adenosine A1 receptors mediate retinotectal presynaptic inhibition: uncoupling by C-kinase and role in LTP during regeneration. *J Neurophysiol* **79,** 501-510.

Zhang C. and Schmidt J. T. (1999) Adenosine A1 and class II metabotropic glutamate receptors mediate shared presynaptic inhibition of retinotectal transmission. *J Neurophysiol* **82,** 2947-2955.

Zhang D., Sucher N. J. and Lipton S. A. (1995) Co-expression of AMPA/kainate receptor-operated channels with high and low Ca2+ permeability in single rat retinal ganglion cells. *Neuroscience* **67,** 177-188.

Zhang X., Zhang M., Laties A. M. and Mitchell C. H. (2005) Stimulation of P2X7 receptors elevates Ca2+ and kills retinal ganglion cells. *Invest Ophthalmol Vis Sci* **46,** 2183-2191.

Zheng F., Gingrich M. B., Traynelis S. F. and Conn P. J. (1998) Tyrosine kinase potentiates NMDA receptor currents by reducing tonic zinc inhibition. *Nat Neurosci* **1,** 185-191.

Zipfel G. J., Babcock D. J., Lee J. M. and Choi D. W. (2000) Neuronal apoptosis after CNS injury: the roles of glutamate and calcium. *J Neurotrauma* **17,** 857-869.